

New *N,N,P*-Ligands and Their Heterobimetallic Complexes

Dissertation zur Erlangung
des Doktorgrades der Naturwissenschaften (Dr. rer. nat.)
genehmigt vom Fachbereich Chemie
der Technischen Universität Kaiserslautern
(D 386)

vorgelegt von
M. Sc. Merve CAYIR

Betreuer der Arbeit: Prof. Dr. W. R. Thiel
Tag der wissenschaftlichen Aussprache: 02.04.2015

Kaiserslautern, 2015

Tag der Wissenschaftliche Aussprache: 02.04.2015

Dekan:

Prof. Dr. C. van Wüllen

Vorsitzender der Prüfungskommission:

Prof. Dr. D. Schrenk

1. Berichterstatter:

Prof. Dr. W. R. Thiel

2. Berichterstatter:

Prof. Dr. H. Sitzmann

Die vorliegende Arbeit wurde im Fachbereich Chemie der Technischen Universität Kaiserslautern im Arbeitskreis von Prof. Dr. W. R. Thiel in der Zeit von Oktober 2010 bis Januar 2015 angefertigt.

To my parents and my dear sister Gizem...

Content

Content	VII
Abbreviations	XI
1 Introduction	1
1.1 Bimetallic Complexes	1
1.1.1 Ligand Design.....	2
1.1.2 <i>P,N</i> -Ligands for Bimetallic Complexes	4
1.1.3 Bimetallic Complexes.....	6
1.1.3.1 Cooperative Effects.....	6
1.1.3.2 Bimetallic Catalysis	7
1.1.3.2.1 Homobimetallic Catalysis	8
1.1.3.2.2 Heterobimetallic Catalysis.....	9
1.2 Gold Chemistry.....	11
1.2.1 Gold Complexes of <i>P,N</i> -Ligands.....	12
1.2.2 Gold Catalyzed Hydroamination Reaction	13
2 Motivation	17
3 Results and Discussion	19
3.1 Heterobimetallic Complexes.....	19
3.1.1 Ligand Synthesis.....	19
3.1.1.1 Route 1	20
3.1.1.1.1 Synthesis of 1,3-Diketones	20
3.1.1.1.2 Synthesis of Enaminones.....	21
3.1.1.1.3 Synthesis of <i>N,N</i> -Ligands.....	24
3.1.1.2 Route 2.....	27
3.1.1.2.1 Synthesis of 2-Hydroxy Pyridylpyrimidines	28
3.1.1.2.2 Synthesis of the 2-Chloro Pyridylpyrimidine	29
3.1.1.3 Route 3.....	36
3.1.1.3.1 Synthesis of Guanidinium Salts.....	37
3.1.1.3.2 Synthesis of <i>N,N,P</i> -Ligands	38
3.1.2 Complex Synthesis	45
3.1.2.1 Synthesis of Gold Complexes	45
3.1.2.2 Synthesis of the Rhodium Complexes	54
3.1.2.3 Synthesis of Heterobimetallic Complexes	58

3.1.2.4	Synthesis of Pd-Au Heterobimetallic Complexes	59
3.1.2.5	Synthesis of Zn-Au Heterobimetallic Complexes	66
3.1.2.6	Synthesis of Ru-Au Heterobimetallic Complexes	71
3.1.3	Catalytic Studies	81
3.1.3.1	Catalytic Hydroamidation	82
3.2	Pyrimidine Ligands with a Paracyclophane Backbone.....	86
3.2.1	(1-Hydroxy-2-pyrimidine-4-amine)[2.2]paracyclophane	87
3.2.2	Synthesis of Substituted Pyrimidines with a Paracyclophane Backbone	89
3.3	Pd(II) Coordinated <i>N,N,C</i> -Complexes	92
3.3.1	Synthesis of <i>N,N,C</i> -Pd Complexes	93
3.3.2	Kinetic Studies.....	97
4	Conclusion and Outlook	103
5	Experimental	107
5.1	General Methods	107
5.2	Instrumental Analysis	107
5.3	Synthesis of 1,3-Diketones	108
5.3.1	1-(Pyridin-2-yl)butane-1,3-dione (1a)	108
5.3.2	4,4-Dimethyl-1-(pyridin-2-yl)pentane-1,3-dione (1b).....	110
5.3.3	1-Phenyl-3-(pyridin-2-yl)propane-1,3-dione (1c).....	111
5.4	Synthesis of Enaminones	112
5.4.1	(<i>Z</i>)-3-Amino-1-(pyridin-2-yl)but-2-en-1-one (2a).....	112
5.4.2	(<i>Z</i>)-3-Amino-4,4-dimethyl-1-(pyridin-2-yl)pent-2-en-1-one (2b)	113
5.4.3	(<i>Z</i>)-3-Amino-3-phenyl-1-(pyridin-2-yl)prop-2-en-1-one (2c)	114
5.4.4	3-(Dimethylamino)-1-(pyridin-2-yl)prop-2-en-1-one (3a)	115
5.4.5	3-(Dimethylamino)-1-(pyridin-2-yl)but-2-en-1-one (3b)	116
5.5	Synthesis of <i>N,N</i> -Ligands	117
5.5.1	4-Methyl-6-(pyridin-2-yl)pyrimidin-2-amine (4a)	117
5.5.2	4-(<i>tert</i> -Butyl)-6-(pyridin-2-yl)pyrimidin-2-amine (4b)	118
5.5.3	4-Phenyl-6-(pyridin-2-yl)pyrimidin-2-amine (4c)	119
5.5.4	4-(<i>tert</i> -Butyl)-6-(pyridin-2-yl)pyrimidin-2-ol (6)	120
5.5.5	4-(<i>tert</i> -Butyl)-2-chloro-6-(pyridin-2-yl)pyrimidine (7)	121
5.5.6	3-((4-(<i>tert</i> -Butyl)-6-(pyridin-2-yl)pyrimidin-2-yl)amino)propan-1-ol (8).....	122
5.6	Synthesis of Aminophosphines.....	123
5.6.1	2-(Diphenylphosphinyl)ethyl-1-amine (9a).....	123
5.6.2	3-(Diphenylphosphinyl)propylamine (9b).....	124

5.7	Synthesis of 1-(Phosphinylalkyl)guanidinium Salts	124
5.7.1	1-(2-(Diphenylphosphinyl)ethyl)guanidinium Sulfate (10a).....	125
5.7.2	1-(3-(Diphenylphosphinyl)propyl)guanidinium Sulfate (10b)	126
5.8	Synthesis of <i>N,N,P</i> -Ligands	127
5.8.1	<i>N</i> -(2-(Diphenylphosphinyl)ethyl)-4-(pyridin-2-yl)pyrimidin-2-amine (11a)	127
5.8.2	<i>N</i> -(2-(Diphenylphosphinyl)ethyl)-4-methyl-6-(pyridin-2-yl)pyrimidin-2-amine (11b)	128
5.8.3	<i>N</i> -(3-(Diphenylphosphinyl)propyl)-4-(pyridin-2-yl)pyrimidin-2-amine (12a).....	130
5.8.4	<i>N</i> -(3-(Diphenylphosphinyl)propyl)-4-methyl-6-(pyridin-2-yl)pyrimidin-2-amine (12b)....	131
5.9	Synthesis of Monometallic Complexes	133
5.9.1	Chlorotetrahydrothiophenegold(I) (13)	133
5.9.2	Au Complex 14a	133
5.9.3	Au Complex 14b	135
5.9.4	Au Complex 15a	136
5.9.5	Au Complex 15b	137
5.9.6	Rh Complex 16	138
5.10	Synthesis of Heterobimetallic Complexes	140
5.10.1	Pd-Au Complex 17a	140
5.10.2	Pd-Au Complex 17b	141
5.10.3	Pd-Au Complex 17c	142
5.10.4	Zn-Au Complex 18a	144
5.10.5	Zn-Au Complex 18b	145
5.10.6	Zn-Au Complex 18c	146
5.10.7	Ru-Au Complex 19a	147
5.10.8	Ru-Au Complex 19b	149
5.10.9	Ru-Au Complex 19c	150
5.10.10	Ru-Au Complex 19d	151
5.11	Synthesis of Pyrimidine Ligands with a Paracyclophane Backbone	153
5.11.1	(<i>E</i>)-3-(Dimethylamino)-1-(1-hydroxy[2.2]paracyclophane)prop-2-en-1-one (20).....	153
5.11.2	1-Hydroxy-2-(2-aminopyrimidin-4-yl)[2.2]paracyclophane (21).....	154
5.11.3	1-Hydroxy-2-(2-(isopropylamino)pyrimidin-4-yl)[2.2]paracyclophane (22a)	155
5.11.4	1-Hydroxy-2-(2-(dimethylamino)pyrimidin-4-yl)[2.2]paracyclophane (22b).....	156
5.11.5	1-Hydroxy-2-(2-(pyrrolidin-1-yl)pyrimidin-4-yl)[2.2]paracyclophane (22c).....	158
5.11.6	1-Hydroxy-2-(2-butylamino-1-yl)pyrimidin-4-yl)[2.2]paracyclophane (22d)	159
5.12	Synthesis of Aryl Substituted Guanidinium Salts.....	160
5.12.1	1-Phenyl guanidinium Sulfate (23a).....	160
5.12.2	1-(4-Fluorophenyl)guanidinium Nitrate (23b)	161
5.12.3	1-(4-Chlorophenyl)guanidinium Nitrate (23c)	162

5.12.4	1-(4-Methoxyphenyl)guanidinium Nitrate (23d).....	163
5.12.5	1-(4-Cyanophenyl)guanidinium Nitrate (23e).....	164
6	References.....	165
7	Appendix.....	179
7.1	Crystal Structure Data.....	179
7.1.1	Crystal Data and Structure Refinement for 14a	179
7.1.2	Crystal Data and Structure Refinement of 15a	180
7.1.3	Crystal Data and Structure Refinement for 22b	181
7.2	Statutory Explanation.....	183
7.3	Acknowledgements.....	184
7.4	Curriculum Vitae	186

Abbreviations

Å	Angstrom
AHPC	5-Acetyl-4-hydrox[2.2]paracyclophane
Bu	Butyl
°C	Celsius
CID	Collision-induced Dissociation
cm	Centimeter
COSY	Correlated Spectroscopy
DCM	Dichloromethane
DMA-DMA	<i>N,N</i> -Dimethylacetamide Dimethyl Acetal
DMF-DMA	<i>N,N</i> -Dimethylformamide Dimethyl Acetal
DMSO	Dimethyl Sulfoxide
dppa	Bis(diphenylphosphino)amine
dppm	Bis(diphenylphosphino)methane
ESI	Electron Spray Ionization
FT-IR	Fourier Transfer Infrared
HMBC	Heteronuclear Multiple Bond Correlation
HMQC	Heteronuclear Multiple Quantum Correlation
Hz	Hertz
IR	Infrared
<i>J</i>	Coupling Constant
M	Molar
Me	Methyl
mm	Millimeter
Ms	Mesyl
NHC	<i>N</i> -Heterocyclic Carbene
NMR	Nuclear Magnetic Resonance
Pc	Paracyclophane
Ph	Phenyl
ppm	Parts Per Million
r.t.	Room Temperature
Tf	Triflyl
THF	Tetrahydrofuran

Abbreviations

tht	Tetrahydrothiophene
Ts	Tosyl
UV-Vis	Ultraviolet-visible
δ	Chemical Shift in ppm
$\tilde{\nu}$	Wave Numbers in cm^{-1}

1 Introduction

1.1 Bimetallic Complexes

Catalysis is one of the most important and fast expanding areas in synthetic chemistry.^[1] The research for developing better catalytic systems in terms of efficiency and selectivity is still continuing. However, the most selective catalysts are found in nature, for instance in enzyme catalyzed reactions. They have been investigated for long times and show unique activities.^[2-5] According to spectroscopic studies which were undertaken to elucidate the structure of the active sites of enzymes, a considerable number of the active sites comprises of two metal centers being in close proximity to each other, thus interact cooperatively. For instance, hemocyanin and tyrosinase enzymes are monooxygenases that both have a dinuclear copper active site (Figure 1). These enzymes activate oxygen and create highly active intermediates for oxidizing catechols to *o*-quinones.^[6,7]

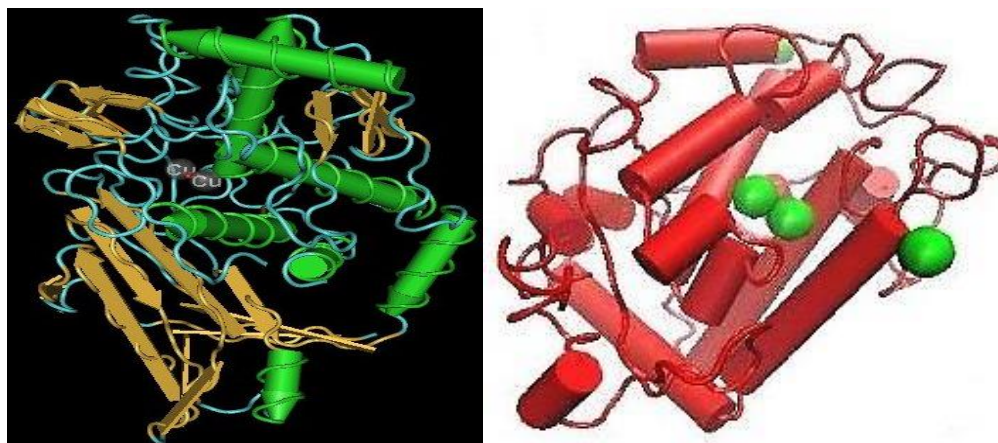


Figure 1. Hemocyanin of an octopus (right), tyrosinase of streptomyces (copper atoms are shown in green, left).^[8,9]

Another example is the superoxide dismutase which is a metalloenzyme bearing two different active metal centers: copper and zinc. It can eliminate the toxic superoxide anion O_2^- by converting it to H_2O_2 and O_2 . While the copper cation coordinates to the superoxide anion, the endorsing of the protein to the required coordination environment is triggered by the zinc cation.^[10,11]

These findings also influenced the design and the synthesis of dinuclear complexes in order to develop better catalysts or to investigate their unique spectroscopic and electrochemical properties.^[12]

1.1.1 Ligand Design

Probably, the most challenging issue for the synthesis of a well-defined bimetallic complex is to design an appropriate ligand system: first it must be able to hold two metal sites, second the steric and electronic properties have to be considered.

In 1970, Robson defined the term “binucleating ligands” which describes polydentate chelating ligands having the capacity to bind two metal atoms and to form binuclear complexes.^[13] They can be divided into two groups according to their coordination modes (Figure 2).

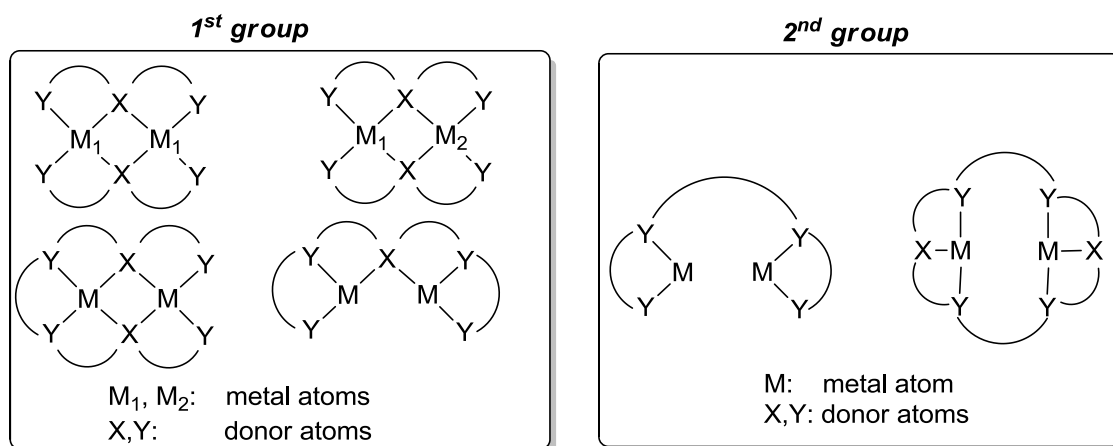


Figure 2. Types of bimetallic complexes with isolated donor sites ligands.

In the first group, compartmental ligands generate homo- and heterobimetallic complexes which share at least one donor atom and have dissimilar donor sets. Here, the central atoms can form a bridge between the two metals.^[14] In the second group, the donor atoms of the ligands are not shared. Here the donor sets are isolated and connected by linkers.

Preliminary reports about complexes derived from binucleating ligands were published in the 1970's. Lever used the phthalhydrazone ligand shown in Figure 3 to synthesize bimetallic complexes of the type $\text{Cu}_2\text{LX}_3(\text{OH})\text{H}_2\text{O}$.^[15] Robson synthesized complexes of

the type LCu_2X ($X = OH$) using the acyclic and cyclic Schiff base ligands acquired from diformylphenols.^[16]

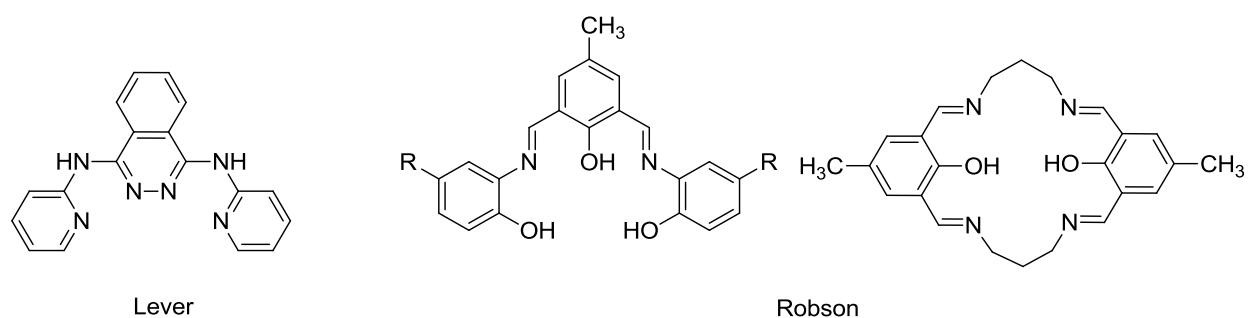


Figure 3. Binucleating ligands used for the synthesis of first bimetallic complexes.

Many other binucleating ligands have been reported since that time. They can also be classified according to the bridging unit between the two metal centers.^[17] Carboxylates are commonly used bridging groups to form bimetallic complexes. In these cases, the two metal centers are coordinated in a *syn, syn* position.^[18]

Furthermore, nitrogen containing heterocycles such as pyrazolate, triazolate, pyradizines, and phthalazines can be included as donor motifs in bridging ligands.^[19,20] Phenolates and alkoxides have been extensively used because of their readily accessibility.^[21,22]

It is also possible to construct bimetallic complexes without bridging ligands. Such systems are called face-to-face bimetallic complexes. Rigid molecular structures hold two metals apart from each other or the metals coordinate with a specific separation distance which results from bridging by small molecules (Figure 4).^[17]

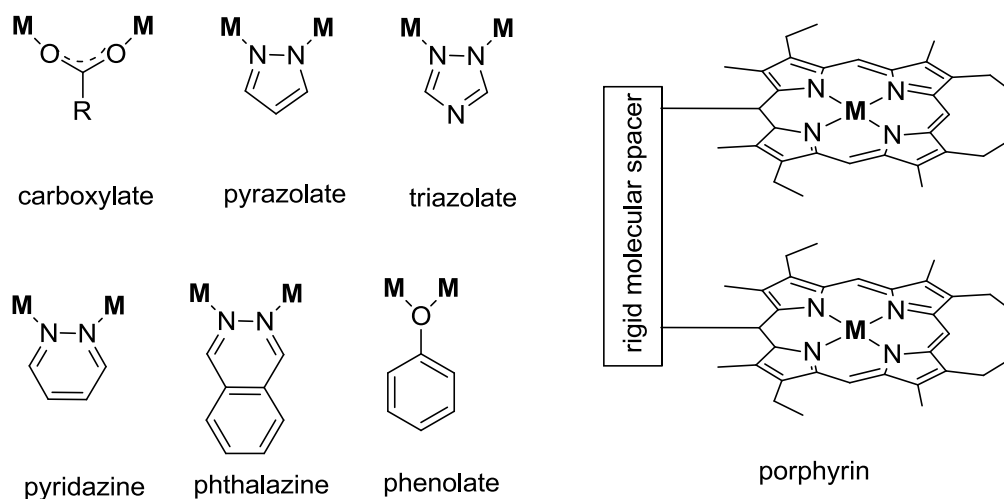



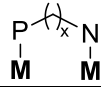
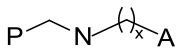
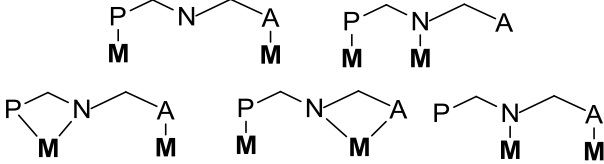
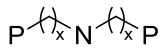
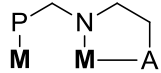
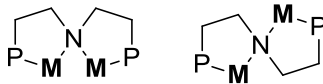
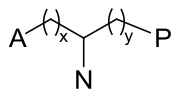
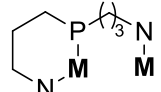
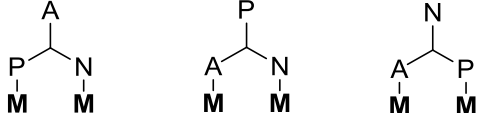
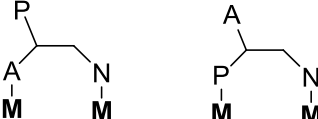
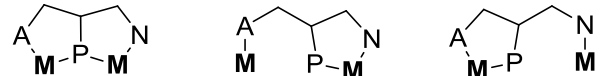
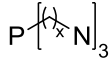
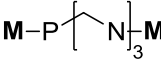

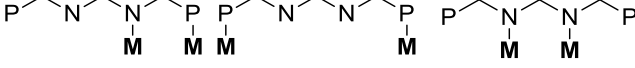
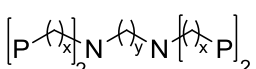
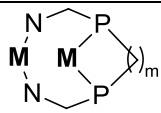
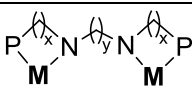
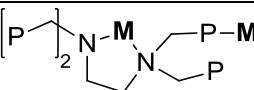
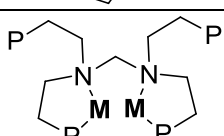
Figure 4. Bridging motifs in bimetallic complexes.

1.1.2 *P,N*-Ligands for Bimetallic Complexes

P,N-Ligands are quite popular hemilabile ligands since they stabilize different oxidation states of metal ions.^[23] While one metal center is stabilized by the weak π -acceptor character of the phosphorous, the σ -donor character of the nitrogen atom enhances the reactivity of a second metal center in e.g. oxidative addition reactions by stabilizing oxidation states.^[24] Therefore, *P,N*-ligands are very attractive to design bimetallic complexes which can show properties and activities other than their monometallic fragments.^[25]

Some selected *P,N*-ligands are summarized in Table 1. The categorization of these ligands is based on the type of bridging units, linkers and metal coordination modes.^[26]

Table 1. Some important *P,N* ligands backbone.^[26]

Bridging unit	No. of atom between <i>P-N</i>	Metal coordination mode
	$x = 1-5$	
	$x = 1$	
	$x = 2$	
	$x = 2$	
	$x = 3$	
	$x = 0, y = 0$	
	$x = 0, y = 1$	
	$x = 1, y = 1$	
	$x = 1$	
	$x = 1, y = 1$	
	$x = 1, y = 2, 3$	
	$x = 2, 3, y = 0-4$	
	$x = 1, y = 2$	
	$x = 2, y = 1$	

1.1.3 Bimetallic Complexes

Bimetallic complexes are prepared from multidentate ligands and two metal atoms or ions. When these metal sites are from the same element, they are called homobimetallic complexes. On the other hand, when the metals are different, they are known as heterobimetallic complexes (Figure 5).



Figure 5. Homo- and heterobimetallic complexes.

1.1.3.1 Cooperative Effects

Bimetallic complexes have gained a distinguished position in the materials science and catalysis due to their unique spectroscopic properties and reactivities. Cooperative effects in multimetallic complexes have been observed in many homogeneous catalytic transformations.^[27] *Cooperativity* is a phenomenon represented by enzymes or receptors which are composed of multiple binding sites. It was originally found in hemoglobin by *Bohr*. He observed that binding of first molecule of oxygen makes binding of second oxygen molecule easier.^[28-30]

Cooperativity can be explained that magnetic, physical and catalytical properties change, when two or more metals are present. Bimetallic complexes can reveal a cooperative effect when the metal sites are positioned within a sufficient distance. It is discussed that if the distance between two metals is about 3.5-5 Å, a bimetallic complex can comprise a cooperative effect. Cooperative effects of bimetallic complexes can be divided into three groups: functional, enthalpic and entropic cooperativities (Figure 6).^[30,31]

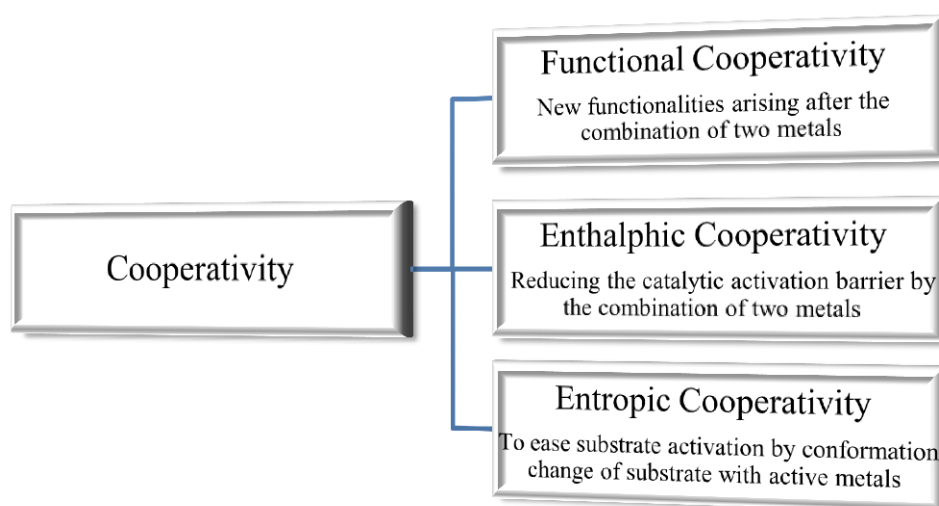


Figure 6. Types of cooperativity.^[30,31]

1.1.3.2 Bimetallic Catalysis

Bimetallic catalysis can be described in a way that two metals work cooperatively in a catalytic process.^[32] From structural point of view, cooperative bimetallic catalysis can be divided into four different types (Figure 7).^[33]

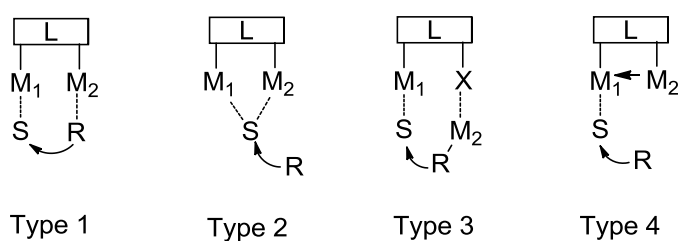


Figure 7. Types of bimetallic catalysis.

In the first type, two metal sites attach to the same ligand. While M_1 activates the substrate (S), the reagent (R) is activated by M_2 . In the second type, both metals activate the substrate simultaneously. In the third type of catalysis one metal interacts with a basic site and activates the reactant. In type 4, one metal activates the substrate and is stabilized by the second metal through metal-metal redox cooperation.^[1,33,34]

1.1.3.2.1 Homobimetallic Catalysis

Structures of enzymes have led to studies on the design of homobimetallic complexes and to investigations of their activities in catalytic reactions. Dias and Grubbs developed the ruthenium catalysts which show 20 times higher activity than their monometallic counterparts in olefin metathesis reactions (Figure 8).^[35] Another example of homobimetallic catalysis was reported by Stanley. The bimetallic rhodium complex was found as a highly active and regioselective catalyst. It catalyzes the hydroformylation of 1-hexene about 40% faster than the monometallic Rh catalyst. This result can be explained by cooperativity between the two rhodium atoms.^[36]

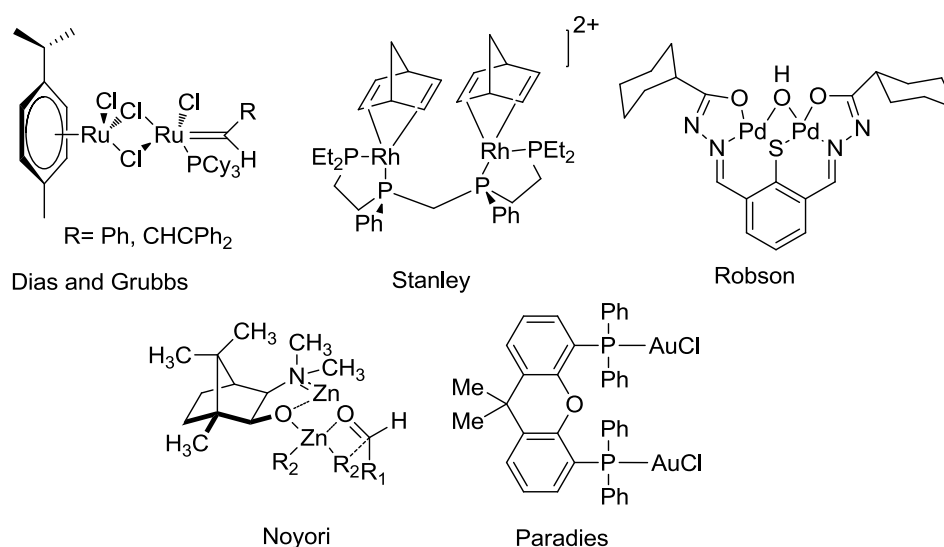


Figure 8. Some examples of homobimetallic catalysts.

Robson and co-workers tested the homobimetallic palladium complex in the hydration of acetonitrile. Coordination of acetonitrile to palladium initiates the catalytic cycle. The next step is the formation of a carbon-oxygen bond which coordinates to two palladium atoms. It is followed by a proton transfer and yields acetamide after quenching with water.^[37] Noyori and co-workers developed the bimetallic zinc catalyst for the enantioselective alkylation of aldehydes. Here, one zinc site behaves as a Lewis acid to activate an electrophile and the other zinc binds to oxygen atom and spreads the nucleophilicity in an enantioselective fashion.^[38]

Recently, Paradies and co-workers synthesized the dinuclear gold complex and tested it in hydroamidation of cyclohexene with tosyl amide. This complex showed higher catalytic activity compared to its monometallic species and PPh_3AuCl .^[39]

1.1.3.2.2 Heterobimetallic Catalysis

Heterobimetallic complexes have attracted special interests due to the fact that the bifunctionality of different metals can lead to unique reactivity.^[40] A large number of heterobimetallic complexes have been synthesized but there are few examples where both metals play active roles in a catalytic cycle. Most heterobimetallic catalysts have been prepared to investigate their structural, spectroscopic, and luminescent properties.

Shibasaki and co-workers developed the BINOL-based bimetallic and tetrametallic complexes shown in Figure 9.^[41] These complexes were tested in various catalytic asymmetric reactions. For example, the bimetallic complex with M_1 and M_2 being aluminum and lithium was found as an efficient catalyst for the conjugate addition of malonates. The reaction was promoted by a cooperation of the two metal centers.^[42]

As another example, the tetrametallic complex with M_1 and M_2 being lithium and lanthanum catalyzes an asymmetric nitroaldol reaction. Combination of an alkali metal and a lanthanide metal improved the reactivity and showed high stereo selectivity with 90% *ee*.^[43] Tetrametallic complexes were successfully applied to other asymmetric reactions such as conjugate additions of malonates using complex with M_1 and M_2 being sodium and lanthanum, respectively,^[44] and aza-Henry reactions using the complex where M_1 and M_2 are potassium and ytterbium.^[45]

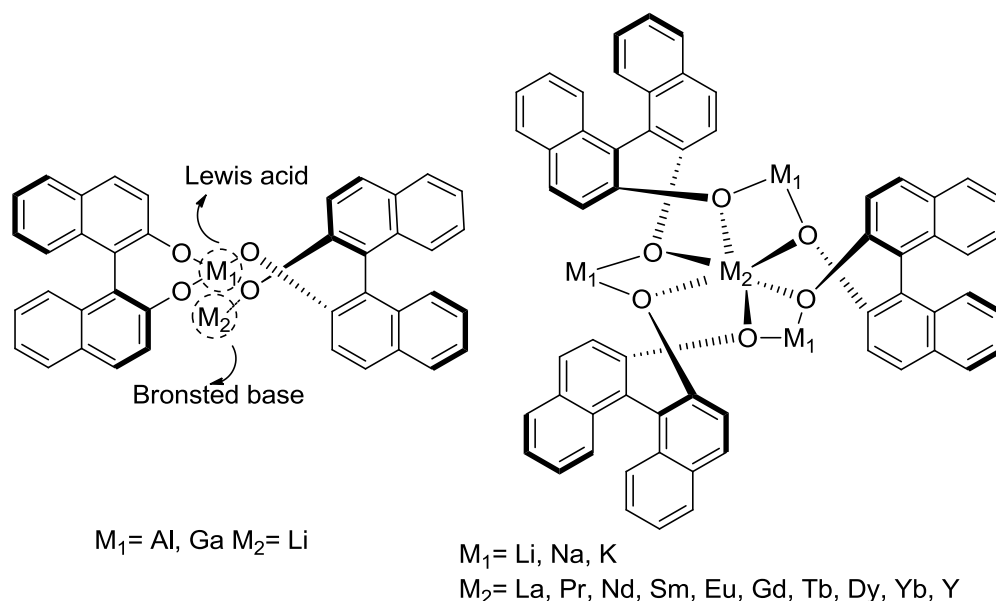
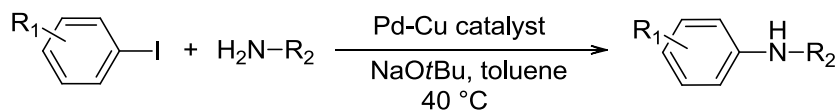


Figure 9. BINOL-based heterobimetallic catalysts.

A highly efficient heterobimetallic Rh-Zr catalyzing the hydroformylation of alkenes was reported by Choukroun.^[46,47] It was proposed that the reaction is carried out by rhodium and zirconium is responsible for a change in electron density at the rhodium site. In 1991, Oro and co-workers developed the heterobimetallic Ru-Rh and Ru-Ir catalyzed hydrogenation of alkenes. Bimetallic catalysts showed superior activity than the corresponding monometallic complexes. It is believed that electronic communication between the two metals through the ligand improves the reactivity.^[48] Recently, Lee and co-workers demonstrated that a conjugate addition of thiophenols to unsaturated enones was efficiently catalyzed by heterobimetallic Zn-Fe complexes. This catalytic activity can be related to synergistic interactions between zinc and iron cations.^[49]

Tsukada and co-workers reported the heterobimetallic Pd-Cu catalyzed coupling reaction of aryl iodides with aniline (Scheme 1). The reaction proceeds at 40 °C and provides diphenylamine in 92–97% yield. Monometallic Pd complexes were tested under identical conditions and showed lower activity compared to the Pd-Cu bimetallic complex.^[50]



Scheme 1. Amination of aryl iodides with aniline catalyzed by a Pd-Cu complex.

The use of heterobimetallic catalysis emerges as a new strategy to increase efficiency and selectivity. However, further studies are still necessary in order to gain a better understanding about the behavior of heterobimetallic complexes in catalytic reactions.

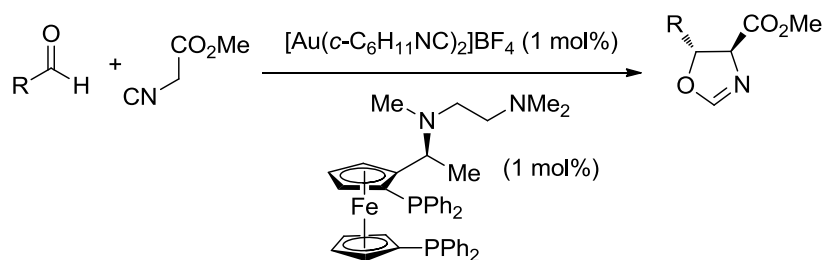
1.2 Gold Chemistry

Gold chemistry became a very attractive topic in materials science, surface chemistry, biology, and homogeneous catalysis.^[51-58] It was believed for long that gold is an inactive metal due to its “chemical inertness” but later it was proved that gold can be used in heterogeneous and as well as in homogeneous catalysis.^[57,59-61] For example, the nucleophilic addition to carbon-carbon multiple bonds is one of the most common reactions that is catalyzed by gold.

AuCl₃ and HAuCl₄ were the first compounds to be used in gold catalysis. Later on, gold complexes carrying phosphine ligands became popular in this field.^[62] A large number of cationic gold complexes were studied in various organic transformations such as the cycloisomerization of enynes, and the hydrofunctionalization of alkenes and alkynes.^[63,64] Especially, gold(I) complexes turned out to be suitable for the π activation of carbon-carbon multiple bonds towards a nucleophilic attack. Owing to its highly electrophilic and soft Lewis acidic character, cationic gold(I) provides good chemoselectivity and functional group compatibility. In addition, low LUMO energies and the weak back donation of gold species can be taken as explanations for the success of gold in catalysis.^[65] The coordination modes of gold(I) complexes are well understood. In general, gold(I) coordinates linearly and forms dicoordinate complexes. Tri- and tetra coordinated gold(I) complexes are quite rare.^[66,67]

A first breakthrough in gold catalysis was achieved by Hayashi and Ito in 1986.^[68] The gold(I) complex of a chiral ferrocenylphosphine was used as an efficient catalyst in the asymmetric aldol condensation and gave dihydrooxazoles in high yield and excellent

enantiomeric excess (Scheme 2). This reaction is also the first example of a catalytic asymmetric aldol reaction.



Scheme 2. Gold catalyzed asymmetric aldol condensation.

1.2.1 Gold Complexes of *P,N*-Ligands

According to Pearson's HSAB concept, gold(I) prefers to coordinate to soft ligands like phosphines, *N*-heterocyclic carbenes (NHC) and organic sulphur compounds.^[69] Especially, gold(I) phosphine complexes have been extensively studied due to their promising anti-tumor activities, chemiluminescent properties, and their activity in catalytic reactions.^[70-72] Recently, gold(I) complexes with *P,N*-ligands have been investigated because of bringing hard and soft donors together. These complexes can contain aurophilic bonds between the gold ions, affecting the structural and photophysical properties of the complexes.^[73] Hereby, the phosphorous atoms should be positioned in close proximity to enable intramolecular gold-gold interactions. For example, bis(diphenylphosphino)methane (dppm) is very proper ligand for an intramolecular aurophilic interaction between gold atoms.^[74,75] Bis(diphenylphosphino)amines (dppa) have relatively close properties compared to dppm. Although some gold(I) complexes of dppa are sensitive towards to light and moisture, a short intramolecular gold-gold interaction in the crystal structure of (dppa)₂Au₂Cl₂ complex was observed by Schmidbaur.^[76] Moreover, *P,N*-ligands can be modified easily from the nitrogen and the phosphorous site leading to different bond angles between P-N-P and also to different conformational structures.^[77]

Besides, gold complexes of *P,N*-ligands can be used in homogeneous catalysis. Hashmi and co-workers reported the gold(I) catalyzed hydration of alkynes using *P,N*-ligands such as PPh₂Py, PINAP and MandyPhos. Complexes of the type [AuPPh₂Py]X (where X = NTf₂, OTf, BF₄) catalyzed the addition of water to 1-pentyne to obtain 2-pentanone

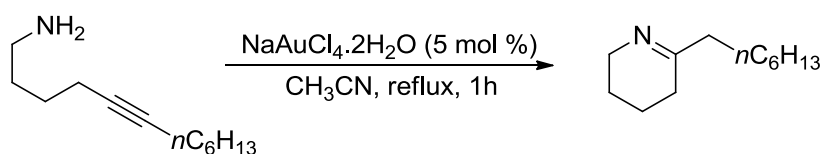
in high yields.^[78] As another example, gold(I) complexes of an imidazolylphosphine ligand were used as catalysts in the multicomponent reaction of benzaldehyde, piperidine and phenylacetylene to synthesize the corresponding propargylamine. These complexes showed high catalytic activities with low catalyst loading (0.5 mol %).^[79]

1.2.2 Gold Catalyzed Hydroamination Reaction

Hydroamination is the addition of an amine N-H bond over a carbon-carbon multiple bond coming from and an alkene, alkyne, diene or allene.^[80] While intramolecular hydroaminations produce nitrogen containing heterocycles, intermolecular hydroaminations are used to obtain acyclic amines.^[81] In earlier times, alkali and lanthanide metals were considered as catalysts in hydroamination reactions. Nowadays, using late transition metals such as Pd, Rh, Ru, and Au has become more popular.^[81]

Gold(I) and gold(III) complexes have been introduced as catalysts in hydroamination reactions since the highly carbophilic Lewis character of gold cations activates carbon-carbon multiple bonds towards a nucleophilic attack.^[82] On the other hand, gold(I) complexes do not have an oxophilic character resulting in good functional group compatibility and high stability against air and moisture.

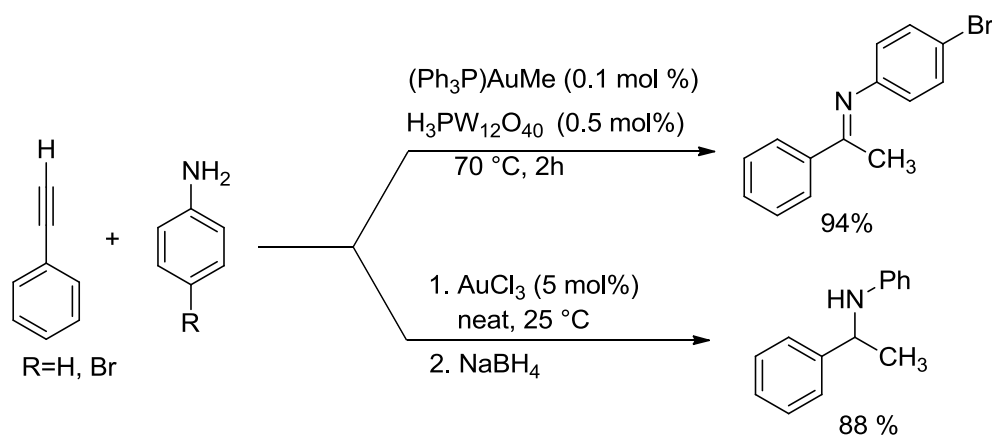
In 1987, the first example of a gold catalyzed intramolecular hydroamination with 5-alkynylamines to obtain tetrahydropyridines was reported by Utimoto. 5-Dodecynylamine was converted to 6-heptyl-2,3,4,5-tetrahydropyridine in the presence of a catalytic amount of NaAuCl₄ (Scheme 3).^[83]



Scheme 3. First gold catalyzed intramolecular hydroamination reaction.

Later, Tanaka developed the acid promoted gold(I) catalyzed intermolecular hydroamination of aromatic and aliphatic alkynes with aniline derivatives to afford ketimines in high yields.^[84] In 2005, Li and co-workers showed that cationic gold(III) complexes can also catalyze intermolecular hydroamination reactions of alkynes with

aniline derivatives. Further reduction of ketimines with sodium borohydride produces corresponding amines (Scheme 4).^[85]



Scheme 4. Gold(I) and gold(III) catalyzed intermolecular hydroamination.

He et al. reported the gold(I) catalyzed hydroamidation of alkenes.^[86] $(\text{Ph}_3\text{P})\text{AuOTf}$ which is prepared by reacting PPh_3AuCl with AgOTf was used as catalyst. A wide range of alkenes including terminal ones were reacted with *p*-toluenesulfonamide to obtain acyclic/cyclic amines in moderate to very high yields.

A general mechanism of the gold(I) catalyzed hydroamination of alkynes was proposed by Tanaka. First, a cationic gold(I) species interacts with an alkyne and an amine to generate complex **A**. This complex is transformed into enamine **B** via an inner-sphere C–N bond formation. After a protodeauration of the enamine **B**, ketimine forms and gold(I) cation is regenerated (Figure 10).^[84]

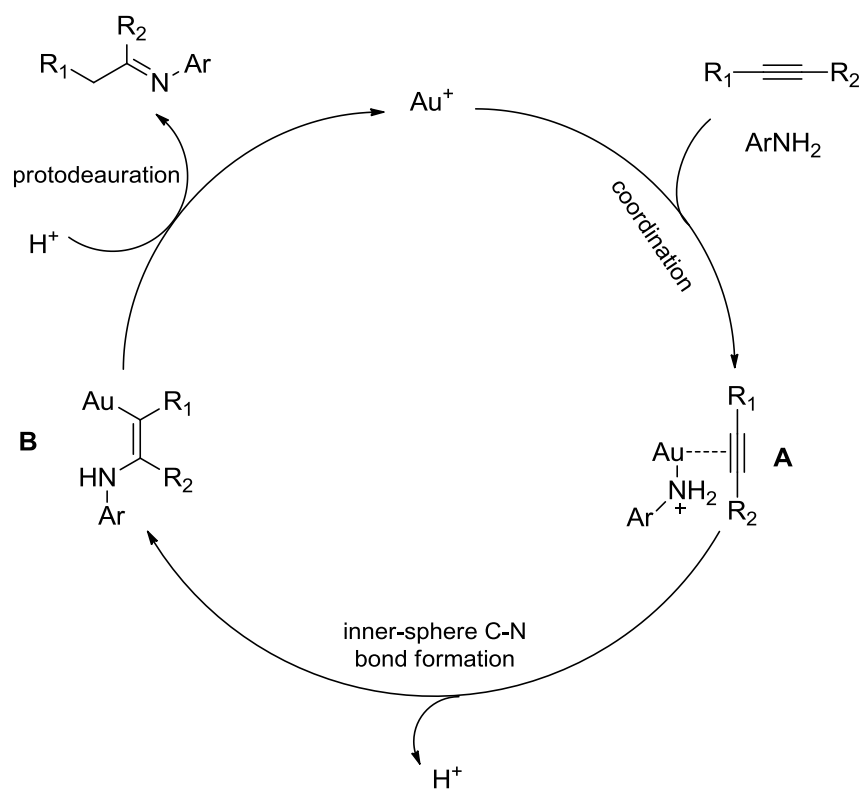


Figure 10. Proposed mechanism of gold catalyzed hydroamination reactions.

2 Motivation

In the recent years, the Thiel group has been interested in the preparation of functionalized phosphine ligands such as pyrimidinylpyridine phosphines,^[87] pyrazole functionalized phosphines,^[88] and imino substituted phosphines.^[89] Transition metal complexes of these ligands showed very good activities in many catalytic transformations.^[26,90] These studies indicate that bi- and tridentate *P,N*-ligand systems are very appropriate precursors to generate catalytically active multimetallic complexes. The aim of this work was to synthesize and characterize novel amino pyridylpyrimidine phosphine ligands. They can be functionalized at the pyrimidine ring and the amino group which will give us an opportunity to build bi- and trimetallic complexes as a part of SBF/TRR-88 3MET project. The target ligand skeleton and possible functionalization modes are shown in Figure 11.

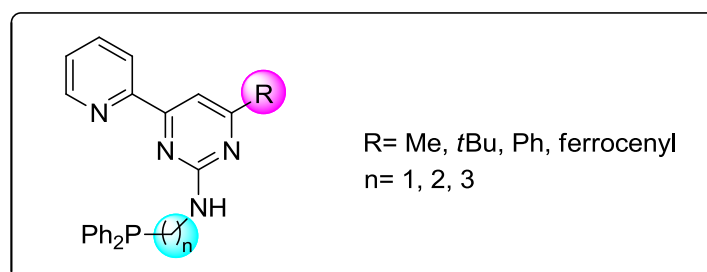


Figure 11. *N,N,P*-Ligands with different substituents on the pyrimidine ring.

Bimetallic complexes are interesting due to their unusual spectroscopic, optical properties and reactivities. When two metal atoms are positioned in close proximity, the complexes can exhibit a unique behavior as a result of the cooperation between two metal atoms. There are several examples in the literature.^[35,91,92] These studies brought the idea to design and synthesize new heterobimetallic complexes of the *N,N,P*-ligands with various metal combinations. These properties should be investigated by the collaboration with SBF/TRR-88 3MET project partners. Figure 12 illustrates the target monometallic gold and rhodium complexes.

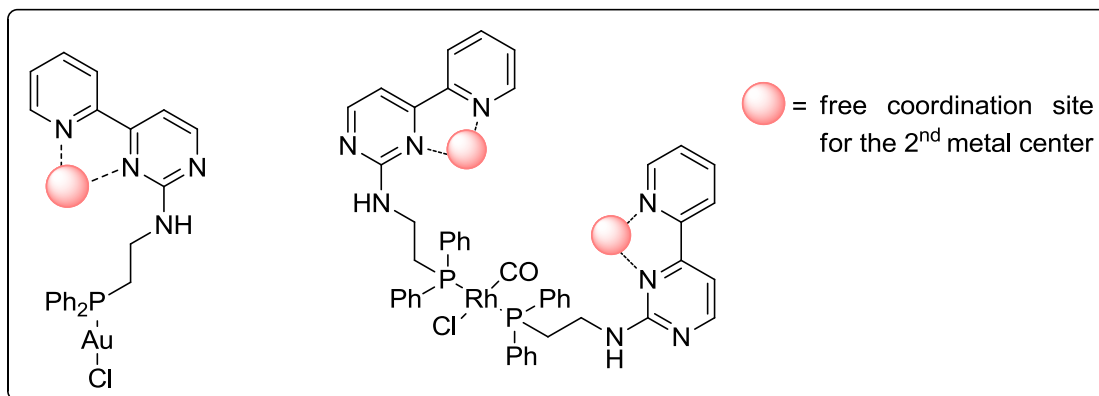


Figure 12. Some examples of monometallic Au and Rh complexes.

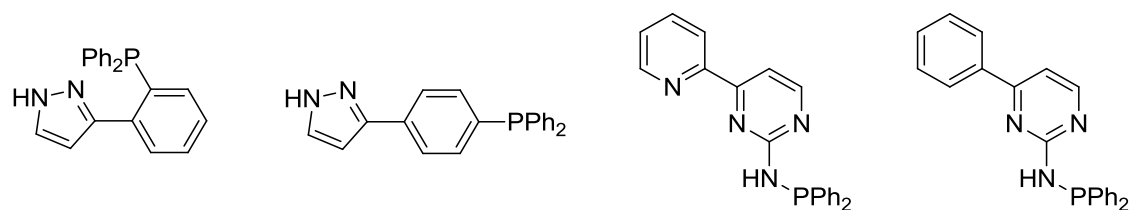
3 Results and Discussion

3.1 Heterobimetallic Complexes

3.1.1 Ligand Synthesis

Multidentate ligands play a significant role in terms of offering different coordination modes. Therefore new complexes are developed continuously with these ligands.^[93] One important property of such multidentate ligands is their possibility to stabilize metal ions in different geometries and oxidation states. Often such ligands are composed of combinations of nitrogen and phosphorous donor sites. Furthermore, multidentate ligands possessing both a hard and a soft donor coordination site are proper building blocks for the preparation of heterobimetallic complexes.^[24,94,95]

The Thiel group has been interested in the chemistry of functionalized phosphine ligands during the last decade. The first phosphine ligands bearing a pyrazole motif were synthesized by the reaction of [2- or 3-(3-dimethylamino-1-oxoprop-2-en-yl)phenyl]diphenylphosphine and hydrazine via cyclocondensation.^[88] Recently, 2-aminopyrimidinyl-functionalized phosphines were obtained by condensing arylmethylketones and *N,N*-dimethylformamide dimethylacetal (DMF-DMA) to produce enaminones which were cyclized with guanidinium salts under basic conditions to give aminopyrimidines. Phosphorylation of the amino group with ClPPh₂ in the presence of a base resulted in the formation of the target aminophosphine ligands (Scheme 5).^[87,96]



Scheme 5. Selected examples of *N,P*-ligands synthesized by the Thiel group.

Multidentate ligands having a pyrimidine group as a hard donor for the coordination with transition metals and a phosphine unit as soft donor are under investigation in the

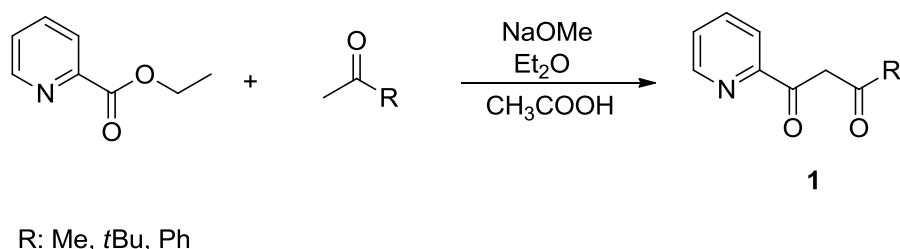
SFB/TRR88 (3MET) in collaboration with the group of Prof. Dr. Stefan Bräse from Karlsruhe Institute of Technology.

Here, we aimed to synthesize ligands bearing different pyridylpyrimidines fragments which are substituted with different phosphinoalkyl chains. The variation of the ligand systems will give us the chance to investigate the steric and electronic requirements for a cooperative activity in catalytic reactions. In the following chapters, different methods for to synthesize of the target aminophosphine ligands will be discussed

3.1.1.1 Route 1

3.1.1.1.1 Synthesis of 1,3-Diketones

1,3-Diketones were used as building blocks in the synthesis of heterocyclic ligands.^[97,98] They were obtained as described in the literature.^[99,100] Exemplarily, ethyl 2-picolinate is reacted with a proper methyl ketone to give diketone **1** via a Claisen condensation reaction (Scheme 6).



Scheme 6. The synthesis of the 1,3-diketones **1**.

The reactions were performed in anhydrous diethyl ether. Hereby, the solution of the methyl ketone in diethyl ether was added dropwise to a suspension of ethyl 2-picolinate and sodium methanolate in diethyl ether. Then, the mixture was heated to reflux for 4 hours. Finally, acetic acid was added to neutralize the sodium salt of the 1,3-diketone **1**. Using this method, three different diketones **1a-c**, in which the substituent R is either methyl, *t*-butyl or phenyl, were synthesized from acetone, pinacolone and acetophenone, respectively.

The 1,3-diketones form a series of tautomers due to keto-enol tautomerism,^[101] which can clearly be identified in the ¹H NMR spectra of the 1,3-diketones (Figure 13).

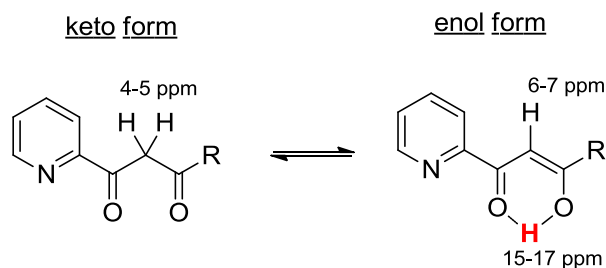


Figure 13. Keto-enol tautomerism of **1**.

The hydroxyl group of the enol form gives a signal at low field between 15 and 17 ppm, which can be explained by the presence of an intramolecular hydrogen bonding between the proton of the hydroxyl group and the oxygen atom of the carbonyl group.

3.1.1.1.2 Synthesis of Enaminones

Enaminones are valuable intermediates to synthesize a wide range of heterocyclic compounds such as pyridines, pyrazoles and pyrimidines.^[102,103] In this chapter, the synthesis of two different types of enaminones will be discussed (Figure 14).

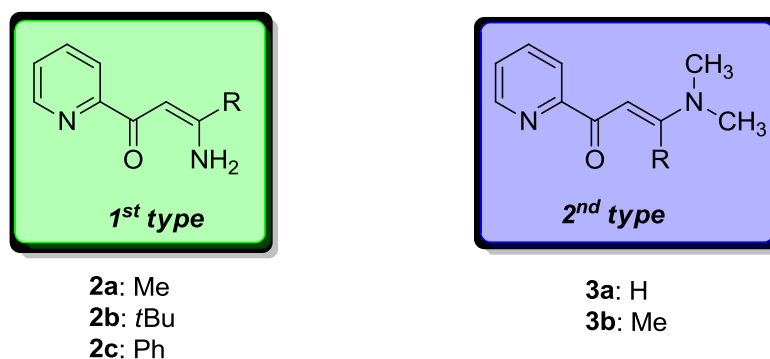
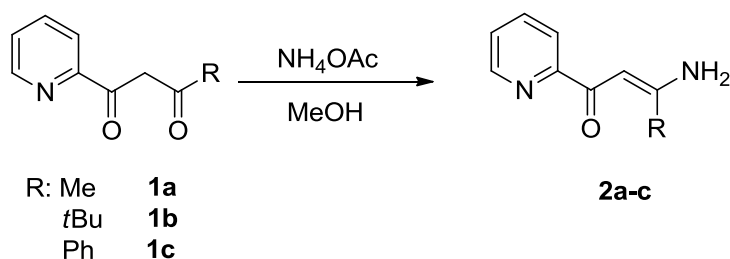


Figure 14. Different types of enaminones.

The first type of enaminones can be easily synthesized from β -diketones.^[104,105] Diketones **1a-c** were reacted with ammonium acetate in anhydrous methanol at reflux temperature for 24 hours to transform them into the target compounds **2a-c** in good yields (Scheme 7).



Scheme 7. Synthesis of the 1st type enaminones.

As an illustrative example, a comparison of the ¹H NMR spectra of the β-diketone **1a** and enaminone **2a** is shown below (Figure 15). The transformation can be proved by the replacement of the hydroxyl unit by the amine which shows a hindered rotation.

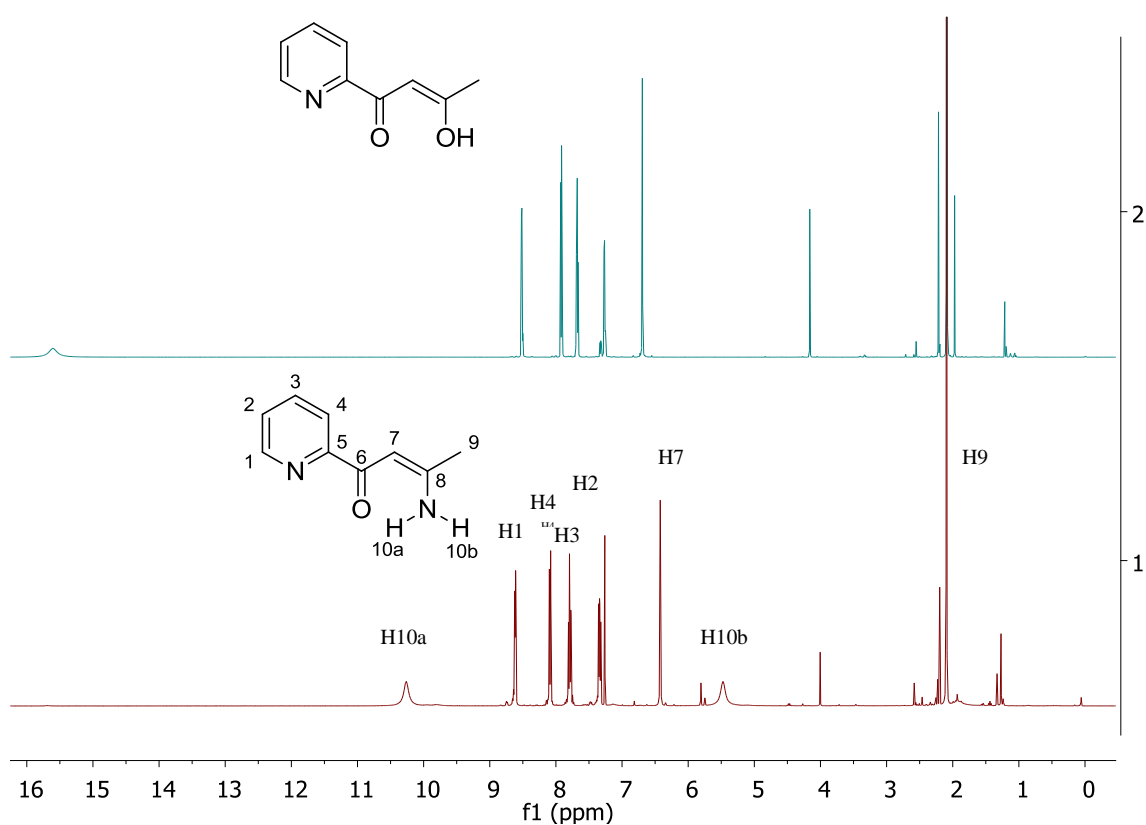
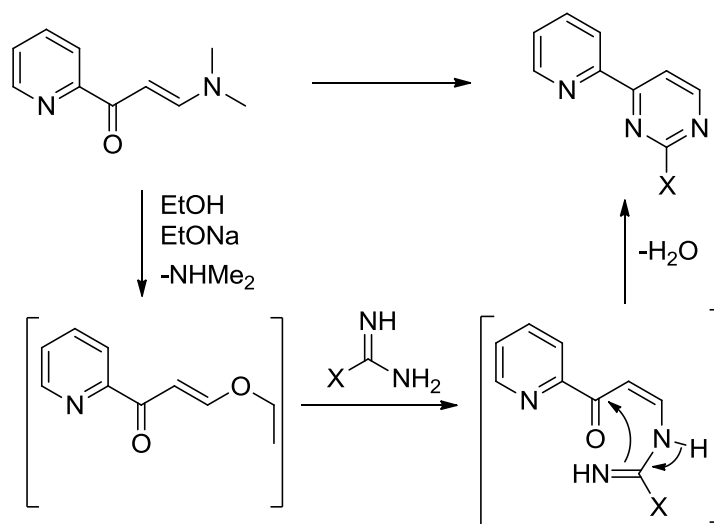


Figure 15. ¹H NMR comparison between **1a** and **2a**.

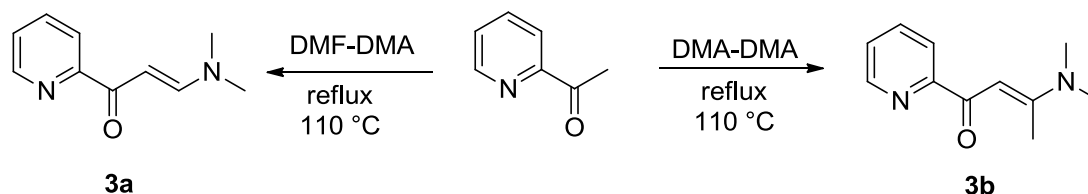
Therefore, the two protons of the amino group are chemically different. The intramolecular hydrogen bond between H10a and the carbonyl oxygen atom lowers the electron density of the proton and thus the resonance of proton shifts to low field (10.3 ppm) whereas the other NH proton appears at 5.4 ppm.

The 2nd type enaminones are suitable precursors to prepare the target pyridylpyrimidines aminophosphine ligands in terms of the reaction mechanism shown in Scheme 8. An important intermediate can be obtained by the displacement of the dimethylamino group with different nucleophiles.^[106] However, a similar reactivity is not found for the 1st type enaminones due to problems in removing of the NH₂ group.



Scheme 8. A proposed mechanism for the pyrimidine synthesis starting from 2nd type enaminones.

The 2nd type enaminones were obtained from 2-acetylpyridine.^[103,107] These enaminones can be derived using by different dimethylacetal compounds. 2-Acetylpyridine was reacted with excess amounts of the dimethyl acetals of dimethylformamide or dimethylacetamide at 110 °C for 24 hours to obtain the target enaminones (Scheme 9).



Scheme 9. Synthesis of the 2nd type enaminones.

The ^1H NMR spectrum of enaminone **3b** reveals two characteristic singlet peaks at 2.69 ppm and 3.11 ppm belonging to the methyl groups attached to the double bond and the two methyl groups of the dimethylamino group, respectively (Figure 16).

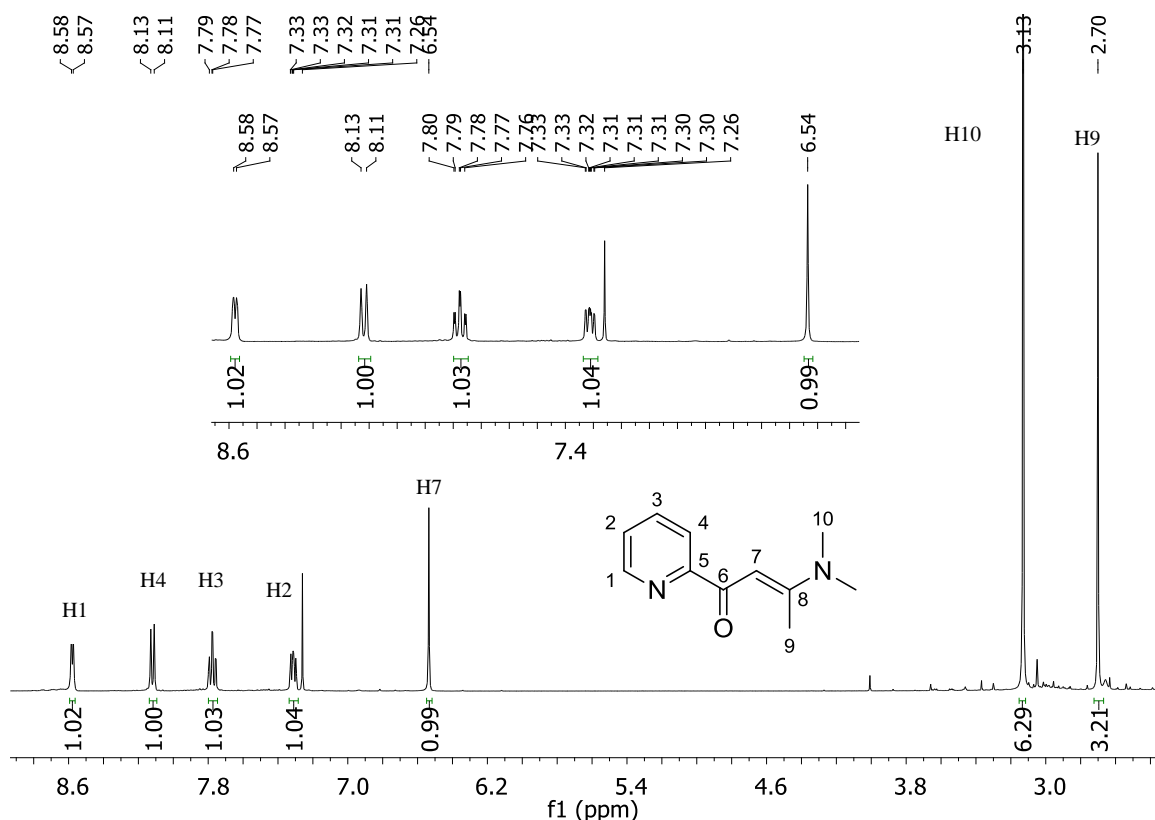


Figure 16. ^1H NMR spectrum of enaminone **3b**.

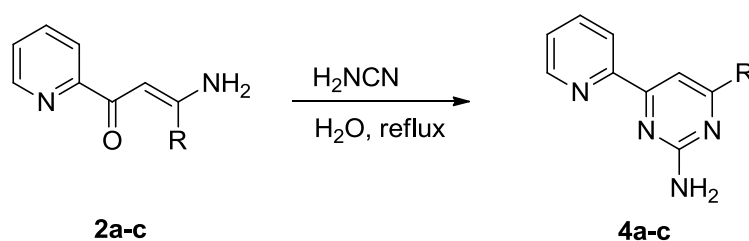
The double bond proton shows a singlet at 6.54 ppm. The pyridine protons give signals in the aromatic region between 7.28 and 8.57 ppm as expected. These 2nd type enaminones were used in “Route 3”. It will be discussed in the following chapters.

3.1.1.1.3 Synthesis of *N,N*-Ligands

The chemistry of polyaza heterocycles (pyrazoles, pyrimidines) is investigated since long.^[108] Some of these pyrazoles and pyrimidines are playing important roles as building blocks to form homo- and heterometallic complexes, which were used as catalysts.^[109] They have also gained applications in the fields of medicinal chemistry and agrochemistry.^[110,111] In the past, the Thiel group has also been interested in such polyaza heterocycles as ligands for homogeneous catalysis.^[87,112,113]

The syntheses of 2-amino-4-(2-pyridyl)pyrimidine and 2,6-bis(2-amino-4-pyrimidyl)pyridine via a ring closure reaction of the corresponding enaminone and guanidinium nitrate were reported by Balovine et al. in 1996.^[103] Vicente et al. described an alternative synthetic pathway for the preparation of pyridylpyrimidine ligands by using β -enaminones and cyanamide.^[114]

In the light of these reports, *N,N*-ligands bearing a pyridylpyrimidine motif were synthesized using an excess amount of aqueous cyanamide and the corresponding 1st type enaminones (Scheme 10). The reaction mixture was heated to reflux in H₂O for 24 hours and the pyridylpyrimidine ligands **4a-c** were isolated after extraction with CHCl₃.



Scheme 10. The synthesis of 6-(pyridin-2-yl)pyrimidin-2-amine.

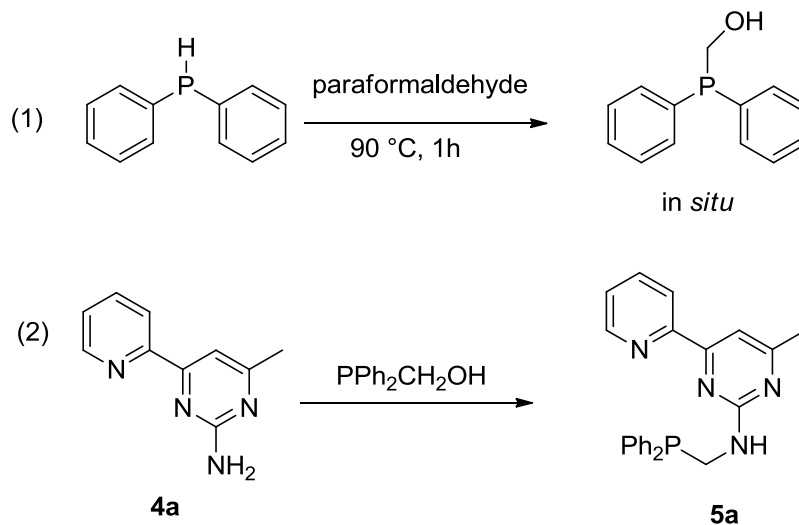
The ¹H NMR spectra prove the formation of the cyclized products. The -NH₂ protons of the pyridylpyrimidines give a broad singlet at 5.20-5.40 ppm in contrast to the starting materials where the two NH₂ protons show different chemical shifts. Another evidence is the resonance of the newly formed aromatic proton of the pyrimidine ring which appears as a singlet for compounds **4a-c** (Table 2).

Table 2. Characteristic ¹H NMR (ppm) shifts of aminopyrimidines.

R	Me(4a)	<i>t</i>Bu(4b)	Ph(4c)
NH₂	5.40	5.23	5.47
Pyrimidine	7.54	7.74	8.14

The next step is the conversion of the prepared aminopyrimidines into aminophosphine substituted pyridylpyrimidines ligands to access mixed ligands combining hard and soft donor atoms and their heterobimetallic complexes.^[115] The synthetic pathway comprises

two steps: first the formation of a hydroxymethylphosphine from diphenylphosphine and paraformaldehyde, second the reaction of this phosphine with the aminopyrimidine to form the target ligands (Scheme 11).^[116]



Scheme 11. A possible synthetic pathway leading to aminophosphinopyrimidines

Various reaction conditions were applied to synthesize the aminophosphinopyrimidine **5a** based on the Mannich-type reaction mechanism discussed above.^[117] Diphenylphosphine was added to a solution of 4-pyridin-2-yl-pyrimidin-2-yl-amine and paraformaldehyde in anhydrous toluene and the reaction mixture was stirred at 65 °C for 24 hours. Although the reaction was carried out under nitrogen atmosphere and using dry and degassed chemicals, there is only a peak typical for phosphine oxide in the ³¹P NMR spectrum at 30 ppm (Figure 17).

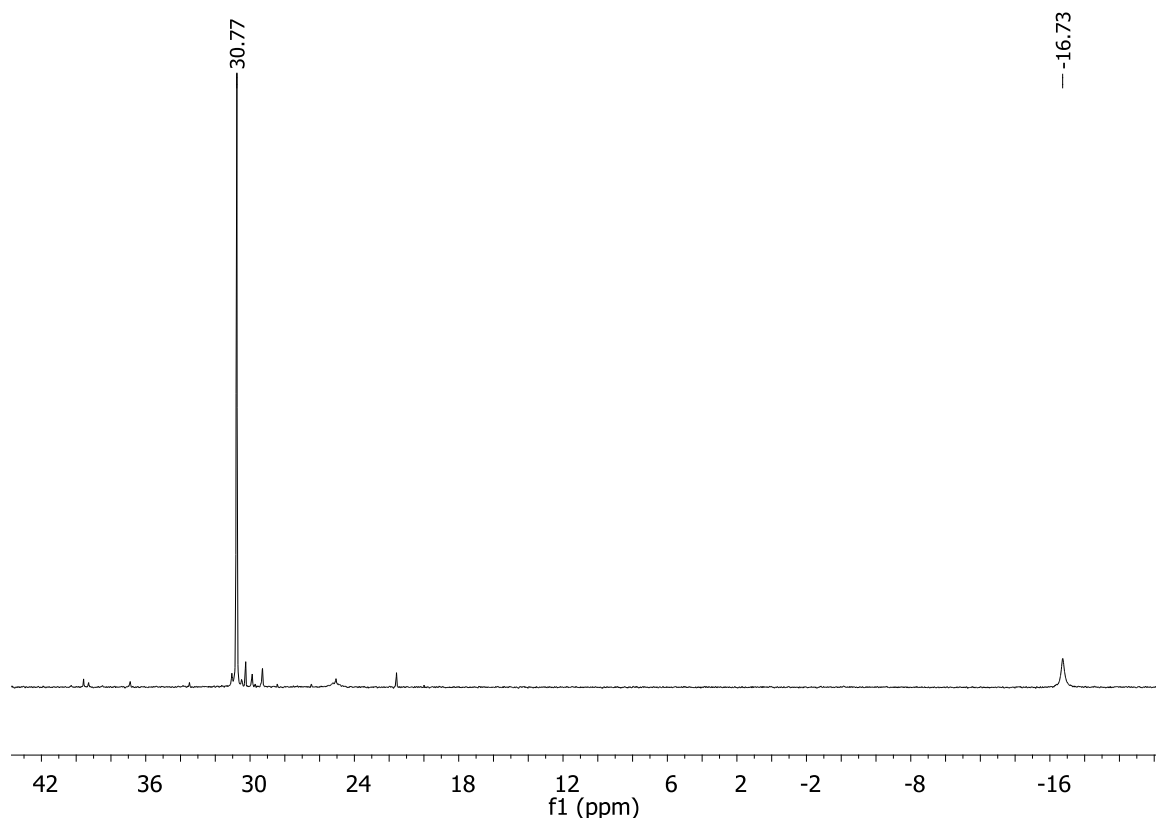


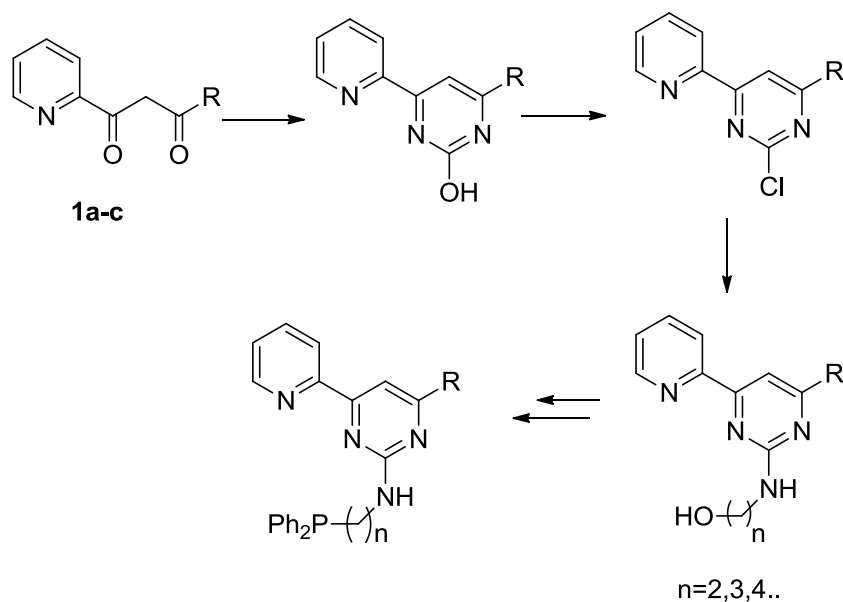
Figure 17. ^{31}P NMR spectrum of the product obtained from the synthesis of **5a**.

The ^1H NMR spectrum of this reaction shows a lot of different signals in the aromatic region which could not be assigned properly. Alternatively, the reaction was performed in a degassed toluene/methanol mixture and the reaction time was increased to 6 days. However, product could not be isolated. The reaction was alternatively carried out in the presence of acid which did not result in any improvement.^[118] All attempts to prepare the aminophosphine **5a** failed and solely the oxidized product was found in addition to the formation of many by-products.

3.1.1.2 Route 2

As mentioned in section 3.1.1, a synthetic route to prepare *N,N,P*-ligands containing soft and hard donor atoms as a precursor for multimetallic complexes was outlined. Since the first route failed in the last step of the synthetic plan, an alternative route was designed. In contrast to the former route, in which the alkyl chain between the hard and soft ligand

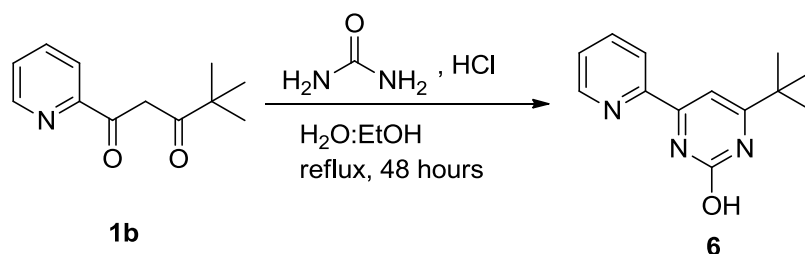
sites is only comprised of one methylene unit, route 2 allows to introduce linkers with longer alkyl chains (Scheme 12).



Scheme 12. Route 2 for the synthesis of the aminophosphine pyrimidine ligands.

3.1.1.2.1 Synthesis of 2-Hydroxy Pyridylpyrimidines

Route 2 starts with the synthesis of 2-hydroxy pyridylpyrimidines. Exemplarily 4,4-dimethyl-1-(pyridin-2-yl)pentane-1,3-dione and an excess of urea were dissolved in a H₂O/EtOH mixture followed by the addition of HCl and heating to reflux for 48 hours. After neutralizing the reaction mixture with Na₂CO₃, the product was filtered off and purified by washing several times with Et₂O (Scheme 13).



Scheme 13. Synthesis of the 2-hydroxy pyridylpyrimidine **6**.

The structure elucidation of compound **6** was done by ¹H and ¹³C NMR spectroscopy. The ¹H NMR spectrum reveals a broad singlet at 8.54 ppm, which is a clear evidence for

the presence of a new pyrimidine ring (Figure 18). The hydroxyl proton gives a broad singlet peak at 12.75 ppm. The chemical shifts of the four protons of the pyridine ring do not show any significant alteration compared to the diketone **1b**.

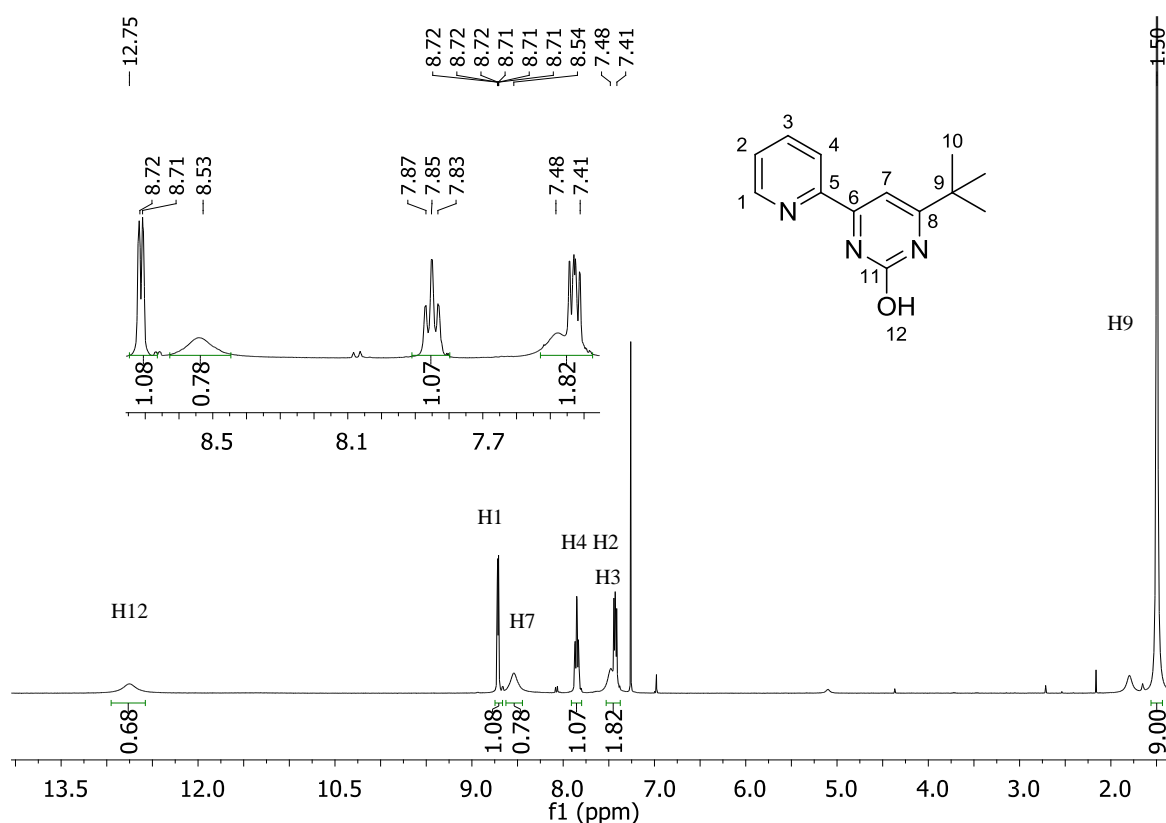


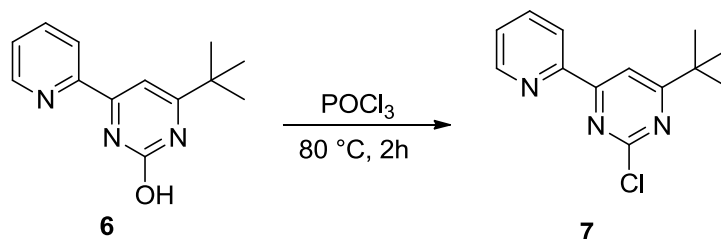
Figure 18. ^1H NMR spectrum of compound **6**.

The ^{13}C NMR spectrum proves the formation of the pyrimidin-2-ol **6** by the disappearance of the peak at 204 ppm which belongs to the carbonyl group of the starting compound. There are nine signals in the aromatic region and two peaks at 36.1 and 28.8 ppm (C9 and C10).

3.1.1.2.2 Synthesis of the 2-Chloro Pyridylpyrimidine

The second step of route 2 is the substitution of the hydroxyl group by chloride using POCl_3 . The direct substitution with an aminophosphine is not possible since the hydroxyl group is not a good leaving group. By the replacement of the hydroxyl unit against a

chloride, an aromatic substitution reaction becomes feasible as long as a strong nucleophile is applied. The chlorination of pyrimidin-2-ol **6** was carried out following a protocol published in the literature which was slightly modified (Scheme 14).^[119] An excess amount of POCl₃ was used as the chlorinating agent. After the consumption of the starting material **6**, the unreacted POCl₃ was removed with a water pump and the residue was neutralized with Na₂CO₃.



Scheme 14. The chlorination of compound **6**.

The ¹H and ¹³C NMR spectra prove the formation of the desired compound. The most significant change is the disappearance of the hydroxyl peak in the ¹H NMR spectrum of compound **7** (Figure 19).

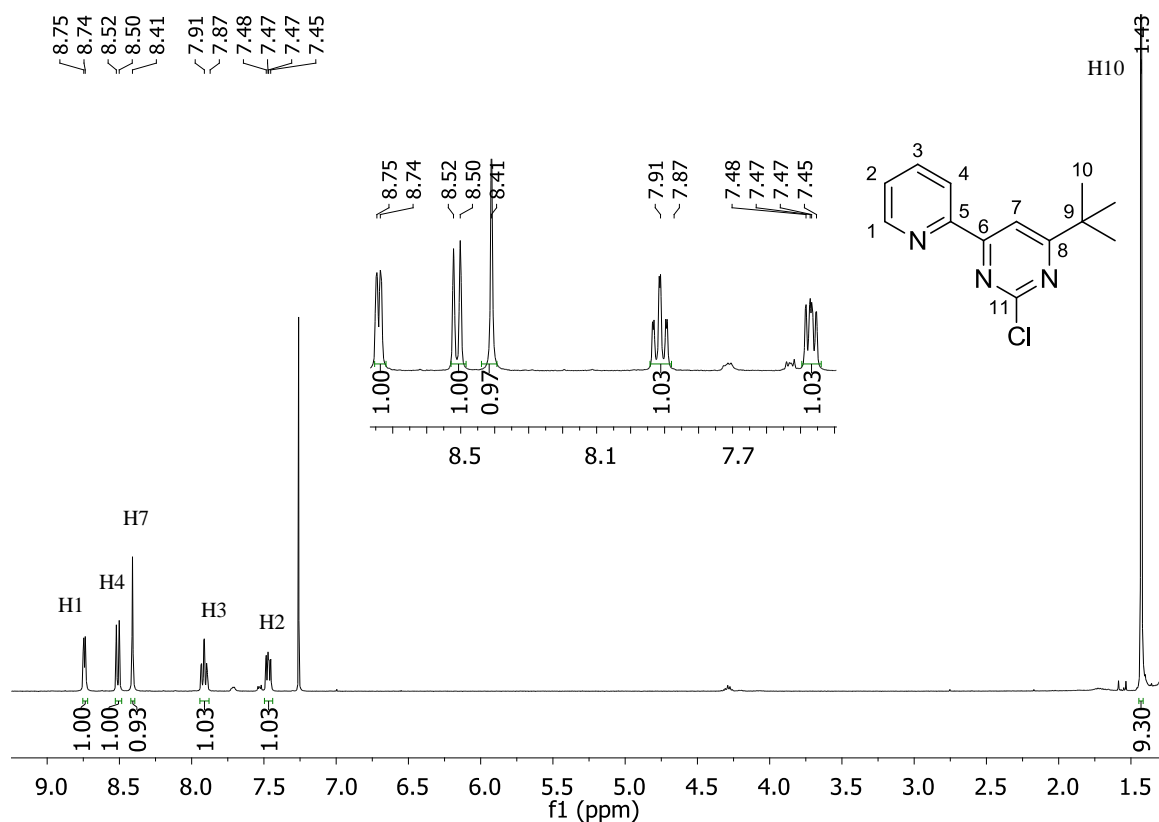


Figure 19. ^1H NMR spectrum of compound **7**.

The proton H7 of the pyrimidine ring gives a singlet at 8.41 ppm (**6**: 8.54 ppm). The protons of the *t*Bu group resonate at 1.43 ppm as a singlet. They shift slightly to higher field compared to the hydroxyl substituted compound **6**.

In ^{13}C NMR spectrum of **7**, the chemical shifts of the carbon atoms resonate slightly shifted lower field compared to **6**. The signal of the carbon atom being functionalized with the chlorine atom appears at 161.0 ppm (Figure 20). Overall there is the expected number of peaks between 183 to 112 ppm belonging to the aromatic carbon atoms of the pyridinyl pyrimidine structure. The *tert*-butyl group gives two peaks at 38.4 and 29.5 ppm being assigned to the quaternary and methyl carbon atoms, respectively.

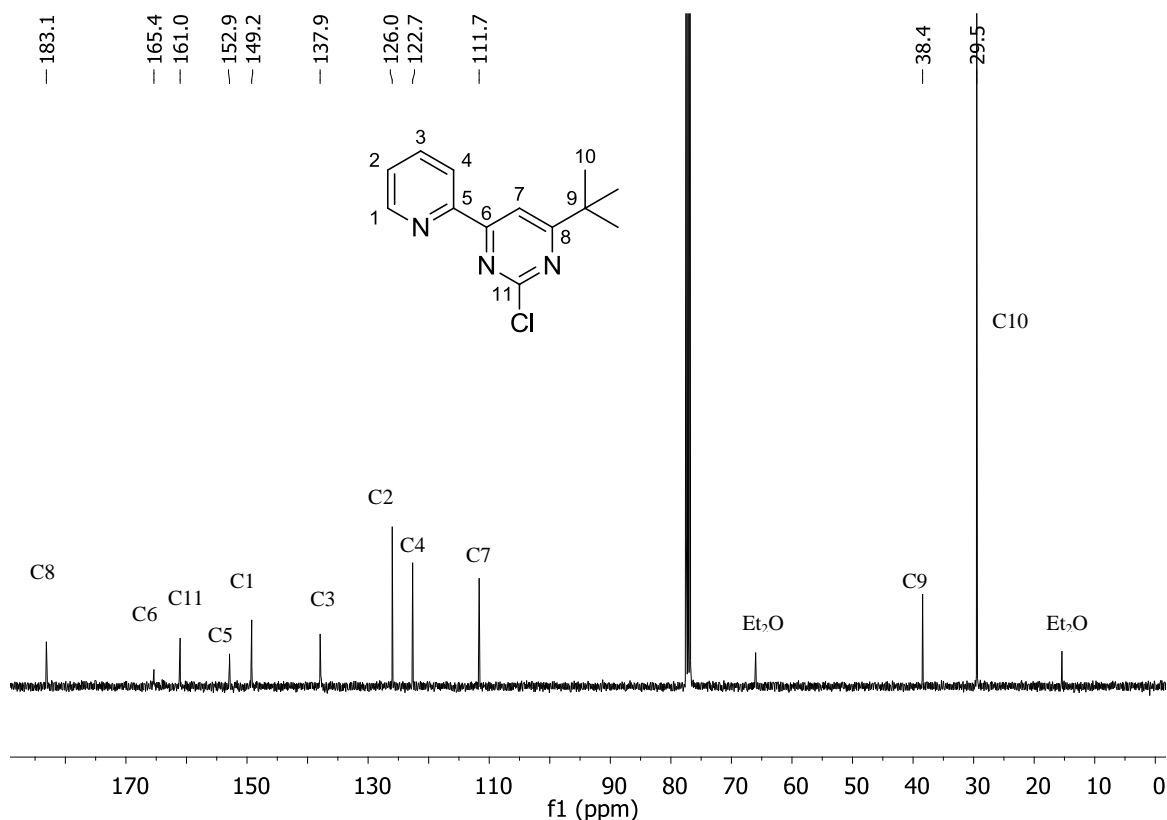
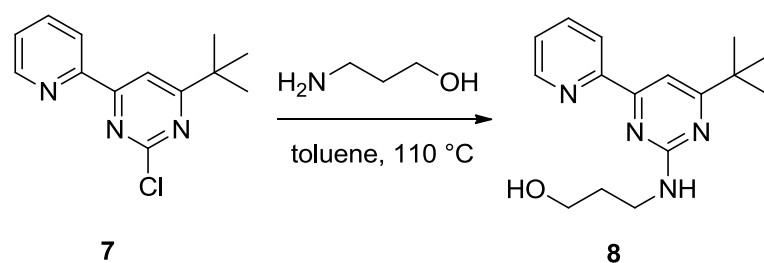


Figure 20. ^{13}C NMR spectrum of compound **7**.

Since the idea of the synthetic route **2** is to introduce alkyl chains with different numbers of methylene units, 3-amino-1-propanol was used as a first nucleophile. Compound **7** and 3-amino-1-propanol were heated to reflux in ethanol for 24 hours as described in the literature^[120]. The reaction follows an aromatic substitution mechanism, whereby the chloride substituent is substituted by the amine. As expected the nucleophilic replacement of the chloride by hydroxyl group of 3-amino-1-propanol does not occur since the amine site is more nucleophilic than the alcohol site. The reaction was monitored by ^1H NMR and no conversion was observed under these reaction conditions. Subsequently, the reaction conditions were modified by using toluene as the solvent and by doubling the amount of 3-amino-1-propanol, which made the desired product **8** accessible in good yield (Scheme 15).



Scheme 15. Synthesis of compound **8**.

The ^1H NMR spectrum of compound **8** reveals three new peaks in the aliphatic region belonging to the propylene chain (Figure 21). A multiplet between 1.77 and 1.83 ppm is assigned for the methylene group in the middle of this chain (H14).

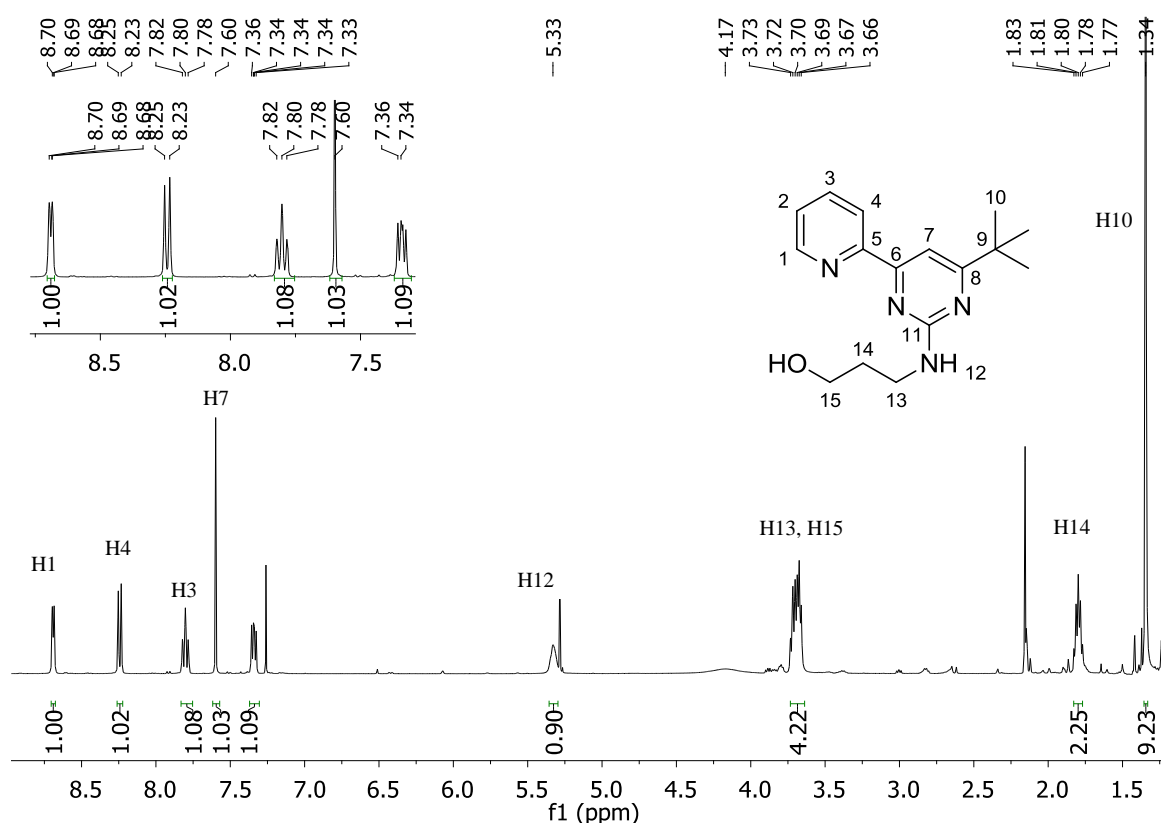


Figure 21. ^1H NMR spectrum of compound **8**.

The other two methylene groups appear as multiplet between 3.66 and 3.73 ppm. Further proof for the formation of the desired compound is given by a broad singlet at 5.33 ppm being assigned to the $-\text{NH}$ proton. The pyrimidine proton H7 gives a singlet at 7.60 ppm and there are the expected four additional signals in the aromatic region being assigned to the protons of the pyridine ring.

The ^{13}C NMR spectrum of compound **8** shows three peaks for the propylene chain in the aliphatic region (Figure 22), and two peaks belonging to the *tert*-butyl group. As expected, there are nine peaks in the aromatic region, which further supports the proposed structure.

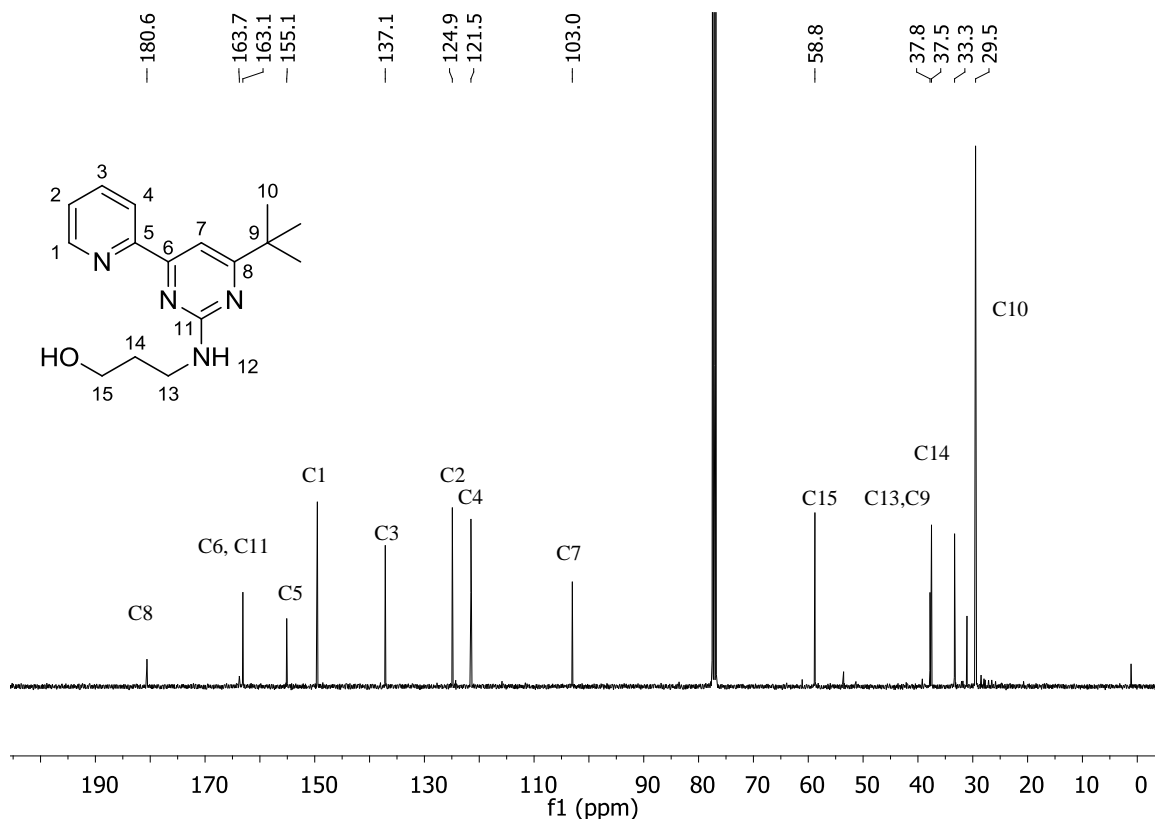
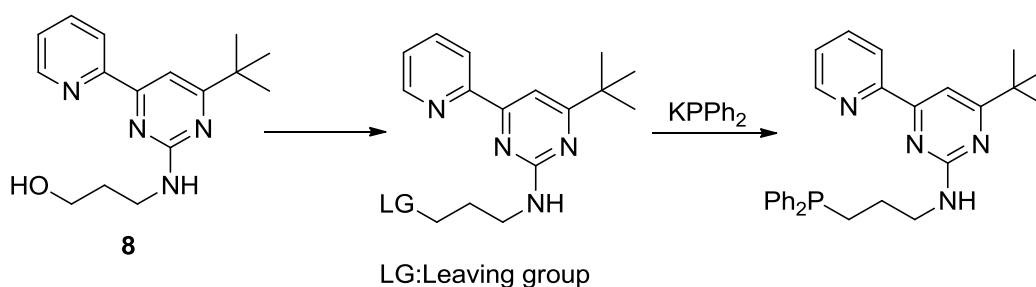


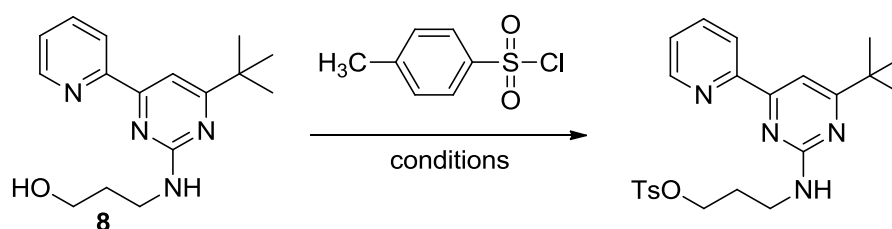
Figure 22. ^{13}C NMR spectrum of compound **8**.

After introducing the aminoalcohol chain to the pyridylpyrimidine ring, a functional group transformation from a hydroxyl unit to a better leaving group was attempted to activate this site for a nucleophilic substitution reaction by a diphenylphosphino group in the next step by using a nucleophilic phosphine source such as potassium diphenylphosphide (Scheme 16).



Scheme 16. Introduction of a diphenylphosphino group.

Alkyl sulfates and sulfonates are excellent leaving groups because of their resonance stabilized structures after leaving. Sulfonates can be used as a precursor for nucleophilic substitution reactions.^[121] These facts led us to choose the tosylate unit as a leaving group. Tosylation of the alcohol **8** could be achieved by using *p*-toluenesulfonyl chloride and a base (Scheme 17), but the reaction was not successful for alcohol **8** after even screening different bases (Table 3).

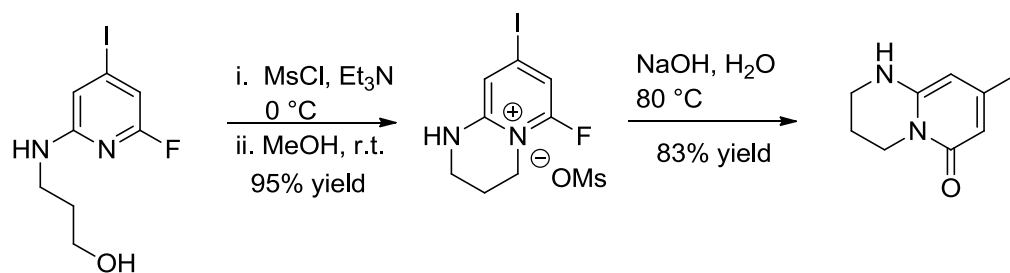


Scheme 17. Unsuccessful tosylation of alcohol **8**.

Table 3. Conditions for the tosylation reactions.

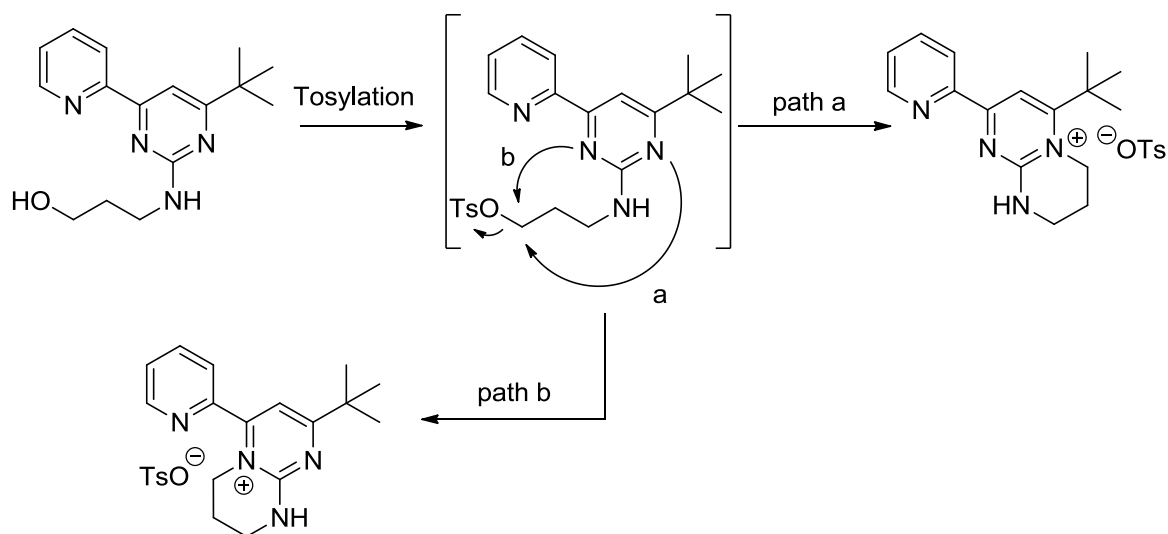
Base	Solvent	Temperature
KOH	THF	0 °C → r.t.
NEt ₃	CH ₃ CN	0 °C → r.t.
NEt ₃	DCM	0 °C → r.t.
K ₂ CO ₃	DCM	0 °C → r.t.

In literature, Gallagher and co-workers presented synthesis of fused pyridinium salts which were subsequently hydrolyzed to bicyclic pyridinones (Scheme 18).^[122]



Scheme 18. Gallagher's approach to bicyclic pyridinones.

Based on Gallagher's report, the failed tosylation reaction can be explained by the similarities of the chemical structure. When the hydroxyl group is tosylated, two possible intramolecular reactions might occur (Scheme 19). Therefore, route 2 was not applicable in our pyridylpyrimidine systems.



Scheme 19. Possible undesired reactions of the tosylated intermediate.

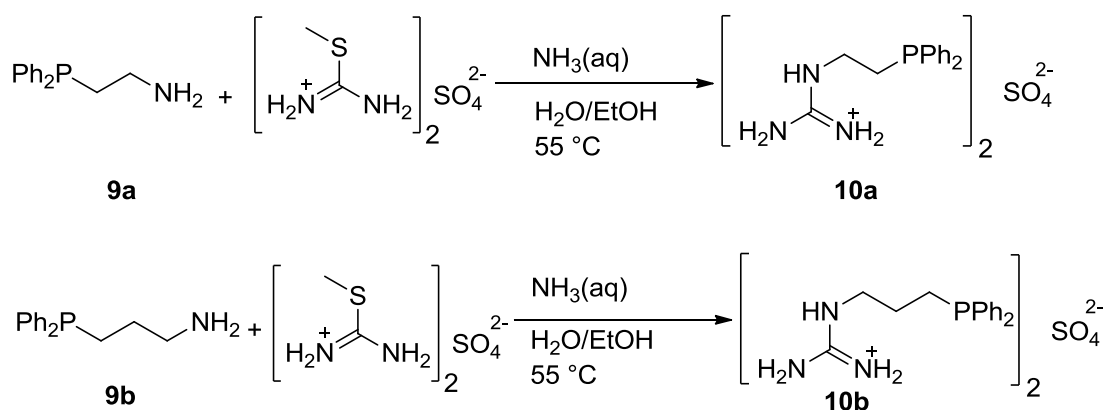
3.1.1.3 Route 3

The results of the experiments on the different pathways described above showed that the 2nd type enaminones **3a** and **3b** are probably the best precursors to synthesize bidentate *N,N,P*-ligand. This approach builds up the pyrimidine unit by a condensation of functional groups involving the required substituents.^[123,124] The proposed mechanism of the condensation was explained in Scheme 8.

The ring closure of compounds **3a** and **3b** with corresponding guanidinium salts was carried out in the presence of NaOMe in EtOH under reflux conditions. The key point of the derivatization of *N,N,P*-ligands was to synthesize the requested guanidinium salts.

3.1.1.3.1 Synthesis of Guanidinium Salts

Guanidinium salts can be synthesized by a series of different methods being published in the literature.^[125-127] The synthesis of our target guanidinium salts was carried out according to a known procedure with slight modifications (Scheme 20).^[125]



Scheme 20. Guanidinium salts **10a** and **10b**.

Diphenylphosphinyl amines,^[128,129] water/EtOH and 25% aqueous ammonia were mixed under a nitrogen atmosphere and the thiourea salt was added upon stirring. The mixture was heated to 55 °C for 24 hours. The smell of the liberated methanethiol indicated that the reaction took place. Then, the mixture was cooled to room temperature and water was decanted from the mixture. The oily residue was stirred with toluene overnight, and the resulting precipitate was collected by filtration to obtain the corresponding guanidinium salts in good yields.

Figure 23 shows exemplarily the ¹H NMR spectrum of guanidinium salt **10a** measured in CD₃OD. The ethylene protons give signals around 2.3 and 3.2 ppm as multiplets due to a coupling with the phosphorous atom. The multiplet between 7.2 and 7.4 ppm is assigned to the protons of the phenyl group.

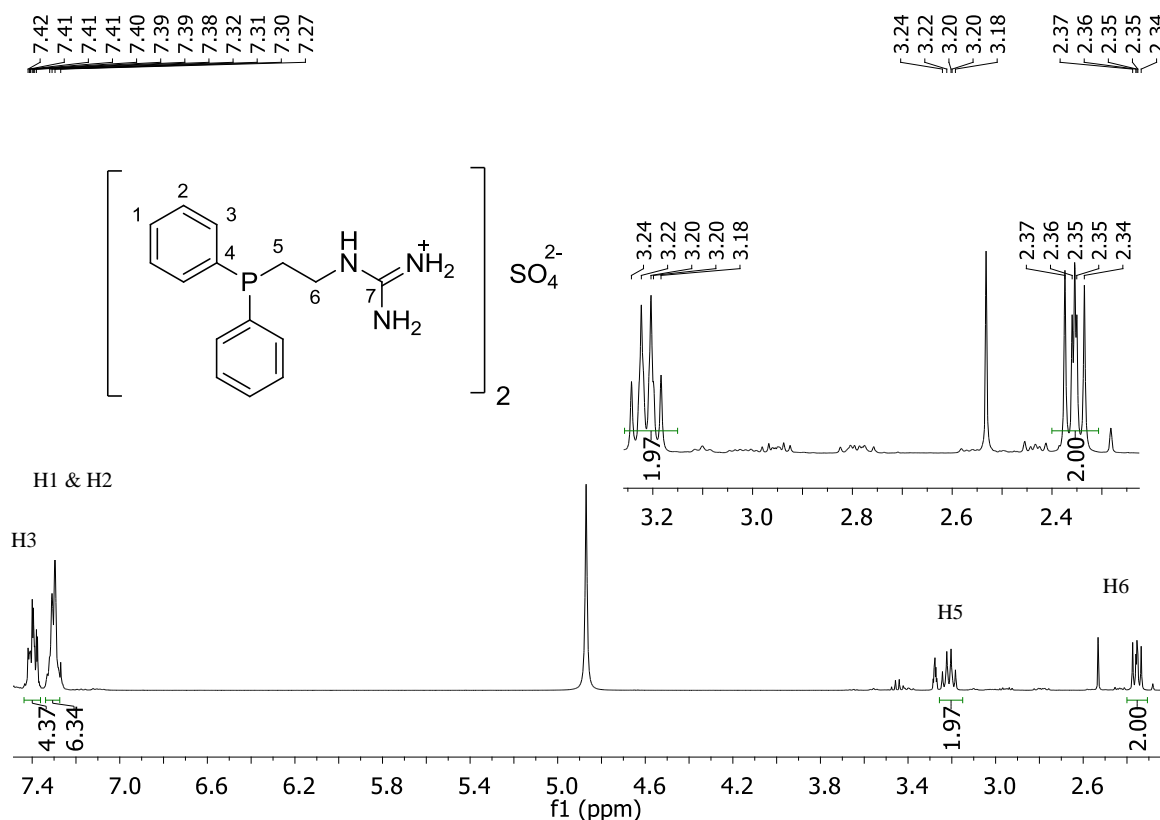


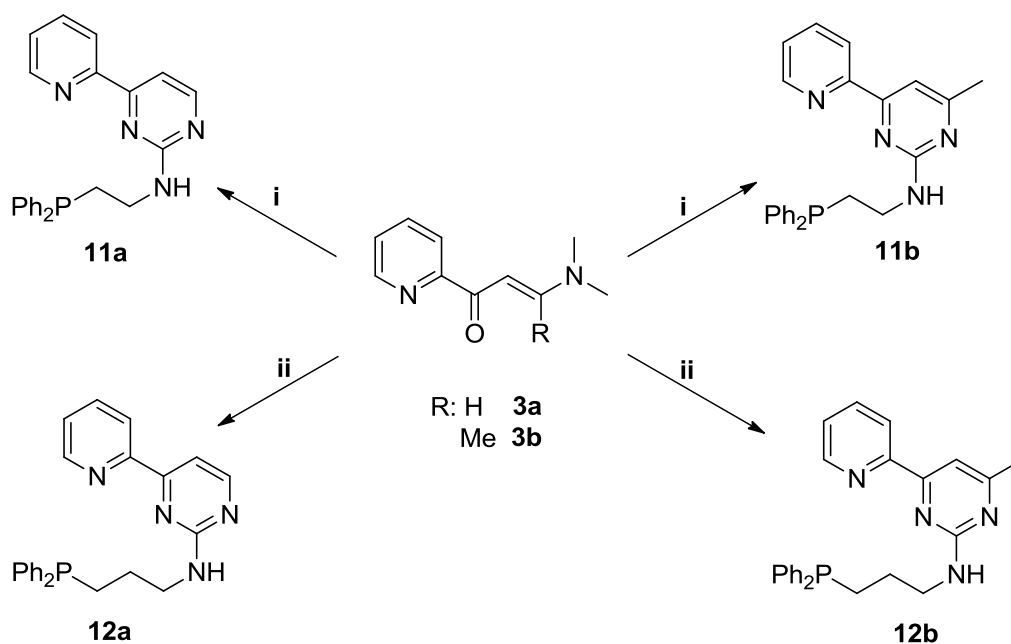
Figure 23. ^1H NMR spectrum of guanidinium salt **10a**.

^{13}C and ^{31}P NMR spectra also prove the formation of the desired guanidinium salt. There is a signal at 158.4 ppm in ^{13}C NMR spectrum which belongs to the guanidinium carbon atom (C7). The ethylene carbon atoms resonate at about 40 and 29 ppm as doublets with coupling constants of $^2J_{\text{C,P}} = 25.6$ and $^1J_{\text{C,P}} = 13.3$ Hz, respectively. The phenyl carbon atoms except those in the para position with respect to the phosphorous atom are also giving doublets at around 140 to 130 ppm due to P,C coupling. The ^{31}P NMR spectrum shows one signal at -21.99 ppm proving that the phosphorus atom was not oxidized.

3.1.1.3.2 Synthesis of *N,N,P*-Ligands

The synthesis of *N,N,P*-ligand starts from 2-acetylpyridine which was transformed to corresponding enaminone as mentioned in Section 3.1.1.1. Then the corresponding aminophosphine guanidinium salt and NaOEt were first refluxed for 30 minutes to activate the guanidinium salt with the base. This step is important because activated guanidinium salts initiate the reaction. Then, the corresponding enaminone was added to this solution and the mixture was heated to reflux for 24 hours. After cooling to room temperature, the solvent was removed and the oily residue was extracted with

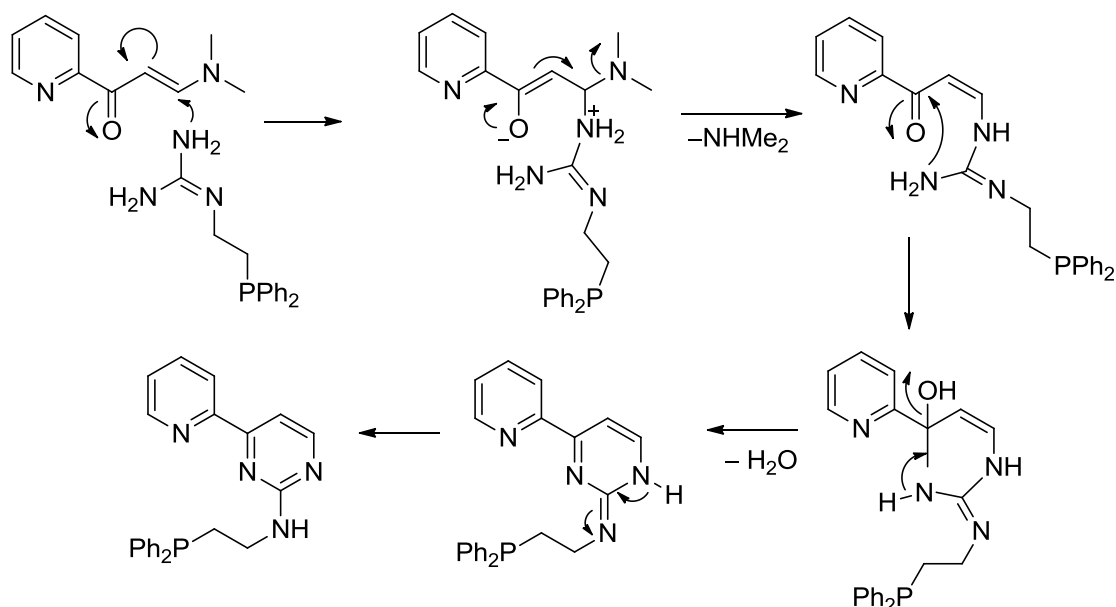
dichloromethane. The *N,N,P*-ligands were purified further by washing the crude products with methanol several times (Scheme 21).



(i) compound **10a**, NaOMe in anhydrous EtOH (ii) compound **10b**, NaOMe in anhydrous EtOH

Scheme 21. Synthesis of *N,N,P*-ligands.

The mechanism of the pyrimidine formation starts with the neutralization of the guanidinium salt with NaOMe or NaOEt. The free activated guanidines then attach the enaminones via a 1,4-addition. While the resulting enolates transform into their keto form, dimethylamine is eliminated. The ligands are formed after dehydration and rearomatization steps (Scheme 22).



Scheme 22. The reaction mechanism of cyclization of enaminone **3a**.

The structure elucidation of compound **11a** is accomplished by ^1H , ^{13}C and ^{31}P NMR spectroscopy. The ^1H NMR spectrum shows two peaks in the aliphatic region which belong to the ethylene chain (Figure 24). The amine proton shows a triplet at 5.41 ppm. Ten protons assigned to the phenyl rings give two sets of multiplets at around 7.7 and 7.4 ppm. The pyrimidine proton, H8, shows a doublet at 8.41 ppm with a coupling constant of 5.0 Hz and the other one (H7) resonates at 7.57 ppm. There are four additional peaks in the aromatic region which belonging to the pyridine ring.

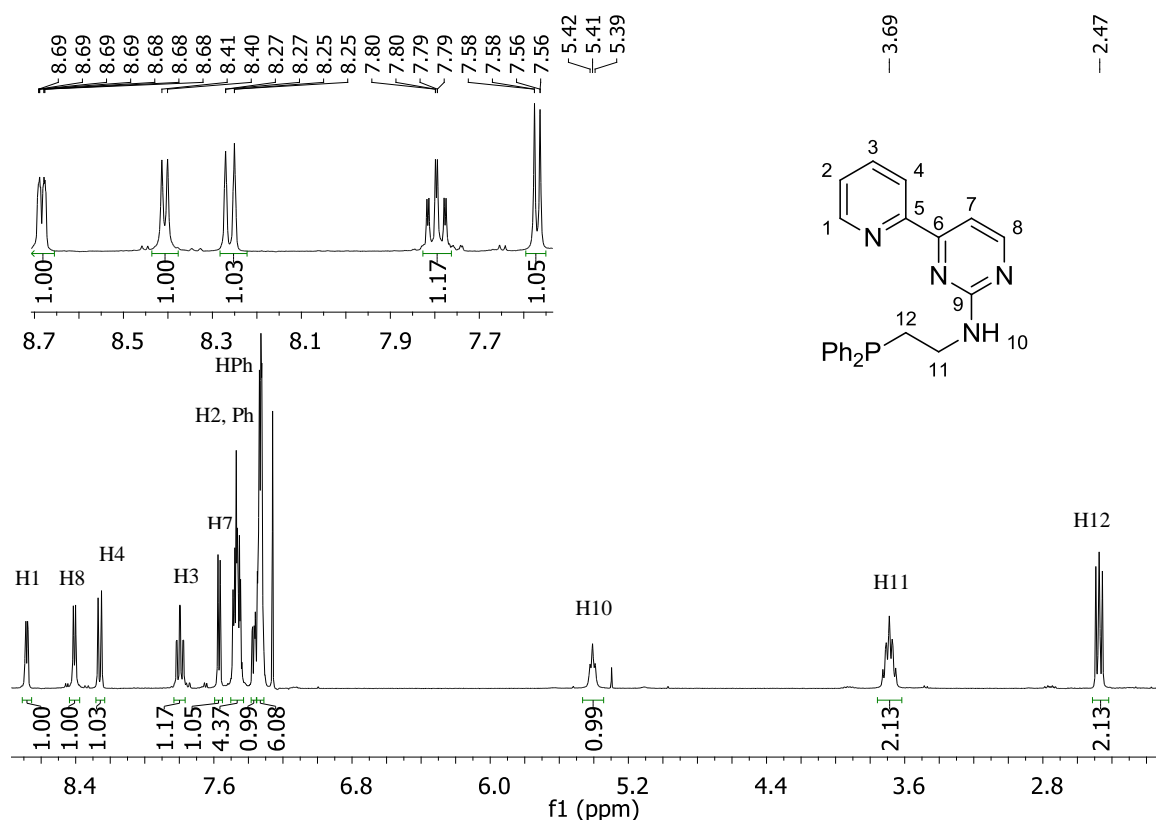


Figure 24. ^1H NMR spectrum of compound **11a**.

The ^{13}C NMR spectrum also proves the formation of compound **11a** (Figure 25). The spectrum of the product shows the characteristic peaks of the pyrimidine ring which reveal after the cyclization: C8 gives a signal at 163.6 ppm, and the peak at 162.3 ppm belongs to the carbon atom attached to the amino group. Another characteristic carbon peak of the pyrimidine group is found around 159.5 ppm and is assigned to the carbon atom being attached to the pyridine ring. C7 shows a peak at 107.1 ppm. The phenyl carbon atoms of the diphenylphosphino group resonate as doublets similar to those of the guanidinium salt **10a**. There are five additional peaks in the aromatic region that belong to the pyridine ring. The ethylene carbon atoms give two different sets of doublets at approximately 39 and 29 ppm. Their chemical shifts are close to the data recorded for the salt **10a**. The assignment of the carbon atoms were done by using HMBC and HMQC techniques. The ^{31}P NMR spectrum shows one peak at -21.26 ppm as expected. This also shows that the phosphorus atom was not oxidized during the synthesis or in the work-up process.

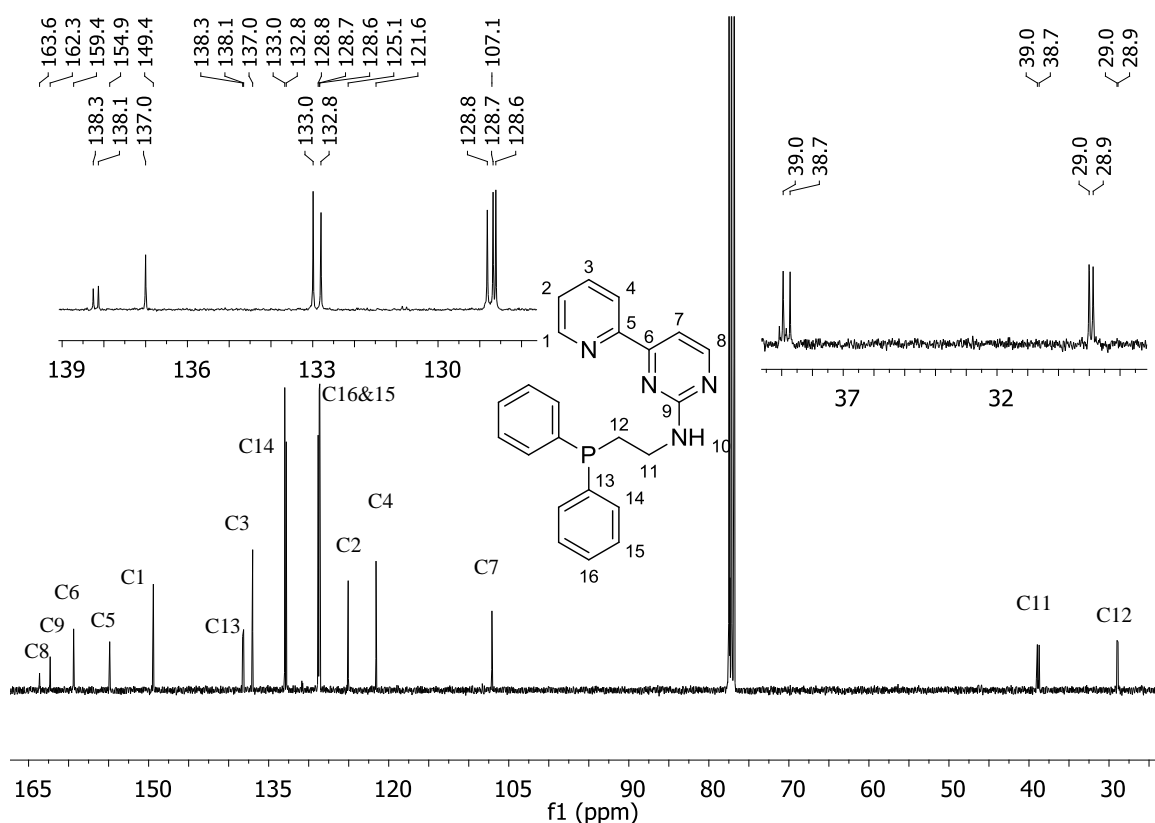


Figure 25. ^{13}C NMR spectrum of compound **11a**.

Compound **11b** was synthesized following the same procedure except using the methyl substituted enaminone as the starting material. The functionalization of the pyrimidine ring causes almost no significant change in the ^1H NMR spectrum compared to the data of compound **11a**. The only difference is the replacement of the proton H8 in compound **11a** by a methyl substituent. This methyl group resonates as a singlet at 2.41 ppm. The comparison of the chemical shifts for the compound **11a** and **11b** is shown in Table 4. The ^{31}P NMR resonance is exactly the same as for compound **11a**, there is one peak at -21.26 ppm. It seems that slightly changing the substituent of the pyrimidine ring does not have any influence on the phosphorous center.

Table 4. ^1H NMR comparison of compound **11a,b**.

Ligand	H1	H2	H3	H4	H7	H8	NH	(N)CH ₂	(P)CH ₂
11a	8.68	7.38	7.79	8.26	7.57	8.41	5.80	3.68	2.47
11b	8.67	7.37	7.79	8.25	7.50	–	5.32	3.69	2.48

After the functionalization of the pyrimidine ring with a methyl group, it was planned to insert a longer chain between the nitrogen and the phosphorous sites to change steric properties of metal complexes. According to the synthetic route for the synthesis of such ligands, this is possible simply by using a guanidinium salt with a longer alkyl chain. The desired ligands **12a** and **12b** were synthesized using the guanidinium salt **10b** with the same procedure as described for the synthesis of **11a,b** (Scheme 21).

The ^1H NMR spectrum of compound **12a** reveals three peaks in the aliphatic region which are belonging to the methylene protons of the propylene unit (Figure 26). The methylene protons attached to the amine give a quartet at 3.60 ppm with a coupling constant of 6.6 Hz, the peak at 1.81 ppm is assigned for the methylene protons next to the phosphorus atom and $-\text{CH}_2$ protons in the middle of chain show a multiplet at 2.16 ppm. The $-\text{NH}$ proton gives a triplet with a coupling constant of 4.8 Hz at 5.22 ppm. The characteristic pyrimidine protons H7 and H8 give a doublet peaks at 7.56 and 8.41 ppm, respectively.

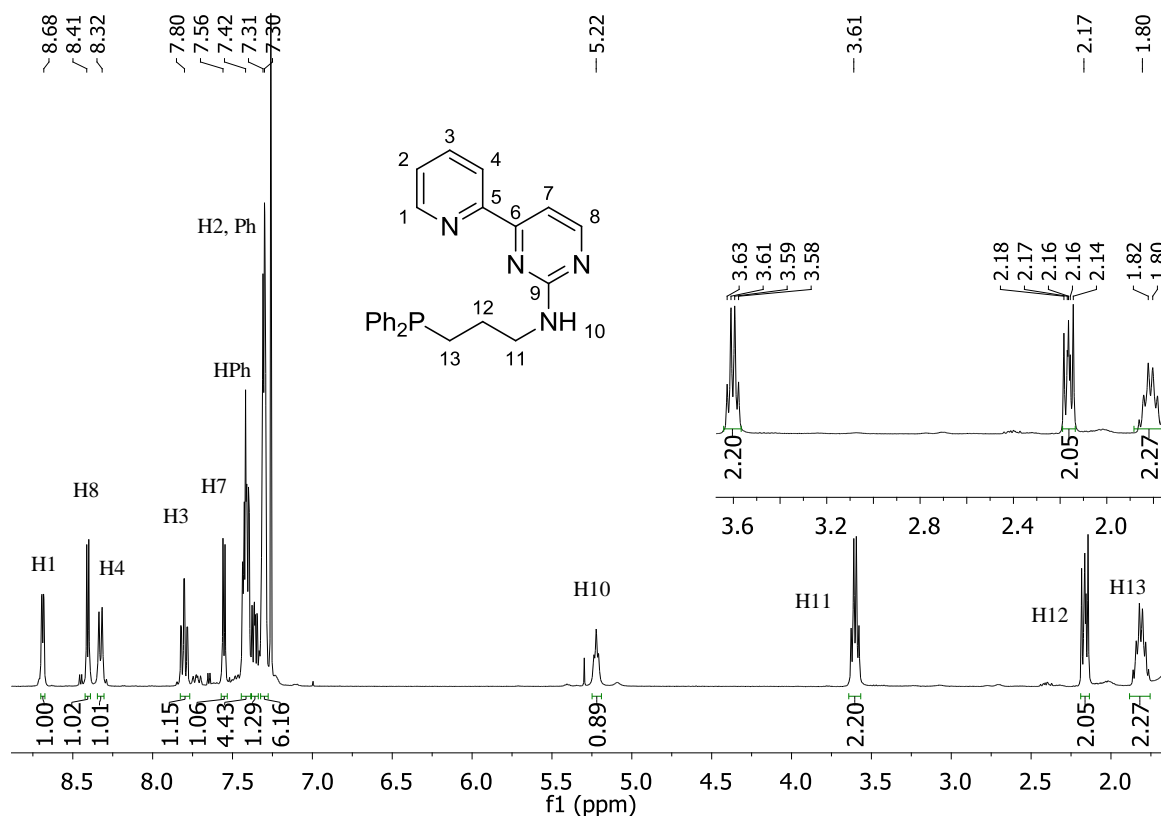


Figure 26. ^1H NMR spectrum of compound **12a**.

The phenyl protons of the diphenylphosphine part resonate as two different sets of multiplets around 7.2 and 7.4 ppm.

The ^{13}C NMR spectrum of compound **12a** shows the expected characteristic carbon peaks. A peak at 163.7 ppm belongs to the newly formed pyrimidine carbon atom C8 and the carbon atom next to the amino group gives a signal at 162.4 ppm. There are also two additional signals which are assigned to the pyrimidine carbons C6 and C7 at 159.3 and 107.1 ppm, respectively. While the peak at 42.7 ppm belongs to the C11, the neighboring carbon atom (C13) of the phosphorus atom reveals a peak at 25.6 ppm. The methylene carbon atom in the middle of the propyl chain shows the signal at 26.2 ppm. All the assignments of the carbon atoms are presented in Figure 27. Furthermore, the ^{31}P NMR spectrum of compound **12a** shows one peak at -16.41 ppm as expected for phosphines.

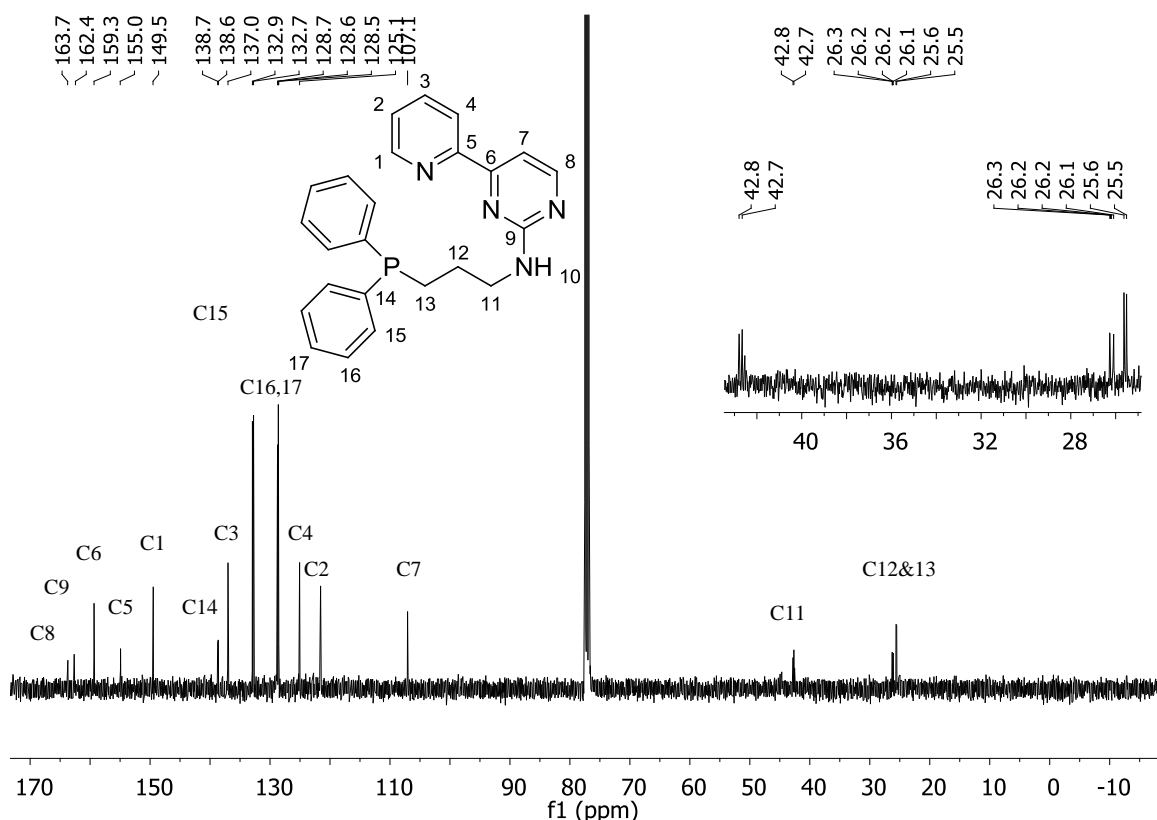


Figure 27. ^{13}C NMR spectrum of compound **12a**.

Compound **12b** was synthesized using the same method described for the synthesis of compound **12a**. The methyl substituted enaminone **3b** was used as the starting material. There is no significant change in the ^1H NMR spectrum compared to the compound **12a**

(Table 5). While the additional methyl protons appear, the H8 proton signal disappears. The ^{31}P NMR shows a peak at -16.37 ppm similar to the resonance of compound **12a**.

Table 5. ^1H NMR comparison of compound **12a** and **12b**.

Ligand	H1	H2	H3	H4	H7	H8	(N)CH2	(P)CH2	CH2
12a	8.69	7.36	7.80	8.33	7.56	8.41	3.60	2.18	1.80
12b	8.68	7.35	7.79	8.33	7.46	-----	3.60	2.16	1.81

3.1.2 Complex Synthesis

Ligands containing hetero donor atoms such as phosphorous and nitrogen have different coordination modes than *N,N*- or *P,P*-ligands. Phosphorous as a soft donor stabilizes metal centers in low oxidation states, while the hard σ -donor character of nitrogen stabilizes electron poor, hard metal centers.^[24] These properties can be advantageous for catalytic reactions by stabilizing intermediates in terms of oxidation state or geometry. On the other hand, multidentate ligands having both hard and soft donor coordination sites are perfect precursors for the preparation of heterobimetallic complexes. These complexes are quite interesting because of their different individual metal centers and thus can show unique functions in catalytic reactions and organometallic chemistry. Heterobimetallic complexes can also show activity for reactions which require cooperative catalysis.^[94,130]

The ligand system aminophosphine pyridylpyrimidine is a suitable candidate for the synthesis of heterobimetallic complexes. However, it requires a smart design to coordinate selectively either the *N,N*-donor site or the phosphorous moiety. Because of this, two different metals which show quite different Lewis acidities were chosen.

3.1.2.1 Synthesis of Gold Complexes

Gold complexes can be mono-, bi- and polynuclear and the coordination number of gold can vary between two and six depending on its oxidation state and the ligand

environment.^[131] The most common oxidation states of a gold cation are +1 and +3 with coordination numbers of two and four, respectively.^[132] Mononuclear gold (I) complexes exist either in linear or bent molecular geometries.^[131]

Gold-phosphine complexes show interesting chemical, biological and physical properties.^[131,133] For example, gold(I)-phosphine derivatives are among the most active gold species used for tumor therapy.^[70] The photoluminescence properties of the cation $[\text{Au}_2-(\mu\text{-dppm})_2]^{2+}$ (dppm = bis(diphenylphosphino)methane) has received much attention. It shows a long-living emission in the visible spectrum.^[134] In the present work gold(I) complexes bearing pyridylpyrimidines-aminophosphine ligands should be prepared (Figure 28).

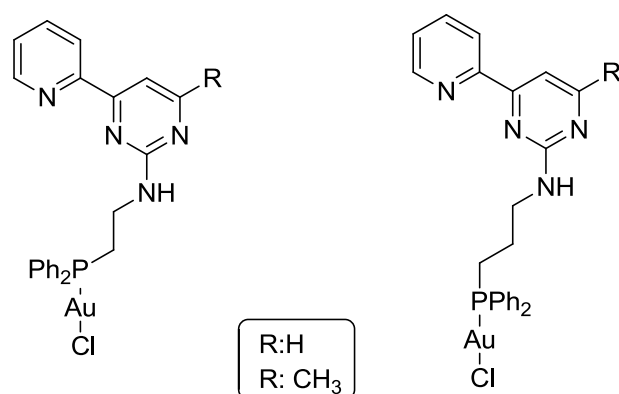
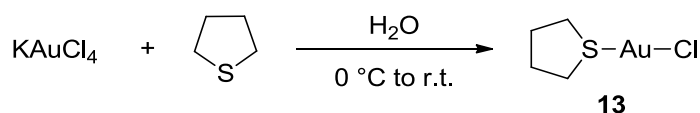


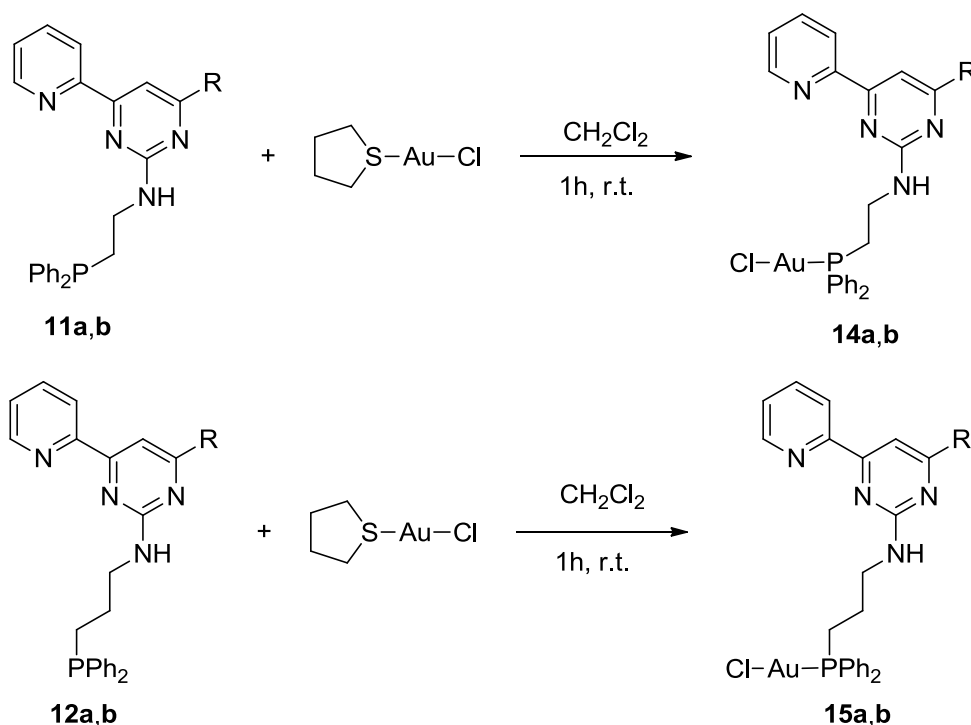
Figure 28. The target gold(I) complexes.

These complexes were prepared using Au(tht)Cl as precursor. The tetrahydrothiophene (tht) ligand is labile and can be easily replaced by other ligands. Since Au(tht)Cl is not commercially available, it was prepared from the reaction of KAuCl_4 and tetrahydrothiophene as described in the literature (Scheme 23).^[135]



Scheme 23. Preparation of Au(tht)Cl.

The target complexes were synthesized from ligands **11a,b** and **12a,b** by simply stirring a solution with Au(tht)Cl for one hour (Scheme 24). After concentrating the solvent and addition of diethyl ether, the products were precipitated and collected by filtration.^[136]



Scheme 24. Synthesis of gold(I) aminophosphine complexes **14a,b** and **15a,b**.

The structural elucidation of compounds **14a,b** was done by means of ^1H , ^{13}C and ^{31}P NMR spectroscopy. Comparison of the ^1H NMR spectra of ligand **11a** and of the gold(I) complex **14a** are shown, that the most significant changes are observed for the chemical shifts of the ethylene protons. After the coordination of the ligand to the gold center, the electron density of the phosphorous site decreases by transferring electron density to the gold cation via a σ bond, which also influences the electron density in the ethylene chains which resonates at lower field. As shown in Figure 29, H12 is the most influenced proton: It resonates about 0.5 ppm at lower field compared to the free ligand. The chemical shift of the second ethylene units also changes around by 0.2 ppm. Similarly, the phenyl protons of the gold (I) complex give a signal around 0.2 ppm at lower field compared to the free ligand. Since the resonances of the pyridylpyrimidine fragments do not change, it can be considered that gold(I) exclusively interacts with the

phosphorous atom as expected. Figure 29 shows all the assignments and a comparison of the spectra of the free ligand **11a** and the gold complex **14a** in detail.

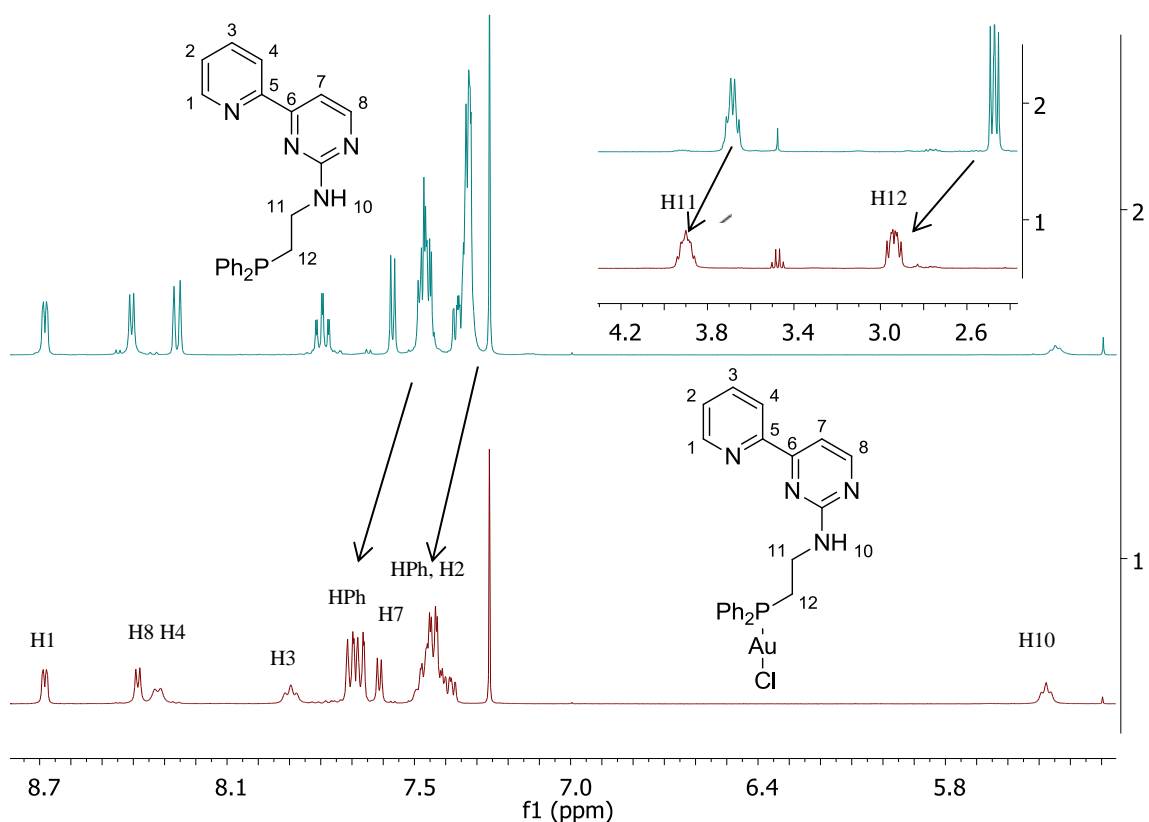


Figure 29. ^1H NMR spectral comparison ligand **11a** (blue) and Au(I) complex **14a** (red).

The ^{13}C NMR spectrum is not influenced significantly by the complexation. The ethylene carbon atoms C11 and C12 give doublets with P,C -coupling constants of 7.8 and 35.5 Hz around 39 and 29 ppm, respectively. The chemical shifts of the phenyl carbon atoms are almost identical to those of the free ligand, there are four carbon signals belonging to the phenyl groups which are at 133.3 ppm as doublet with $J_{PC} = 13.1$ Hz assigned for C14, at 132.1 ppm with a P,C -coupling constant of 2.4 Hz for C16. C15 gives a doublet with $J_{PC} = 11.7$ Hz at 129.4 ppm and the peak at 129.2 ppm with $J_{PC} = 61.0$ Hz belongs to C13. There are also nine additional signals which are assigned for the carbon atoms of the pyridinylpyrimidine ring.

The most significant change is observed in the ^{31}P spectrum. After the coordination, the electron density of the phosphorous atom is decreased and the changes in the electron density directly influences the chemical shift of the phosphorous atom.^[137] As shown in

Figure 30, the free ligand gives signal -22 ppm, while the phosphorous signal shifts to $+24$ ppm after coordination to gold.

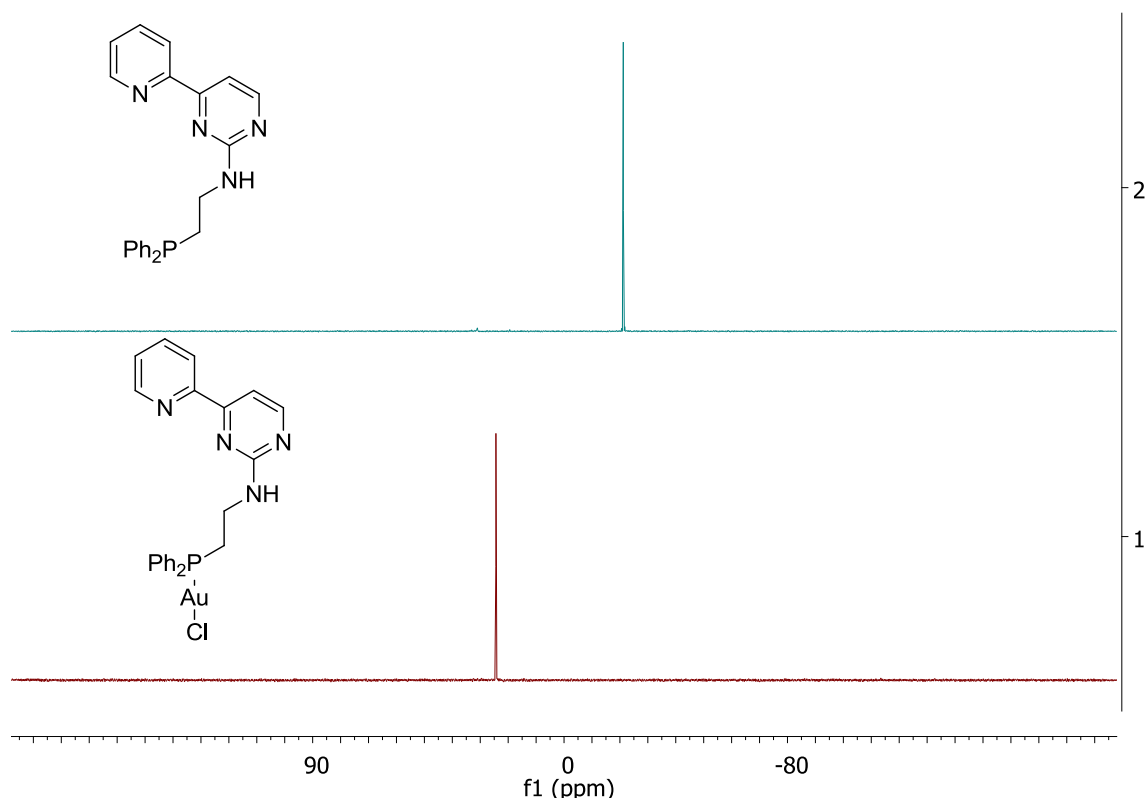


Figure 30. ^{31}P NMR spectral comparison of ligand **11a** (blue) and complex **14a** (red).

Recrystallization of compound **14a** by slow diffusion of diethyl ether into a dichloromethane solution gave suitable crystals for X-ray diffraction analysis (Figure 31). Gold complex **14a** crystallizes in the triclinic space group $P\bar{1}$. The gold atom shows a linear geometry (e.g. $\text{P}(1)\text{--Au}(1)\text{--Cl}(1)$ $178.47(4)^\circ$). The distance between $\text{P}(1)\text{--Au}(1)$ is $2.2309(8)$ Å and $\text{Au}\text{--Cl}$ bond length is $2.2915(8)$ Å. The crystal structure of **14a** also shows that the molecule dimerizes in the solid state via $\pi\text{--}\pi$ stacking interactions of pyridylpyrimidine units (Figure 31). Two intermolecular hydrogen bondings exist in the unit cell. These interactions are observed between $\text{H}(\text{N}8)$ as a hydrogen donor and the pyrimidinyl nitrogen ($\text{N}7$) of the other dimeric structure as an acceptor.

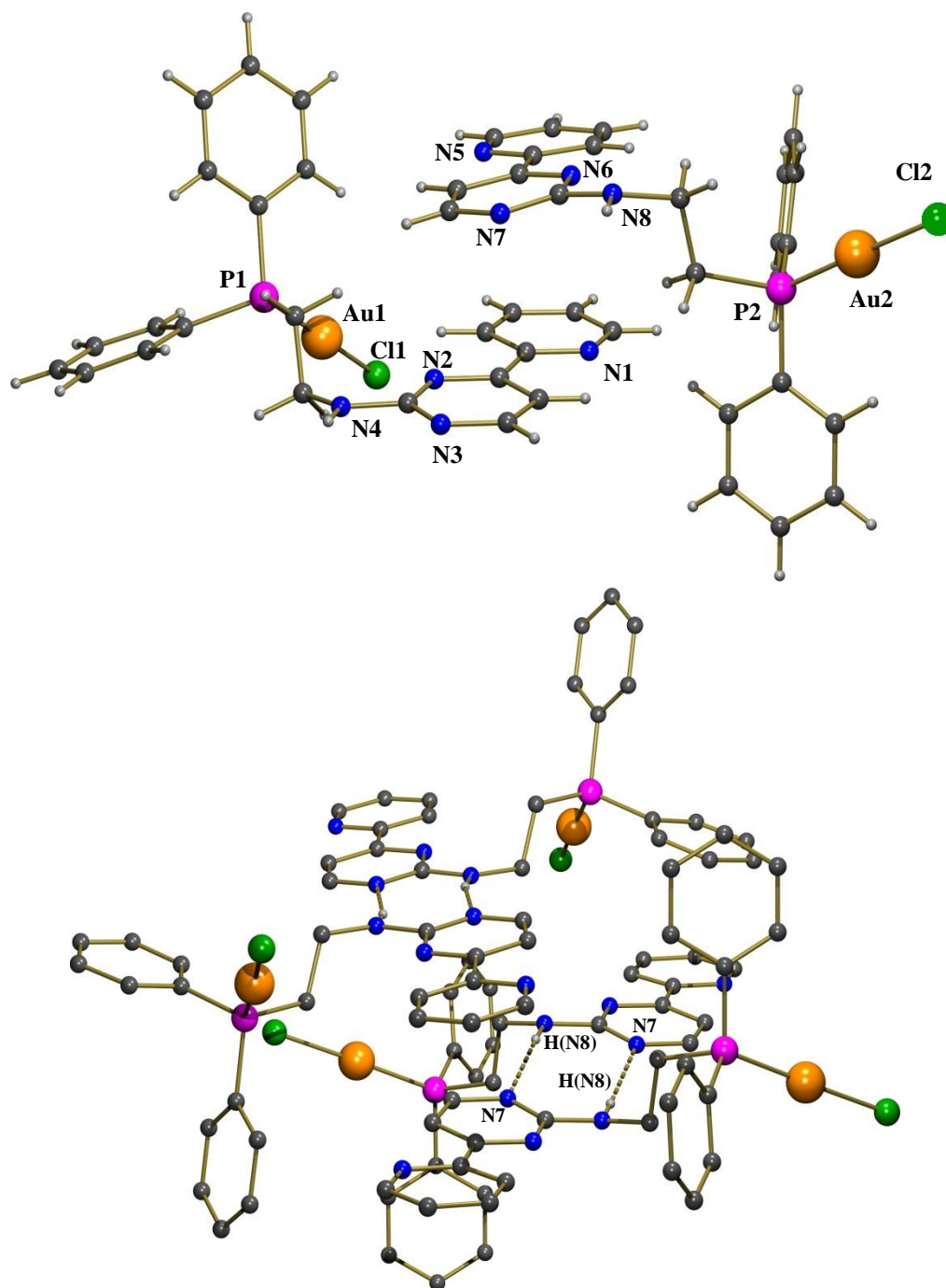


Figure 31. Dimeric structure of gold complex **14a** in the solid states; Characteristic bond lengths [\AA] and angles [$^\circ$]: P(1)-Au(1) 2.2309(8), Au(1)-Cl(1) 2.2915(8), P(1)-Au(1)-Cl(1) 177.86.

Compound **14b** was synthesized using the same method as described for the compound **14a**. Ligand **11b** was used instead of **11a**. There is no significant change in the ^1H NMR spectrum of complex **14b** when it is compared to the spectrum of complex **14a**. Therefore, introduction of a methyl substituent on the pyrimidine ring does not have a big

influence on the spectral parameters of the gold complex. The methyl protons reveal at 2.41 ppm as a singlet, the resonance of the H8 proton is no longer present (Table 6).

Table 6. ^1H NMR chemical shifts of compounds **14a,b**.

Complex	H1	H2	H3	H4	H7	H8	NH	(N)CH ₂	(P)CH ₂
14a	8.68	7.40	7.90	8.32	7.61	8.39	5.48	3.90	2.94
14b	8.68	7.38	7.89	8.31	7.51	–	5.35	3.90	2.93

In the ^{31}P NMR spectrum of complex **14b** shows a most significant change as expected. While the chemical shift of free ligand **11b** is -21.26 ppm, the signal shifts to $+24.07$ ppm in the gold complex **14b**.

The gold complexes of the long chain phosphine ligands **15a,b** were synthesized with the same procedure as described for the synthesis of the gold complexes **14a,b**. The gold complex **15a** was synthesized from ligand **12a** and the gold complex **15b** was synthesized from **12b** using with Au(tht)Cl in CH_2Cl_2 .

The structure elucidation of compound **15a** is done again by ^1H , ^{13}C and ^{31}P NMR spectroscopy. The inset of Figure 32 shows the ^1H NMR spectrum comparison of free ligand and the gold complex. Obviously the most influenced protons are H12 and H13. Their chemical shifts change by around 0.5 ppm towards to lower field with respect to the free ligand **12a**. In addition, the change in the electron density by coordinating the phosphorous atom to the gold cation affects the chemical shifts of the phenyl groups significantly. Their chemical shift values are about 0.2 ppm higher compared to the free ligand. All the assignments of the protons are shown in Figure 32 in detail.

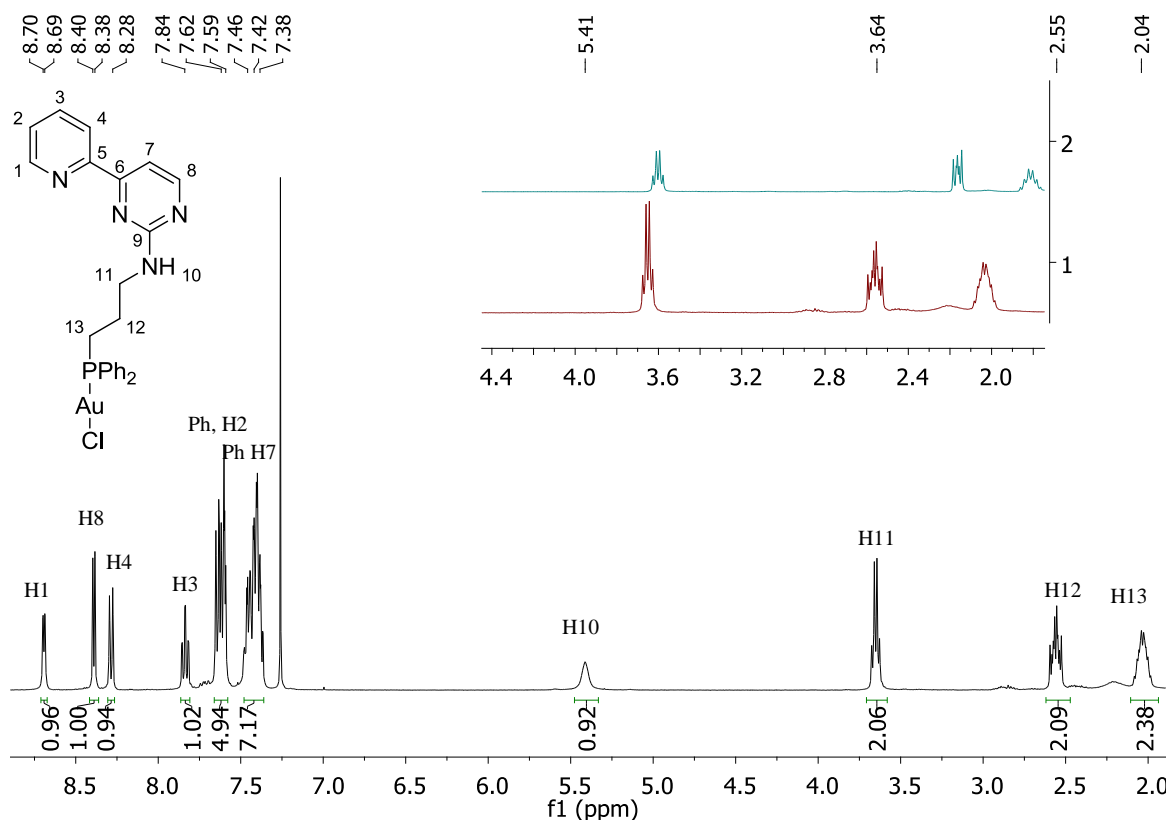


Figure 32. ^1H NMR spectrum of the gold complex **15a**. Inset: ^1H NMR comparison (alkyl region) of free ligand **12a** (blue) and gold complex **15a** (red).

Changing the electron density of the phosphorous atom affects the ^{31}P NMR spectrum as predicted. The signal shifts towards low field from -16.41 ppm to $+29.42$ ppm. This chemical shift change proves the formation of the P-Au bond (Figure 33).

Suitable crystals for compound **15a** for X-Ray crystallographic studies were observed by slow diffusion of Et_2O into CH_2Cl_2 solution. The structure is shown in Figure 34. **15a** crystallizes in triclinic space group $\text{P}\bar{1}$. The bond lengths P(1)-Au(1) and Au(1)-Cl(1) are $2.2304(8)$ Å and $2.2887(9)$ Å, respectively. The angle P(1)-Au(1)-Cl(1) is 173.97° and supports the almost linear coordination of gold(I).

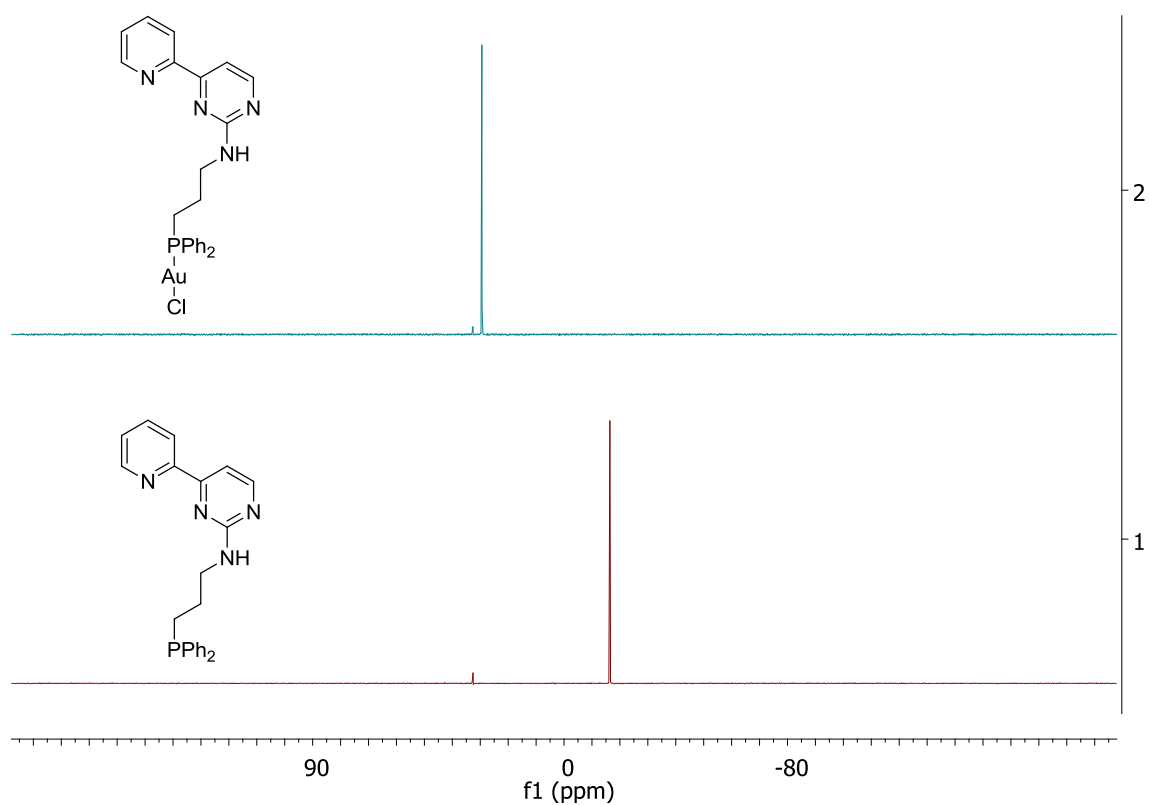


Figure 33. ^{31}P NMR spectrum comparison free ligand **12a** (red) and gold complex **15a** (blue).

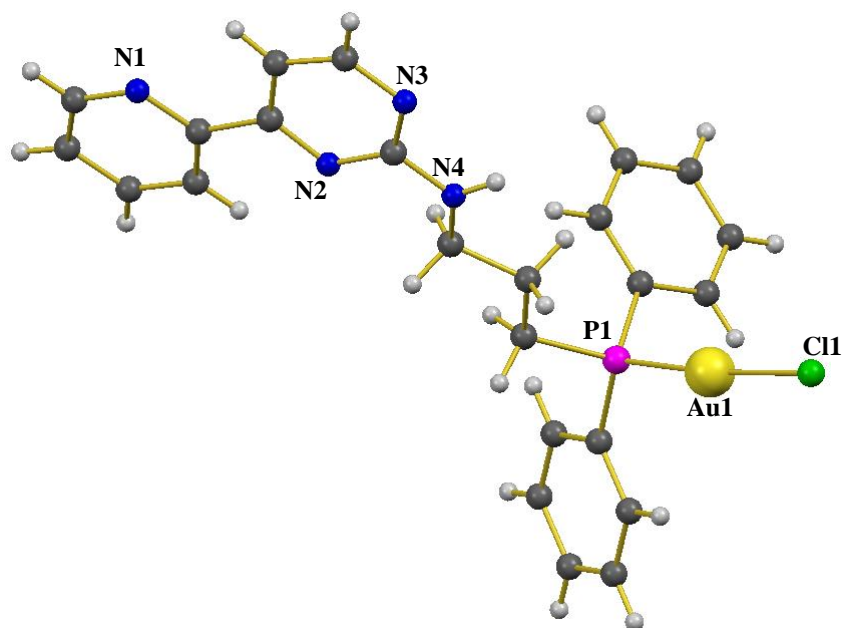


Figure 34. Molecular structure of Au complex **15a** in solid state; characteristic bond lengths [Å] and angles [°]: P(1)-Au(1) 2.2304(8), 2.2887(9), P(1)-Au(1)-Cl(1) 173.97.

There were no significant changes in the ^1H NMR spectrum of compound **15b** compared to compound **15a**. Compound **15b** has a singlet at 2.41 ppm belonging to the methyl protons and the H8 proton signal of compound **15a** is no longer present (Table 7). ^{31}P NMR gives a signal at +29.39 ppm after the coordination with gold(I) cation.

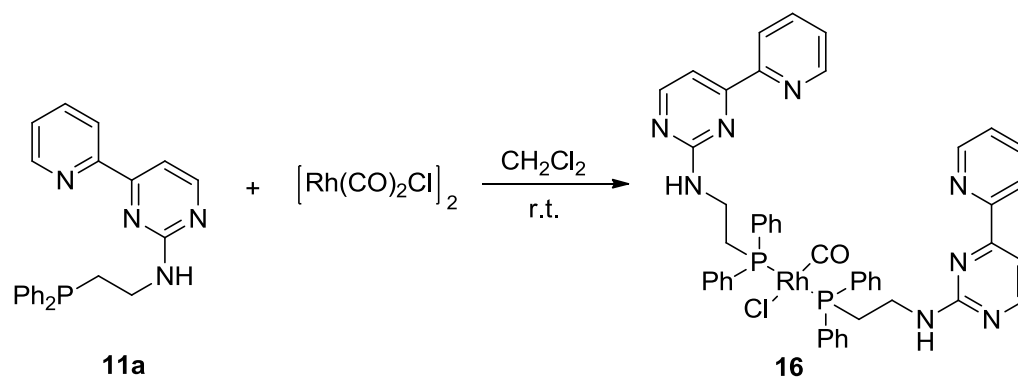
Table 7. ^1H NMR chemical shift of compound **15a,b**.

Complex	H1	H2	H3	H4	H7	H8	(P)CH ₂	(N)CH ₂	CH ₂
15a	8.69	7.36	7.84	8.29	7.61	8.39	3.65	2.56	2.03
15b	8.68	7.37	7.83	8.27	7.50	----	3.65	2.55	2.05

3.1.2.2 Synthesis of the Rhodium Complexes

Rhodium complexes are very active, and often highly selective compounds for catalytic reactions such as the hydroformylation of alkenes,^[138] the carbonylation of methanol and the asymmetric hydrogenation of α -amidocinnamic acid. The latter is used in the synthesis of α -dihydroxyphenylalanine (L-DOPA) a pharmaceutical for controlling the symptoms of Parkinson's disease.^[139-142] Especially, rhodium triphenylphosphine complexes are used in a wide range of catalytic reactions. One class of the most important transformations are catalytic hydrogenations of alkenes, for which, Wilkinson's catalyst $\text{RhCl}(\text{PPh}_3)_3$ is the most prominent example.^[143]

$\text{Trans-RhClCO}(\text{L})_2$ (L= aminophosphine type ligand) complexes can easily be synthesized from the rhodium(I) dicarbonyl chloride dimer. The dimeric rhodium precursor and compound **11a** (4 equiv.) were dissolved in anhydrous dichloromethane and stirred at room temperature for 24 hours (Scheme 25). The color of the reaction mixture changed to dark red after 30 minutes.



Scheme 25. Synthesis of trans-RhClCO(L)₂ **16**.

The structure elucidation of compound **16** is done by ¹H, ¹³C and ³¹P NMR spectroscopy. In the ¹H NMR spectrum, most significant changes are observed for the chemical shifts of the ethylene chain and phenyl ring protons, which are close to the phosphorous atom (Figure 35). They resonate at lower field compared to the free ligand **11a** because of the change in electron density of the complex after complexation with the rhodium cation.

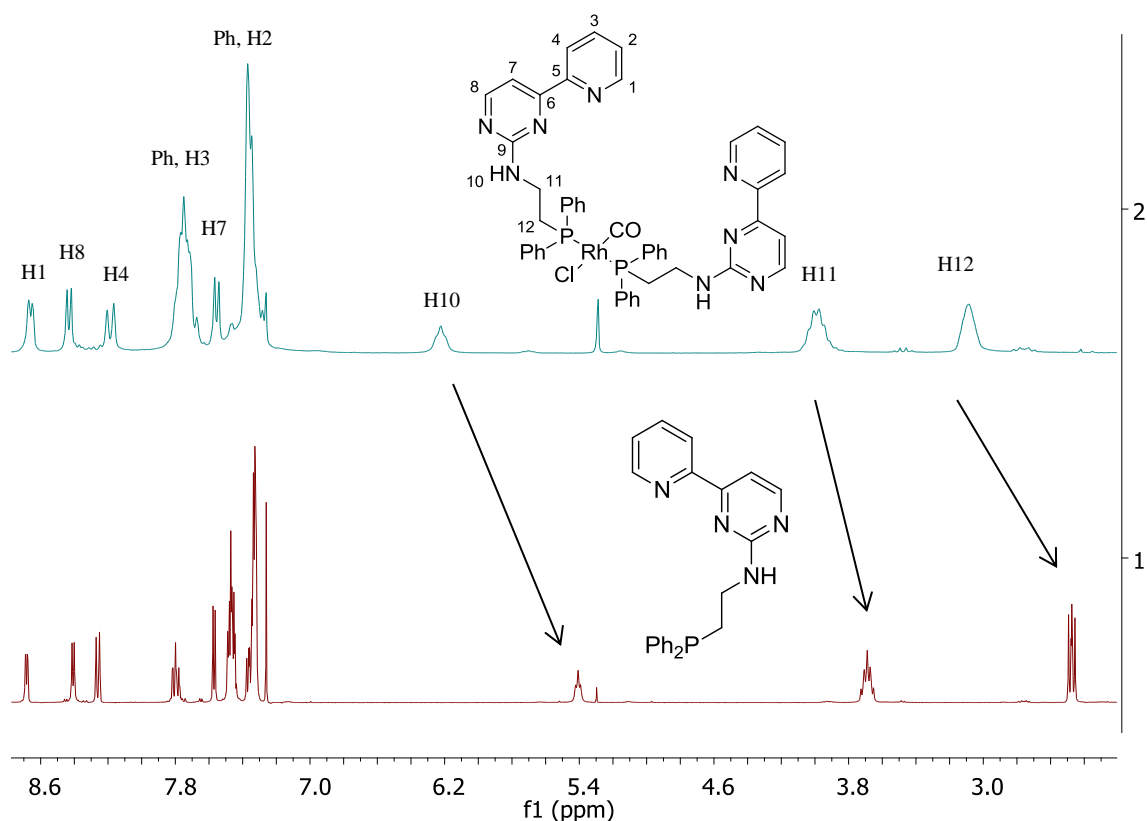


Figure 35. ¹H NMR spectrum comparison of free ligand **11a** and rhodium complex **16**.

The amine proton is also influenced strongly by the coordination of the metal center. The signal shifts about 0.8 ppm to the lower field which can be taken as a hint that there is an interaction (hydrogen bond), probably with the chlorido ligand coordinated in the cis-position to the phosphine ligand. In addition, the signals of the ethylene protons and –NH proton are broadened compared to the **11a**. Moreover, two protons of the pyrimidine ring H7 and H8 give a doublet 7.55 and 8.43 ppm, respectively. The chemical shifts of the pyridine ring protons are not influenced significantly by the coordination of the rhodium center proving a selective interaction with the phosphorous site.

The ^{13}C NMR spectrum proves the coordination to rhodium because rhodium ($I=1/2$) shows coupling with the carbon nuclei. The coupling constant varies between 15 to 70 Hz over one bond.^[144] The rhodium center couples to the phenyl carbon atoms and C12 over the phosphorous atom and they either give a triplet or a doublet of a doublet (Figure 36). The pyrimidinylpyridine carbons are not influenced by the coordination with rhodium center significantly and their chemical shifts are almost identical to the free ligand. The assignments of all carbons are carried out by the help of HMBC and HMQC techniques.

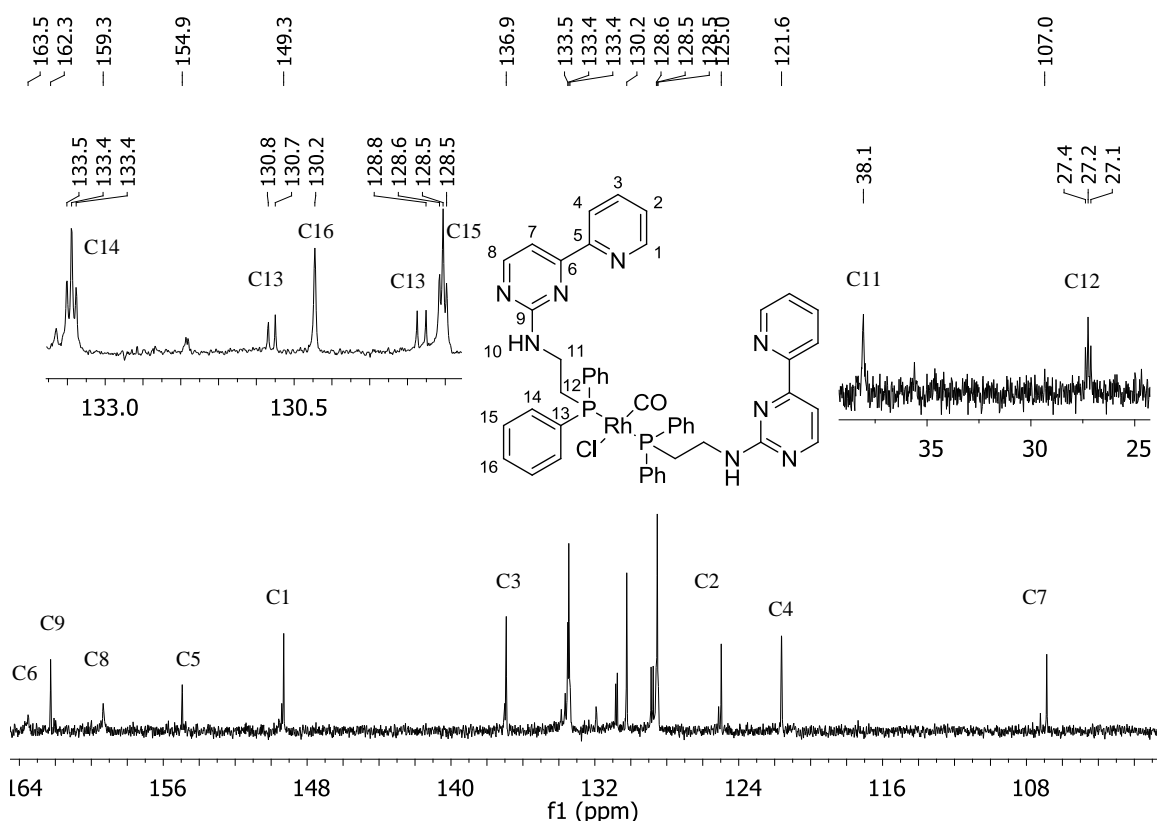


Figure 36. ^{13}C NMR spectra of compound **16**.

Similar to the gold complexes, the ^{31}P NMR spectrum shows the most significant change. The phosphorous signal shifts to lower field from -20 ppm to $+21$ ppm and it gives a characteristic doublet with a coupling constant of $^1J_{\text{Rh},\text{P}} = 122.9$ Hz. The doublet shows that the ligands are coordinated in trans positions to each other (Figure 37).^[145]

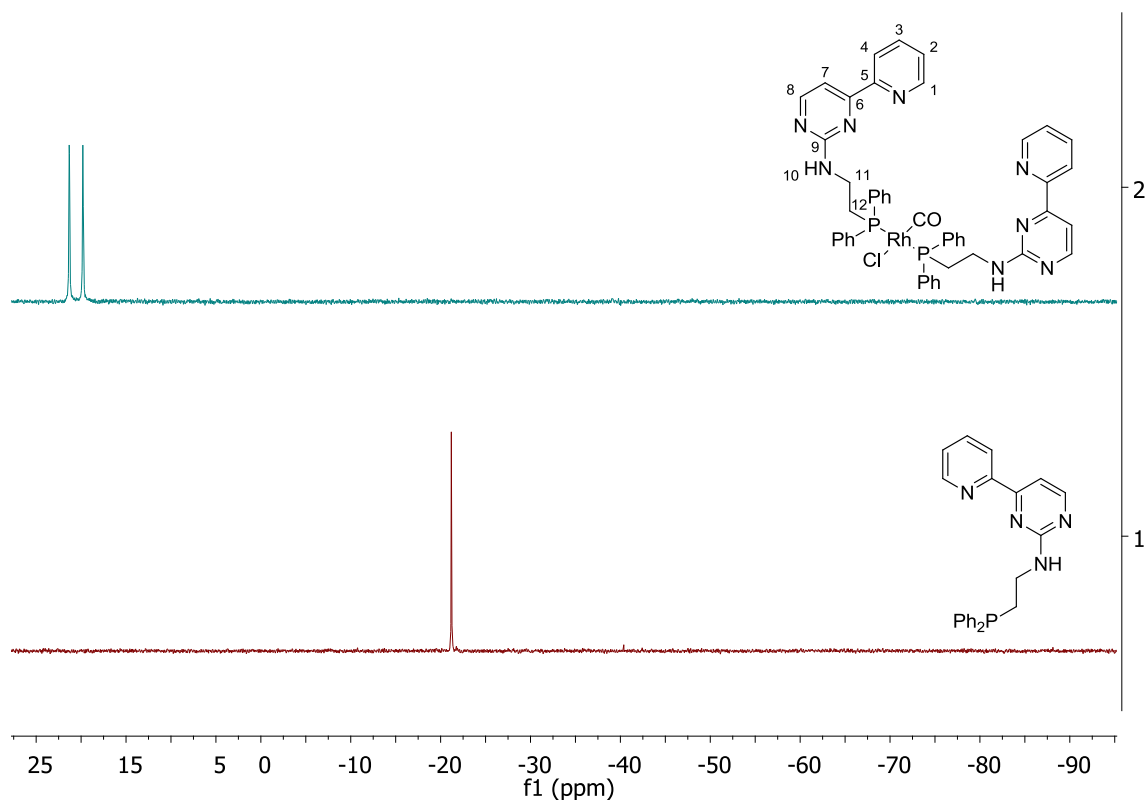


Figure 37. ^{31}P NMR spectrum comparison of free ligand **11a** and complex **16**.

In the IR spectrum of the rhodium complex **16**, one strong absorption band at 1965 cm^{-1} is assigned to carbonyl vibrational band (Figure 38).

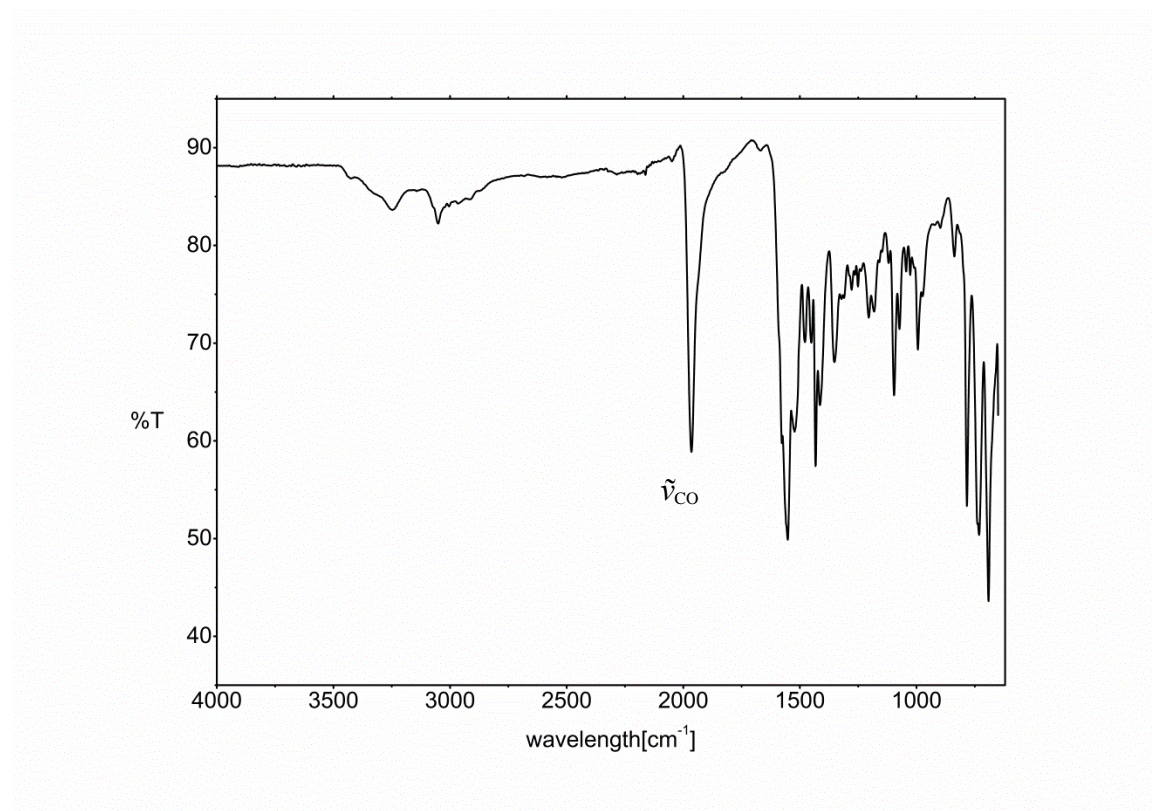


Figure 38. IR spectrum of compound **16**.

3.1.2.3 Synthesis of Heterobimetallic Complexes

Early-late heterobimetallic complexes have attracted great interest in the recent decade due to their unusual catalytic activities which is assigned to the cooperation of different metal sites.^[130,146] In heterobimetallic complexes, each metal center in principle performs those reactions being observed for the monometallic fragments, but by cooperation the two metal sites can also show novel types of reactivity and selectivity.^[117] In Figure 39, some examples of bimetallic complexes are presented which have different catalytic and electronic properties and show different selectivity. The Cu(II)-Pd(II) bimetallic complex connected to the chelate *P,N*-ligand shows higher catalytic activation in the amination reaction of aryl iodides compared to their mononuclear congeners. Another example are Co-salen complexes equipped with d-block Lewis acids (e.g. Co(II), Fe(III), Zn(II)). They show higher enantioselectivity in the kinetic resolution of racemic epichlorohydrin.^[50,147] There are some examples of heterobimetallic systems which show cooperativity; e.g., Rh-

Zn systems for catalytic hydrogenation and hydroborylation or Au-Zn for hydroamidation are few possible examples.^[148-150]

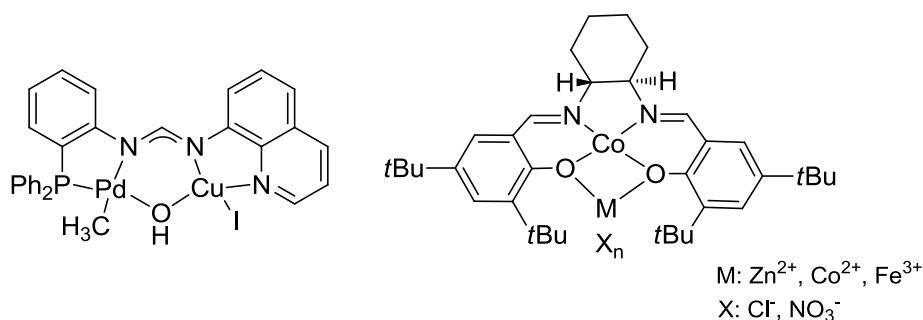
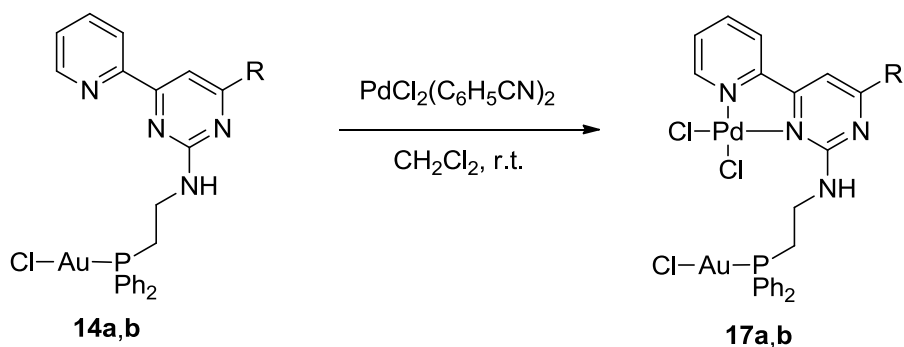


Figure 39. Some examples of bimetallic complexes.

In this study, the aim is to synthesize heterobimetallic complexes of *N,N,P*-ligands presented above (coordination with *N,N*-donor site of the pyridinylpyrimidine ring and phosphorous atom) with several metal combinations to see their applicability in catalytic reactions. In the following, the synthesis of heterobimetallic complexes with three different metal combinations (Pd-Au, Zn-Au and Ru-Au) will be presented. As it is known from Pearson's HSAB concept, gold(I) as a soft metal prefers the coordination to soft donor ligands like phosphines or *N*-heterocyclic carbenes (NHC).^[69,151] After completing the phosphorus coordination site by e.g. kinetically stable gold chloride, the second metal can be easily introduced to the hard *N,N*-donor site of the ligand.

3.1.2.4 Synthesis of Pd-Au Heterobimetallic Complexes

Palladium-gold combinations are known as catalysts for cross coupling reactions in terms of their unique reactivities.^[152] Sarkar reported a dual Pd-Au catalyst for the Sonogashira type cross coupling of arenediazonium salts for the first time.^[153] In order to synthesize Pd-Au systems, PdCl₂(C₆H₅CN)₂ and gold complexes of the aminophosphine ligands were stirred in dichloromethane at room temperature. As soon as the reactions were started, yellow precipitates were observed. After 24 hours, the precipitates were collected via filtration and the resulting yellow solids were washed with CH₂Cl₂ several times to remove the liberated bisbenzotrile (Scheme 26).



Scheme 26. Synthesis of heterobimetallic Pd-Au complexes **17a,b**.

The ^1H , ^{31}P and ^{13}C NMR spectra of compound **17a** prove the formation of the desired complex. ^1H NMR shows a triplet at 9.56 ppm that belongs to the NH proton (Figure 40). The coordination with palladium cation shifts the proton H1 of the pyridine ring towards to lower field compared to the gold complex.

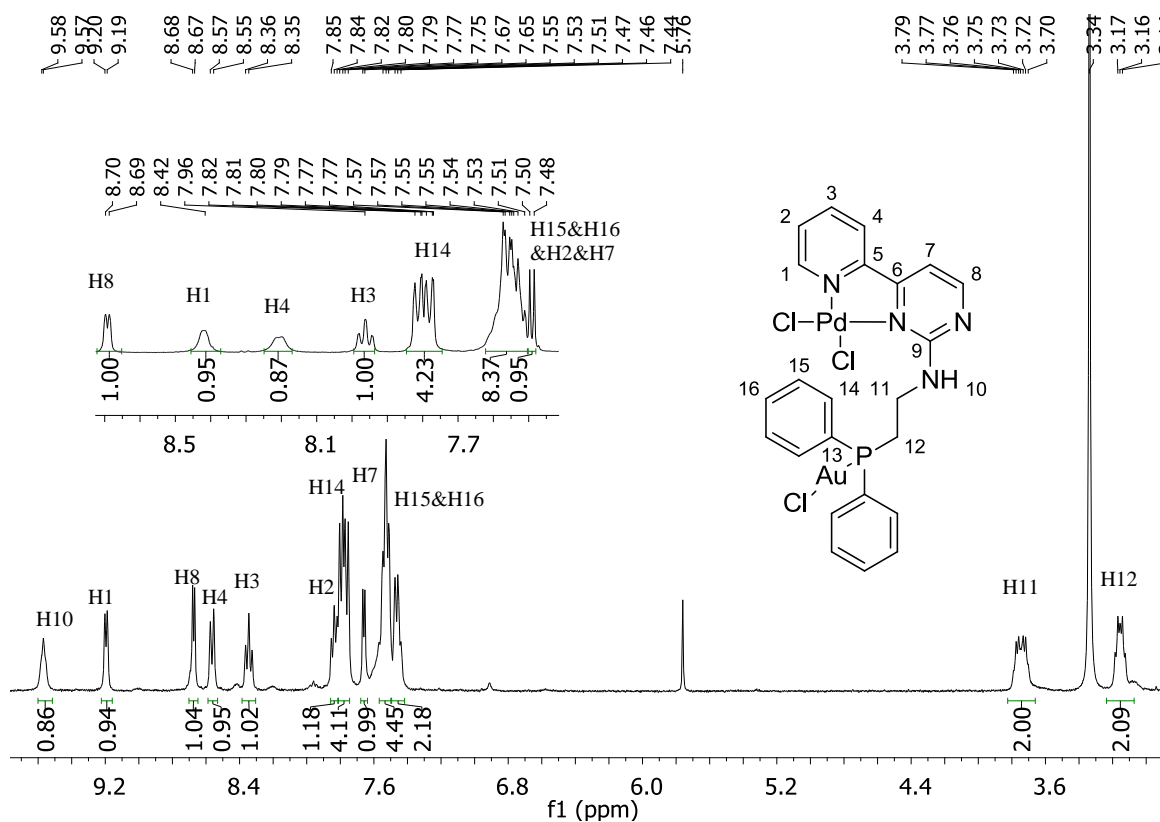


Figure 40. ^1H NMR spectrum of compound **17a**. Inset: ^1H NMR of compound **14a** (aromatic region).

H1 and H2 are the most influenced protons; both are shifted 0.5 ppm towards lower field. There is no significant change in chemical shifts of the ethylene protons. Therefore, the most significant effect of the coordination with palladium metal is observed on the pyridinylpyrimidine ring protons. The inset of the Figure 40 shows the chemical shifts of the gold complex **14a** between 7.48 ppm and 8.70 ppm.

The ^{31}P NMR spectrum of the compound **17a** is not significantly influenced by the coordination of the palladium moiety to the *N,N*-site because there is no direct change in the chemical environment of the phosphorous atom (Figure 41). When the ^{31}P NMR spectra of the ligand **11a**, gold complex **14a** and bimetallic complex **17a** are compared, no significant difference between monometallic and bimetallic complexes is observed in terms of the chemical shift. In other words, the complexation of the phosphine unit with gold cation is quite stable and introducing a second metal cation such as palladium does not cleave the gold phosphorous bond.

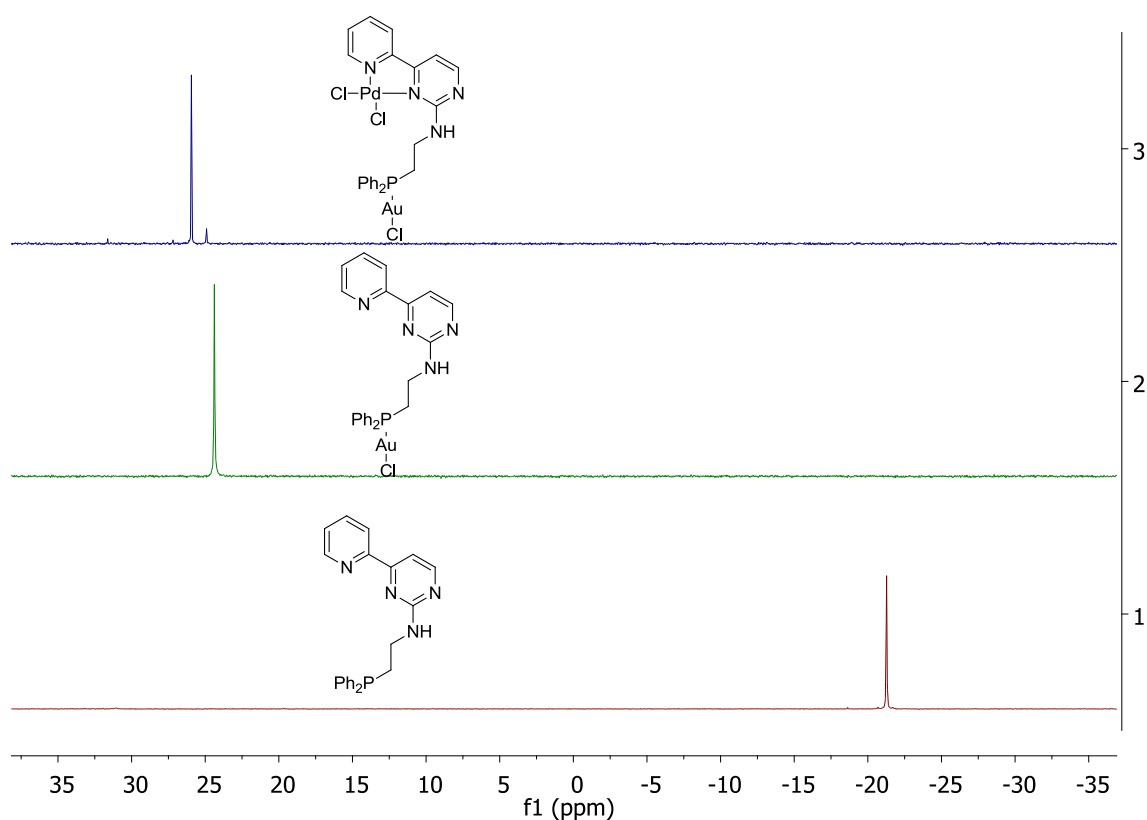


Figure 41. ^{31}P NMR spectral comparison of **11a** (red), **14a** (green) and **17a** (blue).

In the ^{13}C NMR spectrum of the complex **17a**, the carbon atoms cannot be assigned completely because of the low solubility of the complex in almost all solvents. Carbon atoms having hydrogen atoms bond are easily determined by a HMQC correlation. For example, the ethylene carbon atoms resonate at 25.6 ppm and 31.8 ppm (Figure 42).

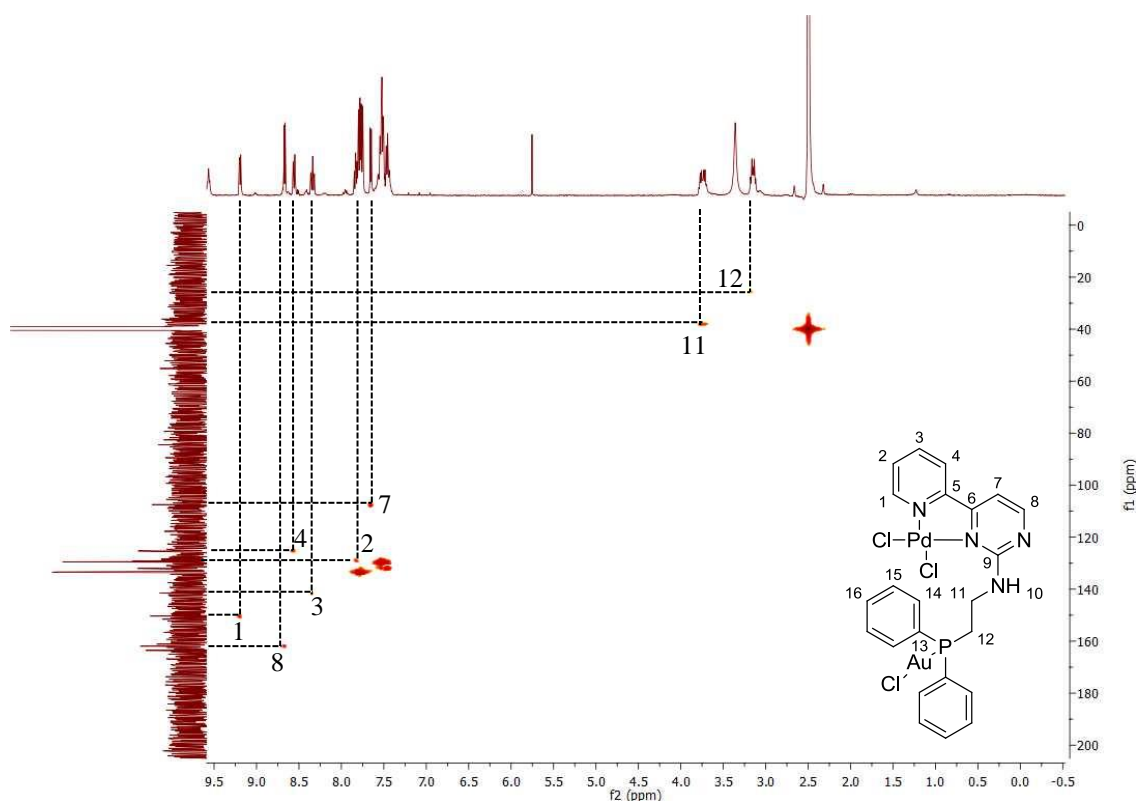


Figure 42. HMQC spectrum of **17a**.

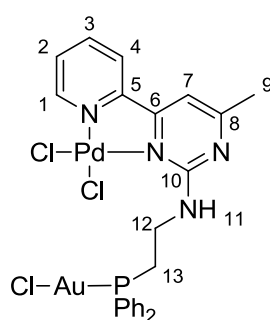
To assign the quaternary carbon signals, the HMBC technique was used. Even though none of the quaternary carbon atoms is visible in the 1D ^{13}C NMR spectrum, some of them can be found when the carbon has a long-range correlation with the neighboring hydrogen atoms over two, three, or four bonds.

Several combinations of solvents were tried to recrystallize **17a** but none of them were successful to give the single crystals of sufficient quality for a X-ray diffraction experiment because of the insolubility of the complex **17a**. Therefore, elemental analysis result is the only proof beside NMR-spectroscopy for the formation of the desired complex (Table 8).

Table 8. Elemental analysis result of **17a**.

$C_{23}H_{21}AuCl_3N_4PPd$	C %	H %	N %
theoretical	34.78	2.67	7.05
found	34.23	2.72	7.06

The complex **17b** was synthesized by reacting the monometallic gold complex **14b** with $PdCl_2(PhCN)_2$.

**Figure 43.** Heterobimetallic complex **17b**.

In 1H NMR spectrum of **17b**, the most significant change is observed in the chemical shift of the pyridine protons. They shift by maximum 0.5 ppm to lower field compared to the gold complex **14b**. All the chemical shifts and a comparison with **17b** and **14b** are shown in detail (Table 9).

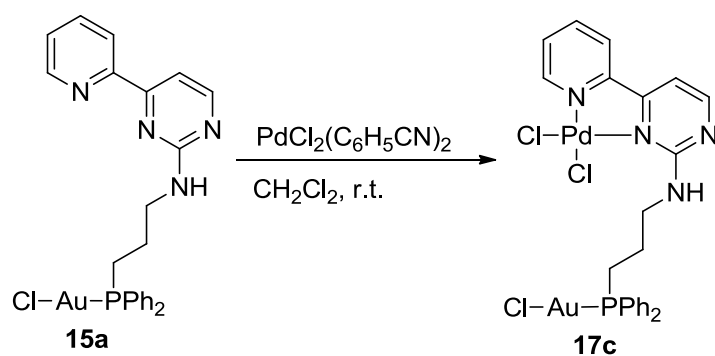
Table 9. 1H NMR comparison between **14b** and **17b**.

complex	H1	H2	H3	H4	H7	H9	H11	H12	H13
14b	8.67	7.49	7.89	8.32	7.90	2.41	5.37	3.90	2.93
17b	9.19	7.62	8.34	8.51	7.86	2.45	9.45	3.80	3.14

There is no significant change in the chemical shift of the phosphorous atom because there is no direct interaction between palladium and this site. In the ^{31}P NMR spectrum, **14b** has a peak at 24.07 ppm, while complex **17b** gives a signal at 26.08 ppm, Because of

the low solubility of **17b**, it was impossible to see signals in ^{13}C NMR spectrum. However, it was possible to find some carbon resonances using HMQC and HMBC analyses.

The bimetallic Pd-Au complex **17c** was prepared from the gold complex **15a** and palladiumbisbenzimidazole dichloride in dichloromethane solution in the same manner (Scheme 27).



Scheme 27. Synthesis of the Pd-Au complex **17c**.

The ^1H NMR spectrum of the compound **17c** shows a triplet at 9.39 ppm that belongs to the amine proton. The pyridine protons are influenced significantly since they shift to lower field by about 0.5 ppm compared to the complex **15a**. There is no significant change in the chemical shift of the phenyl groups and the propyl chain (Figure 44). Similar to the previous cases, the ^{31}P NMR spectrum has no significant change. While the gold complex **15a** has a signal at 29.42 ppm, complex **17c** gives a peak at 30.70 ppm.

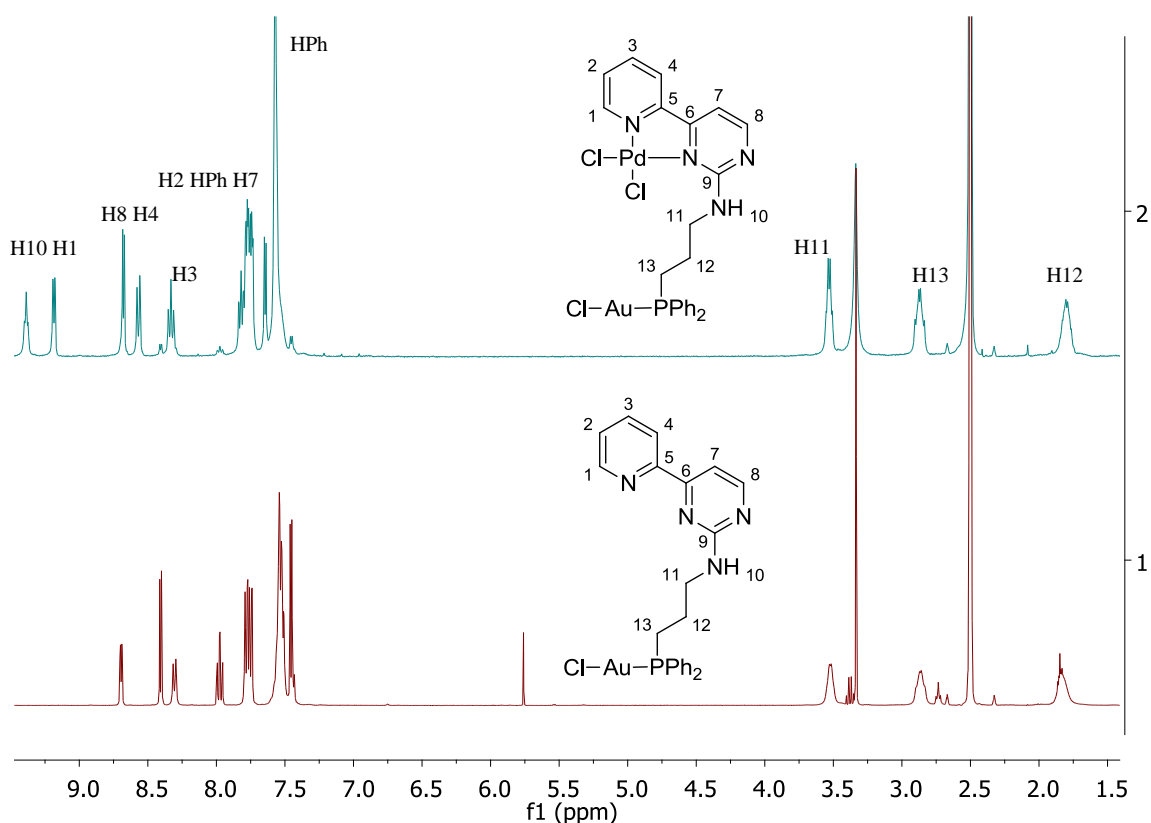


Figure 44. ^1H NMR spectrum comparison of complex **15a** and **17c**.

^{13}C NMR shifts are less sensitive than ^1H NMR shifts. After coordination to palladium, there is no significant change in the chemical shifts of the carbon atoms. The propylene carbon atoms could not be observed in the ^{13}C NMR spectrum but they can be assigned by help of 2D-NMR spectroscopic methods such as HMQC (Figure 45) and HMBC.

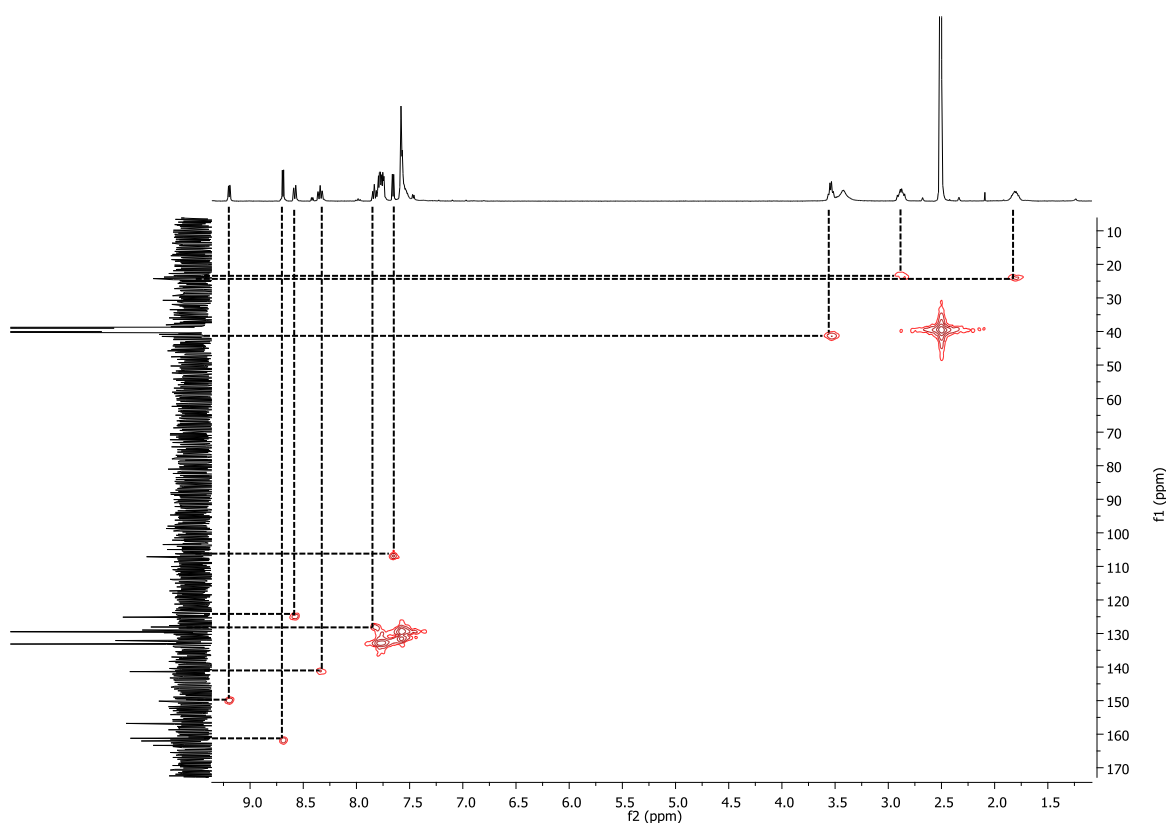


Figure 45. HMQC correlations of complex **17c**.

3.1.2.5 Synthesis of Zn-Au Heterobimetallic Complexes

The aim of the preparation of gold-zinc bimetallic systems is to observe the cooperative interactions of both metals in catalytic transformations such as the hydroamination of olefins.^[154] In literature, the $\text{PPh}_3\text{AuCl}/\text{AgOTf}$ system has been used as catalyst for hydroamination reactions. This reaction does not take place alone with Ph_3PAuCl or AgOTf . A weakly coordinating counter ion like triflate or hexafluoroantimonate is necessary to activate the gold complex.^[154] In our case we expect that gold catalyzes the reaction and zinc binds the substrate.^[150] Thus, broad variety of Zn-Au complexes bearing *N,P*-, *N,N,P*- or *N,N,N,P,P*-ligands are on the list to be investigated for hydroamination reactions.

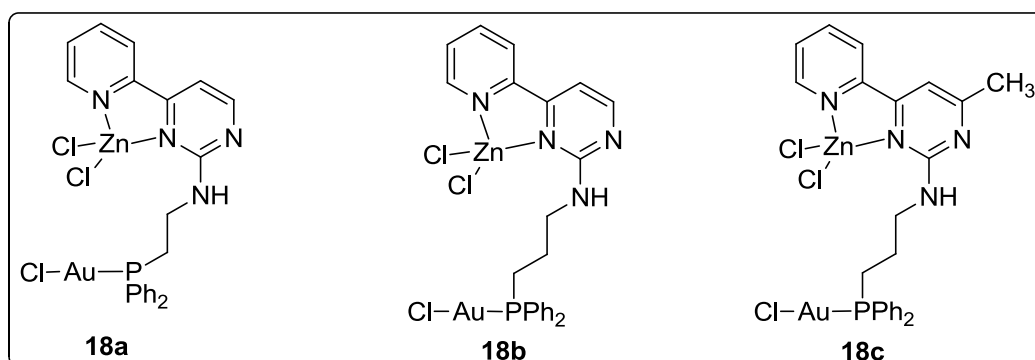
Several reaction conditions were tested to insert zinc cation by reacting the monogold complexes with zinc (II) triflate (Table 9). Unfortunately, the reactions with $\text{Zn}(\text{OTf})_2$ did not produce any of the desired complexes.

Table 10. Reaction conditions for the synthesis of Zn-Au complexes^a.

[Zn]	[Au]	Solvent	[Zn]:[Au]
Zn(OTf) ₂	14a	Ethanol	1:1.1
Zn(OTf) ₂	14a	Acetonitrile	1:1.2
Zn(OTf) ₂	14a	Acetonitrile	1:0.5
Zn(OTf) ₂	14a	Dichloromethane	1:1.1

^a All reactions were carried out at room temperature during 24 hours.

After attempting several reactions with Zn(OTf)₂, Zn(Cl)₂ was used. A solution of gold complexes **14a** and **15a,b** in CH₂Cl₂ was added dropwise to a solution of ZnCl₂ in CH₂Cl₂. The reaction mixtures were stirred at room temperature for 24 hours. The complexes **18a-c** were purified by washing from diethyl ether (Figure 46).

**Figure 46.** Heterobimetallic Zn-Au complexes **18a-c**.

In the ¹H NMR spectrum of the bimetallic complex **18a** recorded in CDCl₃, all signals are broadened. It is most probably due to the dynamic properties of the bimetallic Zn-Au complex. In Figure 47, the most affected proton in terms of the chemical shift is the -NH proton. It shifts by approximately 1.0 ppm to lower field compared to the gold complex **14a**. This is a clear hint for the interaction of the zinc cation with the pyridylpyrimidine ligand.

The pyridylpyrimidine protons H2, H3 and H8 protons also shift towards lower field because the electron density around the *N,N*-donor site is decreased by the coordinated zinc center. The chemical shifts of the ethylene protons H11 and H12 are not influenced

considerably by the insertion of the zinc cation. Figure 47 shows the comparison of the ^1H NMR spectra of the gold complex **14a** and the bimetallic Zn-Au complex **18a**.

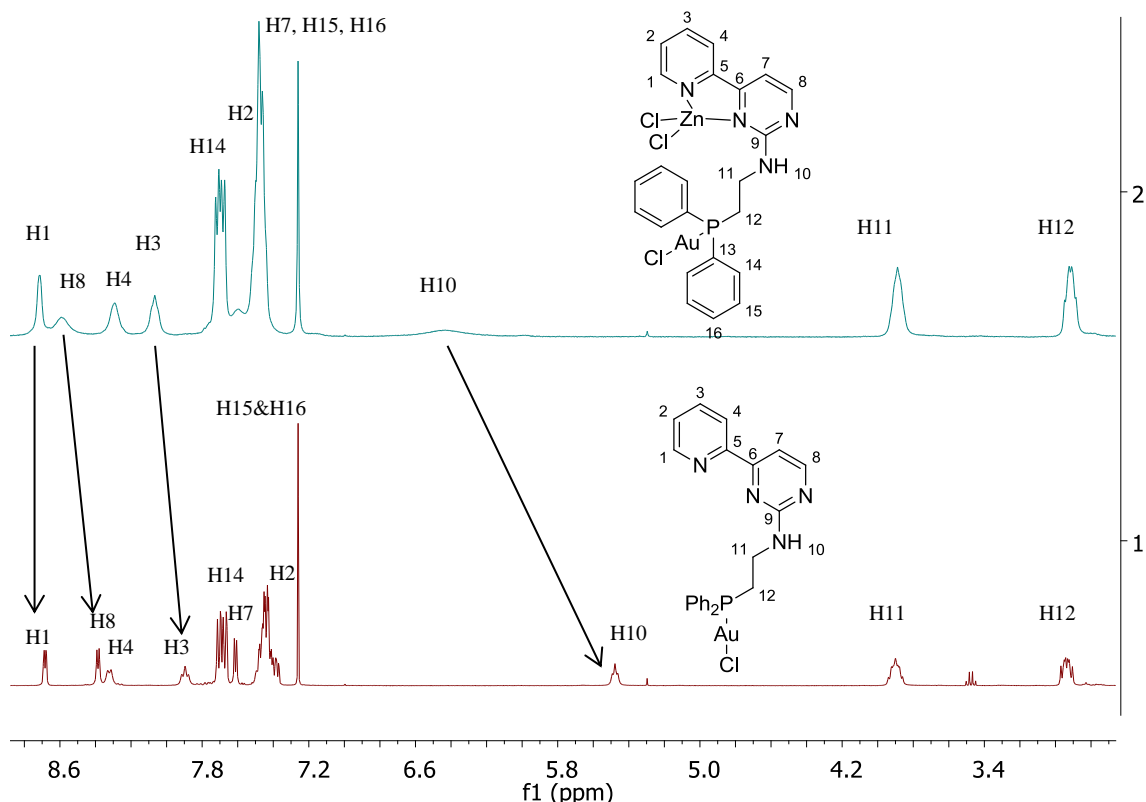


Figure 47. ^1H NMR spectral comparison of the Zn-Au complex **18a** and Au complex **14a**.

In the ^{13}C NMR spectrum, some of the carbon signals could not be obtained due to line broadening and the low solubility of the complex. The assignment of the carbon atoms was done by the help of 2D-NMR spectroscopy. Figure 48 shows the HMQC spectrum of compound **18a**. While the ethylene and phenyl carbons were assigned, it is not possible to see all the carbon-hydrogen correlations.

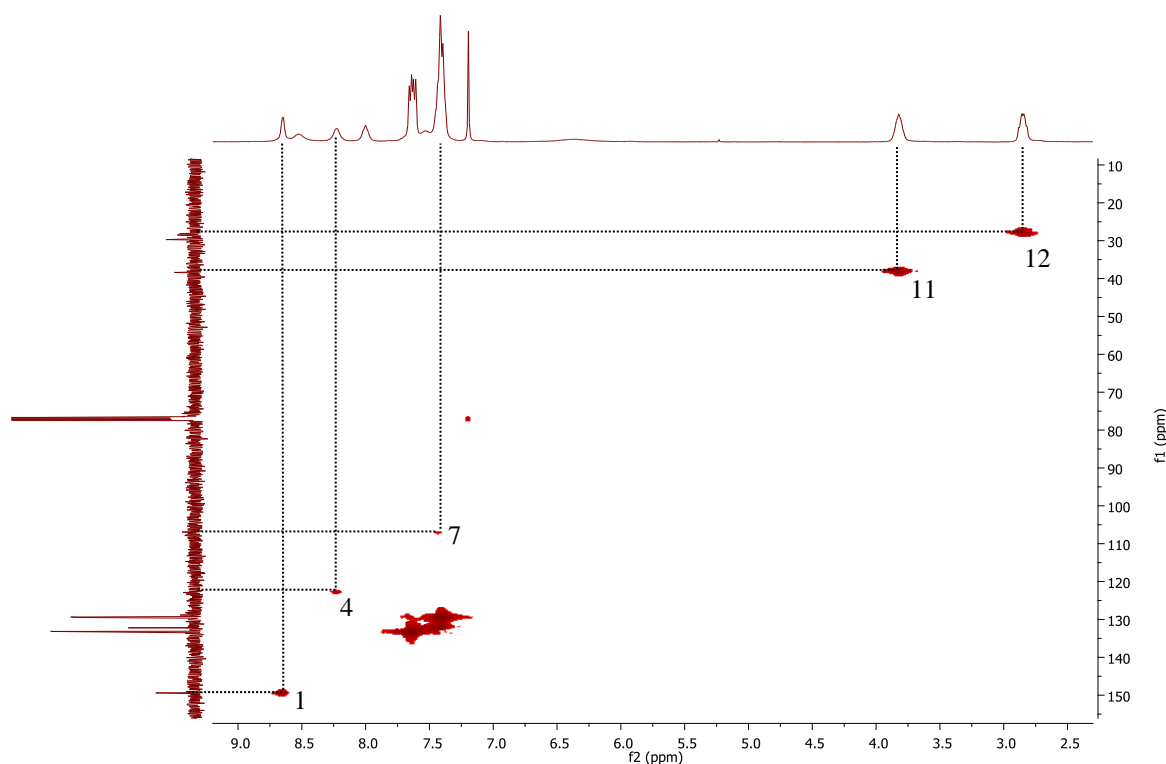


Figure 48. HMQC spectrum of bimetallic Zn-Au complex **18a**.

The ^{31}P NMR spectrum also proves that the insertion of the zinc cation does not interrupt the gold-phosphine part since the bimetallic Zn-Au complex **18a** gives a signal at 23.76 ppm while the Au complex **14a** provides a peak at 24.41 ppm.

Moreover, ESI-MS studies were carried out by Dipl. Chem. Johannes Lang from the research group of Prof. Niedner-Schatteburg. Fragments of the neutral complex **18a** were observed by elimination of a chloride anion and ZnCl_3^- ions from the molecule. The structures of these fragmented ions in gas phase were proposed by the same group, too. With Gaussian 09,^[155] the molecular structures of $[\text{M}-\text{Cl}]^+$ and $[\text{M}-\text{ZnCl}_3]^+$ in the gas phase were optimized by energy minimization (Figure 49). When chloride is split from the molecule, the gold cation can be stabilized by a neighboring chlorido ligand attached to the zinc. The calculated structure of $[\text{M}-\text{Cl}]^+$ also shows an intramolecular hydrogen bonding between the chlorido ligand and the N-H bond. Similar to this fragmented ion, neutral complex **18a** should have an intramolecular hydrogen bonding, as well. This explains the change in chemical shift of the -NH and broadening of signals in ^1H NMR.

By further fragmentation of ZnCl_2 from $[\text{M-Cl}]^+$, naked gold species can be stabilized by the pyridylpyrimidine unit in solution a solvent molecule will probably do this.

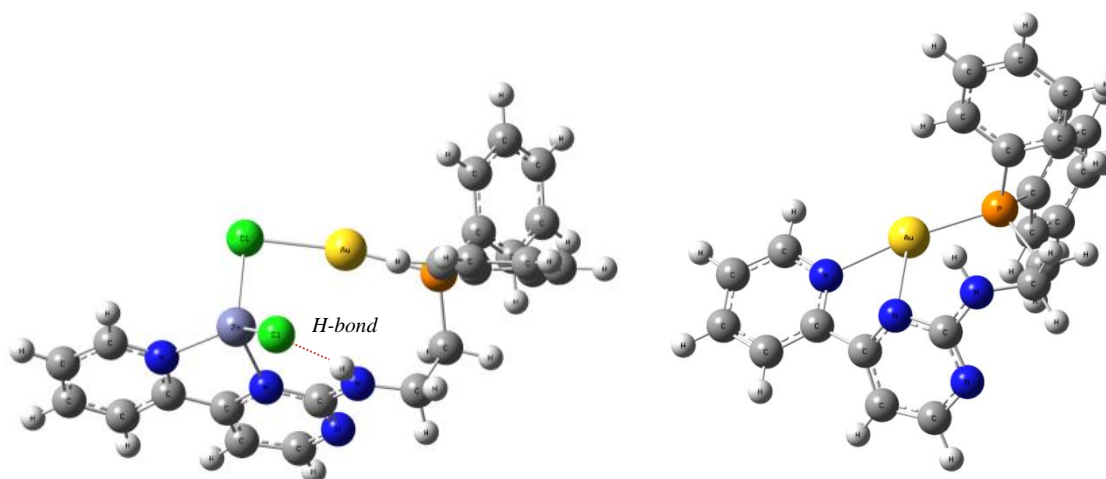


Figure 49. Calculated structures of $[\text{M-Cl}]^+$ (left) and $[\text{M-ZnCl}_3]^+$ (right).

The ^1H NMR data of the complexes **18b,c** are summarized in Table 11. The bimetallic Zn-Au complexes **18b** and **18c** also show peak broadening due to coordinating of the zinc cation. For both complexes, the most influenced proton belongs to the amine site. Similarly, the pyridylpyrimidine protons shift to lower field compared to the corresponding gold complexes. The ^{31}P NMR spectra of both complexes **18b,c** prove that there is no coordination between the phosphorous coordination site and the zinc metal because the chemical shifts of the ^{31}P NMR spectra do not show a significant change. **18b** has the peak at 30.18 ppm and **18c** has the signal at 30.45 ppm.

Table 11. ^1H NMR data of the bimetallic Zn-Au complexes **18b** and **18c**.

Complex	H1	H2	H3	H4	H7	H8	NH	NCH ₂	PCH ₂	CH ₂
18b	8.77	7.44-7.42	8.11	8.26	7.74-7.69	8.63	6.31	3.67	2.64	2.03
18c	8.78	7.48-7.40	8.14	8.23	7.76-7.72	–	6.23	3.67	2.65	2.03

For further investigations, electrospray mass spectrometry studies were carried out by Johannes Lang from the group of Prof. Niedner-Schatteburg. The fragments of the neutral

complex **18b** were observed by the elimination of the chloride ion from the molecular peak and the elimination of ZnCl_2 from the fragmented ion $[\text{M-Cl}]^+$. Figure 50 shows the simulation of those fragments (red line) and their experimental spectra (black line).

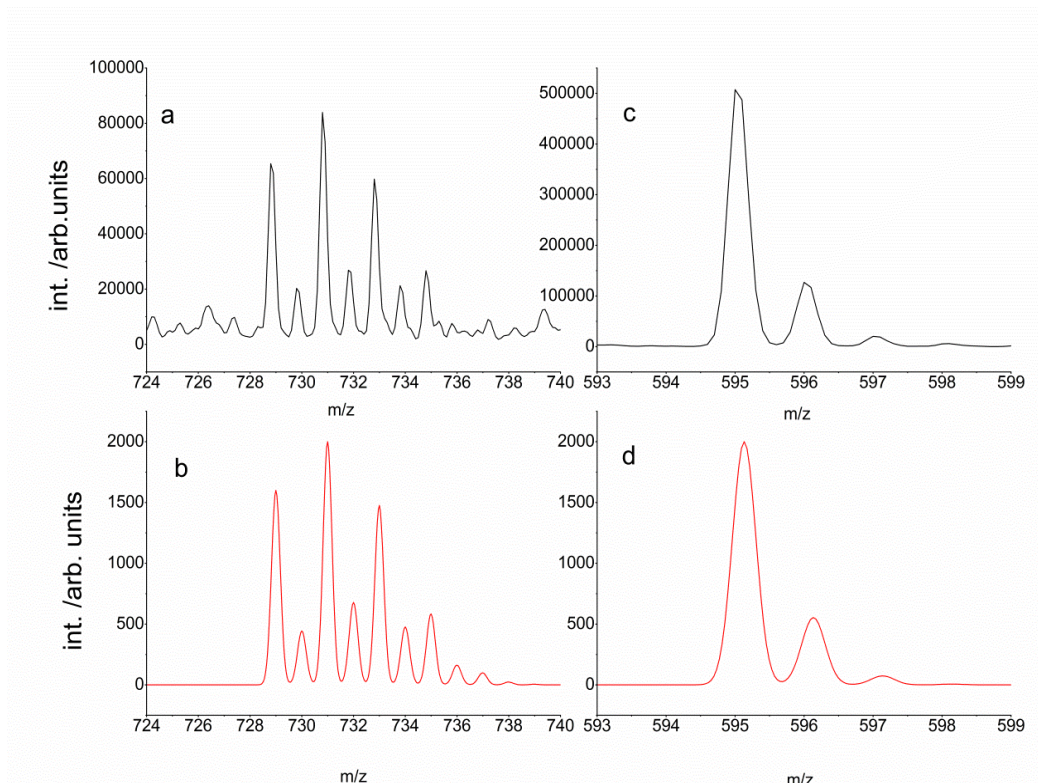
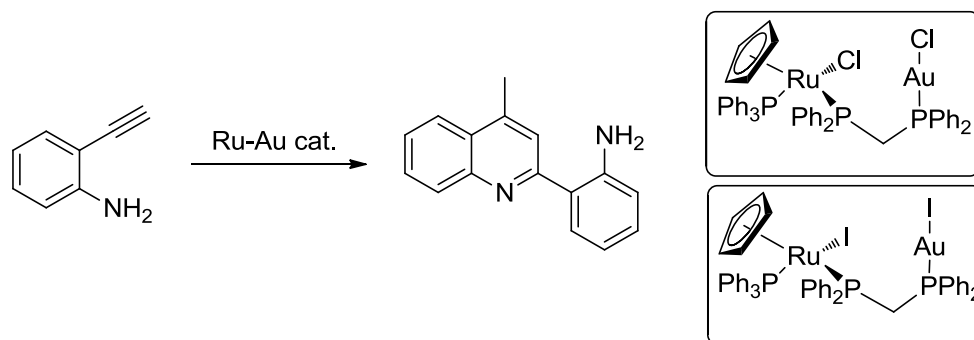


Figure 50. ESI-MS spectra fragment of **18b**. Experimental spectrum of $[\text{M-Cl}]^+$ (a) and simulated spectrum of $[\text{M-Cl}]^+$ (b), experimental spectrum of ZnCl_2 elimination from $[\text{M-Cl}]^+$ (c) and simulated spectrum of ZnCl_2 elimination from $[\text{M-Cl}]^+$ (d).

3.1.2.6 Synthesis of Ru-Au Heterobimetallic Complexes

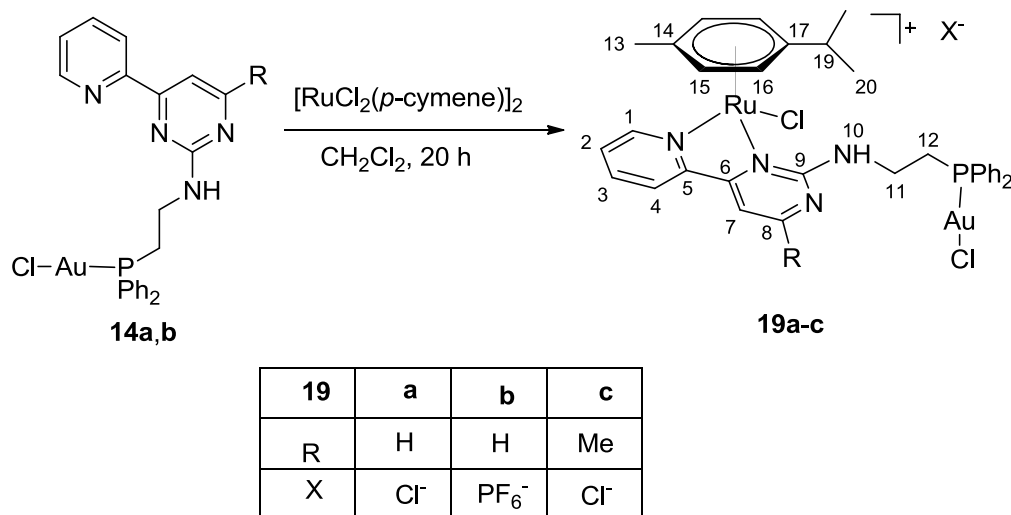
White et al. reported that the cyclization of alkynylanilines can be obtained by the use of a Ru-Au heterobimetallic system. The coordination of the alkyne group to the gold center induces the dimerization of 2-ethynylaniline (Scheme 28).^[156]



Scheme 28. Dimerization of 2-ethynylaniline to a quinoline by Ru-Au bimetallic catalyst.

In this chapter, the synthesis and characterization of heterobimetallic ruthenium-gold complexes of the type of $\text{Cl}_2\text{LRu}(N,N)\text{-PAuCl}$ ($\text{L} = p\text{-cymene}$) bearing a bidentate pyridylpyrimidine motif as a N,N -ligand will be discussed.

Treating the monometallic complexes **14a,b** with half an equivalent of $[\text{RuCl}_2(p\text{-cymene})]_2$ in dichloromethane at room temperature led to the formation of the orange colored heterobimetallic ruthenium-gold complexes **19a-c** in good yields. The chloride ion can be exchanged against a larger and weaker coordinating anion (PF_6^-). The addition of an excess amount of KPF_6 to the reaction mixture of **14a** and $[\text{RuCl}_2(p\text{-cymene})]_2$ in dichloromethane gave the Ru-Au complex **19b** (Scheme 29).



Scheme 29. Synthesis of the heterobimetallic Ru-Au complexes **19a-c**.

The $^1\text{H}, ^1\text{H}$ -COSY experiment of the bimetallic complex **19a** shows all the proton-proton couplings. Coordination of the pyridylpyrimidine to the Lewis acidic ruthenium (II)

center causes a shift of all hydrogen atoms to lower field (Figure 51). H1 and H10 are the most influenced protons that shift from 8.68 and 5.98 ppm (complex **14a**) to 9.72 and 6.89 ppm (complex **19a**), respectively. Since the ruthenium ion is a center of chirality, the diastereotopic methyl groups of isopropyl substituent of the cymene ring appear as two doublets at 0.9 and 1.0 ppm as expected. Accordingly the resonances of the ethylene protons are split into four sets of multiplets between 2.8 and 4.1 ppm. The assignments of all protons are shown in Figure 51.

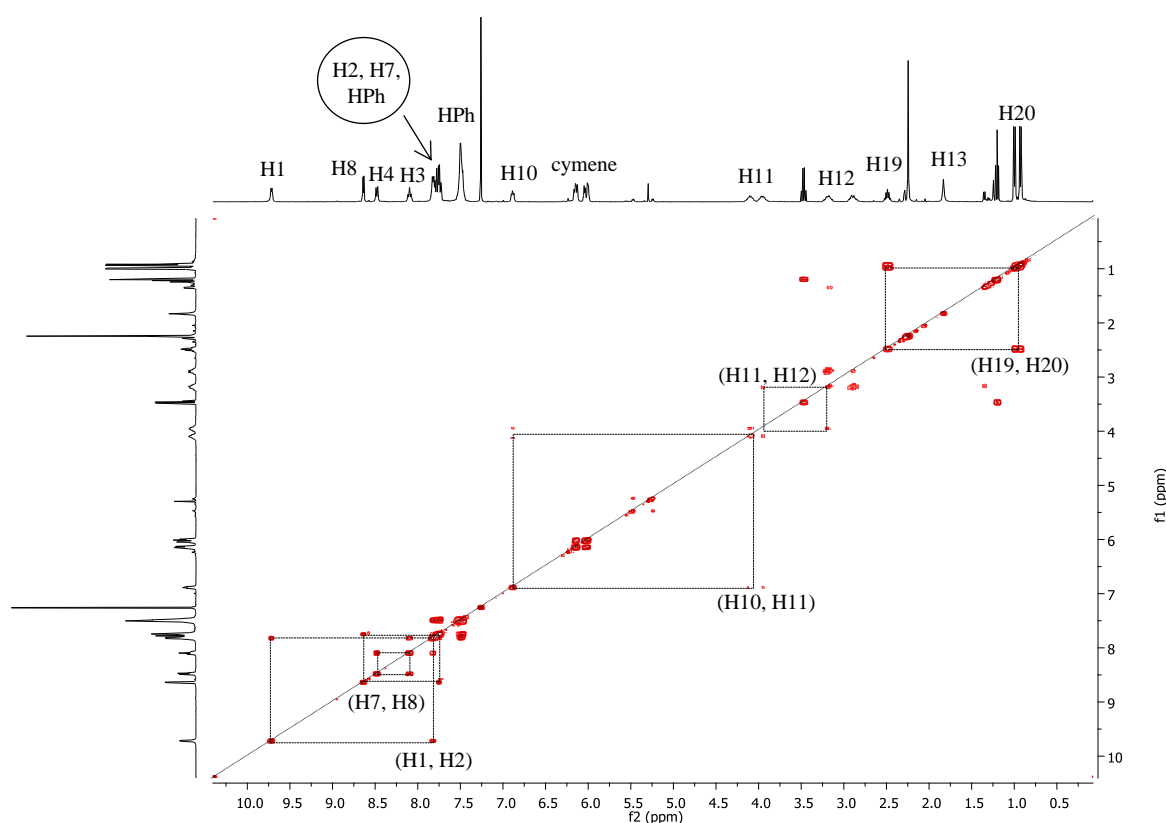


Figure 51. ^1H - ^1H COSY spectrum of **19a**.

In the ^{13}C NMR spectrum, four peaks between 87.0 ppm and 84.0 ppm can be assigned to four magnetically inequivalent aromatic carbons of the cymene ring and the peaks between 31.0 ppm and 19.2 ppm belong to the saturated carbons the cymene group. The ^{31}P NMR spectrum of **19a** has no significant change in the chemical shift after the coordination of ruthenium which proves that the gold cation is still attached to the phosphine and that the ruthenium (II) center coordinates to the *N,N*-donor site. The

heterobimetallic Ru-Au complex **19a** has a resonance at 24.77 ppm, while the gold complex **14a** gives a signal at 24.41 ppm (Figure 52).

Several trials to obtain crystals for X-ray measurement were unsuccessful. Probably the presence of the small counter ion (Cl^-) prevents the growing of crystals. Thus exchange of the chloride against a bigger counter anion such as hexafluorophosphate might solve the problem. Unfortunately, only an oily residue was formed with PF_6^- in several solvent combinations. The ^1H and ^{13}C NMR spectra of the bimetallic complex **19b** are similar to the spectra of compound **19a**, since the only difference is the counter ion. The ^{31}P NMR spectrum of complex **19b** exhibits two signals, one of them belonging to the phosphorous atom of the cation which resonates at +24.6 ppm. The second one is the signal of the PF_6^- ion at -144.2 ppm appearing as a septet (Figure 52).

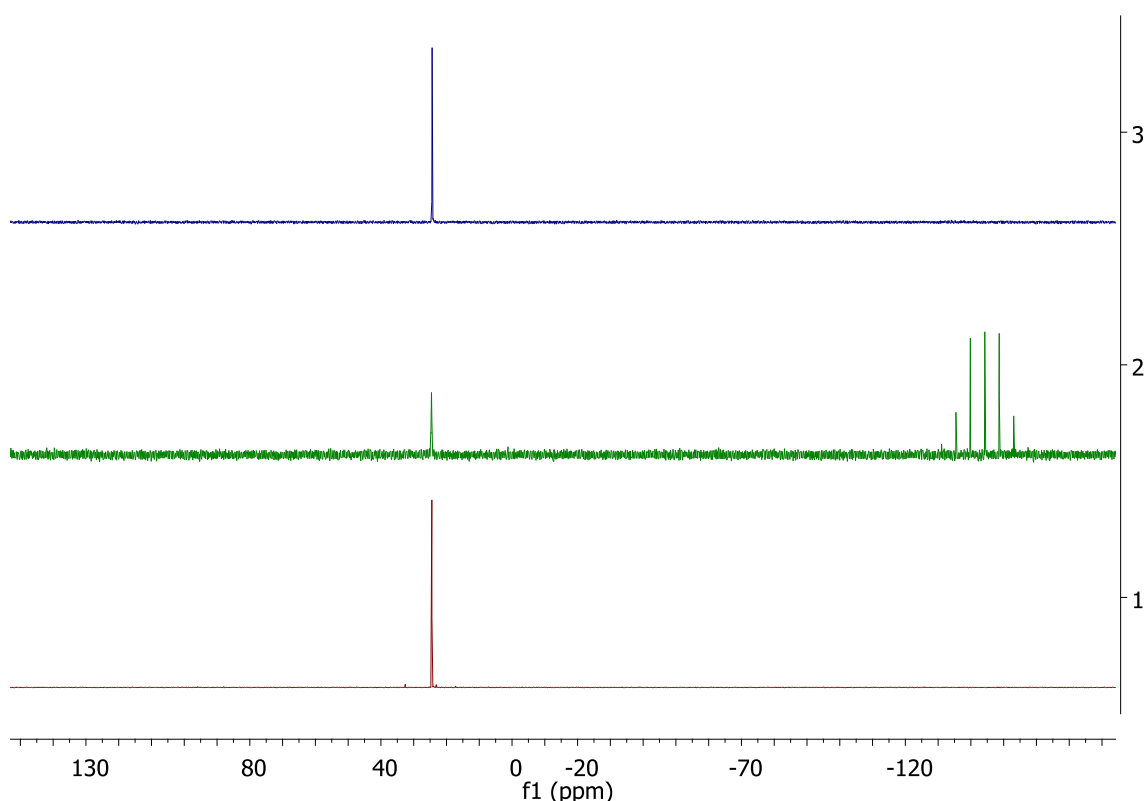
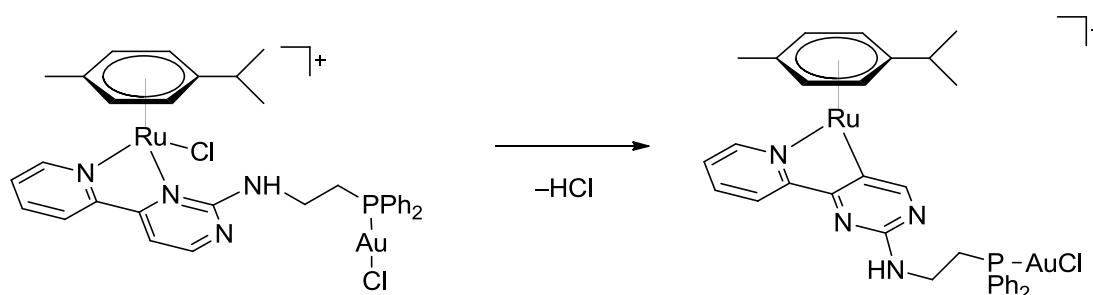


Figure 52. ^{31}P NMR spectral comparison of **19a** (red), **19b** (green) and **14a** (blue).

The ESI-MS spectrum also proves the formation of the heterobimetallic complex **19a**: the molecular ion peak of the ruthenium gold complex $[\text{M}]^+$ with a m/z ratio of 886.8 is detected. During the fragmentation of this peak, HCl elimination is observed to generate

the $[M-HCl]^+$ cation with m/z 850.9. The CH- activation takes places on the ortho carbon atom (Scheme 31).



Scheme 30. HCl dissociation process of **19a**.

Besides this HCl elimination, two additional fragments are detected belonging to the complex $[M-cymene]^+$ and $[M-HCl-cymene]^+$ with m/z values of 754.7 and 716.8, respectively. Figure 53 and Figure 54 show all experimental and simulated spectra of the fragmented ions. Their isotopic patterns fit perfectly to the calculated patterns.

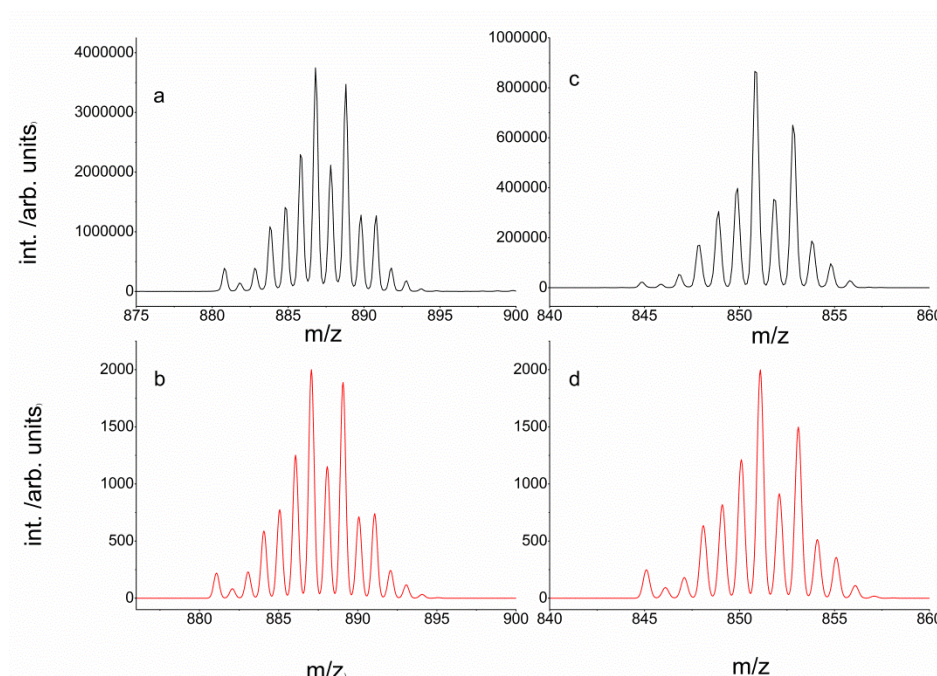


Figure 53. ESI-MS spectra of **19a**. Experimental spectrum of $[M]^+$ (a) and simulated spectrum of $[M]^+$ (b), experimental spectrum of $[M-HCl]^+$ (c) and simulated spectrum of $[M-HCl]^+$ (d).

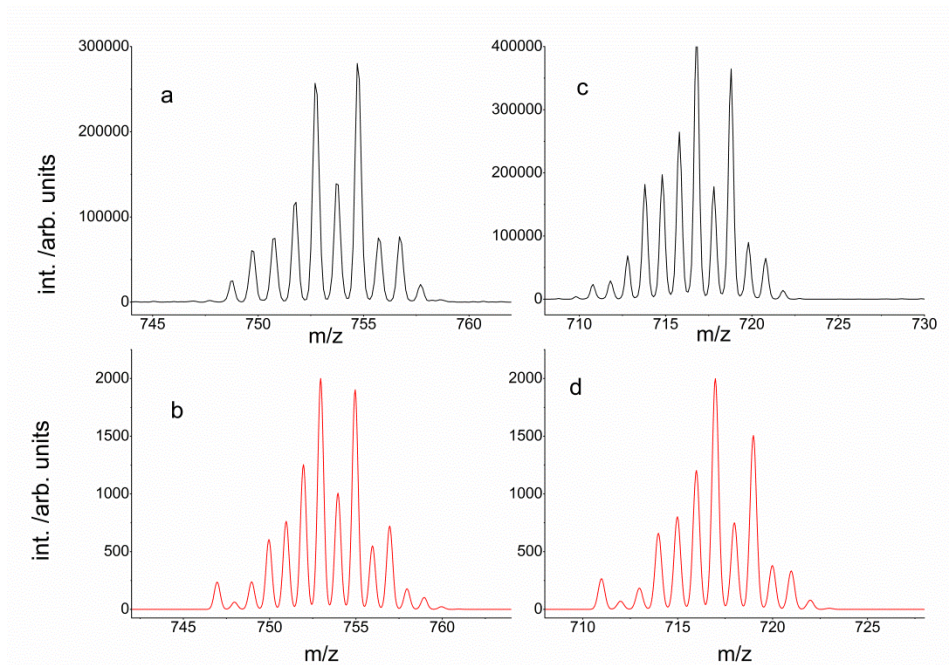


Figure 54. ESI-MS spectra of **19a**. Experimental spectrum $[M\text{-cymene}]^+$ (a) and simulated spectrum of $[M\text{-cymene}]^+$ (b) experimental spectrum of $[M\text{-HCl-cymene}]^+$ (c) and simulated spectrum of $[M\text{-HCl-cymene}]^+$ (d).

The ruthenium gold heterobimetallic complex **19c** was synthesized as shown in Scheme 29. In the ^1H NMR spectrum of compound **19c**, the resonances of the pyridylpyrimidine protons as expected shift to lower field after the coordination with ruthenium. The aromatic protons of the cymene ring give a multiplet between 5.99 and 6.10 ppm. The methyl groups of the cymene isopropyl substituent appear as two doublets at 0.97 ppm and 1.04 ppm. The ethylene protons are diastereotopic as well because of the coordination to a chiral metal center and give four sets of multiplets. All chemical shifts are summarized in Table 12.

Table 12. ^1H and ^{13}C NMR data of compound **19c**.

	1	2	3	4	5	6	7	8	9	NH	11	12	Me
δ_{H}	9.63	7.80	8.10	8.36	–	7.50	7.56	–	–	6.72	4.17 – 3.93	3.21 – 2.82	2.67
δ_{C}	157.0	140.0	146.8	125.0	153.9	162.9	109.5	165.2	161.3	–	44.6	31.2	25.0

The ^{13}C NMR spectrum of **19c** shows four peaks between 89.5 ppm and 84.9 ppm, which belong to the tertiary aromatic carbons of the cymene ligand, the peaks between 31.3 ppm and 15.9 ppm are assigned to the aliphatic carbon atoms of the cymene ring. The ^{31}P NMR spectrum shows one signal at 24.3 ppm and the chemical shift of the phosphorus atom is not affected by the introduction of the ruthenium cation as expected.

ESI-MS studies of **19c** were performed to obtain another proof for the complex formation. It has the molecular ion peak $[\text{M}]^+$ at m/z 902.8 and gives fragments similar as before. Fragmented ions $[\text{M}-\text{HCl}]^+$ at m/z 864.9, $[\text{M}-\text{cymene}]^+$ at m/z 768.7, $[\text{M}-\text{HCl}-\text{cymene}]^+$ at m/z 730.8, and $[\text{M}-\text{Ru}(\text{cymene})\text{Cl}_2-\text{HCl}]^+$ at m/z 595.0 were detected. Figure 55 and Figure 56 represent the experimental and simulated isotopic pattern of all fragmented ions of the complex **19c**.

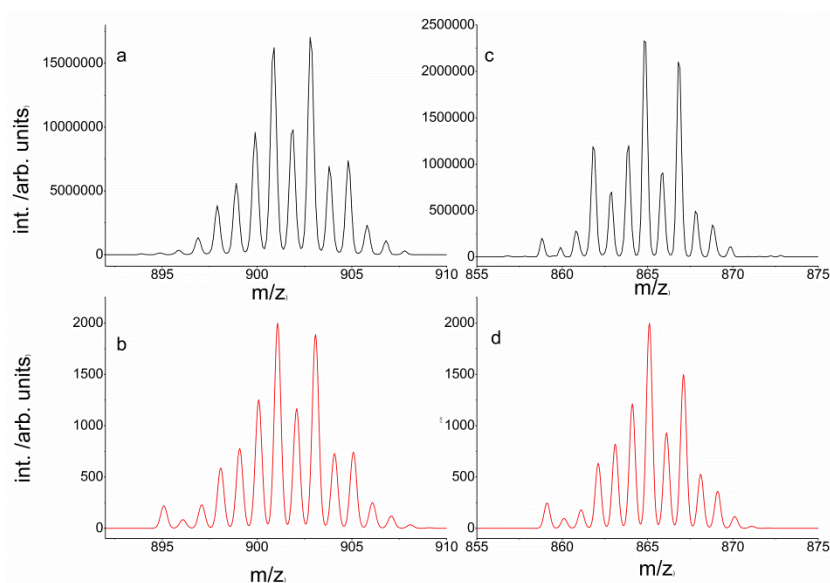


Figure 55. ESI-MS spectra of **19c**. Experimental spectrum of $[\text{M}]^+$ (a), simulated spectrum of $[\text{M}]^+$ (b) and experimental spectrum of $[\text{M}-\text{HCl}]^+$ (c), simulated spectrum of $[\text{M}-\text{HCl}]^+$ (d).

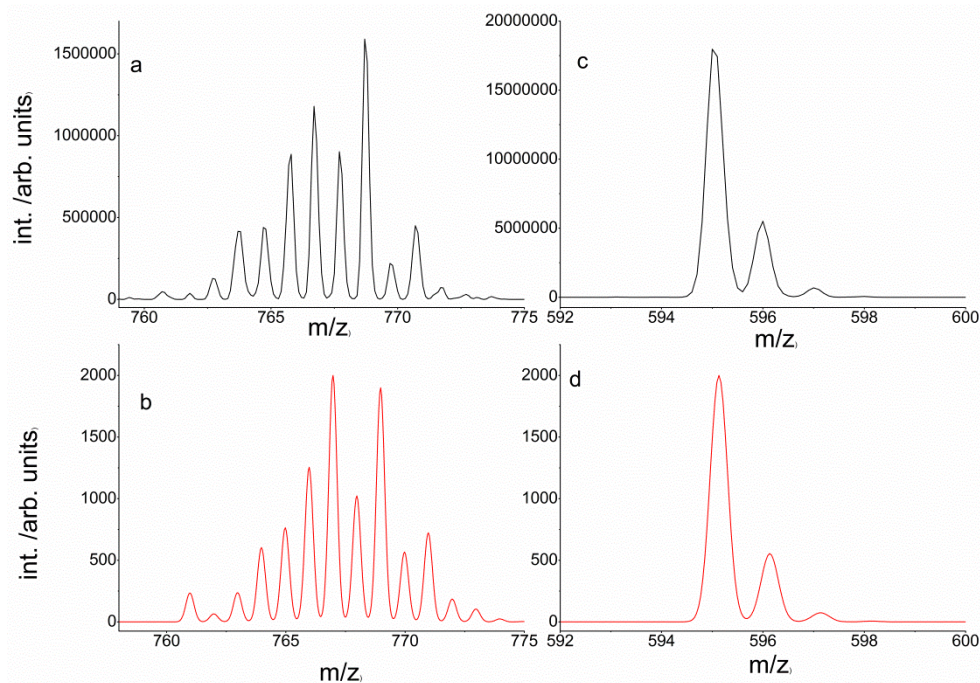
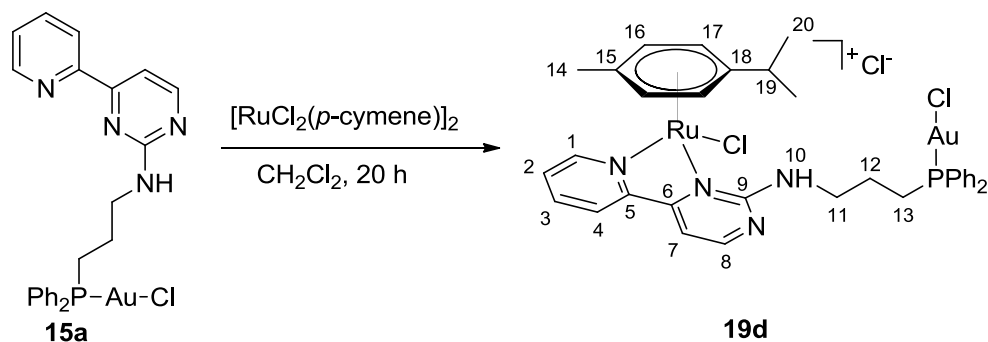


Figure 56. ESI-MS spectra of **19c**. Experimental spectrum of $[M\text{-cymene}]^+$ (a), simulated spectrum of $[M\text{-cymene}]^+$ (b) and experimental spectrum of $[M\text{-Ru}(p\text{-cymene})\text{Cl}_2\text{-HCl}]^+$ (c), simulated spectrum of $[M\text{-Ru}(p\text{-cymene})\text{Cl}_2\text{-HCl}]^+$ (d).

The heterobimetallic Ru-Au complex **19d** was also synthesized from the monometallic gold complex **15a** which has a propylene linker instead of ethylene between the amine and the phosphine. The reaction was carried out in dichloromethane at room temperature (Scheme 31).



Scheme 31. Synthesis of heterobimetallic Ru-Au complex **19d**.

Figure 57 shows the ^1H NMR spectrum of the bimetallic complex **19d**. Attaching the ruthenium center to the pyridylpyrimidine moiety causes a drastic increase in the chemical shift. Most significant changes are observed for H1 and H10 which are shifted

about 1.0 ppm downfield. The aromatic protons of the cymene ring appear as doublet of doublet at 6.08 ppm and 6.19 ppm and the diastereotopic methyl protons of the isopropyl unit give doublets at 0.95 ppm and 1.03 ppm. Then methylene protons of the propyl linker become diastereotopic due to bearing another chiral unit in the complex. The resonance of H11 shifts about 0.5 ppm downfield in comparison to the monometallic complex **15a**.

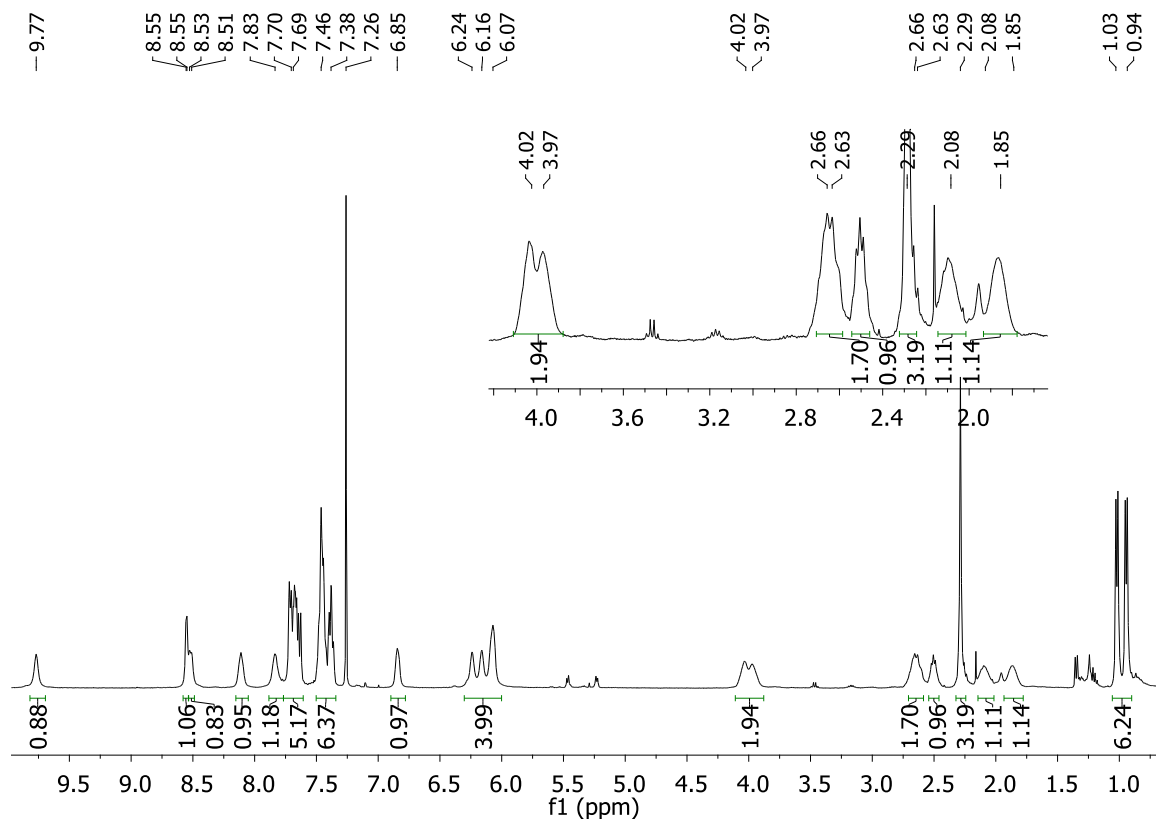


Figure 57. ^1H NMR spectrum of **19d**.

In the ^{13}C NMR spectrum of the bimetallic complex **19d**, C1 shifts from 149.9 to 163.1 ppm due to the coordination of the ruthenium center to the pyridylpyrimidine unit. Similar to the former complexes, the ^{31}P NMR spectrum of the complex **19d** contains one singlet at 28.30 ppm.

Besides the molecular ion peak, $[\text{M}]^+$ at 901.1, similar fragmentation patterns are observed in the mass spectrum of the heterobimetallic complex **19d**. The fragmented ions are identified as $[\text{M}-\text{HCl}]^+$ at m/z 865.1, $[\text{M}-\text{cymene}]^+$ at m/z 768.8, and $[\text{M}-(\text{Ru}(\text{cymene})\text{Cl}_2)]^+$ at m/z 595.0. In Figure 58 the experimental and the simulated isotopic patterns of $[\text{M}]^+$ and $[\text{M}-\text{HCl}]^+$ are shown.

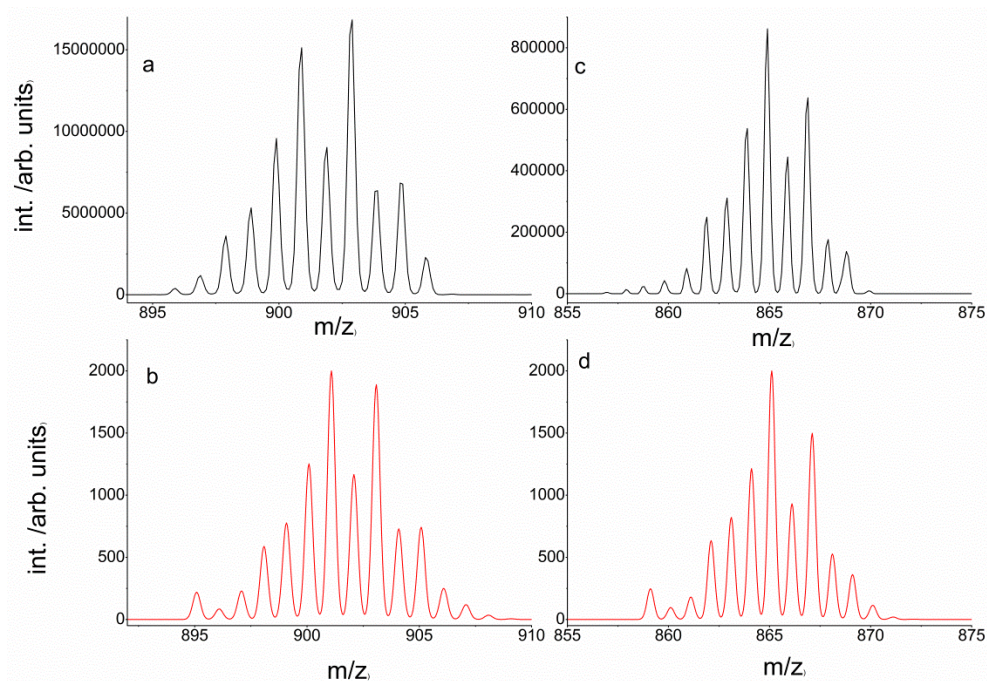


Figure 58. ESI-MS spectra of **19d**. Experimental spectrum of $[M]^+$ (a), and simulated spectrum of $[M]^+$ (b), experimental spectrum of $[M-HCl]^+$ (c) and simulated spectrum of $[M-HCl]^+$ (d).

Collisional-induced dissociation (CID) experiments were also done for the heterobimetallic ruthenium-gold complexes **19a** and **19d**. CID is a mass spectrometry technique to induce fragmentation in the gas phase. Selected ions can be activated in a collision cell by neutral gas molecules (e.g. helium, nitrogen or argon).^[157] After the collision process, the kinetic energy is converted to internal energy and causes bond cleavages leading to characteristic fragmentations. The resulting fragments are analyzed by the mass spectrometer. By the variation of internal kinetic energy of the ions, the added amount of internal energy after collision can be calculated. When the kinetic energy is kept constant, ions which show different reactivity can be compared. When CID curves for the complexes **19a** and **19d** are compared, it is clear that their fragmentation behavior is quite different. For both complexes, the most favorable fragmentation is the cleavage of $RuCl_2$ and a cymene group but they differ compared to each other in terms of the relative abundance of these fragmentation. **19d** gives 80% of the $[M-(RuCl_2-cymene)]$ fragment while **19a** gives same fragment with only 45%. They also show significant differences for the abundance of the HCl cleavage: the proportion of the species after HCl elimination is almost two times higher for the complex **19a** than for the complex **19d**. For

the complex **19a**, the least favorable fragmentation is the cleavage of the cymene group (less than 10%), while for the complex **19d**, this fragmentation is the second most favorable fragment (more than 10%). The least favorable fragment is the cleavage of HCl and cymene groups as less than 10% (Figure 59).

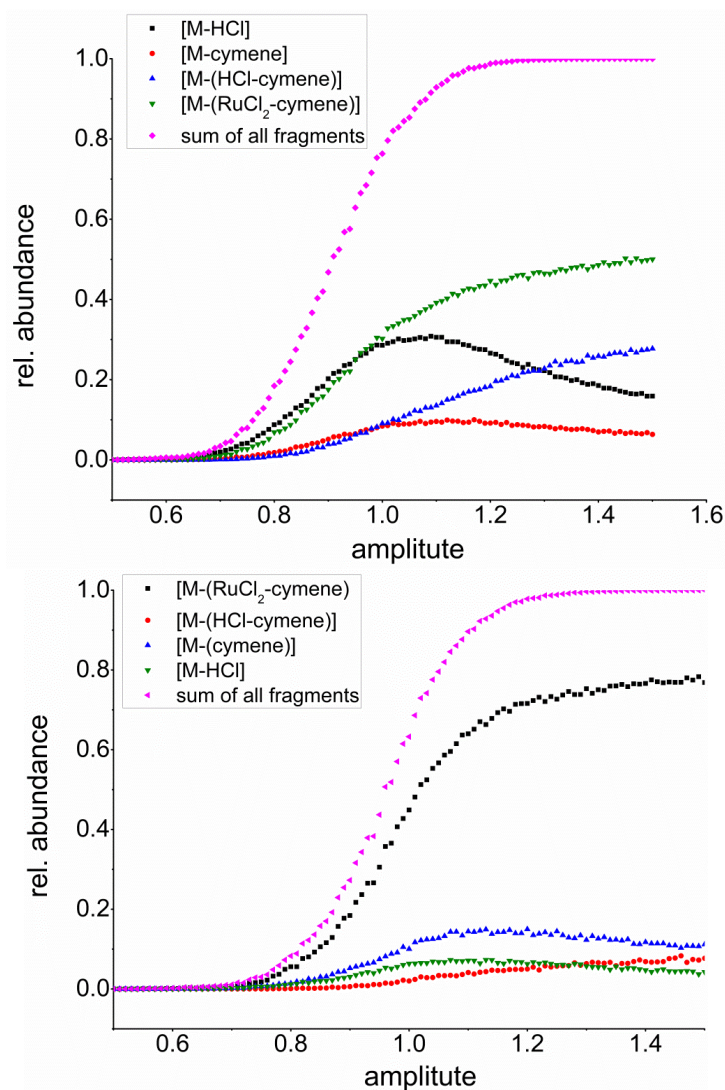


Figure 59. CID curves of complex **19a** (top) and complex **19d** (bottom).

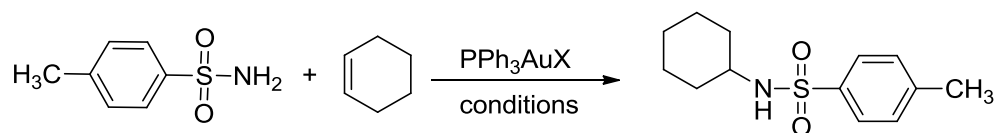
3.1.3 Catalytic Studies

As described before, heterobimetallic complexes are promising candidates for several catalytic reactions, e.g. hydrogenations catalyzed by the combination of Zn-Rh or hydroamidations catalyzed by the combination of Zn-Au. The cooperativity between these different metal centers can cause unique reactivities and higher yields in catalytic reactions. For this purpose, heterobimetallic Zn-Au and monometallic Au complexes were tested in catalytic hydroamidation reactions.

3.1.3.1 Catalytic Hydroamidation

Transition metal-catalyzed hydroamidation of the unactivated olefins is an important method for the preparation of nitrogen containing species.^[86] Palladium, platinum, and ruthenium are the examples that catalyze these type of transformations.^[158-161] However, they have some limitations. For instance, β -hydride elimination can be observed to produce unsaturated hydrocarbons as a by-product when palladium is used as a catalyst. A second major drawback of these methods is high catalyst loading for the intermolecular hydroamination reactions. Cationic gold(I) has the ability to activate the unactivated alkenes efficiently since it acts as a Lewis acid which activates carbon-carbon multiple bonds. This ability makes gold complexes appropriate candidates to become potential catalysts for the hydroamidation of alkenes.^[154,162,163]

Cyclohexene and *p*-toluenesulfonamide were chosen as model substrates to test the activity of novel catalysts for the hydroamidation transformation. The product, *N*-cyclohexyl-*p*-toluenesulfonamide can be synthesized in the presence of PPh_3AuX where X is triflate, hexafluoroantimonate, or tetrafluoroborate (Scheme 32).



Scheme 32. Hydroamidation of cyclohexene with TsNH₂.

In general, PPh_3AuX complexes are prepared in situ by mixing PPh_3AuCl and a silver salt to generate the cationic gold species which is the crucial active species for the reaction.^[39,86] There are two general mechanistic cycles proposed for the hydroamidation reaction: in one of them the activation of the olefin, in the other one, the amine activation is considered as the key point of the mechanism. For the gold(I) catalyzed hydroamidation reactions, mechanistic studies based on NMR experiments show that olefin is activated by gold(I).^[86,164]

A plausible reaction mechanism for the hydroamidation of cyclohexene was proposed by Ujaque et al. (Figure 60).^[165] The first step is the formation of an active gold species, then the substrate coordinates to the cationic gold center. Next, *p*-toluenesulfonamide as a

nucleophile attacks the alkene. The last step is the substrate-assisted protodeauration of the gold-amine intermediate.

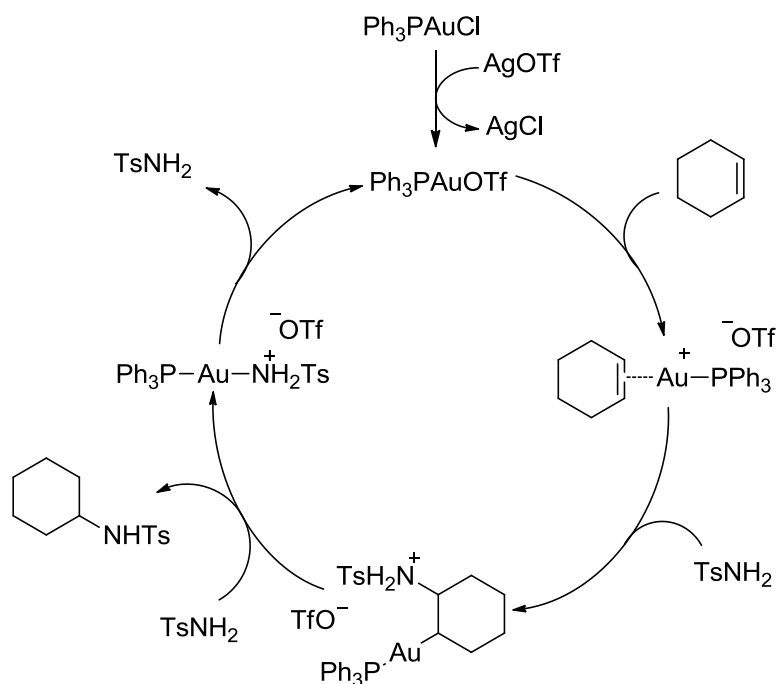


Figure 60. Possible catalytic cycle in the hydroamidation of cyclohexene.

Based on this information, the monometallic gold complex **14a** and the bimetallic Zn-Au complex **18a** were tested in the hydroamidation reaction of cyclohexene with *p*-toluenesulfonamide (Table 13).

Table 13. Reaction conditions for the hydroamidation of cyclohexene.

Entry	Au (mol%)	Ag (mol%)	Solvent	Temp.	Time	Yield ^a
1	PPh ₃ AuCl (4%)	AgSbF ₆ (4.4%)	DCE	90 °C	4 h	60%
2	14a (4.4%)	AgSbF ₆ (4.4%)	DCE	90 °C	4 h	N.R.
3	14a (5%)	AgSbF ₆ (15%)	Toluene	90 °C	24 h	N.R. ^b
4	14a (5%)	AgOTf (15%)	Toluene	90 °C	24 h	65% ^{b,c}
5	–	AgOTf	Toluene	90 °C	24 h	N.R. ^b
6	14a (5%)	–	Toluene	90 °C	24 h	N.R. ^b
7	18a (4%)	AgSbF ₆ (4.4%)	DCE	90 °C	4 h	N.R.
8	18a (10%)	AgSbF ₆ (11%)	Toluene	110 °C	24 h	N.R.
9	18a (5%)	AgOTf (15%)	Toluene	90 °C	24 h	N.R. ^b

^a NMR yield. ^b 3:1 mol ratio of cyclohexene/TsNH₂ was used. ^c Unexpected product

The gold complex **14a** and gold-zinc complex **18a** did not catalyze the hydroamidation reaction of cyclohexene after trying several conditions but in one case, an unexpected compound was obtained in 65% yield (entry 4). The ¹H NMR spectrum of the crude sample shows that the unexpected product is *N*-(cyclohex-2-enyl)-4-methylbenzenesulfonamide which is the oxidized form of the desired hydroamidated product (Figure 61).^[166]

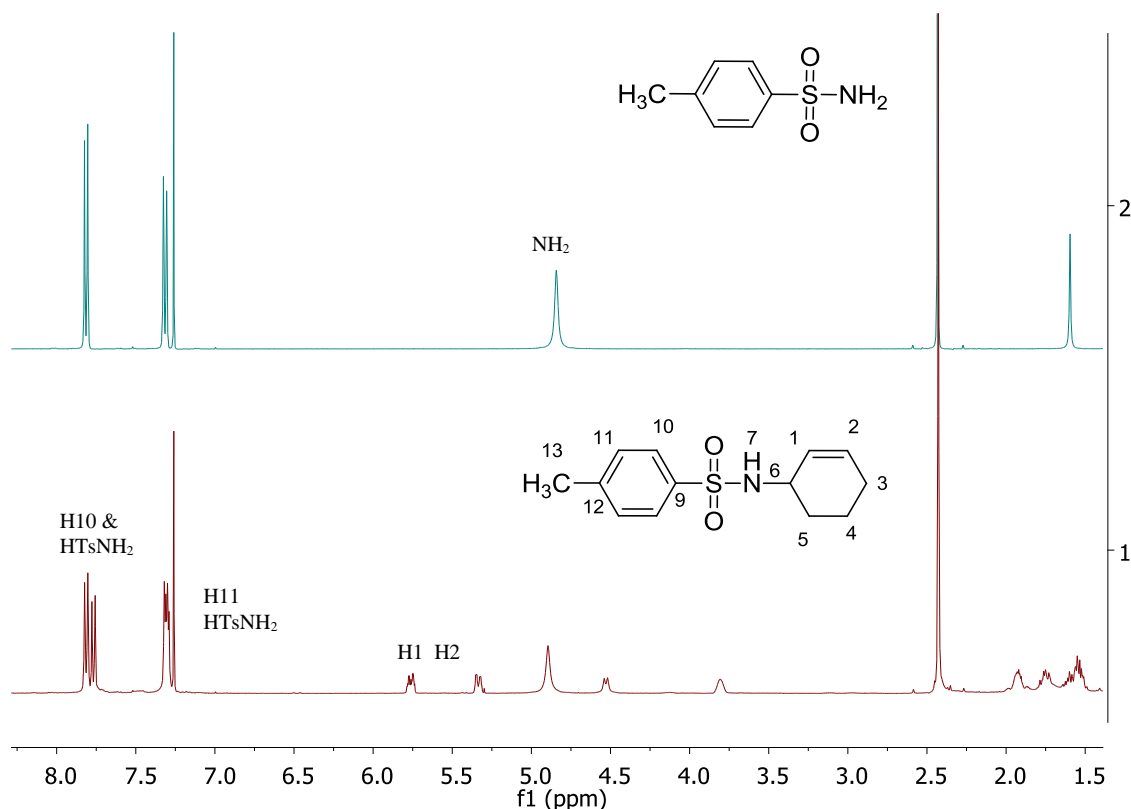


Figure 61. ^1H NMR comparison of TsNH_2 (top), mixture of TsNH_2 and unexpected hydroamidation product(bottom).

The ratio of *p*-toluenesulfonamide and *N*-(cyclohex-2-enyl)-4-methylbenzenesulfonamide was calculated as 3:4 by integrating the characteristic signals of each component. However, the formation of this unexpected product was not reproducible under the identical conditions. It can be suggested that the allylic C-H bond activation is done via a radical reaction pathway catalyzed by a trace amount of an impurity.

The catalytic studies showed that the complexes **14a** and **18a** are not active for the hydroamidation reaction of cyclohexene under these conditions. The reason might be the generating of the active cationic gold (I) species with the silver salt. In addition to this, gold(I) species are not very stable. For example, when the fluorinated counter anions were included, the product could not be isolated.^[167,168] Another possibility is that the secondary amine in the complex might inhibit the reaction by coordinating to the cationic gold species.

3.2 Pyrimidine Ligands with a Paracyclophane Backbone

[2.2]Paracyclophane was synthesized first by Brown and Farthing as a pyrolysis product of *p*-xylene which is extracted from a polymer.^[169] They have a planar chirality which makes them interesting for designing chiral ligands for asymmetric, metal catalyzed reactions. For example, [2.2]phanephos ligands are planar chiral systems which were produced by introducing two diphenylphosphine groups to the paracyclophane. Their rhodium complexes are very efficient catalysts in asymmetric hydrogenation reactions and show excellent enantioselectivities. The palladium complexes of *N,S*- and *N,Se*-ligands which were derived from [2.2]paracyclophane are also very active catalysts in asymmetric allylic alkylation reactions (Figure 62).^[170,171]

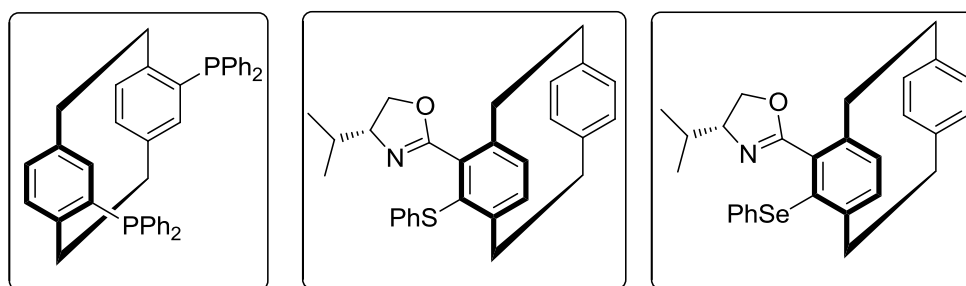
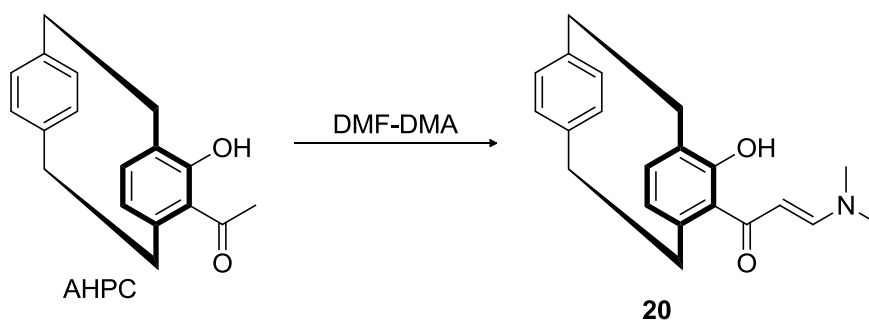


Figure 62. Examples of chiral paracyclophanes.

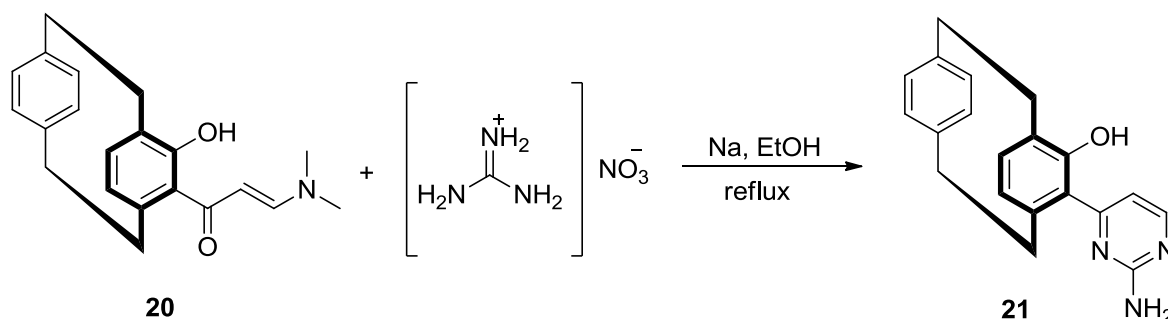
The synthetic route to pyrimidine ligands containing a paracyclophane backbone starts with the preparation of 5-acetyl-4-hydroxy[2.2]paracyclophane (AHPC). The synthesis was carried in the group of Prof. Dr. Stefan Bräse from Karlsruhe Institute of Technology. AHPC was then converted into the enaminone **20** using DMF-DMA (Scheme 33).^[172]



Scheme 33. Synthesis of enaminone **20**.

3.2.1 (1-Hydroxy-2-pyrimidine-4-amine)[2.2]paracyclophane

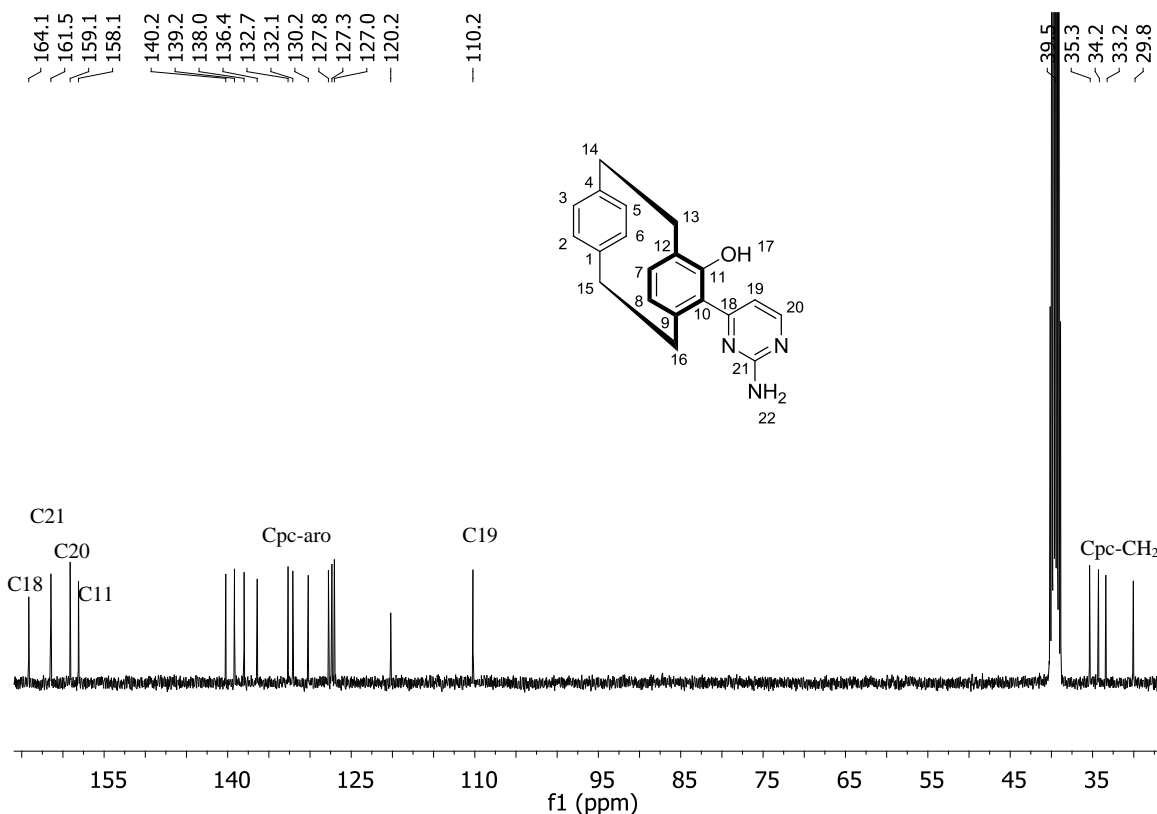
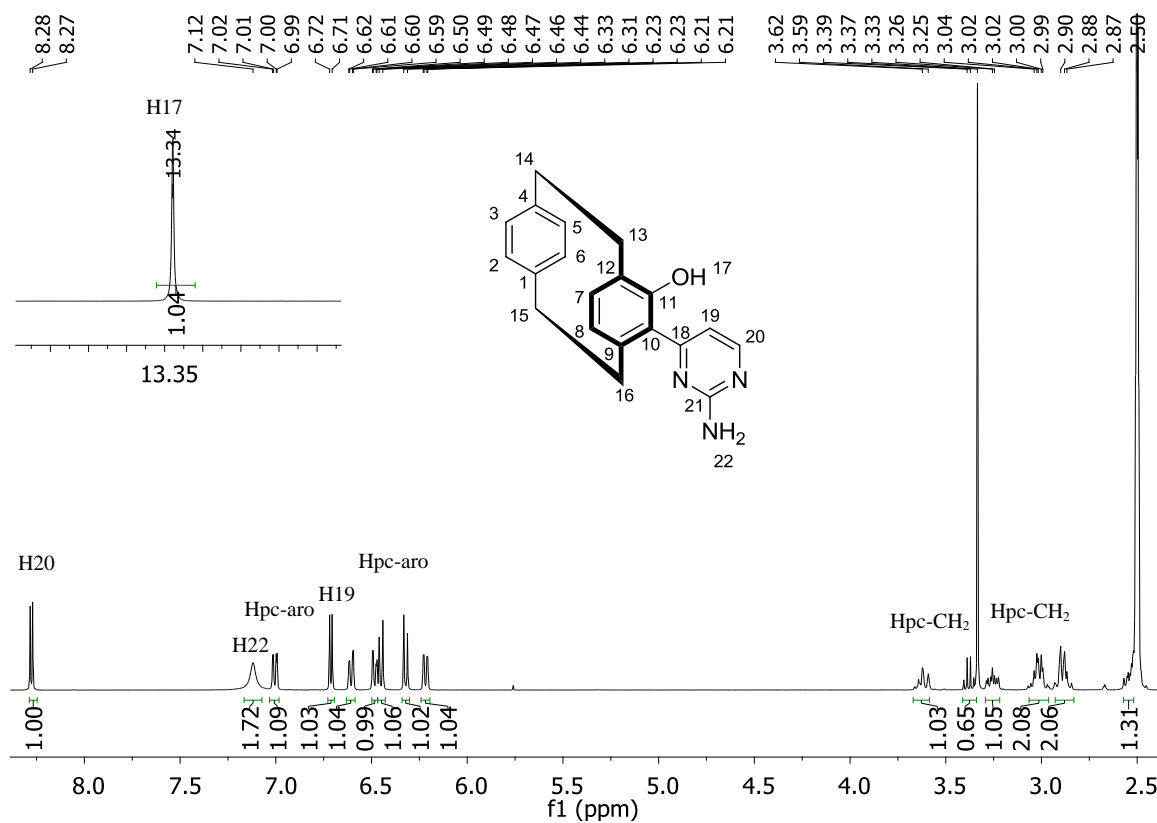
The target pyrimidinylparacyclophane **21** was obtained from the reaction of the enaminone **20** with an excess amount of guanidinium nitrate in the presence of sodium ethanolate under reflux conditions. After an extractive work-up with CH_2Cl_2 and crystallization a yellow solid was obtained in 65% yield (Scheme 34).



Scheme 34. Synthesis of pyrimidine **21**.

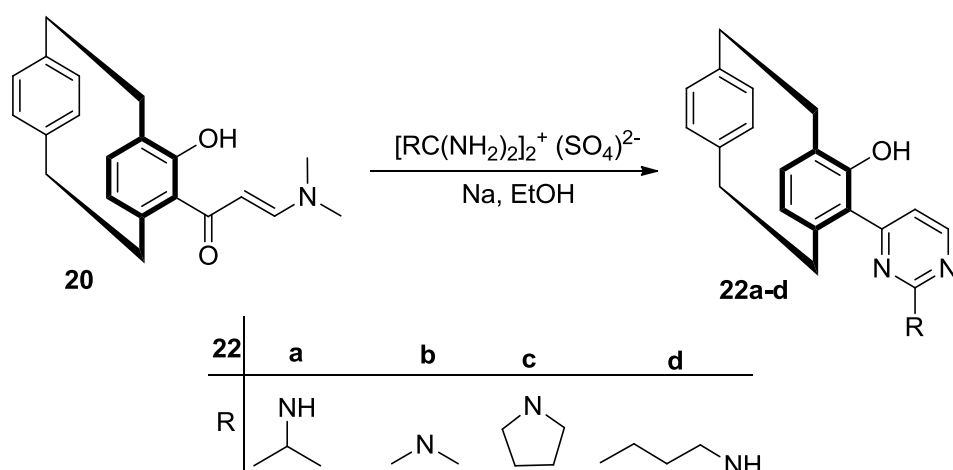
The ^1H NMR spectrum of **21** reveals a singlet at 7.12 ppm which belongs to the amine protons (Figure 63). Two protons of the pyrimidine ring, H19 and H20 appear as doublets at 6.71 ppm and 8.28 ppm, respectively. The other signals in the aromatic region belong to aromatic protons of paracyclophane ring. All methylene protons of the paracyclophane ring give multiplets between 2.52 ppm and 3.66 ppm. Moreover, the phenolic proton shows a broad singlet at 13.34 ppm as expected.

The ^{13}C NMR spectrum of compound **21** shows four peaks between 30.1 ppm and 35.4 ppm which are the signals of the methylene carbon atoms of the paracyclophane ring. The peak at 110.2 ppm belongs to C19. The spectrum reveals three additional peaks for the pyrimidine ring at 164.2 ppm, 161.5 ppm and 159.1 ppm that are assigned for C18, C21 and C20, respectively. There are also twelve peaks in the unsaturated carbon region which belong to the paracyclophane aromatic carbon atoms. The quaternary carbon attached to the hydroxyl group gives a signal at 158.1 ppm (Figure 64).



3.2.2 Synthesis of Substituted Pyrimidines with a Paracyclophane Backbone

Similar to the previous reaction, various pyrimidine ligands can easily be prepared, when R substituted guanidinium salts are used. Pyrimidinylparacyclophanes **22a-d** were obtained in good yields by treating the enaminone **20** with a proper guanidinium sulfate in the presence of NaOEt in ethanol under reflux conditions (Scheme 35). The substituted guanidinium precursors were prepared in our group by Dr. Leila Taghizadeh.^[173] Contrary to the synthesis of **21**, excess amounts of guanidinium sulfates were used (5–10 equivalents) for the synthesis of **22a-d**.



Scheme 35. Synthesis of pyrimidines **22a-d**.

The ¹H NMR spectrum of **22a** reveals a doublet at 1.26 ppm which belongs to the methyl protons of the isopropyl unit and the methine proton (H23) gives a signal 4.04 ppm as a broad singlet. Doublets at 8.32 ppm and 6.98 ppm belong to the pyrimidine protons and the NH proton shows a singlet at 7.61 ppm. The hydroxyl proton gives a signal at 13.23 ppm as a singlet. The methylene protons of the paracyclophane ring show multiplets between 2.54 ppm and 3.63 ppm (Figure 65).

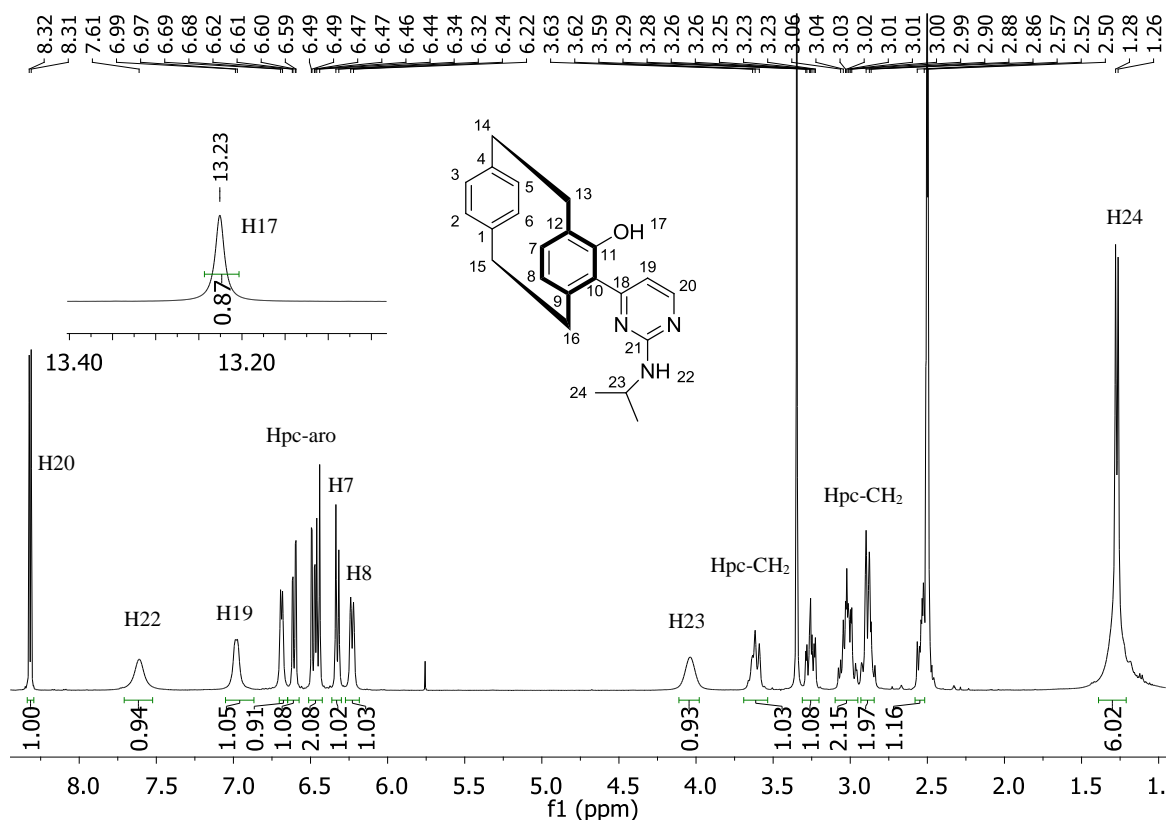


Figure 65. ^1H NMR spectrum of **22a**.

The ^{13}C NMR spectrum also proves the formation of the isopropyl substituted pyrimidine paracyclophane **22a**. It shows three new peaks in the saturated region (Figure 66). The peaks at 42.4 ppm belong to the methine carbon atom (C23), the peaks at 22.3 ppm and 22.4 ppm are the signals of methyl carbon atoms (C24a and C24b). The other four peaks in this saturated region belong to the methylene carbon atoms. There are also four new signals in the aromatic carbon region; the peak at 164.0 ppm is the signal of C18 which is connected to the paracyclophane ring, C21 gives a signal at 159.6 ppm. The other pyrimidine ring carbon atoms resonate at 158.7 ppm and 110.0 ppm.

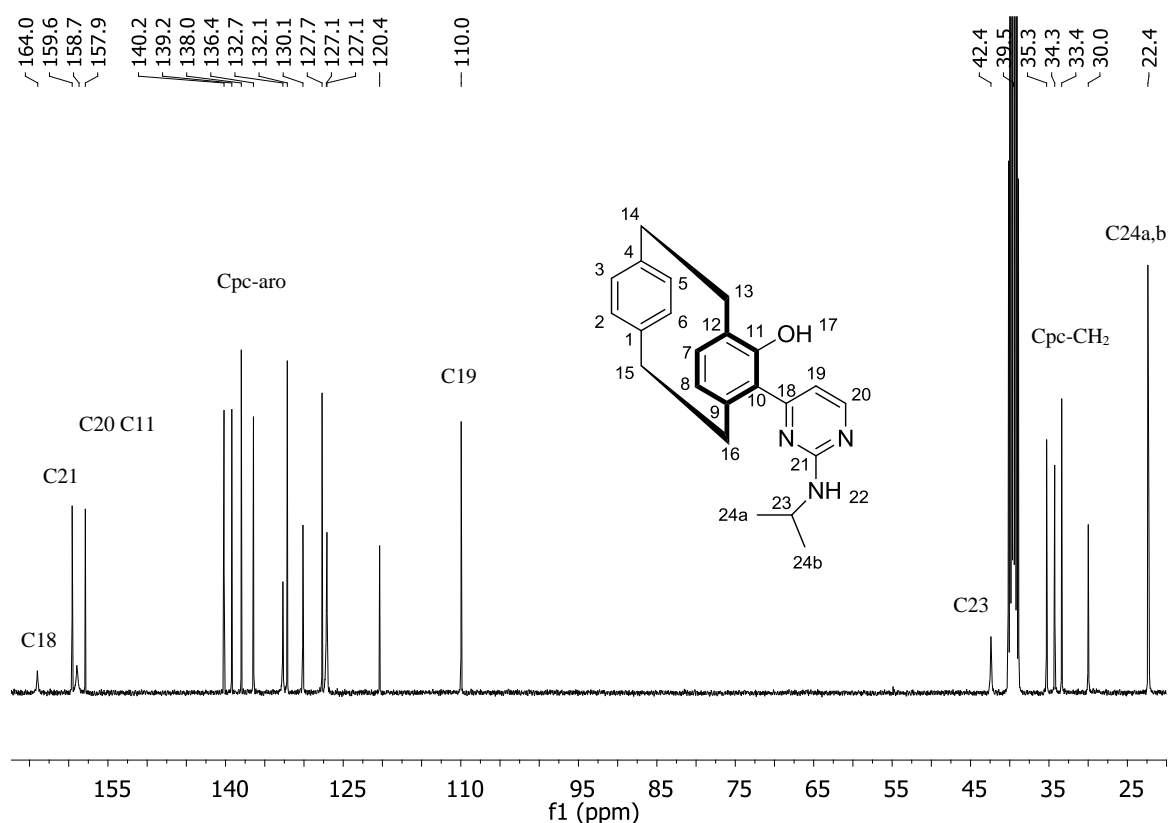


Figure 66. ^{13}C NMR spectrum of **22a**.

In the ^1H NMR spectrum of **22b**, H19 and H20 resonate as doublets at 6.75 ppm and 8.40 ppm. The signal at 13.01 ppm belongs to the hydroxyl proton. When the chemical shifts of compounds **21**, **22a**, and **22b** are compared, it is found that changing the alkyl substituent of the amine causes no significant change in the chemical shifts of the aromatic protons. In the ^{13}C NMR spectrum of pyrimidine **22b**, there are four additional carbon signals which belong to the pyrimidine carbon atoms and methyl carbon atoms give the signal at 37.4 ppm.

The ^1H NMR spectra of the compounds **22c,d** are similar in terms of the chemical shifts of the pyrimidine protons. While H19 of compound **22c** gives a doublet at 6.66 ppm, the same proton in compound **22d** resonates as doublet at 6.69 ppm. Similarly, the chemical shift values of H20 for both compounds have small differences. Methylene protons of the pyrrolidine unit in **22c** give multiplets between 2.13 ppm and 3.72 ppm, the butyl group of compound **22d** has four sets of multiplets in addition to the methylene protons of the paracyclophane backbone. The methylene groups attached to the nitrogen atom resonate downfield compared to the other $-\text{CH}_2$ protons as expected.

Recrystallization of the compound **22b** by slow evaporation of the solvent ($\text{CH}_2\text{Cl}_2/\text{EtOH}$) gave suitable crystals for X-ray diffraction analysis (Figure 67). The compound crystallizes in a monoclinic space group $P2_1/n$.

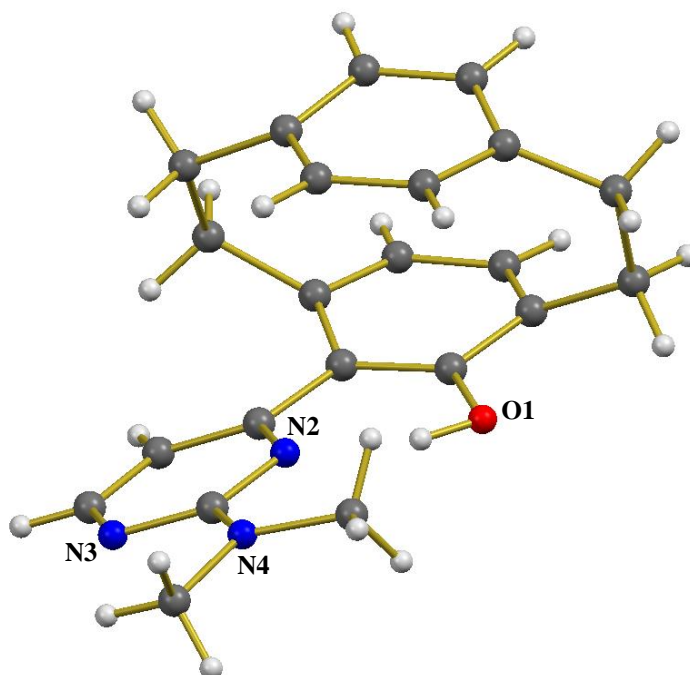


Figure 67. The molecular structure of pyrimidine **22b** in the solid state.

The synthesis of substituted paracyclophanes and their complexes are also interest of SFB/TRR88 (3MET) with the collaboration of Prof. Dr. Stefan Bräse group. The enantiomerically pure or enriched ligands and complexes are expected to show activities in asymmetric catalytic reactions.^[172] Furthermore, extending the pyrimidine ligands with a paracyclophane ring gives an opportunity to synthesize bimetallic complexes like Cu-Pd which could be suitable catalysts for the decarboxylative cross coupling arylation.

3.3 Pd(II) Coordinated *N,N,C*-Complexes

Palladacycles are complexes that contain at least one intramolecular palladium-carbon bond stabilized by one donor atom (N, O, S) and they are one of the most popular and important classes of cyclometallated compounds due to their extensive use in catalysis, organic synthesis, material science and C-H bond activation. The main reason of these rich applications of palladacycles is their redox change between the Pd(II)/Pd(0) oxidation states.^[174,175] There are several ways to generate palladacycles such as oxidative

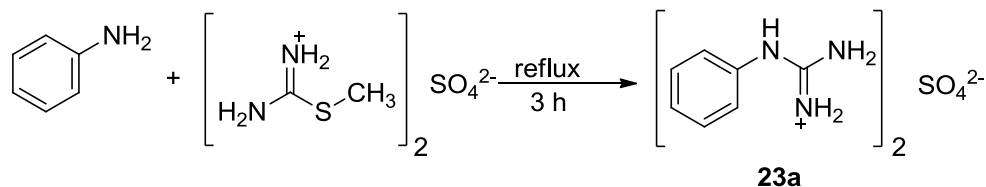
addition, transmetalation, nucleophilic addition to the unsaturated bonds or C-H activation. C-H bond activation is one of the most simple and most direct ways for the formation of palladacycles.^[176] The factors which affect the convenience and the mechanism of cyclopalladation are still under investigations. In the proposed mechanism, there is an intramolecular attack of the palladium site to the carbon atom which results in the formation of the chelate ring and elimination of the proton with the leaving group giving the activation of the C-H bond.^[169,177]

Cyclopalladation reactions have been studied since a long time but there are few examples which support the reaction mechanism with kinetic studies.^[178-181] Here, we aimed to synthesize *N,N,C*-coordinated palladium complexes and to explain the reaction mechanism with supporting kinetic measurements.

3.3.1 Synthesis of *N,N,C*-Pd Complexes

The Thiel group has recently reported the synthesis of (2-amino-pyrimidine-4-yl)pyridine ligands and the catalytic activation of their ruthenium complexes in transfer hydrogenation reactions. It is found that these ligands can show C-H bond activation on the pyrimidine site.^[87] Based on this knowledge, it was aimed to synthesize (2-amino-pyrimidine-4-yl)pyridine ligands bearing a phenylamino group. After the formation of *N,N*-coordinated Pd(II) complexes, C-H activation occurs on the phenyl ring. The first synthesis of these ligands and complexes has been performed by Dr. Leila Taghizadeh Ghoochany.^[173]

Here, the preparation of the aryl substituted guanidinium salts is showed in detail. There are several methods to synthesize the guanidinium salts depending on the functional groups of the guanidinium moiety.^[125-127] Two different routes can be used to prepare the target guanidinium salts. The first method is applied for the synthesis of the α -phenyl guanidinium sulfate.^[182] 2-Methyl-2-thiopseudourea hemisulfate and two equivalents of freshly distilled aniline were heated under reflux conditions (Scheme 36). During the reaction, methanethiol was released. After 3 hours, the product crystallized and was washed with ethanol until a colorless solid was obtained.



Scheme 36. Synthesis of α -phenyl guanidinium sulfate **23a**.

The ^1H NMR spectrum of compound **23a** does not show the -NH protons (Figure 68). Since the measurement was done in D_2O , all NH protons are exchanged against deuterium. The phenyl protons are observed clearly: the *meta* protons give a signal at 7.49 ppm as a triplet, the peak at 7.39 ppm belongs to the proton in the *para* position resonating as a triplet and the protons at the *ortho* position group give a doublet at 7.29 ppm.

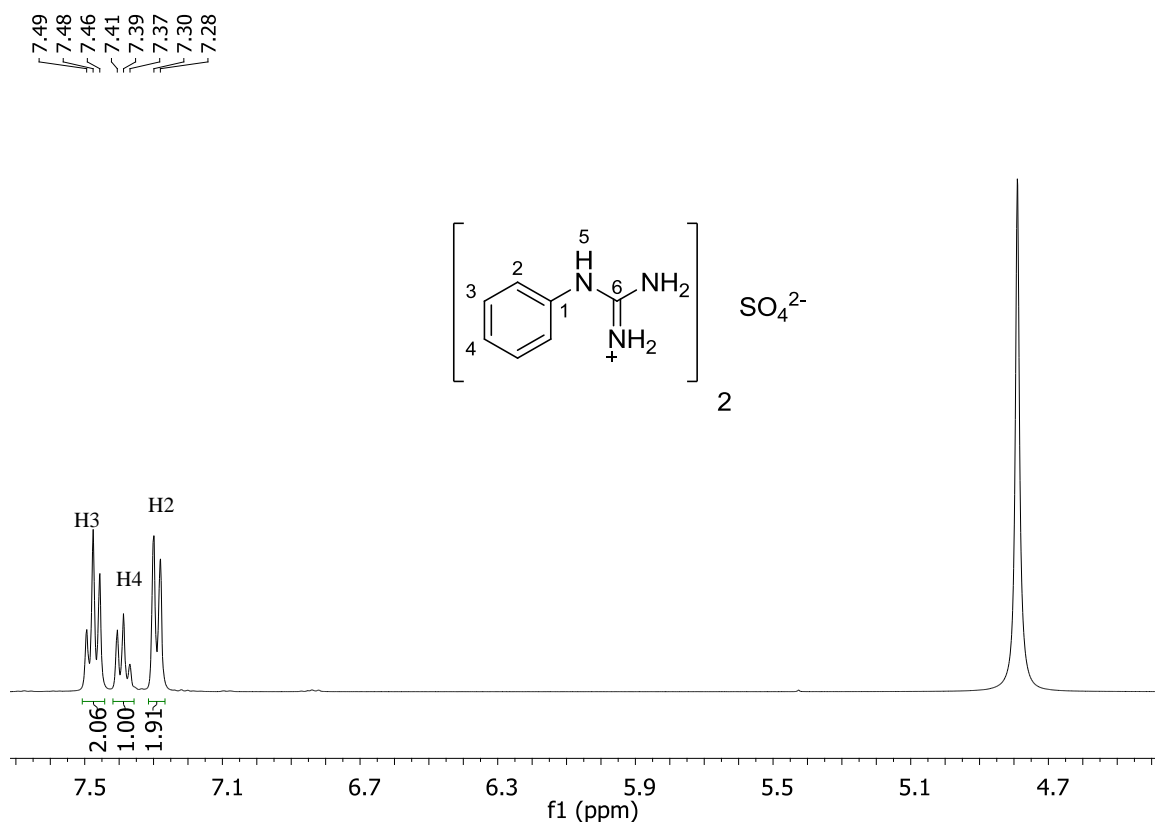


Figure 68. ^1H NMR of **23a** in D_2O .

The ^{13}C NMR spectrum reveals a peak at 156.3 ppm which belongs to the carbon atom connected to three nitrogen atoms (C6). The quaternary carbon atom attached to the -NH

group resonates at 134.0 ppm. Further three peaks at 129.9 ppm, 128.0 ppm and 125.8 ppm belong to the *meta*, *para* and *ortho* carbons, respectively (Figure 69).

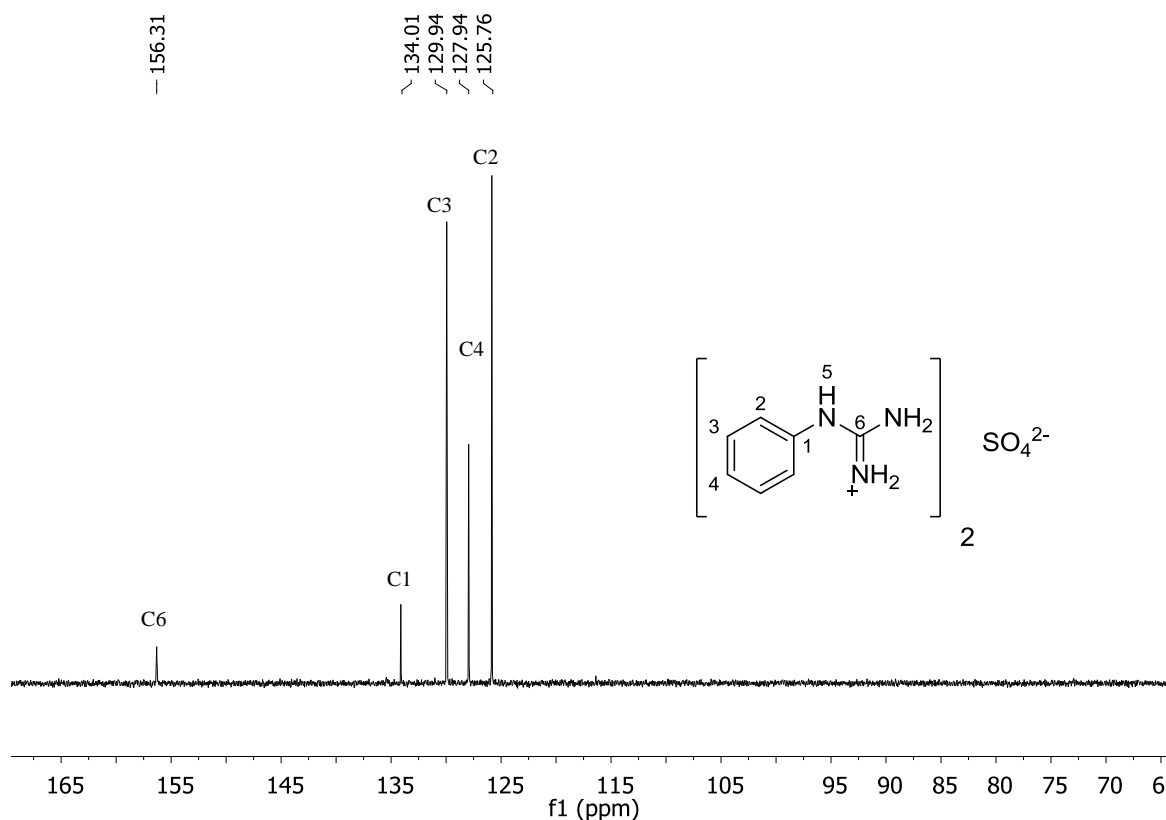
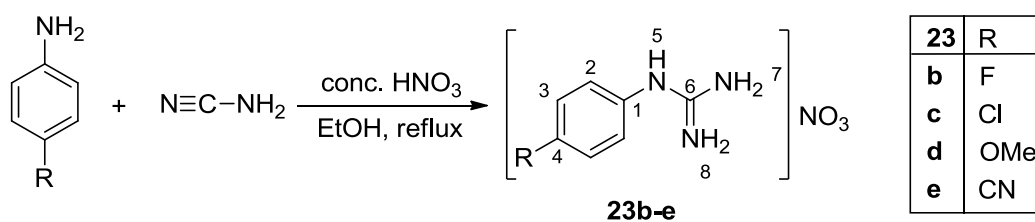


Figure 69. ^{13}C NMR spectrum of **23a**.

The second route is applied for the synthesis of *para* substituted aryl guanidinium salts. The arylamine was dissolved in ethanol. Concentrated nitric acid and a 50% aqueous solution of cyanamide (1.5 equivalents) were added to the solution. The reaction mixture was refluxed for 16 hours and cooled down to 0 °C. After adding diethyl ether, the solution was kept in refrigerator overnight and the resulting solids were collected by filtration (Scheme 37).



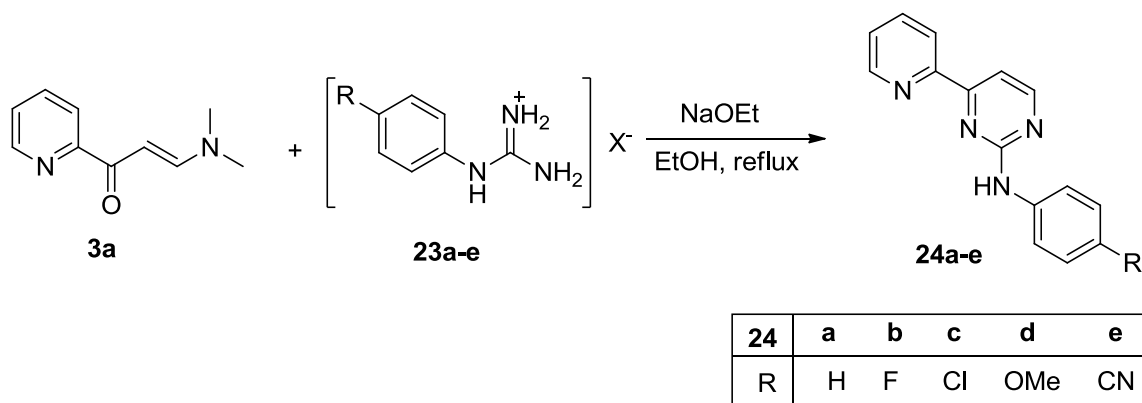
Scheme 37. Synthesis of guanidinium salts **23b-e**.

Table 14 summarizes all ^1H and ^{13}C NMR data of compounds **23b-e**. It can be seen from the table, that functionalization of the phenyl ring in the *para* position influences the ^1H NMR resonances of the hydrogen atoms. The electron-donating methoxy group leads to a shift of the phenyl group to higher field compared to the other guanidinium nitrates. Phenyl protons of compound **23e** resonate at lower field relative to the other salts because the presence of electron-withdrawing cyano group causes a downfield shift.

Table 14. ^1H and ^{13}C NMR data of **23b-e**.

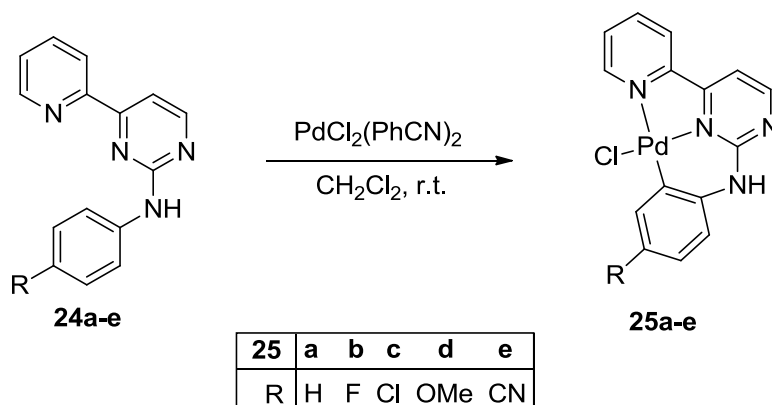
Compound	1	2	3	4	5	6	7	8	R	
23b	δ_{H}	–	7.35-7.29	7.25-7.16	–	–	–	–	–	
	δ_{C}	130.0	128.5	116.7	161.8	–	156.6	–	–	
23c	δ_{H}	–	7.29-7.16	7.48	–	–	–	–	–	
	δ_{C}	133.0	127.4	129.9	132.9	–	156.3	–	–	
23d	δ_{H}	–	7.18	7.00	–	9.40	–	7.23	7.23	3.77
	δ_{C}	127.5	127.3	114.9	158.2	–	156.3	–	–	55.4
23e	δ_{H}	–	7.40	7.88	–	10.04	–	7.66	7.66	–
	δ_{C}	118.6	123.4	133.9	140.7	–	155.3	–	–	107.5

As it was mentioned above, the synthesis and characterization of the ligands and complexes was carried out by. The *N,N,C*-ligands were synthesized by the condensation of a proper aryl guanidinium salt with (*E*)-3-(dimethylamino)-1-(pyridin-2-yl)prop-2-en-1-one in ethanol in the presence of NaOEt (Scheme 38). Both guanidinium nitrates and sulfates can be used in this reaction.



Scheme 38. Synthesis of the *N,N,C*-ligands **24a-e**.

The reaction of ligands **24a-e** with one equivalent of $\text{PdCl}_2(\text{PhCN})_2$ in dichloromethane at room temperature gave the desired tetra coordinate $\text{Pd}(\text{N,N,C})\text{Cl}_2$ complexes in almost quantitative yields (Scheme 39).



Scheme 39. Synthesis of $\text{Pd}(\text{N,N,C})\text{Cl}_2$ complexes **25a-e**.

3.3.2 Kinetic Studies

The reaction mechanism for the formation of cyclopalladated complexes was explained by kinetic experiments and the activation parameters for the complex formation were obtained by the help of these studies.

The kinetic studies of formation the $\text{Pd}(\text{N,N,C})\text{Cl}_2$ were carried out in collaboration with Adam Walli from the group of Prof. Dr. Franc Meyer at the University of Göttingen. The measurements were performed by UV-Vis spectrometry monitoring the spectral changes (Figure 70). Although the complex formation reactions (**25a-e**) were accomplished in

CH_2Cl_2 , the solubilities of the **25a-e** are quite poor in this solvent. Therefore, a mixture of $\text{CH}_2\text{Cl}_2/\text{DMSO}$ (1:1) was used as the solvent for the kinetic measurements to dissolve the complexes completely and to obtain a homogeneous solution. Figure 70 shows the absorption spectral changes graph of the reaction of $\text{PdCl}_2(\text{PhCN})_2$ with **24a** in $\text{CH}_2\text{Cl}_2/\text{DMSO}$ solution at 40°C . The isosbestic points of the UV-Vis spectrum are at 383 nm and 345 nm and the spectral changes are observed within the first 60 s after the addition of 0.66 mM of *N,N,C*-ligand to the palladium precursor. The isosbestic points at 433 nm and 355 nm are obtained 90 s after mixing. Based on this result, we proposed that the faster step is the coordination the pyrimidinylpyridine part of the ligand to the palladium metal which is followed by the cyclometalation as the rate determining step.

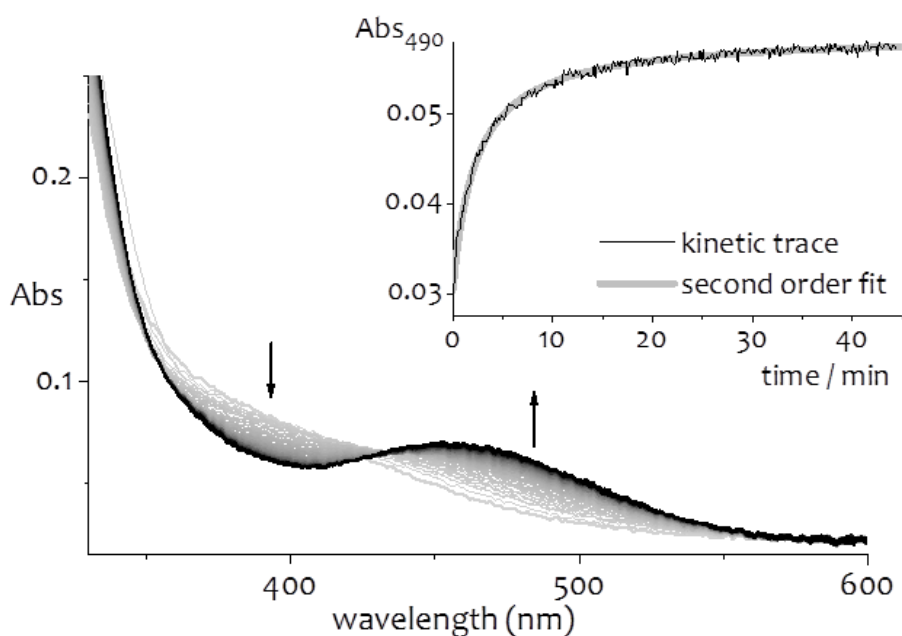


Figure 70. The absorption spectral changes of complex formation **25a**. Bold grey curve: $t = 90$ s after mixing; bold black curve: $t = 40$ min.

The inset in Figure 70 shows the spectral changes of the slow cyclometalation step that fits to a second order kinetic. The second order rate constant k differs for different ligands **25a-e**. The reaction rate is accelerated as the electron donor ability of the R substituent in ligands increases. It is an obvious sign that the reaction forms a positive charge during the rate determining step which is also supported by the Hammett analysis (plot of $(\log k/k_h)$ vs Hammett constants σ_{meta}).^[183,184] In Figure 71, the methoxy substituted ligand **25d** is

excluded and represented in grey because the average of the four measurements is not regarded in the fit due to large deviations between different measurements.

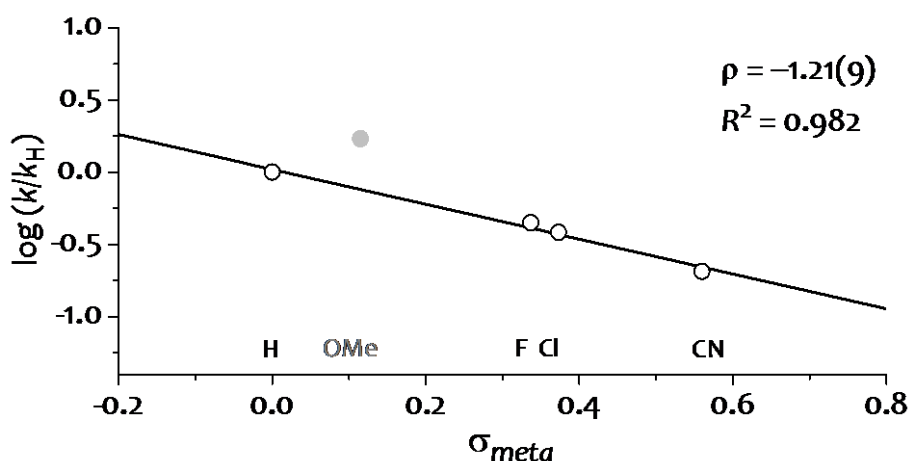


Figure 71. Hammett plot for the formation of complexes **25a-e** at 25 °C.

From the Hammett plot, a good linear correlation is acquired ($R^2=0.982$) with a negative slope/Hammett reaction constant ρ of -1.21 ± 0.09 at 25 °C. When the reactions were carried out at different temperatures, the ρ constant changed around -1 over the investigated temperature range. (An analogous plot with Hammett-Brown constants σ^+_{meta} gives a similar good correlation fit ($R^2=0.966$) and the same value for the reaction constant. However, the reaction constants σ and σ^+ are very similar for *meta* substituents) Therefore, it is proposed that an electrophilic aromatic substitution mechanism occurs which is indicated in Figure 72. In the proposed mechanism, the palladium metal acts as an electrophile. A proton is abstracted from the Pd-*N,N,C* complex by a chloride ion which behaves as a base. Generally, a second order kinetic suggests an intermolecular reaction during the proton abstraction.

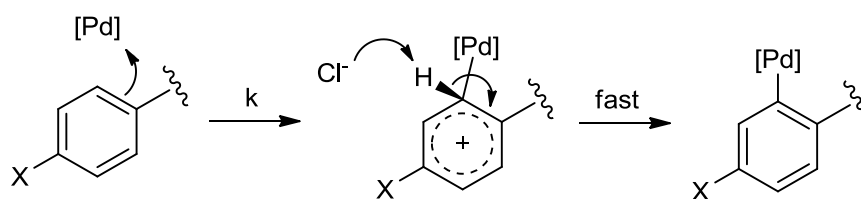


Figure 72. Proposed mechanism for the formation palladium complexes **25a-e**.

Full kinetic investigations were carried out in addition to the Hammett analysis in the temperature ranges between -10 and $+45$ °C. Temperature dependent respective rate constants were used to determine activation parameters for the rate limiting step. The Eyring plots are depicted in Figure 73.

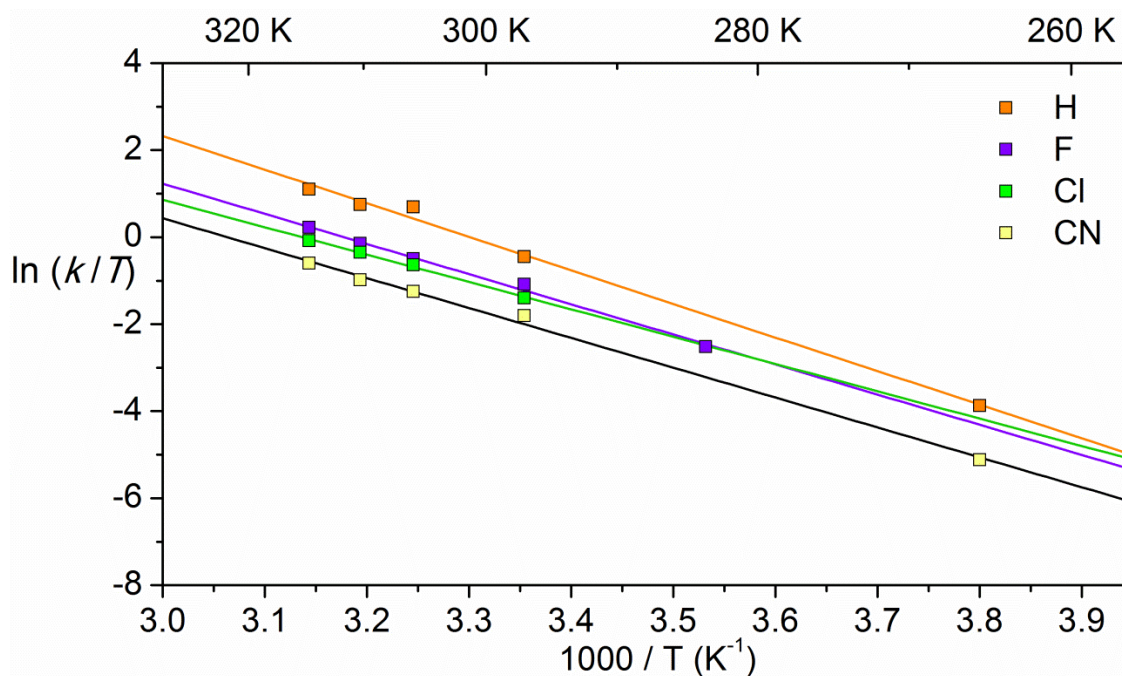


Figure 73. Eyring plots of the second order rate constants k for the formation of the complexes **25a-e** with linear regressions.

When the slopes of the linear fits in the Eyring plot are compared, it is observed that they are almost equal and derive the enthalpies of activation ΔH^\ddagger between 12.5 - 15.3 kcal mol⁻¹ (Table 15). However, the activation parameters could not be calculated for the methoxy substituted compound **25d** because the rate constants were not reproducible. Therefore, the rate constant was observed only at 25 °C. The entropies of activation ΔS^\ddagger are between 3.4 - 8.0 cal K⁻¹ mol⁻¹. While a decreasing trend in ΔH^\ddagger can be observed with more electron withdrawing substituents, a similar trend is more obvious for ΔS^\ddagger .

Table 15. Activation parameters for the reaction PdCl₂(PhCN)₂ with *N,N,C*- ligands.

X	k_{298} [M ⁻¹ min ⁻¹]	R^2	ΔH^\ddagger [kcal mol ⁻¹]	ΔS^\ddagger [cal K ⁻¹ mol ⁻¹]	ΔG_{298}^\ddagger [kcal mol ⁻¹]
OMe	335.4				
H	197.5	0.993	15.32 ± 0.65	3 ± 2	14.31 ± 0.93
F	88.1	0.993	13.76 ± 0.60	-4 ± 2	14.79 ± 0.84
Cl	75.7	0.993	12.48 ± 0.65	-8 ± 2	14.88 ± 0.91
CN	40.5	0.995	13.64 ± 0.49	-5 ± 2	15.25 ± 0.69

According to the Eyring plots, the parallel linear fits shift down to lower values with more electron withdrawing substituents. This results in entropies which are more negative, rendering the reactions to be less entropically favored and more ordered transition states are indicated. Entropies around zero are difficult to interpret.^[185] However, since the entropies are mostly negative, an associative mechanism in the rate determining step is favored, which is in accordance with the mechanism stated in Figure 72.

4 Conclusion and Outlook

In summary, three different synthesis plans were evaluated in order to prepare aminophosphine substituted pyridylpyrimidines. The pyridylpyrimidine aminophosphine ligands were finally synthesized via a cyclization process starting from 3-(dimethylamino)-1-(pyridin-2-yl)prop-2-en-1-one or 3-(dimethylamino)-1-(pyridine-2-yl)but-2-en-1-one with excess amounts of the corresponding phosphine functionalized guanidinium salts in the presence of a base (Figure 74). For this step, the synthesis of proper guanidinium salts was crucial. Thus two different guanidinium salts were prepared from 2-(diphenylphosphinyl)ethylamine or 3-(diphenyl-phosphinyl)propylamine.

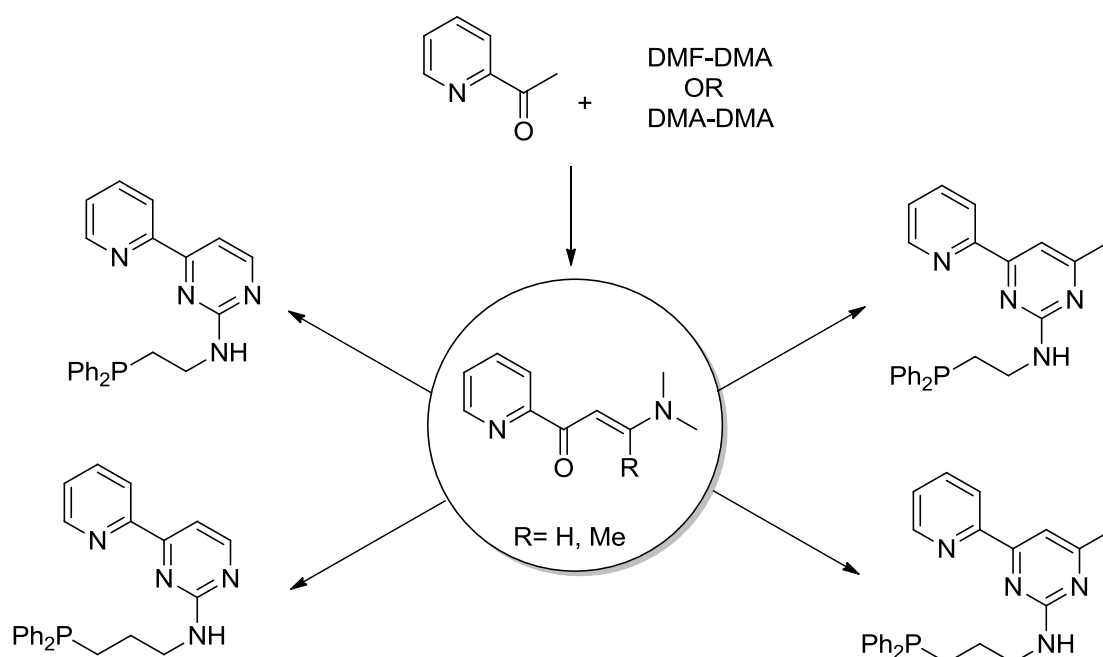


Figure 74. Synthesis of pyridylpyrimidine aminophosphine ligands.

These bidentate *N,N,P*-ligands were applied for the synthesis of bimetallic complexes, and as a part of SFB/TRR-88 3MET investigations. They contain hard (nitrogen) and soft (phosphorous) donor sites allowing the coordination of two different metal centers. First, the gold(I) complexes of all *N,N,P*-ligands were synthesized using Au(tht)Cl as the gold precursor. The gold center coordinates only to the phosphorous donor which has been proved by X-Ray crystallography and ³¹P NMR spectroscopy. After introducing the gold center, the synthesis of the heterobimetallic complexes with different metal combination

was achieved. For this purpose, $\text{Pd}(\text{PhCN})_2\text{Cl}_2$, ZnCl_2 , $[\text{Ru}(p\text{-cymene})\text{Cl}_2]$ were used as metal sources (Figure 75).

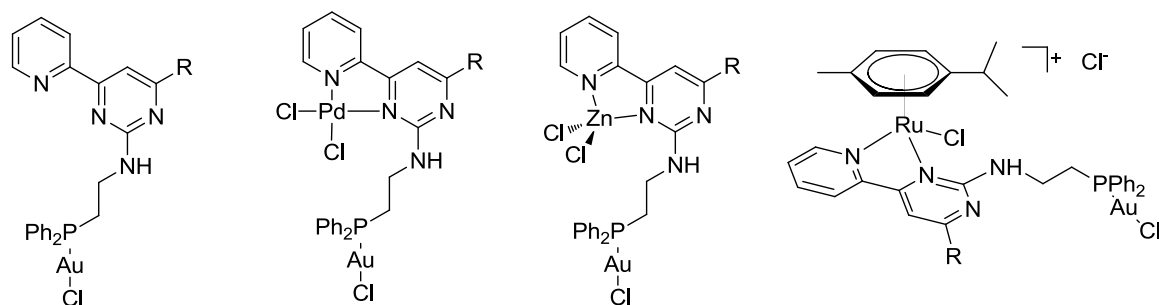


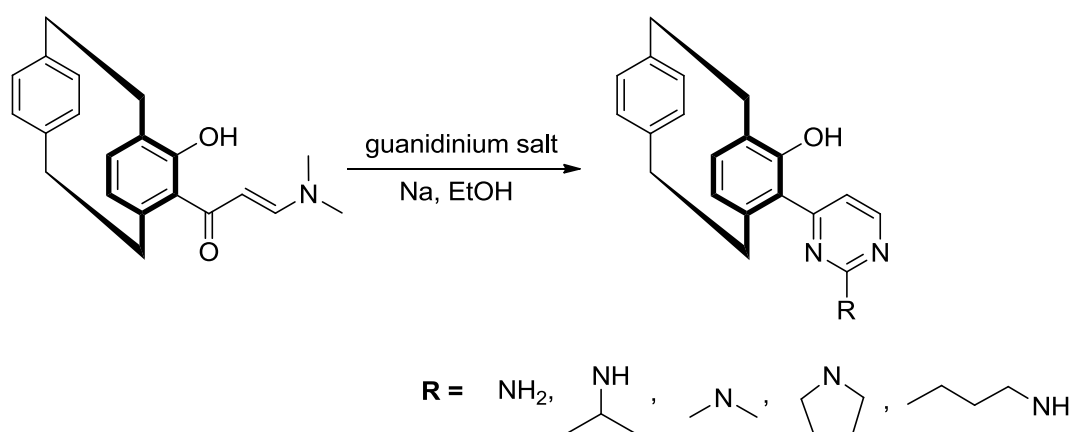
Figure 75. Some of the synthesized mono- and bimetallic complexes.

The second metal centers coordinated to the *N,N* donor site which was characterized by the help of NMR spectroscopy. Moreover, ESI-MS measurements were carried out by Johannes Lang from the physical chemistry at the TU Kaiserslautern.

Rhodium was additionally used as a second metal for the synthesis of mono metallic complexes. Here, rhodium (I) dicarbonyl chloride dimer was chosen as the rhodium source and the trans-coordinated complex $\text{RhClCO}(\text{L})_2$ ($\text{L} = (2\text{-amino})\text{pyridylpyrimidinyl}$ diphenylphosphino ligand) was successfully synthesized. The characterization of this complex was done by NMR and IR spectroscopy. In the IR spectrum of this compound, there was one strong absorption band at 1965 cm^{-1} being assigned to the carbonyl stretching vibration. Bi- and trimetallic complexes with this rhodium compound can be synthesized in future. Here different metal combinations might be possible such as Rh-Zn or Rh-Ru probably showing catalytic activities in different organic transformation reactions.

The fully characterized Au(I) and Au-Zn complexes of *N,N,P*-ligands described above were tested as catalysts for the hydroamidation reaction of cyclohexene with *p*-toluenesulfonamide. They did not show catalytic activity under the conditions tested. Further studies to understand the catalytic activities and cooperativity between the two metal atoms are required. In addition, these complexes have the potential to show activity in other transformations such as a gold catalyzed hydroarylation and a gold-palladium catalyzed coupling reactions.

As the group is a member of SFB/TRR-88 3MET, there several collaborations with other working groups at TU Kaiserslautern and Karlsruhe Institute of Technology were important for the success of this work. One of them was the collaboration with the group of Prof. Dr. Stefan Bräse, which aimed to introduce chiral paracyclophane moieties to the pyrimidine linkers substituted with an amino or an aminophosphine group. The starting compounds hydroxyl [2.2]paracyclophane and 5-acetyl-4-hydroxy[2.2]paracyclophane (AHPC) were synthesized at the KIT. The synthesis of an hydroxyl [2.2]paracyclophane substituted enaminone was accomplished using AHPC and DMF-DMA. Five different paracyclophane substituted aminopyrimidine ligands were synthesized by a cyclization reaction with excess amounts of guanidinium salts under basic conditions (Scheme 40).



Scheme 40. Synthesis of paracyclophane substituted aminopyrimidines.

The characterization of the synthesized compounds was carried out by NMR, FT-IR spectrometry, and also by single crystal X-Ray measurements. These ligands can be also functionalized with aminophosphine unit. Introduction of the metal centers to these chiral ligands and their application in asymmetric catalytic reactions can be performed in future.

Dr. Leila Taghizadeh Ghoochany had synthesized some 2-(arylamino)pyrimidin-4-yl)pyridine ligands and their palladium complexes in the past and found C-H activation occurring at the phenyl ring of the 2-(2-phenylaminopyrimidin-4-yl)pyridine ligand. In my work I investigated the reaction mechanism by kinetic studies. The kinetic measurements of the cyclopalladation reaction were carried out by using UV-Vis spectroscopy in Göttingen. According to the spectral studies of the cyclometalation step, the reaction fits a second order kinetics. It was proposed that the mechanism of the

cyclopalladation reaction is similar to an electrophilic aromatic substitution at aniline site with palladium center acting as the electrophile (Figure 76).

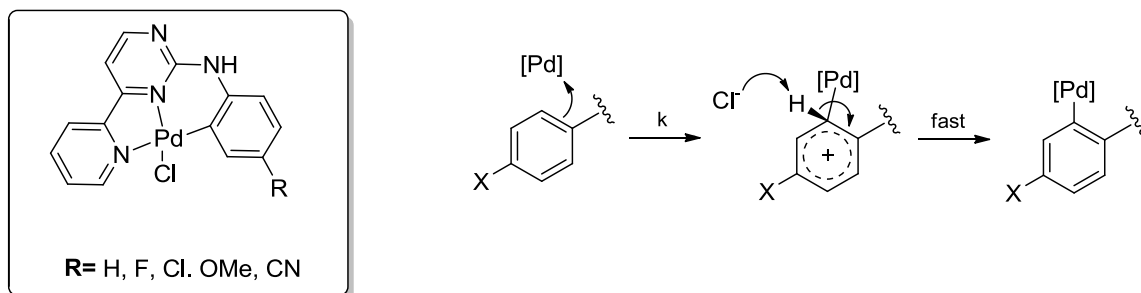


Figure 76. Proposed mechanism for the formation of Pd-*N,N,C*-complexes.

In addition to this, a full kinetic investigation was performed at different temperatures. According to the temperature dependent rate constants, the activation parameters were calculated. Eyring plots $\ln(k/T)$ vs T^{-1} gave activation enthalpies ΔH^\ddagger in the range between 12.5-15.3 kcal mol⁻¹ and also showed the entropies of activation being quite small between 3.4 and -8.0 cal K⁻¹ mol⁻¹ which can be interpreted that the reactions are less entropically favored and more ordered in the transition state.

5 Experimental

5.1 General Methods

All air and moisture sensitive reactions were performed under nitrogen atmosphere using the Schlenk techniques with dry solvents. The chemicals were purchased from ACROS, Sigma Aldrich, ABCR, Merck, STREM Chemicals and Alfa Easer and used without further purification unless otherwise noted.

5.2 Instrumental Analysis

NMR Spectroscopy

- Bruker AVANCE 200 (^1H : 200.1 MHz, ^{13}C : 50.3 MHz, ^{31}P : 81.0 MHz)
- Bruker AVANCE 400 (^1H : 400.1 MHz, ^{13}C : 100.6 MHz, ^{31}P : 162.0 MHz)
- Bruker AVANCE 600 (^1H : 600.1 MHz, ^{13}C : 150.9 MHz, ^{31}P : 243.0 MHz)

The chemical shifts were given in δ ppm value [ppm]. As an internal standard, the resonance signals of the residual protons of the deuterated solvents were for the ^1H spectra; Chloroform: 7.26 ppm, D_2O : 4.79 ppm, DMSO: 2.50 ppm, Methanol: 3.31 ppm and the residual signals for ^{13}C spectra Chloroform: 77.16 ppm, DMSO: 39.52 ppm, Methanol: 40.00 ppm. For ^{31}P NMR spectra, 85% phosphoric acid was used as the external standard. Abbreviation: s = singlet, d = doublet, t = triplet, q = quartet, m = multiplet and br. = broad.

Elemental Analysis

The percentage of carbon, hydrogen, nitrogen and sulfur was determined at the analytical laboratory of the TU Kaiserslautern Chemistry using with *Vario MICRO cube* elemental analyzer by the Firma Elementar.

ESI-MS Spectroscopy

The ESI-MS measurements were performed in the Physical Chemistry by Dipl.–Chem. Johannes Lang from Prof. Dr. Gereon Niedner-Schatteburg working group.

Bruker Esquire 6000plus ion trap spectrometer was used for all the measurements. 10^{-3} - 10^{-4} molar solutions of the samples were prepared in the acetonitrile.

Infrared (IR) Spectroscopy

The infrared spectra were recorded using with a *Perkin Elmer FT-ATR-IR 1000* spectrometer containing a diamond coated ZnSe-window. Abbreviation: w = weak, m = medium, s = strong.

X-Ray Absorption Spectroscopy

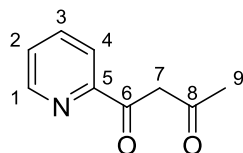
The measurement of crystal structures were carried out by Dr. Yu Sun on an Oxford Diffraction Gemini S Ultra. The detailed data of the crystal structures are given in Appendix.

Kinetic Measurements

The kinetic studies were performed using with UV-Vis spectroscopy at University of Göttingen. Measurements were done directly in the reaction solutions with an all quartz immersion probe in a custom made reaction tube (transmission measurement with 1 mm optical path, Hellma Analytics). Cary 50 Bio spectrometer was used to record time-dependent UV-Vis spectra every ~10 s by the use of a fiber optical connection. Temperature controls of the solutions were accomplished with Lauda ECO RE 630 cryostat.

5.3 Synthesis of 1,3-Diketones

5.3.1 1-(Pyridin-2-yl)butane-1,3-dione (1a)



To a well stirred solution of 2.70 g (50.0 mmol) of NaOMe in 50 ml anhydrous Et₂O, a solution of 7.50 g (50.0 mmol) of ethyl picolinate in 25 ml Et₂O was added dropwise over 20 minutes. After the addition was completed, a solution of 5.80 g of acetone (100 mmol) in 25 ml Et₂O was added dropwise over 20 minutes under nitrogen atmosphere. After refluxing for 3 hours, the solution was cooled down to room temperature and 100 ml of iced water was added. The resulting solution was acidified with 3.00 ml of glacial acetic acid. The organic phase was washed three times with water and dried over Na₂SO₄. The product was obtained after removing all volatiles under reduced pressure.

Yield: 6.10 g (37.4 mmol, 74 %, yellow liquid).

Elemental Analysis: C₉H₉NO₂ (163.17 g/mol)

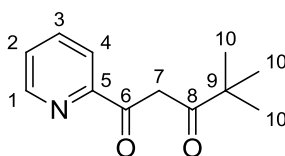
Calculated : C: 66.25% H: 5.56% N: 8.58%

Found : C: 65.46% H: 5.62% N: 8.40%

¹H NMR (600.1 MHz, CDCl₃, 20 °C) of the enol form: δ 15.62 (s, 1H, OH), 8.53 (dd, ³J_{HH} = 4.8 Hz and ⁴J_{HH} = 1.8 Hz, 1H, H1), 7.93 (d, ³J_{HH} = 7.8 Hz, 1H, H4), 7.69 (td, ³J_{HH} = 7.8 Hz and ⁴J_{HH} = 1.7 Hz, 1H, H3), 7.27 (ddd, ³J_{HH} = 7.6 Hz, ³J_{HH} = 4.8 Hz and ⁴J_{HH} = 1.1 Hz, 1H, H2), 6.70 (s, 1H, H7), 2.09 (s, 3H, H9) ppm.

¹³C NMR (151.0 MHz, CDCl₃, 20 °C) of the enol form: δ 194.8 (s, C6), 180.7 (s, C8), 151.9 (s, C5), 149.1 (s, C1), 136.9 (s, C3), 126.2 (s, C2), 122.0 (s, C4), 97.2 (s, C7), 25.9 (s, C9) ppm.

IR $\tilde{\nu}$ (cm⁻¹): 3456 (w), 3065 (w), 3006 (w), 2970 (w), 1981 (w), 1737 (m), 1724 (m), 1605 (s), 1578 (s), 1563 (s), 1426 (s), 1354 (s), 1284 (s), 1231 (s), 1217 (s), 1079 (m), 1043 (w), 1020 (w), 990 (s), 937 (m), 847 (m), 785 (s), 746 (s), 690 (m).

5.3.2 4,4-Dimethyl-1-(pyridin-2-yl)pentane-1,3-dione (1b)

To a well stirred solution of 2.70 g (50.0 mmol) of NaOMe in 50 ml anhydrous Et₂O, a solution of 7.50 g (50.0 mmol) of ethyl picolinate in 25 ml Et₂O was added dropwise over 20 minutes. After the addition was completed, a solution of 10.0 g of pinacolone (100 mmol) in 25 ml Et₂O was added dropwise over 20 minutes under nitrogen atmosphere. After refluxing for 3 hours, the solution was cooled down to room temperature and 100 ml of iced water was added. The resulting solution was acidified with 3.00 ml of glacial acetic acid. The organic phase was washed three times with water and dried over Na₂SO₄. The product was obtained after removing all volatiles under reduced pressure.

Yield: 7.60 g (37.0 mmol, 74 %, yellow liquid).

Elemental Analysis: C₁₂H₁₅NO₂ (205.26 g/mol)

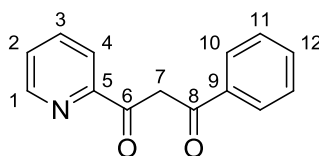
Calculated : C: 70.22% H: 7.37% N: 6.82%

Found : C: 69.65% H: 7.17% N: 6.90%

¹H NMR (600.1 MHz, CDCl₃, 20 °C) of the enol form: δ 16.09 (s, 1H, OH), 8.53 (dd, ³J_{HH} = 5.0 Hz and ⁴J_{HH} = 1.7 Hz, 1H, H1), 7.95 (d, ³J_{HH} = 7.9 Hz, 1H, H4), 7.68 (td, ³J_{HH} = 7.7 Hz and ⁴J_{HH} = 1.7 Hz, 1H, H3), 7.26 (ddd, ³J_{HH} = 7.6 Hz, ³J_{HH} = 5.0 and ⁴J_{HH} = 1.0 Hz, 1H, H2), 6.90 (s, 1H, H7), 1.47 (s, 9H, H10) ppm.

¹³C NMR (151.0 MHz, CDCl₃, 20 °C) of the enol form: δ 204.2 (s, C6), 181.6 (s, C8), 152.2 (s, C5), 149.0 (s, C1), 136.8 (s, C3), 125.9 (s, C2), 121.8 (s, C4), 92.6 (s, C7), 40.0 (s, C9), 27.1 (s, C10) ppm.

5.3.3 1-Phenyl-3-(pyridin-2-yl)propane-1,3-dione (1c)



To a well stirred solution of 2.70 g (50.0 mmol) of NaOMe in 50 ml anhydrous Et₂O, a solution of 7.50 g (50.0 mmol) of ethyl picolinate in 25 ml Et₂O was added dropwise over 20 minutes. After the addition was completed, a solution of 12.0 g of acetophenone (100 mmol) in 25 ml Et₂O was added dropwise over 20 minutes under nitrogen atmosphere. After refluxing for 3 hours, the solution was cooled down to room temperature and 100 ml of iced water was added. The resulting solution was acidified with 3.00 ml of glacial acetic acid. The organic phase was washed three times with water and dried over Na₂SO₄. The product was obtained after removing all volatiles under reduced pressure.

Yield: 9.30 g (41.3 mmol, 62 %, yellow solid).

Elemental Analysis: C₁₄H₁₁NO₂(225.24 g/mol) + 0.15H₂O

Calculated : C: 73.77% H: 5.00% N: 6.14%

Found : C: 73.77% H: 5.01% N: 6.17%

¹H NMR (200 MHz, CDCl₃, 20 °C): δ 8.63 (ddd, ³J_{HH} = 4.7 Hz, ⁴J_{HH} = 1.6 Hz and ⁵J_{HH} = 0.8 Hz, 1H, H1), 8.08 (d, ³J_{HH} = 7.9 Hz, 1H H4), 8.01-8.00 (m, 1H, H3), 7.98-7.96 (m, 1H, H2), 7.50-7.31 (m, 5H, H_{Ph}) ppm.

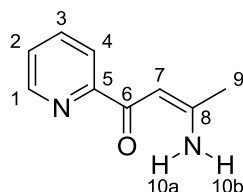
¹³C NMR (100.6 MHz, CDCl₃, 20 °C): δ 186.6 (s, C6), 183.6 (s, C8), 152.6 (s, C5), 149.4 (s, C1), 137.5 (s, C3), 135.5 (s, C9), 132.9 (s, C2), 128.9 (s, C_{Ph}), 127.7 (s, C_{Ph}), 126.6 (s, C12), 122.4 (s, C4), 93.9 (s, C7) ppm.

IR $\tilde{\nu}$ (cm⁻¹): 3456 (w), 3055 (w), 2970 (w), 1979 (w), 1738 (m), 1682 (w), 1599 (m), 1535 (s), 1455 (s), 1422 (m), 1266 (w), 1250 (w), 1230 (w), 1213 (m), 1145 (w), 1086

(m), 1067 (m), 1041 (m), 1022 (m), 993 (s), 952 (w), 909 (w), 796 (m), 771 (s), 749 (s), 707 (s), 686 (s).

5.4 Synthesis of Enaminones

5.4.1 (Z)-3-Amino-1-(pyridin-2-yl)but-2-en-1-one (2a)



5.60 g (34.0 mmol) of 1-(Pyridin-2-yl)butane-1,3-dione (**1a**) was dissolved in 70 ml of dry MeOH. 6.60 g (85.0 mmol) of NH₄OAc were added to this solution. After refluxing for 24 hours at 70 °C, the reaction mixture was cooled down to room temperature and was quenched with 50 ml H₂O. It was then extracted three times with 50 ml Et₂O. The organic phases were collected and dried over Na₂SO₄. The solvent was removed under reduced pressure to obtain the pure product.

Yield: 4.50 g (27.7 mmol, 82 %, yellow solid).

Elemental Analysis: C₉H₁₀N₂O (162.19 g/mol)

Calculated : C: 66.65% H: 6.21% N: 17.27%

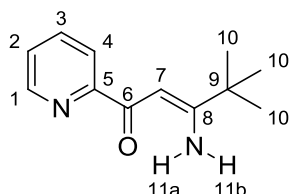
Found : C: 66.37% H: 6.10% N: 17.10%

¹H NMR (400.1 MHz, CDCl₃, 20 °C): δ 10.26 (s, 1H, H10a), 8.61 (dd, ³J_{HH} = 4.9 Hz and ⁴J_{HH} = 1.7 Hz, 1H, H1), 8.09 (d, ³J_{HH} = 7.9 Hz, 1H, H4), 7.79 (td, ³J_{HH} = 7.7 and ⁴J_{HH} = 1.4 Hz, 1H, H3), 7.35-7.32 (m, 1H, H2), 6.42 (s, H7), 5.48 (s, 1H, H10b), 2.09 (s, 3H, H9) ppm.

¹³C NMR (100.6 MHz, CDCl₃, 20 °C): δ 187.5 (s, C6), 164.7 (s, C8), 156.2 (s, C5), 148.6 (s, C1), 137.0 (s, C3), 125.4 (s, C2), 121.8 (s, C4), 91.7 (s, C7), 23.1 (s, C9) ppm.

IR $\tilde{\nu}$ (cm⁻¹): 3337 (w), 3191 (w), 2970 (w), 1738 (s), 1601 (m), 1581 (w), 1560 (m), 1522 (s), 1461 (w), 1438 (w), 1374 (s), 1314 (s), 1276 (m), 1249 (w), 1228 (s), 1217 (s), 1146 (w), 1116 (m), 1090 (m), 1059 (m), 996 (m), 971 (w), 914 (w), 849 (m), 822 (w), 779 (s), 747 (s), 689 (m).

5.4.2 (Z)-3-Amino-4,4-dimethyl-1-(pyridin-2-yl)pent-2-en-1-one (2b)



7.00 g (34.0 mmol) of 4,4-Dimethyl-1-(pyridin-2-yl)pentane-1,3-dione (**1b**) was dissolved in 70 ml of dry MeOH. 6.60 g (85.0 mmol) of NH₄OAc were added to this solution. After refluxing for 24 hours at 70 °C, the reaction mixture was cooled down to room temperature and was quenched with 50 ml H₂O. It was then extracted three times with 50 ml Et₂O. The organic phases were collected and dried over Na₂SO₄. The solvent was removed under reduced pressure to obtain the pure product.

Yield: 4.30 g (21.1 mmol, 62 %, yellow liquid).

Elemental Analysis: C₁₂H₁₆N₂O (204.27 g/mol) + 0.25H₂O

Calculated : C: 69.04% H: 7.97% N: 13.42%

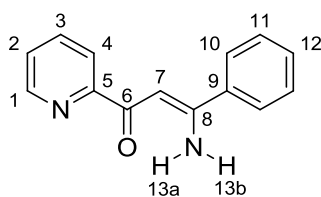
Found : C: 69.06% H: 7.76% N: 13.28%

¹H NMR (400.1 MHz, CDCl₃, 20 °C): δ 9.80 (s, 1H, H11a), 8.50 (d, ³J_{HH} = 4.6 Hz, 1H, H1), 7.79 (d, ³J_{HH} = 7.9 Hz, 1H, H4), 7.64 (td, ³J_{HH} = 7.7 Hz and ⁴J_{HH} = 2.0 Hz, H3), 7.22 (dd, ³J_{HH} = 7.7 and ³J_{HH} = 4.6 Hz, 1H, H2), 7.09 (s, 1H, H11b), 5.91 (s, H7), 1.13 (s, 9H, H10) ppm.

^{13}C NMR (100.6 MHz, CDCl_3 , 20 °C): δ 206.1 (s, C6), 156.4 (s, C8), 151.3 (s, C5), 148.8 (s, C1), 136.7 (s, C3), 124.8 (s, C2), 120.1 (s, C4), 87.6 (s, C7), 42.1 (s, C9), 27.6 (s, C10) ppm.

IR $\tilde{\nu}$ (cm^{-1}): 3436 (w), 3265 (w), 2969 (m), 2867 (w), 1739 (s), 1619 (s), 1583 (m), 1560 (s), 1519 (m), 1456 (s), 1434 (m), 1362 (m), 1306 (s), 1254 (w), 1217 (m), 1131 (s), 1093 (w), 1059 (w), 1043 (m), 1008 (m), 993 (s), 911 (w), 776 (s), 766 (s), 743 (w), 700 (m), 669 (w).

5.4.3 (Z)-3-Amino-3-phenyl-1-(pyridin-2-yl)prop-2-en-1-one (2c)



7.70 g (34.0 mmol) of 1-Phenyl-3-(pyridin-2-yl)propane-1,3-dione (**1c**) was dissolved in 70 ml of dry MeOH. 6.60 g (85.0 mmol) of NH_4OAc were added to this solution. After refluxing for 24 hours at 70 °C, the reaction mixture was cooled down to room temperature and was quenched with 50 ml H_2O . It was then extracted three times with 50 ml Et_2O . The organic phases were collected and dried over Na_2SO_4 . The solvent was removed under reduced pressure to obtain the pure product.

Yield: 4.40 g (19.6 mmol, 58 %, pale yellow solid).

Elemental Analysis: $\text{C}_{14}\text{H}_{12}\text{N}_2\text{O}$ (224.26 g/mol)

Calculated : C: 74.98% H: 5.39% N: 12.49%

Found : C: 74.95% H: 5.28% N: 12.46%

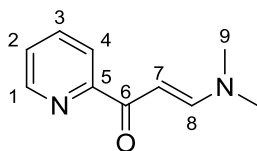
^1H NMR (600.1 MHz, CDCl_3 , 20 °C): δ 10.29 (s, 1H, H13a), 8.69 (d, $^3J_{\text{HH}} = 4.6$ Hz, 1H, H1), 7.98-7.97 (m, 2H, H10), 7.94 (d, $^3J_{\text{HH}} = 8.0$ Hz, 1H, H4), 7.82 (td, $^3J_{\text{HH}} = 7.8$ Hz and

$^4J_{\text{HH}} = 1.6$ Hz, 1H, H3), 7.50-7.40 (m, 4H, H11, H12 and H13b), 7.41 (dd, $^3J_{\text{HH}} = 7.4$ Hz and $^3J_{\text{HH}} = 4.8$ Hz, 1H, H2), 6.52 (s, 1H, H7) ppm.

^{13}C NMR (151.0 MHz, CDCl_3 , 20 °C): δ 190.7 (s, C6), 157.4 (s, C8), 151.2 (s, C5), 149.2 (s, C1), 140.6 (s, C9), 137.3 (s, C3), 131.2 (s, C2), 128.5 (s, C_{Ph}), 127.3 (s, C_{Ph}), 125.5 (s, C_{Ph}), 120.7 (s, C4), 89.2 (s, C7) ppm.

IR $\tilde{\nu}$ (cm^{-1}): 3378 (m), 3246 (m), 3056 (w), 3015 (w), 2970 (w), 1739 (s), 1610 (s), 1575 (w), 1561 (m), 1523 (s), 1490 (w), 1456 (s), 1429 (s), 1365 (s), 1323 (m), 1296 (m), 1285 (m), 1252 (w), 1231 (s), 1217 (s), 1175 (w), 1162 (w), 1151 (m), 1094 (m), 1069 (m), 1051 (m), 993 (m), 891 (w), 812 (m), 799 (w), 742 (s), 723 (s), 690 (s).

5.4.4 3-(Dimethylamino)-1-(pyridin-2-yl)prop-2-en-1-one (3a)



Under nitrogen atmosphere, 10.8 g (88.3 mmol) of 2-acetylpyridine and 24 ml (177 mmol) of DMF-DMA were mixed and refluxed at 110 °C for 24 hours. After evaporating the solvent, the residue was washed three times with 20 ml hexane and three times with 20 ml diethyl ether.

Yield: 11.6 g (65.8 mmol, 75%, yellow solid).

Elemental Analysis: $\text{C}_{10}\text{H}_{12}\text{N}_2\text{O}$ (176.22 g/mol)

Calculated : C: 68.16% H: 6.86% N: 15.90%

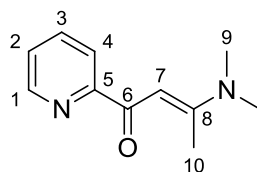
Found : C: 68.00% H: 6.81% N: 15.77%

^1H NMR (400.1 MHz, DMSO-d_6 , 20 °C): δ 8.62 (dd, $^3J_{\text{HH}} = 4.8$ Hz and $^4J_{\text{HH}} = 1.5$ Hz, 1H, H1), 8.14 (d, $^3J_{\text{HH}} = 7.8$ Hz, 1H, H4), 7.91 (d, $^3J_{\text{HH}} = 12.6$ Hz, 1H, H8), 7.80 (td,

$^3J_{\text{HH}} = 7.7$ Hz and $^4J_{\text{HH}} = 1.8$ Hz, 1H, H3), 7.36 (ddd, $^3J_{\text{HH}} = 7.4$ Hz, $^3J_{\text{HH}} = 4.8$ and $^4J_{\text{HH}} = 1.2$ Hz, 1H, H2), 6.45 (d, $^3J_{\text{HH}} = 12.6$ Hz, 1H, H7), 3.17 (s, 3H, H9), 2.99 (s, 3H, H9) ppm.

^{13}C NMR (100.6 MHz, DMSO- d_6 , 20 °C): δ 186.7 (s, C6), 156.1 (s, C8), 154.9 (s, C5), 147.9 (s, C1), 137.0 (s, C3), 125.7 (s, C2), 122.0 (s, C4), 91.01 (s, C7), 45.3 (s, C9), 37.7 (s, C9) ppm.

5.4.5 3-(Dimethylamino)-1-(pyridin-2-yl)but-2-en-1-one (3b)



Under nitrogen atmosphere, 1.50 g (14.4 mmol) of 2-acetylpyridine and 4.00 ml (24.8 mmol) of *N,N* dimethyl acetamide dimethyl acetal were mixed and refluxed at 110 °C for 24 hours. After evaporating the solvent, the residue was washed three times with 20 ml hexane and three times with 20 ml diethyl ether.

Yield: 1.50 g (7.88 mmol, 64 %, brown solid).

Elemental Analysis: $\text{C}_{11}\text{H}_{14}\text{N}_2\text{O}$ (190.24 g/mol) + 0.15 H_2O

Calculated : C: 68.48% H: 7.47% N: 14.52%

Found : C: 68.63% H: 7.32% N: 14.45%

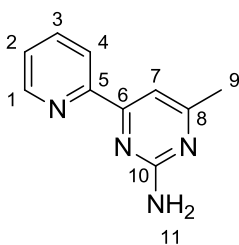
^1H NMR (400.1 MHz, CDCl_3 , 20 °C): δ 8.58 (d, $^3J_{\text{HH}} = 4.0$ Hz, 1H, H1), 8.12 (d, $^3J_{\text{HH}} = 7.9$ Hz, 1H, H4), 7.78 (td, $^3J_{\text{HH}} = 7.7$ Hz, $^4J_{\text{HH}} = 1.7$ Hz, 1H, H3), 7.31 (ddd, $^3J_{\text{HH}} = 7.4$ Hz, $^3J_{\text{HH}} = 4.8$ Hz and $^4J_{\text{HH}} = 1.1$ Hz, 1H, H2), 6.54 (s, 1H, H7), 3.13 (s, 6H, H9), 2.70 (s, 3H, H10) ppm.

^{13}C NMR (100.6 MHz, CDCl_3 , 20 °C): δ 185.6 (s, C6), 165.2 (s, C8), 158.0 (s, C5), 147.9 (s, C1), 136.8 (s, C3), 124.9 (s, C2), 121.9 (s, C4), 91.0 (s, C7), 40.4 (s, C9), 16.7 (s, C10) ppm.

IR $\tilde{\nu}$ (cm^{-1}): 3047 (w), 1590 (w), 1540 (w), 1529 (s), 1420 (w), 1410 (m), 1381 (m), 1350 (w), 1231 (w), 1086 (m), 1026 (m), 993 (m), 924 (m), 866 (m), 787 (m), 747 (m), 695 (m), 681 (m).

5.5 Synthesis of N,N-Ligands

5.5.1 4-Methyl-6-(pyridin-2-yl)pyrimidin-2-amine (4a)



To a solution 5.40 g (33.4 mmol) of precursor **2a** in 20 ml of H_2O , 5.70 g (66.8 mmol) 50 % of aqueous cyanamide solution were added. After refluxing for 24 hours at 100 °C, the reaction mixture was extracted three times with 20 ml CHCl_3 . The organic phases were combined and dried over Na_2SO_4 . The solvent was removed under reduced pressure to obtain the pure product.

Yield: 3.80 g (20.4 mmol, 61 %, yellow solid).

Elemental Analysis: $\text{C}_{10}\text{H}_{10}\text{N}_4$ (186.21 g/mol).

Calculated : C: 64.50% H: 5.41% N: 30.09%

Found : C: 62.23% H: 5.35% N: 27.20%

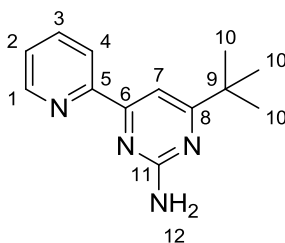
^1H NMR (400.1 MHz, CDCl_3 , 20 °C): δ 8.68 (d, $^3J_{\text{HH}} = 4.0$ Hz, 1H, H1), 8.31 (d, $^3J_{\text{HH}} = 7.9$ Hz, 1H, H4), 7.80 (td, $^3J_{\text{HH}} = 7.8$ Hz and $^4J_{\text{HH}} = 1.7$ Hz, 1H, H3), 7.54 (s, 1H,

H7), 7.36 (ddd, $^3J_{\text{HH}} = 7.5$ Hz, $^3J_{\text{HH}} = 4.8$ Hz and $^4J_{\text{HH}} = 0.9$ Hz, 1H, H2), 5.40 (s, 2H, H11), 2.45 (s, 3H, H9) ppm.

^{13}C NMR (100.6 MHz, CDCl_3 , 20 °C): δ 169.0 (s, C8), 164.3 (s, C6), 162.8 (s, C10), 154.5 (s, C5), 149.5 (s, C1), 137.1 (s, C3), 125.2 (s, C2), 121.9 (s, C4), 107.7 (s, C7), 24.0 (s, C9) ppm.

IR $\tilde{\nu}$ (cm^{-1}): 3487 (w), 3321 (w), 3181 (w), 2970 (w), 1738 (s), 1650 (s), 1592 (w), 1572 (s), 1551 (s), 1438 (m), 1378 (m), 1351 (m), 1288 (w), 1230 (m), 1218 (m), 1146 (w), 1092 (w), 1048 (w), 993 (m), 878 (m), 844 (w), 783 (s), 745 (m), 737 (m), 685 (m).

5.5.2 4-(*tert*-Butyl)-6-(pyridin-2-yl)pyrimidin-2-amine (4b)



To a solution 3.20 g (15.7 mmol) of precursor **2b** in 15 ml CH_3OH , 6.60 g (78.5 mmol) of 50 % aqueous cyanamide solution were added. After refluxing at 65 °C for 48 hours, 10 ml of H_2O were added to the solution and the product was precipitated. The solid was collected by filtration and dried in *vacuo*.

Yield: 2.10 (9.33 mmol, 59 %, pale yellow solid).

Elemental Analysis: $\text{C}_{13}\text{H}_{16}\text{N}_4$ (228.29 g/mol) + 0.15 H_2O .

Calculated : C: 67.59% H: 7.11% N: 24.25%

Found : C: 67.41% H: 6.93% N: 24.43%

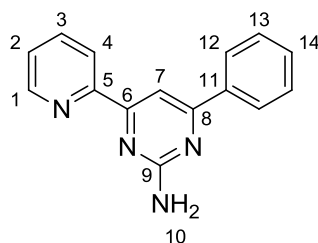
^1H NMR (400.1 MHz, CDCl_3 , 20 °C): δ 8.70 (d, $^3J_{\text{HH}} = 4.8$ Hz 1H, H1), 8.30 (d, $^3J_{\text{HH}} = 7.9$ Hz, 1H, H4), 7.80 (td, $^3J_{\text{HH}} = 7.8$ Hz and $^4J_{\text{HH}} = 1.7$ Hz, 1H, H3), 7.69 (s, 1H,

H7), 7.35 (ddd, $^3J_{\text{HH}} = 7.8$ Hz, $^3J_{\text{HH}} = 4.9$ Hz and $^4J_{\text{HH}} = 1.3$ Hz, 1H, H2), 5.23 (s, 2H, H12), 1.35 (s, 9H, H10) ppm.

^{13}C NMR (100.6 MHz, CDCl_3 , 20 °C): δ 180.3 (s, C8), 164.3 (s, C6), 162.8 (s, C11), 155.1 (s, C5), 149.5 (s, C1), 137.1 (s, C3), 125.0 (s, C2), 121.8 (s, C4), 103.8 (s, C7), 37.7 (s, C9), 29.5 (s, C10) ppm.

IR $\tilde{\nu}$ (cm^{-1}): 3309 (w), 3194 (w), 2971 (m), 2956 (w), 1739 (s), 1624 (m), 1561 (m), 1536 (s), 1478 (m), 1446 (m), 1365 (s), 1352 (s), 1230 (s), 1217 (s), 1205 (s), 1167 (w), 1143 (w), 1091 (m), 1048 (w), 995 (m), 968 (w), 906 (w), 871 (m), 852 (m), 789 (s), 751 (m), 743 (m), 715 (w), 676 (m).

5.5.3 4-Phenyl-6-(pyridin-2-yl)pyrimidin-2-amine (4c)



To a solution of 2.90 g (12.9 mmol) of precursor **2c** in 15 ml H_2O , 2.70 g (32.3 mmol) of 50 % aqueous cyanamide solution were added. After refluxing for 24 hours at 100 °C, the product was extracted three times with 20 ml CHCl_3 . The organic phases were combined and dried over Na_2SO_4 . The solvent was removed under reduced pressure.

Yield: 1.60 g (6.44 mmol, 48 %, yellow solid).

Elemental Analysis: $\text{C}_{15}\text{H}_{12}\text{N}_4$ (248.28 g/mol) + 0.25 H_2O .

Calculated : C: 71.27% H: 4.98% N: 22.16%

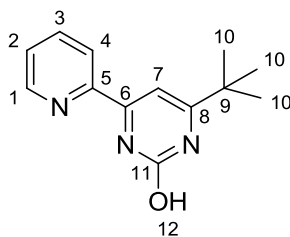
Found : C: 71.82% H: 4.94% N: 21.67%

^1H NMR (400.1 MHz, CDCl_3 , 20 °C): δ 8.73 (dd, $^3J_{\text{HH}} = 4.7$ Hz and $^4J_{\text{HH}} = 0.7$ Hz, 1H, H1), 8.38 (d, $^3J_{\text{HH}} = 7.8$ Hz, 1H, H4), 8.14-8.13 (m, 3H, H12 and H7), 7.83 (td, $^3J_{\text{HH}} = 7.74$ and $^4J_{\text{HH}} = 1.71$ Hz, 1H, H3), 7.49-7.48 (m, 3H, H13 and H14), 7.38 (ddd, $^3J_{\text{HH}} = 7.4$ Hz, $^3J_{\text{HH}} = 4.7$ Hz and $^4J_{\text{HH}} = 1.0$ Hz, 1H, H2), 5.47 (s, 2H, H10) ppm.

^{13}C NMR (100.6 MHz, CDCl_3 , 20 °C): δ 166.5 (s, C6), 164.8 (s, C9), 163.3 (s, C8), 154.5 (s, C5), 149.5 (s, C1), 137.2 (s, C11), 137.1 (s, C3), 130.9 (s, C14), 128.9 (s, C13), 127.4 (s, C12), 125.3 (s, C2), 121.8 (s, C4), 104.5 (s, C7) ppm.

IR $\tilde{\nu}$ (cm^{-1}): 3329 (m), 3204 (m), 3058 (w), 2971 (w), 1737 (m), 1638 (m), 1589 (w), 1528 (s), 1499 (m), 1474 (m), 1457 (s), 1358 (s), 1287 (m), 1254 (w), 1230 (s), 1217 (m), 1207 (m), 11154 (w), 1128 (w), 1092 (m), 994 (m), 922 (w), 862 (m), 834 (m), 794 (m), 766 (s), 743 (m), 684 (s).

5.5.4 4-(*tert*-Butyl)-6-(pyridin-2-yl)pyrimidin-2-ol (**6**).



7.30 g (122 mmol) urea and 5.00 g (24.4 mmol) of 4,4-Dimethyl-1-(pyridin-2-yl)pentane-1,3-dione (**1b**) were dissolved in H_2O :ethanol mixture (18 ml:3 ml). The mixture was heated to 95 °C. When the reflux was started, 18 ml (40.0 mmol) concentrated HCl solution were added slowly to the reaction mixture. After 48 hours, the reaction was cooled down to room temperature and neutralized with 2M Na_2CO_3 solution. The precipitate was collected by filtration and washed with Et_2O until the filtrate was colorless.

Yield: 4.00 g (17.4 mmol, 72 %, colorless solid).

Elemental Analysis: $\text{C}_{13}\text{H}_{15}\text{N}_3\text{O}$ (229.30 g/mol) + 1.1 H_2O .

Calculated : C: 62.68% H: 6.96% N: 16.87%

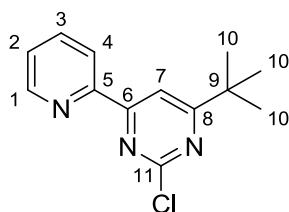
Found : C: 63.23% H: 6.44% N: 17.40%

¹H NMR (400.1 MHz, CDCl₃, 20 °C): δ 12.75 (s, 1H, H12), 8.71 (dd, ³J_{HH} = 4.9 Hz and ⁴J_{HH} = 1.8 Hz, 1H, H1), 8.54 (br. s, 1H, H7), 7.85 (td, ³J_{HH} = 7.8 Hz and ⁴J_{HH} = 1.9 Hz, 1H, H4), 7.48-7.41 (m, 2H, H2 and H3), 1.50 (s, 9H, H10) ppm.

¹³C NMR (100.6 MHz, CDCl₃, 20 °C): δ 170.0 (s, C8), 160.4 (s, C6), 155.2(s, C11), 153.8 (s, C5), 149.4 (s, C1), 126.1 (s, C3), 123.2 (s, C2), 122.1 (s, C4), 98.0 (s, C7), 36.1 (s, C9), 28.8 (s, C10) ppm.

IR $\tilde{\nu}$ (cm⁻¹): 3305 (w), 3193 (w), 2970 (m), 2957 (m), 2867 (w), 1739 (s), 1623 (s), 1561 (s), 1536 (s), 1477 (m), 1445 (s), 1365 (m), 1351 (s), 1230 (s), 1217 (s), 1205 (s), 1166 (w), 1142 (w), 1091 (m), 1048 (w), 995 (m), 968 (w), 907 (w), 871 (m), 852 (m), 789 (s), 743 (m), 751 (m), 743 (m), 716 (w), 676 (m).

5.5.5 4-(*tert*-Butyl)-2-chloro-6-(pyridin-2-yl)pyrimidine (7)



1.20 g (5.20 mmol) of compound 4-(*tert*-Butyl)-6-(pyridin-2-yl)pyrimidin-2-ol (**6**) and 9 ml (100 mmol) of POCl₃ were mixed and heated at 80 °C. After 1 hour, unreacted POCl₃ was removed under vacuum. The residue was poured on 20.0 g of iced water and neutralized with 5M Na₂CO₃ solution. After neutralization, the precipitated solid was collected by filtration.

Yield: 865 mg (3.49 mmol, 66 %, colorless solid).

Elemental Analysis: C₁₃H₁₄ClN₃ (247.70 g/mol).

Calculated : C: 63.03% H: 5.70% N: 16.96%

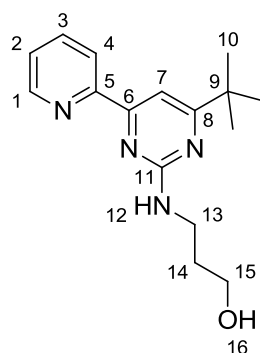
Found : C: 63.11% H: 5.88% N: 16.70%

¹H NMR (400.1 MHz, CDCl₃, 20 °C): δ 8.74 (d, ³J_{HH} = 4.8 Hz, 1H, H1), 8.51 (d, ³J_{HH} = 8.0 Hz, 1H, H4), 8.41 (s, 1H, H7), 7.91 (td, ³J_{HH} = 7.8 Hz and ⁴J_{HH} = 1.6 Hz, 1H, H3), 7.47 (ddd, ³J_{HH} = 7.7 Hz, ³J_{HH} = 4.8 Hz and ⁴J_{HH} = 1.3 Hz, 1H, H2), 1.43 (s, 9H, H10) ppm.

¹³C NMR (100.6 MHz, CDCl₃, 20 °C): δ 183.1 (s, C8), 165.4 (s, C6), 161.1 (s, C11), 152.9 (s, C5), 149.2 (s, C1), 138.0 (s, C3), 126.0 (s, C2), 122.7 (s, C4), 111.7 (s, C7), 38.4 (s, C9), 29.5 (s, C10) ppm.

IR $\tilde{\nu}$ (cm⁻¹): 3457 (w), 3065 (w), 2971 (m), 2958 (m), 2868 (w), 1739 (s), 1656 (m), 1592 (m), 1579 (m), 1562 (s), 1519 (s), 1471 (s), 1447 (w), 1408 (m), 1355 (s), 1295 (m), 1256 (s), 1239 (m), 1216 (s), 1145 (m), 1086 (m), 1046 (m), 995 (m), 938 (w), 887 (s), 841 (s), 801 (s), 775 (s), 743 (m), 736 (m), 677 (m), 667 (m).

5.5.6 3-((4-(*tert*-Butyl)-6-(pyridin-2-yl)pyrimidin-2-yl)amino)propan-1-ol (8)



2.00 g (8.00 mmol) of precursor **7** and 6.00 ml (72.0 mmol) of 3-amino-1-propanol were dissolved in 50 ml of dry toluene under nitrogen atmosphere and refluxed at 110 °C. After 24 hours, the reaction mixture was cooled down to room temperature. The solvent was removed under reduced pressure and the residue was treated with CH₂Cl₂ and H₂O. The

phases were separated. Then, the organic phases were collected and dried over Na_2SO_4 . The solvent was removed under reduced pressure.

Yield: 1.40 g (4.88 mmol, 62 % yield, colorless solid).

Elemental Analysis: $\text{C}_{16}\text{H}_{22}\text{N}_4$ (286.38 g/mol) + 0.4 CH_2Cl_2 .

Calculated : C: 64.72% H: 7.55% N: 18.41%

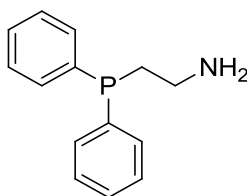
Found : C: 65.35% H: 7.81% N: 17.92%

^1H NMR (400.1 MHz, CDCl_3 , 20 °C): δ 8.69 (dd, $^3J_{\text{HH}} = 4.0$ Hz and $^4J_{\text{HH}} = 0.7$ Hz, 1H, H1), 8.24 (d, $^3J_{\text{HH}} = 7.9$ Hz, 1H, H4), 7.80 (t, $^3J_{\text{HH}} = 7.7$ Hz, 1H, H3), 7.60 (s, 1H, H7), 7.36-7.33 (m, 1H, H2), 5.33 (s, 1H, H12), 4.17 (br. s, 1H, H16), 3.73-3.66 (m, 4H, H13 and H15), 1.83-1.77 (m, 2H, H14), 1.34 (s, 9H, H10) ppm.

^{13}C NMR (100.6 MHz, CDCl_3 , 20 °C): δ 180.6 (s, C8), 163.7 (s, C6), 163.1 (s, C11), 155.1 (s, C5), 149.5 (s, C1), 137.1 (s, C3), 124.9 (s, C2), 121.5 (s, C4), 103.0 (s, C7), 58.8 (s, C15), 37.8 (s, C13), 37.5 (s, C9), 33.3 (s, C14), 29.5 (s, C10) ppm.

5.6 Synthesis of Aminophosphines

5.6.1 2-(Diphenylphosphinyl)ethyl-1-amine (9a)

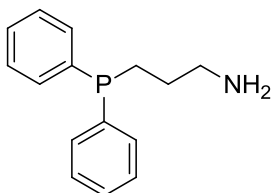


The title compound was synthesized according to the literature procedure.^[128] A flame-dried flask was charged with a magnetic stirring bar, 2.93 g (423 mmol) granulated lithium, and 37.3 g (141 mmol) PPh_3 under nitrogen atmosphere. 125 ml of THF were added to the reaction flask and the reaction mixture was stirred overnight at room

temperature. The dark-red solution was filtered through a glass frit. To this filtrate, 29.0 g (127 mmol) 2-bromoethylamine hydro bromide were added slowly. A highly exothermic reaction started. The reaction mixture was stirred for another 30 minutes and then quenched with H₂O. The solution was concentrated in *vacuo* and washed three times with 25 ml hexane. The remaining colorless slurry was extracted with toluene and the organic phase filtered through a short column filled with neutral Al₂O₃. Toluene was evaporated in *vacuo* to obtain the aminophosphine **9a** as yellow oil which was used without further purification.

Yield: 25.0 g (109 mmol, 86 %, pale yellow oil).

5.6.2 3-(Diphenylphosphinyl)propylamine (**9b**)

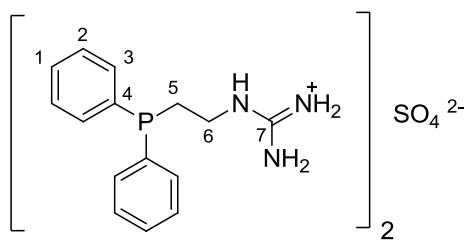


The title compound was synthesized using the same procedure as for compound **9a** starting from 1.15 g (165 mmol) granulated lithium, 14.4 g (55.0 mmol) PPh₃ and 11.2 g (50.0 mmol) 3-bromopropyl amine hydrobromide.

Yield: 10.9 g (44.8 mmol, 90 %, colorless oil).

5.7 Synthesis of 1-(Phosphinylalkyl)guanidinium Salts

The corresponding aminophosphine and 25% aqueous ammonia solution were mixed in H₂O under a nitrogen atmosphere. 2-Methyl-2-thiopseudourea-hemisulfate (2.0 equiv.) was added to this solution upon stirring. The reaction mixture was heated at 55 °C for 24 hours. After cooling to room temperature, water was decanted from the mixture and the solid was washed with H₂O twice. The oily residue was stirred in toluene overnight; the precipitate was filtered and dried in *vacuo*.

5.7.1 1-(2-(Diphenylphosphinyl)ethyl)guanidinium Sulfate (10a)


The title compound was synthesized according to general procedure for 1-(phosphinylalkyl)guanidinium salts from 23.2 g (101 mmol) of aminophosphine **9a**.

Yield: 27.1 g (42.2 mmol, 84 %, pale yellow solid).

Elemental Analysis: C₃₀H₃₈N₆O₄P₂S (658.69 g/mol) + 2H₂O

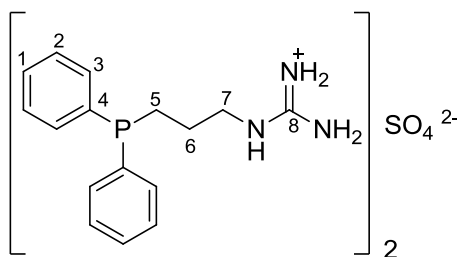
Calculated : C: 54.70% H: 6.12% N: 12.76% S: 4.87%

Found : C: 53.25% H: 5.81% N: 12.42% S: 4.74%

¹H NMR (400.1 MHz, CD₃OD, 20 °C): δ 7.45-7.41 (m, 4H, H3), 7.36-7.31 (m, 6H, H1 and H2), 3.28-3.22 (m, 2H, H6), 2.41-2.37 (m, 2H, H5) ppm. Since the NH protons exchange with deuterium in CD₃OD, the amino protons cannot be assigned.

¹³C NMR (100.6 MHz, CD₃OD, 20 °C): δ 158.4 (s, C7), 138.9 (d, ¹J_{PC} = 12.2 Hz, C4), 133.8 (d, ²J_{PC} = 19.4 Hz, C3), 130.0 (s, C1), 129.7 (d, ³J_{PC} = 6.8 Hz, C2), 39.9 (d, ²J_{PC} = 25.6 Hz, C6), 28.7 (d, ¹J_{PC} = 13.3 Hz, C5) ppm.

³¹P NMR (161.98 MHz, CD₃OD, 20 °C): δ -21.99 (s) ppm.

5.7.2 1-(3-(Diphenylphosphinyl)propyl)guanidinium Sulfate (10b)

The title compound was synthesized according to the general procedure for 1-(phosphinylalkyl)guanidinium salts from 10.9 g (45.0 mmol) aminophosphine **9b**.

Yield: 11.2 g (16.7 mmol, 74 %, colorless solid).

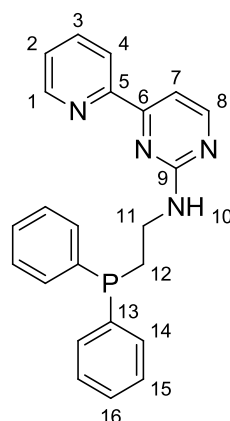
^1H NMR (400.1 MHz, CD_3OD , 20 °C): δ 7.43-7.39 (m, 4H, H3), 7.35-7.31 (m, 6H, H1 and H2), 3.23 (t, $^3J_{\text{HH}} = 7.0$ Hz, 2H, H7), 2.13-2.07 (m, 2H, H5), 1.71-1.61 (m, 2H, H6) ppm.

^{13}C NMR (100.6 MHz, CD_3OD , 20 °C): δ 158.6 (s, C8), 139.7 (d, $^1J_{\text{PC}} = 12.5$ Hz, C4), 133.7 (d, $^2J_{\text{PC}} = 18.9$ Hz, C3), 129.8 (s, C1), 129.6 (d, $^3J_{\text{PC}} = 6.7$ Hz, C2), 43.2 (d, $^3J_{\text{PC}} = 14.8$ Hz, C7), 26.6 (d, $^1J_{\text{PC}} = 17.6$ Hz, C5), 25.8 (d, $^2J_{\text{PC}} = 11.7$ Hz, C6) ppm.

^{31}P NMR (161.98 MHz, CD_3OD , 20 °C): δ -17.00 (s) ppm.

5.8 Synthesis of N,N,P-Ligands

5.8.1 N-(2-(Diphenylphosphinyl)ethyl)-4-(pyridin-2-yl)pyrimidin-2-amine (11a)



To a solution of 2.40 g (3.80 mmol) of 1-(2-(diphenylphosphinyl)ethyl)guanidine sulfate (**10a**) in 20 ml dry EtOH, 0.50 g (9.00 mmol) of NaOMe were added under nitrogen atmosphere. The reaction mixture was stirred at 78 °C. After 30 minutes, 1.00 g (6.00 mmol) of 3-(dimethylamino)-1-(pyridin-2-yl)prop-2-en-1-one (**3a**) were added to the solution and refluxed for 24 hours. The mixture was cooled down to room temperature and all volatiles were evaporated. The residue was extracted three times with 20 ml dichloromethane and three times with 20 ml H₂O. The combined organic phases were dried over Na₂SO₄. After evaporating the solvent, the product was obtained by washing two times with 20 ml dry MeOH.

Yield: 1.10 g (2.80 mmol, 46 %, colorless solid).

Elemental Analysis: C₂₃H₂₁N₄P (384.42 g/mol) + 0.4 H₂O.

Calculated : C: 70.54% H: 5.61% N: 14.31%

Found : C: 70.45% H: 5.51% N: 14.39%

¹H NMR (400.1 MHz, CDCl₃, 20 °C): δ 8.68 (ddd, ³J_{HH} = 4.8 Hz, ⁴J_{HH} = 1.6 Hz and ⁵J_{HH} = 0.8 Hz, 1H, H1), 8.41 (d, ³J_{HH} = 5.1 Hz, 1H, H8), 8.26 (d, ³J_{HH} = 7.9 Hz, 1H, H4), 7.79 (td, ³J_{HH} = 7.8 Hz and ⁴J_{HH} = 1.8 Hz, 1H, H3), 7.57 (d, ³J_{HH} = 5.1 Hz, 1H, H7), 7.79-

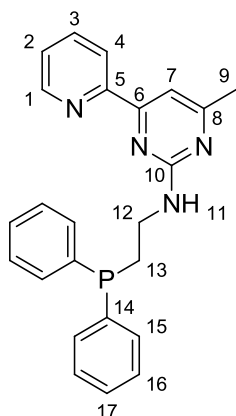
7.44 (m, 4H, H_{Ph}), 7.38-7.36 (m, 1H, H₂), 7.35-7.31 (m, 6H, H_{Ph}), 5.41 (t, ³J_{HH} = 5.8 Hz, 1H, H₁₀), 3.72-3.65 (m, 2H, H₁₁), 2.49-2.46 (m, 2H, H₁₂) ppm.

¹³C NMR (100.6 MHz, CDCl₃, 20 °C): δ 163.6 (s, C₈), 162.3 (s, C₉), 159.5 (s, C₆), 154.9 (s, C₅), 149.4 (s, C₁), 138.2 (d, ¹J_{PC} = 12.2 Hz, C₁₃), 137.0 (s, C₃), 133.0 (d, ²J_{PC} = 18.8 Hz, C₁₄), 128.8 (s, C₁₆), 128.7 (d, ³J_{PC} = 6.7 Hz, C₁₅), 125.1 (s, C₂), 121.6 (s, C₄), 107.1 (s, C₇), 38.8 (d, ²J_{PC} = 22.7 Hz, C₁₁), 28.9 (d, ¹J_{PC} = 13.2 Hz, C₁₂) ppm.

³¹P NMR (161.98 MHz, CDCl₃, 20 °C): δ -21.26 (s) ppm.

IR $\tilde{\nu}$ (cm⁻¹): 3245 (w), 3052 (w), 2148 (w), 1596 (m), 1578 (m), 1563 (s), 1535 (m), 1480 (w), 1455 (m), 1432 (m), 1415 (s), 1360 (s), 1325 (w), 1306 (w), 1291 (w), 1281 (w), 1253 (w), 1239 (w), 1204 (m), 1177 (w), 1157 (w), 1124 (m), 1092 (m), 1074 (m), 1043 (w), 1026 (w), 994 (m), 907 (w), 895 (w), 879 (w), 840 (m), 785 (s), 747 (s), 784 (s), 716 (m), 680 (s).

5.8.2 N-(2-(Diphenylphosphinyl)ethyl)-4-methyl-6-(pyridin-2-yl)pyrimidin-2-amine (11b)



Under nitrogen atmosphere, 400 mg (6.70 mmol) of NaOMe were added to a solution of 1.80 g (2.80 mmol) of 1-(2-(diphenylphosphinyl)ethyl)guanidinium sulfate (**10a**) in 20 ml dry EtOH. The reaction mixture was heated to 78 °C. After stirring for 30 minutes, 900 mg (4.73 mmol) of 3-(dimethylamino)-1-(pyridin-2-yl)but-2-en-1-one (**3b**) were added to

the mixture and refluxed for 24 hours. The solvent was evaporated and the residue was extracted three times with 20 ml of dichloromethane and washed three times with 20 ml of H₂O. The organic phases were combined and dried over Na₂SO₄. After evaporating the solvent, the product was obtained by washing two times with 20 ml dry MeOH.

Yield: 750 mg (1.88 mmol, 42 %, colorless solid).

Elemental Analysis: C₂₄H₂₃N₄P (398.45 g/mol)

Calculated : C: 72.35% H: 5.82% N: 14.06%

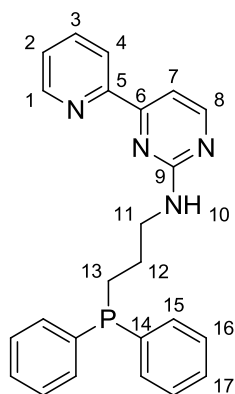
Found : C: 71.23% H: 5.81% N: 14.00%

¹H NMR (400.1 MHz, CDCl₃, 20 °C): δ 8.67 (ddd, ³J_{HH} = 4.8 Hz, ⁴J_{HH} = 1.6 and ⁵J_{HH} = 0.8 Hz, 1H, H1), 8.25 (d, ³J_{HH} = 7.9 Hz, 1H, H4), 7.79 (td, ³J_{HH} = 7.8 Hz and ⁴J_{HH} = 1.8 Hz, 1H, H3), 7.50-7.44 (m, 5H, H15 and H7), 7.37-7.32 (m, 7H, H2, H16 and H17), 5.32 (t, ³J_{HH} = 6.0 Hz, 1H, H11), 3.73-3.66 (m, 2H, H12), 2.48-2.44 (m, 2H, H13), 2.41 (s, 3H, H9) ppm.

¹³C NMR (100.6 MHz, CDCl₃, 20 °C): δ 169.2 (s, C8), 163.1 (s, C10), 162.3 (s, C6), 155.0 (s, C5), 149.2 (s, C1), 138.1 (d, ¹J_{PC} = 12.2 Hz, C14), 136.9 (s, C3), 132.8 (d, ²J_{PC} = 18.9 Hz, C15), 128.7 (s, C17), 128.5 (d, ³J_{PC} = 6.8 Hz, C16), 124.8 (s, C2), 121.6 (s, C4), 106.6 (s, C7), 39.0 (s, C12), 28.9 (d, ¹J_{PC} = 13.4 Hz, C13), 24.3 (s, C9) ppm.

³¹P NMR (161.98 MHz, CDCl₃, 20 °C): δ -21.26 (s) ppm.

IR $\tilde{\nu}$ (cm⁻¹): 3252 (m), 3070 (w), 2929 (8w), 1598 (m), 1581 (m), 1557 (s), 1479 (m), 1456 (w), 1432 (m), 1373 (m), 1347 (s), 1304 (w), 1223 (w), 1185 (w), 1134 (m), 1099 (w), 1087 (w), 1024 (w), 995 (m), 938 (w), 843 (m), 802 (m), 784 (s), 747 (s), 735 (s), 696 (s).

5.8.3 N-(3-(Diphenylphosphinyl)propyl)-4-(pyridin-2-yl)pyrimidin-2-amine (12a)

To a solution of 2.06 g (3.08 mmol) of 1-(3-(Diphenylphosphinyl)propyl)guanidinium sulfate (**10b**) in 20 ml dry EtOH, 0.50 g (9.00 mmol) of NaOMe were added under nitrogen atmosphere. The reaction mixture was stirred at 78 °C. After 30 minutes, 1.00 g (6.00 mmol) of 3-(dimethylamino)-1-(pyridin-2-yl)prop-2-en-1-one (**3a**) were added to the solution and refluxed for 24 hours. The mixture was cooled down to room temperature and all volatiles were evaporated. The residue was extracted three times with 20 ml dichloromethane and three times with 20 ml H₂O. The combined organic phases were dried over Na₂SO₄. After evaporating the solvent, the product was obtained by washing two times with 20 ml dry MeOH.

Yield: 0.80 g (2.01 mmol, 41 %, colorless solid).

Elemental Analysis: C₂₄H₂₃N₄P (398.45 g/mol) + 0.5 H₂O.

Calculated : C: 70.75% H: 5.94% N: 13.75%

Found : C: 70.58% H: 5.79% N: 13.92%

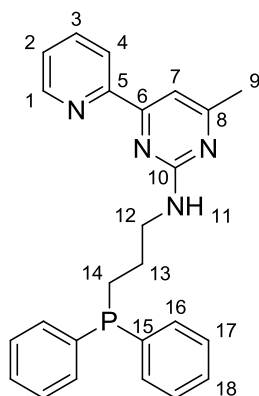
¹H NMR (400.1 MHz, CDCl₃, 20 °C): δ 8.69 (dd, ³J_{HH} = 4.6 Hz and ⁴J_{HH} = 0.7 Hz, 1H, H1), 8.41 (d, ³J_{HH} = 5.1 Hz, 1H, H8), 8.33 (d, ³J_{HH} = 7.9 Hz, 1H, H4), 7.80 (td, ³J_{HH} = 7.7 Hz and ⁴J_{HH} = 1.8 Hz, 1H, H3), 7.56 (d, ³J_{HH} = 5.1 Hz, 1H, H7), 7.44-7.39 (m, 4H, H15), 7.36 (ddd, ³J_{HH} = 7.5 Hz, ³J_{HH} = 4.8 Hz and ⁴J_{HH} = 1.0 Hz, 1H, H2), 7.31-7.29 (m, 6H, H16 and H17), 5.26 (t, ³J_{HH} = 4.8 Hz, 1H, H10), 3.60 (q, ³J_{HH} = 6.6 Hz, 2H, H11), 2.18-2.14 (m, 2H, H13), 1.86-1.77 (m, 2H, H12) ppm.

^{13}C NMR (100.6 MHz, CDCl_3 , 20 °C): δ 163.7 (s, C8), 162.4 (s, C9), 159.3 (s, C6), 155.0 (s, C5), 149.5 (s, C1), 138.7 (d, $^1J_{\text{PC}} = 12.6$ Hz, C14), 137.0 (s, C3), 132.8 (d, $^2J_{\text{PC}} = 18.4$ Hz, C15), 128.7 (s, C17), 128.6 (d, $^3J_{\text{PC}} = 6.6$ Hz, C16), 125.1 (s, C2), 121.5 (s, C4), 107.1 (s, C7), 42.7 (d, $^3J_{\text{PC}} = 14.0$ Hz, C11), 26.2 (d, $^2J_{\text{PC}} = 17.2$ Hz, C12), 25.6 (d, $^1J_{\text{PC}} = 11.3$ Hz, C13) ppm.

^{31}P NMR (161.98 MHz, CDCl_3 , 20 °C): δ -16.41 (s) ppm.

IR $\tilde{\nu}$ (cm^{-1}): 3350 (w), 3050 (w), 2962 (w), 1600 (m), 1558 (s), 1481 (m), 1434 (m), 1389 (w), 1362 (w), 1184 (w), 1161 (w), 1103 (m), 1055 (w), 1027 (w), 997 (w), 881 (w), 770 (w), 740 (m), 691 (s).

5.8.4 *N*-(3-(Diphenylphosphinyl)propyl)-4-methyl-6-(pyridin-2-yl)pyrimidin-2-amine (12b)



Under nitrogen atmosphere, 400 mg (6.70 mmol) of NaOMe were added to a solution of 2.09 g (3.13 mmol) of 1-(3-(Diphenylphosphinyl)propyl) guanidinium sulfate (**10b**) in 20 ml dry EtOH. The reaction mixture was heated to 78 °C. After stirring for 30 minutes, 900 mg (4.73 mmol) of 3-(dimethylamino)-1-(pyridin-2-yl)but-2-en-1-one (**3b**) were added to the mixture and refluxed for 24 hours. The solvent was evaporated and the residue was extracted three times with 20 ml of dichloromethane and washed three times with 20 ml of H_2O . The organic phases were combined and dried over Na_2SO_4 . After evaporating the solvent, the product was obtained by washing two times with 20 ml dry MeOH.

Yield: 800 mg (1.94 mmol, 37 %, pale yellow solid).

Elemental Analysis: C₂₅H₂₅N₄P (412.47 g/mol) + 0.6H₂O

Calculated : C: 70.81% H: 6.26% N: 13.19%

Found : C: 70.80% H: 6.24% N: 13.26%

¹H NMR (400.1 MHz, CDCl₃, 20 °C): δ 8.68 (d, ³J_{HH} = 4.0 Hz, 1H, H1), 8.33 (d, ³J_{HH} = 7.9 Hz, 1H, H4), 7.79 (td, ³J_{HH} = 7.7 Hz and ⁴J_{HH} = 1.7 Hz, 1H, H3), 7.46 (s, 1H, H7), 7.43-7.39 (m, 4H, H16), 7.35 (ddd, ³J_{HH} = 7.6 Hz, ³J_{HH} = 4.8 Hz and ³J_{HH} = 1.1 Hz, 1H, H2), 7.31-7.29 (m, 6H, H17 and H18), 3.60 (t, ³J_{HH} = 6.8 Hz, 2H, H12), 2.41 (s, 3H, H9), 2.18-2.14 (m, 2H, H14), 1.85-1.76 (m, 2H, H13) ppm.

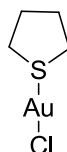
¹³C NMR (100.6 MHz, CDCl₃, 20 °C): 169.5 (s, C8), 163.5 (s, C10), 162.9 (s, C6), 155.4 (s, C5), 149.5 (s, C1), 139.0 (d, ¹J_{PC} = 12.7 Hz, C15), 137.2 (s, C3), 133.0 (d, ²J_{PC} = 18.4 Hz, C16), 128.9 (s, C18), 128.8 (d, ³J_{PC} = 6.6 Hz, C17), 125.1 (s, C2), 121.9 (s, C4), 106.8 (s, C7), 42.8 (d, ³J_{PC} = 13.9 Hz, C12), 26.4 (d, ²J_{PC} = 16.2 Hz, C13), 25.8 (d, ¹J_{PC} = 11.7 Hz, C14), 24.7 (s, C9) ppm.

³¹P NMR (161.98 MHz, CDCl₃, 20 °C): δ -16.37 (s) ppm.

IR $\tilde{\nu}$ (cm⁻¹): 3254 (m), 3072 (w), 2956 (w), 2918 (w), 1606 (m), 1585 (m), 1562 (s), 1479 (w), 1461 (w), 1432 (m), 1420 (m), 1374 (w), 1358 (m), 1349 (m), 1300 (w), 1256 (m), 1220 (w), 1204 (w), 1181 (w), 1090 (m), 1021 (m), 995 (m), 887 (w), 845 (w), 798 (m), 780 (s), 743 (s), 728 (s), 694 (s).

5.9 Synthesis of Monometallic Complexes

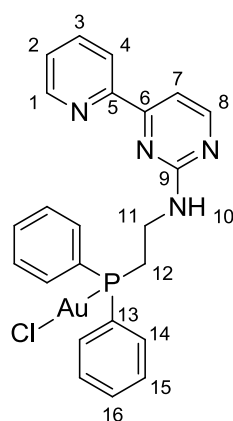
5.9.1 Chlorotetrahydrothiophenegold(I) (13)



The title compound was synthesized according to literature.^[135] To an orange solution of 800 mg (2.07 mmol) of KAuCl_4 in 10 ml H_2O , 0.56 ml (6.21 mmol) of tetrahydrothiophene were added dropwise at 0 °C. The reaction mixture was stirred for 30 minutes and the precipitate was filtered off, washed two times with 5 ml of water and two times with 5 ml of diethyl ether under nitrogen atmosphere. The resulting white solid was dried in *vacuo*. Chlorotetrahydrothiophenegold(I) was used as a gold precursor for the synthesis of monogold complexes without further purification.

Yield: 586 mg (1.83 mmol, 88%, colorless solid).

5.9.2 Au Complex 14a



156 mg (0.40 mmol) of **11a** were added to a solution of 130 mg (0.40 mmol) of $\text{Au}(\text{tth})\text{Cl}$ in 10 ml CH_2Cl_2 . After stirring for 1 hour at room temperature, the solution was concentrated and product was precipitated by adding 5 ml of Et_2O . The product was collected by filtration and dried in *vacuo*.

Yield: 222 mg (0.36 mmol, 89%, colorless solid).

Elemental Analysis: C₂₃H₂₁AuClN₄P (616.84 g/mol)

Calculated : C: 44.78% H: 3.43% N: 9.08%

Found : C: 44.22% H: 3.59% N: 10.70%

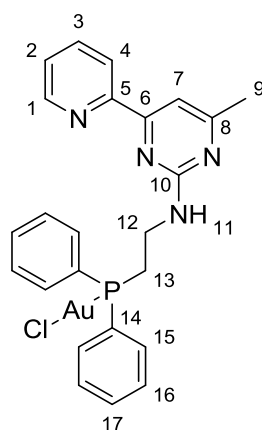
¹H NMR (400.1 MHz, CDCl₃, 20 °C): δ 8.68 (d, ³J_{HH} = 4.0 Hz, 1H, H1), 8.39 (d, ³J_{HH} = 5.0 Hz, 1H, H8), 8.32 (d, ³J_{HH} = 7.4 Hz, 1H, H4), 7.90 (t, ³J_{HH} = 7.5 Hz, 1H, H3), 7.71-7.66 (m, 4H, H14), 7.61 (d, ³J_{HH} = 5.0 Hz, 1H, H7), 7.49-7.41 (m, 6H, H15 and H16), 7.41-7.39 (m, 1H, H2), 5.48 (t, ³J_{HH} = 6.0 Hz, 1H, H10), 3.94-3.86 (m, 2H, H11), 2.97 -2.90 (m, 2H, H12) ppm.

¹³C NMR (100.6 MHz, CDCl₃, 20 °C): δ 163.9 (s, C6), 161.7 (s, C9), 159.3 (s, C8), 154.3 (s, C5), 149.2 (s, C1), 137.4 (s, C3), 133.3 (d, ²J_{PC} = 13.3 Hz, C14), 132.1 (d, ⁴J_{PC} = 2.4 Hz, C16), 129.4 (d, ³J_{PC} = 11.7 Hz, C15), 129.2 (d, ¹J_{PC} = 61.0 Hz, C13), 125.3 (s, C2), 121.8 (s, C4), 107.8 (s, C7), 38.7 (d, ²J_{PC} = 7.8 Hz, C13), 28.5 (d, ¹J_{PC} = 35.5 Hz, C12) ppm.

³¹P NMR (161.98 MHz, CDCl₃, 20 °C): δ 24.39 (s) ppm.

IR $\tilde{\nu}$ (cm⁻¹): 3239 (w), 3051 (w), 2962 (w), 1551 (s), 1522 (m), 1479 (w), 1452 (w), 1434 (m), 1413 (m), 1354 (m), 1255 (w), 1180 (w), 1100 (m), 1074 (w), 1044 (w), 1026 (w), 995 (m), 785 (s), 641 (s), 680 (s).

5.9.3 Au Complex 14b



200 mg (0.50 mmol) of **11b** were added to the solution of 170 mg (0.50 mmol) of Au(tht)Cl in 10 ml of CH₂Cl₂. After stirring for 1 hour at room temperature, the solution was concentrated and product was precipitated by adding 5 ml of Et₂O. The product was collected by filtration and dried in *vacuo*.

Yield: 233 mg (0.37 mmol, 74 %, colorless solid).

Elemental Analysis: C₂₄H₂₃AuClN₄P (630.87g/mol) + 1.5 H₂O

Calculated : C: 43.82% H: 3.98% N: 8.52%

Found : C: 43.88% H: 3.69% N: 8.22%

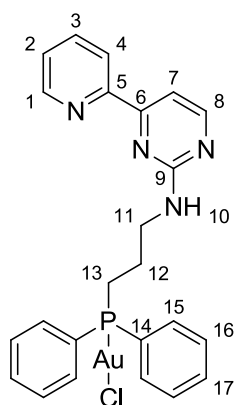
¹H NMR (400.1 MHz, CDCl₃, 20 °C): δ 8.69 (ddd, ³J_{HH} = 4.8 Hz, ⁴J_{HH} = 1.8 Hz and ⁵J_{HH} = 0.9 Hz, 1H, H1), 8.34 (d, ³J_{HH} = 7.4 Hz, 1H, H4), 7.91 (t, ³J_{HH} = 7.4 Hz, 1H, H3), 7.75-7.60 (m, 4H, H15), 7.54 (s, 1H, H7), 7.52-7.44 (m, 6H, H16 and H17), 7.40 (ddd, ³J_{HH} = 7.4 Hz, ³J_{HH} = 4.8 Hz and ⁴J_{HH} = 1.0 Hz, 1H, H2), 5.39 (t, ³J_{HH} = 6.0 Hz, 1H, H11), 3.96-3.88 (m, 2H, H12), 2.98-2.92 (m, 2H, H13), 2.44 (s, 3H, H9) ppm.

¹³C NMR (100.6 MHz, CDCl₃, 20 °C): δ 169.4 (s, C8), 161.8(s, C10), 157.6 (s, C6), 154.5 (s, C5), 149.2 (s, C1), 137.2 (s, C3), 133.2 (d, ²J_{PC} = 13.3 Hz, C15), 131.9 (d, ⁴J_{PC} = 2.1 Hz, C17), 129.3 (d, ³J_{PC} = 11.7 Hz, C16), 129.1 (d, ¹J_{PC} = 60.8 Hz, C14), 125.0 (s, C2), 121.8 (s, C4), 107.2 (s, C7), 38.5 (d, ²J_{PC} = 8.3 Hz, C12), 28.4 (d, ¹J_{PC} = 36.4 Hz, C13), 23.9 (s, C9) ppm.

^{31}P NMR (161.98 MHz, CDCl_3 , 20 °C): δ 24.07 (s) ppm.

IR $\tilde{\nu}$ (cm^{-1}): 3249 (w), 3076 (w), 1738 (w), 1604 (m), 1582 (w), 1559 (s), 1480 (w), 1459 (w), 1435 (m), 1376 (w), 1349 (m), 1311 (w), 1258 (w), 1225 (w), 1204 (w), 1180 (w), 1136 (w), 1104 (m), 993 (m), 943 (w), 881 (w), 801 (w), 781 (m), 755 (m), 738 (s), 702 (s), 691 (s).

5.9.4 Au Complex 15a



200 mg (0.50 mmol) of **12a** were added to a solution of 160 mg (0.50 mmol) of Au(tht)Cl in 10 ml of CH_2Cl_2 . After stirring for 1 hour at room temperature, the solution was concentrated and product was precipitated by adding 5 ml Et_2O . The product was collected by filtration and dried in *vacuo*.

Yield: 260 mg (0.41 mmol, 82 %, colorless solid).

Elemental Analysis: $\text{C}_{24}\text{H}_{23}\text{AuClN}_4\text{P}$ (630.87 g/mol) + 1.4 H_2O

Calculated : C: 43.94% H: 3.96% N: 8.54%

Found : C: 44.11% H: 3.94% N: 8.31%

^1H NMR (400.1 MHz, CDCl_3 , 20 °C): δ 8.69 (d, $^3J_{\text{HH}} = 4.0$ Hz, 1H, H1), 8.39 (d, $^3J_{\text{HH}} = 5.2$ Hz, 1H, H8), 8.29 (d, $^3J_{\text{HH}} = 7.9$ Hz, 1H, H4), 7.84 (td, $^3J_{\text{HH}} = 7.9$ Hz and $^4J_{\text{HH}} = 1.7$ Hz, 1H, H3), 7.65-7.59 (m, 5H, H2 and H15), 7.48-7.36 (m, 7H, H7, H16 and

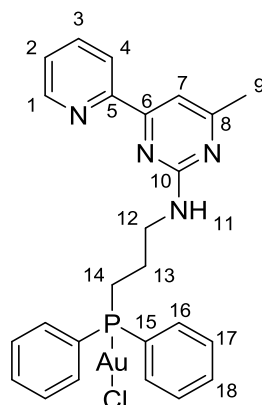
H17), 5.41 (s, 1H, H10), 3.65 (q, $^3J_{\text{HH}} = 6.3$ Hz, 2H, H11), 2.62-2.49 (m, 2H, H13), 2.09-1.94 (m, 2H, H12) ppm.

^{13}C NMR (100.6 MHz, CDCl_3 , 20 °C): δ 164.4 (s, C6), 162.3 (s, C9), 159.1 (s, C8), 154.8 (s, C5), 149.9 (s, C1), 137.5 (s, C3), 133.6 (d, $^2J_{\text{PC}} = 13.1$ Hz, C15), 132.5 (d, $^4J_{\text{PC}} = 2.4$ Hz, C17), 129.7 (d, $^3J_{\text{PC}} = 11.7$ Hz, C16), 129.6 (d, $^1J_{\text{PC}} = 60.1$ Hz, C14), 125.6 (s, C2), 122.0 (s, C4), 107.8 (s, C7), 42.1 (d, $^3J_{\text{PC}} = 18.1$ Hz, C11), 30.2 (s, C12), 26.2 (d, $^1J_{\text{PC}} = 39.0$ Hz, C13) ppm.

^{31}P NMR (161.98 MHz, CDCl_3 , 20 °C): δ 29.42 (s) ppm.

IR $\tilde{\nu}$ (cm^{-1}): 3250 (w), 3050 (w), 2970 (w), 1740 (m), 1595 (m), 1553 (s), 1479 (w), 1434 (s), 1377 (w), 1344 (w), 1236 (w), 1204 (w), 1158 (w), 1103 (m), 1024 (w), 995 (w), 878 (w), 841 (w), 786 (m), 767 (w), 786 (m), 739 (s), 690 (s).

5.9.5 Au Complex 15b



206 mg (0.50 mmol) of **12b** were added to the solution of 160 mg (0.50 mmol) of Au(tht)Cl in 10 ml of CH_2Cl_2 . After stirring for 1 hour at room temperature, the solution was concentrated and product was precipitated by adding 5 ml of Et_2O . The product was collected by filtration and dried in *vacuo*.

Yield: 162 mg (0.25 mmol, 50 %, colorless solid).

Elemental Analysis: $\text{C}_{25}\text{H}_{25}\text{AuClN}_4\text{P}$ (644.89 g/mol) + 1.6 H_2O

Calculated : C: 44.57% H: 4.22% N: 8.32%

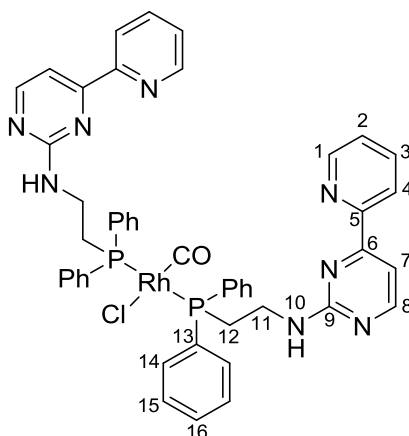
Found : C: 44.95% H: 3.95% N: 7.90%

¹H NMR (400.1 MHz, CDCl₃, 20 °C): δ 8.68 (dd, ³J_{HH} = 4.6 Hz and ⁴J_{HH} = 1.7 Hz, 1H, H1), 8.27 (d, ³J_{HH} = 7.9 Hz, 1H, H4), 7.83 (td, ³J_{HH} = 7.8 Hz and ⁴J_{HH} = 1.7 Hz, 1H, H3), 7.64-7.59 (m, 4H, H16), 7.50 (s, 1H, H7), 7.46-7.35 (m, 7H, H2, H17 and H18), 5.14 (t, ³J_{HH} = 6.0 Hz, 1H, H11), 3.65 (q, ³J_{HH} = 6.4 Hz, 2H, H12), 2.59-2.52 (m, 2H, H14), 2.41 (s, 3H, H9), 2.09-1.98 (m, 2H, H13) ppm.

¹³C NMR (100.6 MHz, CDCl₃, 20 °C): δ 169.4 (s, C8), 163.4 (s, C10), 162.6 (s, C6), 155.0 (s, C5), 149.4 (s, C1), 137.2 (s, C3), 133.3 (d, ²J_{PC} = 12.9 Hz, C16), 132.1 (d, ⁴J_{PC} = 2.4 Hz, C18), 129.4 (d, ³J_{PC} = 11.6 Hz, C17), 129.3 (d, ¹J_{PC} = 60.3 Hz, C15), 125.1 (s, C2), 121.8 (s, C4), 107.1 (s, C7), 41.8 (d, ³J_{PC} = 18.3 Hz, C12), 25.9 (d, ¹J_{PC} = 39.4 Hz, C14), 25.8 (d, ²J_{PC} = 3.0 Hz, C13), 24.9 (s, C9) ppm.

³¹P NMR (161.98 MHz, CDCl₃, 20 °C): δ 29.39 (s) ppm.

5.9.6 Rh Complex 16



To a solution of 90.0 mg (0.23 mmol) tetracarbonyldi- μ -chlorodirhodium(I) in 5 ml of CH₂Cl₂, a solution of 345 mg (0.90 mmol) of *N*-(2-(diphenylphosphino)ethyl)-4-(pyridin-2-yl)pyrimidin-2-amine (**11a**) in 5ml of CH₂Cl₂ were added. The reaction mixture was

stirred at room temperature for 24 hours. The solvent was evaporated and the compound was dried under reduced pressure.

Yield: 334 mg (0.35 mmol, 80 %, red solid).

Elemental Analysis: C₄₇H₄₂ClN₈OP₂Rh (935.21) + 1.6 H₂O

Calculated : C: 58.56% H: 4.73% N: 11.62%

Found : C: 58.66% H: 4.70% N: 11.52%

¹H NMR (400.1 MHz, CDCl₃, 20 °C): δ 8.66 (d, ³J_{HH} = 4.1 Hz, 1H, H1), 8.43 (d, ³J_{HH} = 5.0 Hz, 1H, H8), 8.19 (d, ³J_{HH} = 7.8 Hz, 1H, H4), 7.77-7.67 (m, 5H, H3 and H14), 7.55 (d, ³J_{HH} = 5.0 Hz, 1H, H7), 7.37-7.28 (m, 7H, H2, H15 and H16), 6.22 (s, 1H, H10), 4.01-3.96 (m, 2H, H11), 3.10-3.05 (m, 2H, H12) ppm.

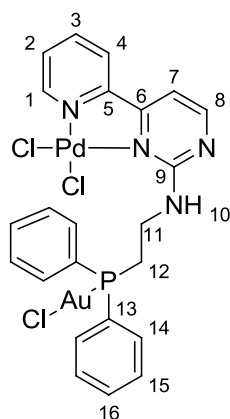
¹³C NMR (100.6 MHz, CDCl₃-d₆, 20 °C): δ 163.5 (s, C6), 162.3 (s, C9), 159.3 (s, C8), 154.9 (s, C5), 136.9 (s, C3), 133.4 (t, J_{RhPC} = 6.3 Hz, C14), 130.2 (s, C16), 129.7 (dd, J_{RhPC} = 200.5 and 11.8 Hz, C13), 128.5 (t, J_{RhPC} = 4.8 Hz, C15), 125.0 (s, C2), 121.6 (s, C4), 107.0 (s, C7), 38.1 (s, C11), 27.2 (t, J_{RhPC} = 13.2 Hz, C12) ppm.

³¹P NMR (161.98 MHz, CDCl₃, 20 °C): δ 20.56 (d, ¹J_{RhP} = 122.8 Hz) ppm.

IR $\tilde{\nu}$ (cm⁻¹): 3200 (w), 3051 (w), 2963 (w), 1966 (s), 1552 (s), 1522 (m), 1478 (w), 1451 (w), 1432 (m), 1412 (w), 1350 (m), 1261 (w), 1182 (w), 1096 (m), 1073 (w), 1026 (w), 995 (m), 784 (s), 740 (s), 682 (s).

5.10 Synthesis of Heterobimetallic Complexes

5.10.1 Pd-Au Complex 17a



To a solution 140 mg (0.22 mmol) of gold complex **14a** in 5 ml of CH_2Cl_2 , 86.0 mg (0.22 mmol) of bis(benzonitrile)palladium(II) chloride in 5 ml of CH_2Cl_2 were added dropwise under nitrogen atmosphere. After stirring for 24 hours at room temperature, the precipitate was filtered, washed two times with 5 ml of CH_2Cl_2 and dried in *vacuo*.

Yield: 90.0 mg (0.11 mmol, 51.0 %, yellow solid).

Elemental Analysis: $\text{C}_{23}\text{H}_{21}\text{AuCl}_3\text{N}_4\text{PPd}$ (794.17 g/mol).

Calculated : C: 34.78% H: 2.67% N: 7.05%

Found : C: 34.23% H: 2.72% N: 7.06%

^1H NMR (200.1 MHz, $\text{DMSO}-d_6$, 20 °C): δ 9.57 (t, $^3J_{\text{HH}} = 5.7$ Hz, 1H, H10), 9.20 (d, $^3J_{\text{HH}} = 5.9$ Hz, 1H, H1), 8.67 (d, $^3J_{\text{HH}} = 4.9$ Hz, 1H, H8), 8.56 (d, $^3J_{\text{HH}} = 7.9$ Hz, 1H, H4), 8.35 (t, $^3J_{\text{HH}} = 7.8$ Hz, 1H, H3), 7.85-7.82 (m, 1H, H2), 7.80-7.75 (m, 4H, H14), 7.66 (d, $^3J_{\text{HH}} = 4.9$ Hz, H7), 7.57-7.44 (m, 6H, H15 and H16), 3.79-3.70 (m, 2H, H11), 3.19 -3.13 (m, 2H, H12) ppm.

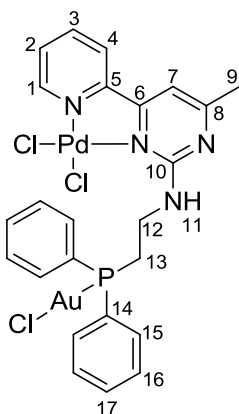
^{13}C NMR (100.6 MHz, $\text{DMSO}-d_6$, 20 °C): δ 163.3 (s, C6), 161.7 (s, C8), 160.9 (s, C9), 156.5 (s, C5), 150.1 (s, C1), 141.3 (s, C3), 133.2 (d, $^2J_{\text{PC}} = 13.4$ Hz, C14), 131.8 (s, C16),

129.33 (d, $^3J_{PC} = 11.5$ Hz, C15), 129.30 (d, $^1J_{PC} = 60.7$ Hz, C13), 128.6 (s, C2), 125.0 (s, C4), 107.3 (s, C7), 37.8 (s, C11), 25.6 (s, C12) ppm.

^{31}P NMR (161.98 MHz, DMSO- d_6 , 20 °C): δ 25.96 (s) ppm.

IR $\tilde{\nu}$ (cm^{-1}): 3205 (w), 3118 (w), 3048 (w), 2924 (w), 1739 (m), 1591 (s), 1570 (w), 1497 (m), 1485 (w), 1467 (s), 1448 (w), 1435 (s), 1420 (w), 1378 (w), 1354 (s), 1312 (w), 1264 (w), 1232 (m), 1217 (m), 1205 (m), 1176 (w), 1157 (m), 1120 (m), 1105 (s), 1083 (w), 1057 (w), 1036 (w), 1009 (m), 984 (m), 953 (w), 891 (m), 840 (w), 827 (s), 813 (s), 784 (s), 769 (s), 741 (s), 718 (s), 700 (s), 687 (s), 668 (m).

5.10.2 Pd-Au Complex 17b



To a solution 142 mg of (0.22 mmol) gold complex **14b** in 5 ml of CH_2Cl_2 , 86.0 mg (0.22 mmol) of bis(benzonitrile)palladium(II) chloride in 5 ml of CH_2Cl_2 were added dropwise under nitrogen atmosphere. After stirring for 24 hours at room temperature, the precipitate was filtered, washed two times with 5 ml of CH_2Cl_2 and dried under vacuum.

Yield: 100 mg (0.12 mmol, 56 %, yellow solid).

Elemental Analysis: $\text{C}_{24}\text{H}_{23}\text{AuCl}_3\text{N}_4\text{PPd}$ (808.19 g/mol)

Calculated : C: 35.67% H: 2.87% N: 6.93%

Found : C: 34.67% H: 2.84% N: 6.73%

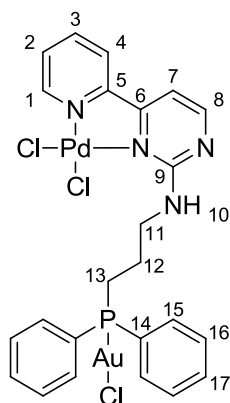
^1H NMR (200.1 MHz, DMSO- d_6 , 20 °C): δ 9.45 (br. s, 1H, H11), 9.19 (dd, $^3J_{\text{HH}} = 5.8$ Hz and $^4J_{\text{HH}} = 1.1$ Hz, 1H, H1), 8.51 (dd, $^3J_{\text{HH}} = 7.7$ Hz and $^4J_{\text{HH}} = 0.8$ Hz, 1H, H4), 8.34 (td, $^3J_{\text{HH}} = 7.9$ Hz and $^4J_{\text{HH}} = 1.4$ Hz, 1H, H3), 7.82-7.76 (m, 5H, H2 and H15), 7.62 (s, 1H, H7), 7.56-7.46 (m, 6H, H16 and H17), 3.83-3.73 (m, 2H, H12), 3.17-3.09 (m, 2H, H13), 2.45 (s, 3H, H9) ppm.

^{13}C NMR could not be measured because of the low solubility of the complex.

^{31}P NMR (161.98 MHz, DMSO- d_6 , 20 °C): δ 26.08 (s) ppm.

IR $\tilde{\nu}$ (cm^{-1}): 3226 (m), 3147 (w), 3103 (w), 3055 (w), 1738 (m), 1608 (s), 1583 (s), 1491 (m), 1474 (m), 1435 (s), 1390 (m), 1355 (s), 1310 (w), 1217 (m), 1165 (m), 1109 (m), 1086 (w), 1053(w), 1014 (w), 1001 (w), 948 (w), 870 (w), 847 (w), 789 (m), 771 (m), 742 (s), 710 (m), 692 (s).

5.10.3 Pd-Au Complex 17c



To a solution 141 mg (0.22 mmol) of gold complex **15a** in 5 ml of CH_2Cl_2 , 86.0 mg (0.22 mmol) of bis(benzonitrile)palladium(II) chloride in 5 ml of CH_2Cl_2 were added dropwise under nitrogen atmosphere. After stirring for 24 hours at room temperature, the precipitate was filtered, washed two times with 5 ml of CH_2Cl_2 and dried in *vacuo*.

Yield: 130 mg (0.16 mmol, 72 %, yellow solid).

Elemental Analysis: C₂₄H₂₃AuCl₃N₄PPd (808.19 g/mol).

Calculated : C: 35.67% H: 2.87% N: 6.93%

Found : C: 35.13% H: 2.96% N: 6.86%

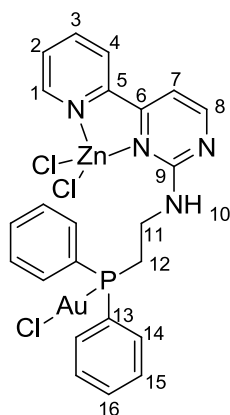
¹H NMR (400.1 MHz, DMSO-*d*₆, 20 °C): δ 9.39 (t, ³J_{HH} = 5.1 Hz, 1H, H10), 9.19 (dd, ³J_{HH} = 5.9 Hz and ⁴J_{HH} = 1.5 Hz, 1H, H1), 8.68 (d, ³J_{HH} = 4.8 Hz, 1H, H8), 8.57 (dd, ³J_{HH} = 8.2 Hz and ⁴J_{HH} = 1.5 Hz, 1H, H4), 8.33 (td, ³J_{HH} = 7.8 Hz and ⁴J_{HH} = 1.5 Hz, 1H, H3), 7.82 (ddd, ³J_{HH} = 7.5 Hz, ³J_{HH} = 5.9 Hz and ⁴J_{HH} = 1.5 Hz, 1H, H2), 7.79-7.73 (m, 4H, H15), 7.64 (d, ³J_{HH} = 4.8 Hz, 1H, H7), 7.58-7.54 (m, 6H, H16 and H17), 3.53 (q, ³J_{HH} = 6.4 Hz, 2H, H11), 2.91-2.84 (m, 2H, H13), 1.85-1.75 (m, 2H, H12) ppm.

¹³C NMR (100.6 MHz, DMSO-*d*₆, 20 °C): δ 163.4 (s, C6), 162.0 (s, C8), 161.2 (s, C9), 156.8 (s, C5), 150.1 (s, C1), 141.3 (s, C3), 133.1 (d, ²J_{PC} = 13.1 Hz, C15), 132.1 (d, ⁴J_{PC} = 2.4 Hz, C17), 129.5 (d, ³J_{PC} = 11.5 Hz, C16), 129.3 (d, ¹J_{PC} = 59.5 Hz, C14), 128.1 (s, C2), 125.1 (s, C4), 41.5 (d, ³J_{PC} = 60.4 Hz, C11), 24.2 (d, ²J_{PC} = 4.2 Hz, C12), 23.3 (d, ¹J_{PC} = 107.9 Hz, C13) ppm.

³¹P NMR (161.98 MHz, DMSO-*d*₆, 20 °C): δ 30.70 (s) ppm.

IR ν (cm⁻¹): 3359 (w), 3050 (w), 2970 (w), 1739 (m), 1599 (m), 1558 (s), 1481 (m), 1435 (m), 1361 (m), 1217 (m), 1104 (m), 1056 (w), 1028 (w), 997 (w), 881 (w), 788 (m), 770 (m), 743 (s), 690 (s).

5.10.4 Zn-Au Complex 18a



To a solution 33.0 mg (0.24 mmol) of ZnCl_2 in 5 ml of CH_2Cl_2 , a solution of 150 mg (0.24 mmol) of gold complex **14a** in 5 ml of CH_2Cl_2 were added dropwise under nitrogen atmosphere. After stirring at room temperature for 24 hours, the solvent was evaporated and the compound was washed with Et_2O .

Yield: 140 mg (0.19 mmol, 77 %, colorless solid).

Elemental Analysis: $\text{C}_{23}\text{H}_{21}\text{AuCl}_3\text{N}_4\text{PZn}$ (753.1 g/mol)

Calculated : C: 36.68% H: 2.81% N: 7.44%

Found : C: 38.20% H: 3.04% N: 7.79%

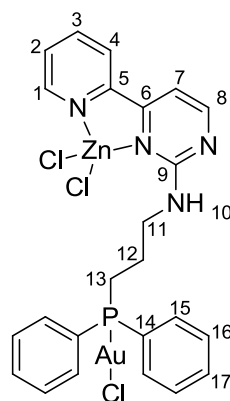
^1H NMR (400.1 MHz, CDCl_3 , 20 °C): δ 8.76 (m, 1H, H1), 8.68 (br. s, 1H, H8), 8.26 (br. s, 1H, H4), 8.14 (br. s, 1H, H3), 7.73-7.68 (m, 5H, H2 and H14), 7.53-7.46 (m, 7H, H7, H15 and H16), 6.52 (s, 1H, H10), 3.90-3.85 (m, 2H, H11), 2.91 (td, $^2J_{\text{PH}} = 10.8$ Hz and $^3J_{\text{HH}} = 7.8$ Hz, 2H, H12) ppm.

^{13}C NMR (100.6 MHz, CDCl_3 , 20 °C): δ 160.6 (s, C8), 149.5 (s, C1), 133.4 (d, $^2J_{\text{PC}} = 13.4$ Hz, C14), 132.3 (d, $^4J_{\text{PC}} = 2.7$ Hz, C16), 129.7 (s, C), 129.6 (d, $^3J_{\text{PC}} = 11.8$ Hz, C15), 129.0 (s, C), 123.0 (s, C4), 107.0 (s, C7), 38.6 (d, $^2J_{\text{PC}} = 10.0$ Hz, C11), 28.5 (d, $^1J_{\text{PC}} = 36.4$ Hz, C12) ppm. Some of the carbon signals are missing due to line broadening and low solubility of the complex.

^{31}P NMR (161.98 MHz, CDCl_3 , 20 °C): δ 23.53 (s) ppm.

IR $\tilde{\nu}$ (cm^{-1}): 3321 (w), 3054 (w), 2924 (w), 1570 (s), 1485 (m), 1464 (m), 1432 (s), 1357 (s), 1313 (w), 1266 (w), 1215 (m), 1186 (w), 1140 (w), 1103 (m), 1077 (w), 1051 (w), 997 (m), 887 (w), 830 (w), 779 (s), 741 (s), 689 (s), 663 (m).

5.10.5 Zn-Au Complex 18b



To a solution 34.0 mg (0.25 mmol) of ZnCl_2 in 5 ml of CH_2Cl_2 , a solution 158 mg (0.25 mmol) gold complex **15a** in 5 ml of CH_2Cl_2 were added dropwise under nitrogen atmosphere. After stirring at room temperature for 24 hours, the solvent was evaporated and the compound was washed with Et_2O .

Yield: 140 mg (0.18 mmol, 73 %, colorless solid).

Elemental Analysis: $\text{C}_{24}\text{H}_{23}\text{AuCl}_3\text{N}_4\text{PZn}$ (767.16 g/mol)

Calculated : C: 37.68% H: 3.02% N: 7.30%

Found : C: 38.44% H: 3.18% N: 7.40%

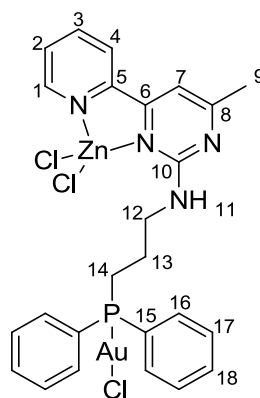
^1H NMR (400.1 MHz, CDCl_3 , 20 °C): δ 8.77 (d, $^3J_{\text{HH}} = 4.2$ Hz, 1H, H1), 8.63 (br. s, 1H, H8), 8.26 (d, $^3J_{\text{HH}} = 8.0$ Hz, 1H, H4), 8.11 (br. s, 1H, H3), 7.80-7.69 (m, 5H, H2 and H15), 7.48-7.41 (m, 7H, H7, H16 and H17), 6.31 (s, 1H, H10), 3.67 (q, $J_{\text{HH}} = 6.08$ Hz, 2H, H11), 2.68-2.61 (m, 2H, H13), 2.03 (m, 2H, H12) ppm.

^{13}C NMR (100.6 MHz, CDCl_3 , 20 °C): δ 149.5 (s, C1), 133.5 (d, $^2J_{\text{PC}} = 13.3$ Hz, C15), 132.1 (d, $^4J_{\text{PC}} = 2.8$ Hz, C17), 129.5 (d, $^3J_{\text{PC}} = 11.6$ Hz, C16), 129.1 (d, $^1J_{\text{PC}} = 60.3$ Hz, C14), 122.9 (s, C4), 106.7 (s, C7), 41.9 (d, $^3J_{\text{PC}} = 17.5$ Hz, C11), 25.4 (d, $^1J_{\text{PC}} = 39.7$ Hz, C13), 25.2 (d, $^2J_{\text{PC}} = 3.9$ Hz, C12) ppm. Some of the carbon signals are missing due to line broadening and low solubility of the complex.

^{31}P NMR (161.98 MHz, CDCl_3 , 20 °C): δ 30.18 (s) ppm.

IR $\tilde{\nu}$ (cm^{-1}): 3457 (w), 3301 (w), 3017 (w), 2971 (w), 1739 (s), 1567 (m), 1487 (w), 1464 (w), 1434 (m), 1365 (s), 1354 (s), 1229 (s), 1217 (s), 1206 (s), 1104 (m), 1055 (w), 1024 (w), 997 (w), 896 (w), 828 (w), 780 (m), 742 (m), 691 (m), 658 (w).

5.10.6 Zn-Au Complex 18c



To a solution 20.0 mg (0.14 mmol) of ZnCl_2 in 5 ml of CH_2Cl_2 , a solution 91.0 mg (0.14 mmol) of the gold complex **15b** in 5 ml of CH_2Cl_2 were added dropwise under nitrogen atmosphere. After stirring at room temperature for 24 hours, the solvent was evaporated and the compound was washed with Et_2O .

Yield: 62 mg (0.08 mmol, 57 %, grey solid).

Elemental Analysis: C₂₅H₂₅AuCl₃N₄PZn (781.19 g/mol)

Calculated : C: 38.44% H: 3.23% N: 7.17%

Found : C: 38.39% H: 3.94% N: 6.57%

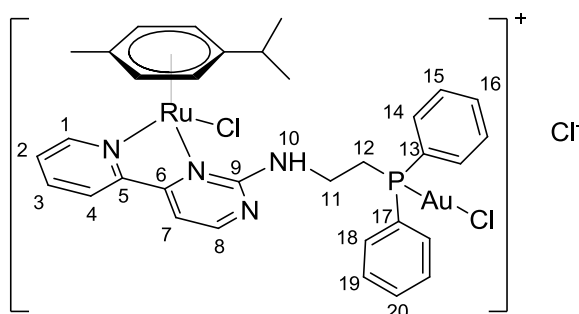
¹H NMR (400.1 MHz, CDCl₃, 20 °C): δ 8.78 (d, ³J_{HH} = 4.4 Hz, 1H, H1), 8.23 (d, J_{HH} = 8.0 Hz, 1H, H4), 8.14 (br. s, 1H, H3), 7.76-7.72 (m, 5H, H2 and H16), 7.49-7.40 (m, 7H, H7, H17 and H18), 6.23 (s, 1H, H11), 3.67 (q, ³J_{HH} = 6.0 Hz, 2H, H12), 2.68-2.62 (m, 2H, H14), 2.52 (s, 3H, H9), 2.08-1.98 (m, 2H, H13) ppm.

¹³C NMR (100.6 MHz, CDCl₃, 20 °C): δ 149.4 (s, C1), 133.5 (d, ²J_{PC} = 13.2 Hz, C16), 132.1 (d, ⁴J_{PC} = 2.4 Hz, C18), 129.4 (d, J_{PC} = 11.6 Hz, C17), 129.2 (d, ¹J_{PC} = 60.0 Hz, C15), 122.8 (s, C4), 106.5 (s, C7), 41.8 (d, ³J_{PC} = 12.9 Hz, C12), 29.8 (s, C9), 25.4 (s, C13), 25.3 (d, J_{PC} = 39.2 Hz, C14) ppm. Some of the carbon signals are missing due to line broadening and low solubility of the complex.

³¹P NMR (161.98 MHz, CDCl₃, 20 °C): δ 30.45 (s) ppm.

IR $\tilde{\nu}$ (cm⁻¹): 3450 (w), 3100 (w), 2962 (w), 1568 (s), 1485 (m), 1435 (m), 1380 (w), 1349 (m), 1260 (m), 1150 (w), 1102 (m), 1023 (m), 822 (w), 797 (s), 779 (s), 742 (m), 690 (s).

5.10.7 Ru-Au Complex 19a



A solution 120 mg (0.20 mmol) of gold complex **14a** in 5 ml of CH₂Cl₂ were added dropwise to a solution 61.0 mg (0.10 mmol) of [RuCl₂(*p*-cymene)]₂ in 5 ml of CH₂Cl₂.

After stirring for 20 hours at room temperature, the solution was concentrated and the product was precipitated by adding 10 ml Et₂O. The product was collected by filtration, and was washed twice with Et₂O. Yellow product was dried in *vacuo*.

Yield: 123 mg (0.13 mmol, 66 %, yellow solid).

Elemental Analysis: C₃₃H₃₅AuCl₃N₄PRu (923.04g/mol) + 1.85 H₂O

Calculated : C: 41.44% H: 4.08% N: 5.86%

Found : C: 41.66% H: 3.95% N: 5.64%

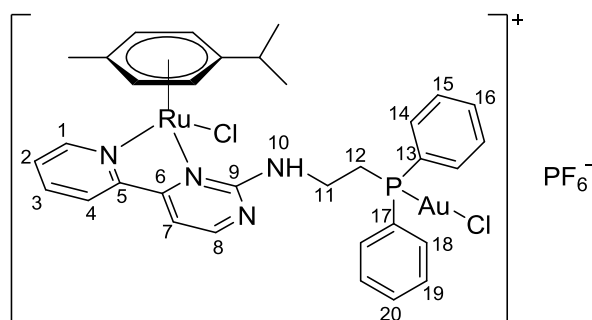
¹H NMR (400.1 MHz, CDCl₃, 20 °C): δ 9.72 (d, ³J_{HH} = 4.9 Hz, 1H, H1), 8.63 (d, ³J_{HH} = 4.7 Hz, 1H, H8), 8.50 (d, ³J_{HH} = 7.9 Hz, 1H, H4), 8.09 (t, ³J_{HH} = 7.6 Hz, 1H, H3), 7.83-7.72 (m, 6H, H2, H7, H14 and H18), 7.52-7.45 (m, 6H, H15, H16, H19 and H20), 6.89 (dd, ³J_{HH} = 7.2 Hz and ³J_{HH} = 4.5 Hz, 1H, H10), 6.17-6.14 (m, 2H, H_{cymene}), 6.04-6.00 (m, 2H, H_{cymene}), 4.16-3.91 (m, 2H, H11), 3.23-2.86 (m, 2H, H12), 2.48 (septet, ³J_{HH} = 6.9 Hz, 1H, H_{cymene}), 2.24 (s, 3H, H_{cymene}), 0.99 (d, ³J_{HH} = 6.9 Hz, 3H, H_{cymene}), 0.91 (d, ³J_{HH} = 6.9 Hz, 3H, H_{cymene}) ppm.

¹³C NMR (100.6 MHz, CDCl₃, 20 °C):δ 163.5 (s, C6), 162.3 (s, C9), 161.0 (s, C8), 157.4 (s, C1), 153.7 (s, C5), 140.1 (s, C3), 133.5 (d, ²J_{PC} = 13.6 Hz, C14,18), 132.4 (d, ⁴J_{PC} = 2.1 Hz, C16,20), 130.0 (s, C2), 129.6 (d, ³J_{PC} = 11.7 Hz, C15,19), 128.9 (d, ¹J_{PC} = 61.5 Hz, C16), 128.6 (d, ¹J_{PC} = 61.5 Hz, C17), 125.6 (s, C4), 109.4 (s, C7), 105.9 (s, C_{cymene}), 105.0 (s, C_{cymene}), 87.4 (s, C_{cymene}), 85.8 (s, C_{cymene}), 85.0 (s, C_{cymene}), 84.7 (s, C_{cymene}), 40.1 (d, ²J_{PC} = 9.5 Hz, C11), 31.2 (s, C_{cymene}), 28.0 (d, ¹J_{PC} = 36.4 Hz, C12), 22.3 (s, 2C, C_{cymene}), 19.1 (s, C_{cymene}) ppm.

³¹P NMR (161.98 MHz, CDCl₃, 20 °C): δ 24.77 (s) ppm.

IR $\tilde{\nu}$ (cm⁻¹): 3349 (w), 3031 (w), 2970 (w), 1739 (m), 1592 (m), 1563 (s), 1527 (w), 1482 (w), 1458 (w), 1435 (m), 1353 (m), 1263 (w), 1216 (m), 1138 (w), 1104 (m), 1056 (w), 1029 (w), 997 (w), 884 (w), 773 (m), 743 (m), 692 (s).

5.10.8 Ru-Au Complex 19b



A solution of 123 mg (0.20 mmol) of gold complex **14a** in 5 ml of CH_2Cl_2 were added dropwise to a solution 63.0 mg (0.10 mmol) of $[\text{RuCl}_2(p\text{-cymene})]_2$ in 5 ml of CH_2Cl_2 . 44.2 mg (0.24 mmol) of KPF_6 were also added to the reaction mixture. After stirring for 20 hours at room temperature, excess KPF_6 and KCl were removed via filtration. The filtrate was concentrated and the product was precipitated by adding 10 ml of Et_2O . The product was collected by filtration, was washed twice with Et_2O and dried in *vacuo*.

Yield: 162 mg (0.16 mmol, 78 %, yellow solid).

Elemental Analysis: $\text{C}_{35}\text{H}_{35}\text{AuCl}_2\text{F}_6\text{N}_4\text{P}_2\text{Ru}$ (1032.55/mol).

Calculated : C: 38.39% H: 3.42% N: 5.43%

Found : C: 38.75% H: 3.60% N: 5.39%

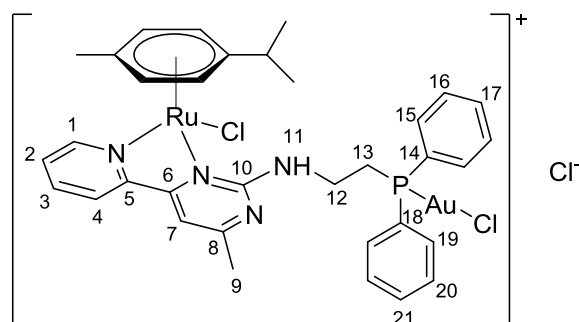
^1H NMR (400.1 MHz, CDCl_3 , 20 °C): δ 9.31 (d, $^3J_{\text{HH}} = 5.4$ Hz, 1H, H1), 8.64 (d, $^3J_{\text{HH}} = 4.8$ Hz, 1H, H8), 8.18 (d, $^3J_{\text{HH}} = 7.9$ Hz, 1H, H4), 8.08 (t, $^3J_{\text{HH}} = 7.7$ Hz, 1H, H3), 7.81-7.71 (m, 5H, H2, H14 and H18), 7.54-7.48 (m, 6H, H15, H16, H19 and H20), 7.45 (d, $^3J_{\text{HH}} = 4.8$ Hz, 1H, H7), 6.72 (dd, $^3J_{\text{HH}} = 7.3$ Hz and $^3J_{\text{HH}} = 4.3$ Hz, 1H, H10), 5.85 (d, $^3J_{\text{HH}} = 6.0$ Hz, 1H, H_{cymene}), 5.80-5.77 (m, 2H, H_{cymene}), 5.70 (d, $^3J_{\text{HH}} = 6.0$ Hz, 1H, H_{cymene}), 4.09-3.84 (m, 2H, H11), 3.13-2.82 (m, 2H, H12), 2.50 (septet, $^3J_{\text{HH}} = 6.9$ Hz, 1H, H_{cymene}), 2.17 (s, 3H, H_{cymene}), 1.02 (d, $^3J_{\text{HH}} = 6.9$ Hz, 3H, H_{cymene}), 0.96 (d, $^3J_{\text{HH}} = 6.9$ Hz, 3H, H_{cymene}) ppm.

^{13}C NMR (100.6 MHz, CDCl_3 , 20 °C): δ 163.6 (s, C6), 162.1 (s, C9), 161.1 (s, C8), 156.3 (s, C1), 153.8 (s, C5), 140.2 (s, C3), 133.5 and 133.4 (d, $^2J_{\text{PC}} = 13.7$ Hz, C14 and

C18), 132.6 and 132.5 (d, $^4J_{PC} = 2.6$ Hz, C16 and C20), 129.8 (s, C2), 129.7 and 129.6 (d, $^3J_{PC} = 11.9$ Hz, C15 and C19), 125.1 (s, C4), 109.0 (s, C7), 106.8 (s, C_{cymene}), 104.3 (s, C_{cymene}), 86.8 (s, C_{cymene}), 85.2 (s, C_{cymene}), 85.1 (s, C_{cymene}), 84.6 (s, C_{cymene}), 39.0 (s, C11), 31.3 (s, C_{cymene}), 27.9 (d, $^1J_{PC} = 36.7$ Hz, C12), 22.3 (s, C_{cymene}), 22.0 (s, C_{cymene}), 18.8 (s, C_{cymene}) ppm.

^{31}P NMR (161.98 MHz, CDCl₃, 20 °C): δ 24.30 (s, 1P, R(Ph)₂P–Au), –144.45 (septet, $^1J_{PF} = 712.7$ Hz, 1P, PF₆) ppm.

5.10.9 Ru-Au Complex 19c



A solution of 126 mg (0.20 mmol) of gold complex **14b** in 5 ml of CH₂Cl₂ were added dropwise to a solution 63.0 mg (0.10 mmol) of [RuCl₂(*p*-cymene)]₂ in 5 ml of CH₂Cl₂. After stirring for 20 h at room temperature, the solution was concentrated and the product was precipitated by adding 10 ml Et₂O. The product was collected by filtration, was washed twice with Et₂O and dried in *vacuo*.

Yield: 125 mg (0.13 mmol, 67 %, yellow solid).

Elemental Analysis: C₃₄H₃₇AuCl₃N₄PRu (937.06g/mol) + 3.75 H₂O

Calculated : C: 40.65% H: 4.46% N: 5.58%

Found : C: 40.14% H: 3.92% N: 5.40%

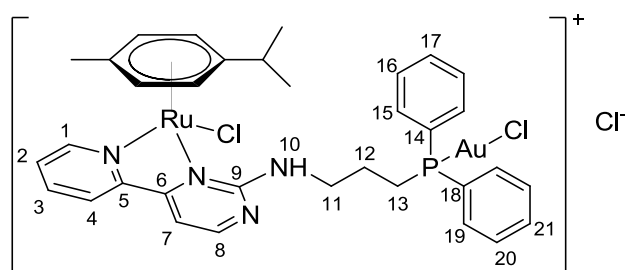
^1H NMR (400.1 MHz, CDCl_3 , 20 °C): δ 9.63 (d, $^3J_{\text{HH}} = 5.3$ Hz, 1H, H1), 8.36 (d, $^3J_{\text{HH}} = 7.9$ Hz, 1H, H4), 8.10 (t, $^3J_{\text{HH}} = 7.6$ Hz, 1H, H3), 7.86-7.72 (m, 5H, H2, H15 and H19), 7.56 (s, 1H, H7), 7.54-7.45 (m, 6H, H16, H17, H20 and H21), 6.72 (dd, $^3J_{\text{HH}} = 7.6$ Hz and $^3J_{\text{HH}} = 4.4$ Hz, 1H, H11), 6.09 (d, $^3J_{\text{HH}} = 5.8$ Hz, 1H, H_{cymene}), 6.05-6.01 (m, 2H, H_{cymene}), 5.99 (d, $^3J_{\text{HH}} = 5.8$ Hz, 1H, H_{cymene}), 4.17-3.93 (m, 2H, H12), 3.21-2.82 (m, 2H, H13), 2.67 (s, 3H, H9), 2.55 (septet, $^3J_{\text{HH}} = 6.9$ Hz, 1H, H_{cymene}), 2.25 (s, 3H, H_{cymene}), 1.04 (d, $^3J_{\text{HH}} = 6.9$ Hz, 3H, H_{cymene}), 0.97 (d, $J_{\text{HH}} = 6.9$ Hz, 3H, H_{cymene}) ppm.

^{13}C NMR (100.6 MHz, CDCl_3 -*d*6, 20 °C): δ 168.2 (s, C8), 162.9 (s, C6), 161.3 (s, C10), 157.0 (s, C1), 153.9 (s, C5), 146.8 (s, C3), 140.0 (s, C2), 133.5 and 133.4 (d, $^2J_{\text{PC}} = 13.7$ Hz, C15 and C19), 132.5 and 132.4 (d, $^4J_{\text{PC}} = 2.7$ Hz, C17 and C21), 129.7 and 129.6 (d, $^3J_{\text{PC}} = 11.9$ Hz, C16 and C20), 129.2 (s, C14 and C18), 125.0 (s, C4), 109.5 (s, C7), 106.1 (s, C_{cymene}), 104.5 (s, C_{cymene}), 89.7 (s, C_{cymene}), 87.0 (s, C_{cymene}), 85.5 (s, C_{cymene}), 85.0 (s, C_{cymene}), 44.6 (s, C12), 31.3 (s, C_{cymene}), 31.2 (d, $^1J_{\text{PC}} = 39.3$ Hz, C13), 25.0 (s, C9), 22.4 (s, C_{cymene}), 22.3 (s, C_{cymene}), 19.1 (s, C_{cymene}) ppm.

^{31}P NMR (161.98 MHz, CDCl_3 , 20 °C): δ 24.30 (s) ppm.

IR $\tilde{\nu}$ (cm^{-1}): 3351 (w), 3100 (w), 2970 (w), 1738 (m), 1600 (m), 1560 (s), 1482 (m), 1435 (m), 1362 (m), 1217 (m), 1162 (w), 1104 (m), 1056 (w), 1029 (w), 997 (w), 881 (w), 791 (w), 770 (m), 743 (s), 691 (s).

5.10.10 Ru-Au Complex 19d



A solution of 126 mg (0.20 mmol) of gold complex **15a** in 5 ml of CH_2Cl_2 were added dropwise to a solution of 63.0 mg (0.10 mmol) of $[\text{RuCl}_2(p\text{-cymene})]_2$ in 5 ml of CH_2Cl_2 . After stirring for 20 hours at room temperature, the solution was concentrated and the

product was precipitated by adding 10 ml of Et₂O. The precipitate was collected by filtration and washed twice with Et₂O. The product was obtained after drying in *vacuo*.

Yield: 140 mg (0.15 mmol, 78 %, yellow solid).

Elemental Analysis: C₃₄H₃₇AuCl₃N₄PRu (937.06 g/mol) + 2 H₂O

Calculated : C: 41.97% H: 4.25% N: 5.76%

Found : C: 41.32% H: 4.40% N: 5.40%

¹H NMR (400.1 MHz, CDCl₃, 20 °C): δ 9.76 (d, ³J_{HH} = 3.6 Hz, 1H, H1), 8.56 (d, ³J_{HH} = 4.5 Hz, 1H, H8), 8.49 (d, ³J_{HH} = 7.6 Hz, 1H, H4), 8.11 (t, ³J_{HH} = 6.7 Hz, 1H, H3), 7.86-7.83 (m, 1H, H2), 7.72-7.63 (m, 5H, H7, H15 and H19), 7.50-7.37 (m, 6H, H16, H17, H20 and H21), 6.85 (dd, ³J_{HH} = 6.7 Hz and ³J_{HH} = 4.5 Hz, 1H, H10), 6.24 (d, ³J_{HH} = 4.7 Hz, 1H, H_{cymene}), 6.15 (d, ³J_{HH} = 5.4 Hz, 1H, H_{cymene}), 6.10 (d, ³J_{HH} = 4.7 Hz, 1H, H_{cymene}), 6.06 (d, ³J_{HH} = 5.4 Hz, 1H, H_{cymene}), 4.07-3.91 (m, 2H, H11), 2.73-2.57 (m, 2H, H13), 2.51 (septet, ³J_{HH} = 6.8 Hz, 1H, H_{cymene}), 2.29 (s, 3H, H_{cymene}), 2.12-1.83 (m, 2H, H12), 1.03 (d, ³J_{HH} = 6.8 Hz, 3H, H_{cymene}), 0.95 (d, J_{HH} = 6.8 Hz, 3H, H_{cymene}) ppm.

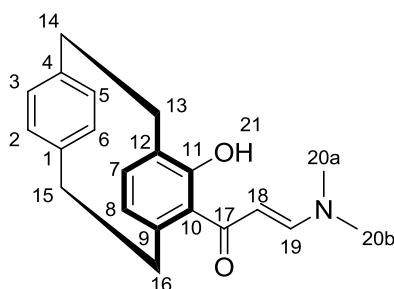
¹³C NMR (100.6 MHz, CDCl₃, 20 °C): δ 163.1 (s, C9), 162.0 (s, C6), 160.9 (s, C8), 157.5 (s, C1), 153.6 (s, C5), 140.0 (s, C3), 133.5 and 133.2 (d, ²J_{PC} = 13.1 Hz, C15 and C19), 132.2 and 132.1 (d, ⁴J_{PC} = 2.40 Hz, C17 and C21), 129.9 (s, C2), 129.5 (d, ³J_{PC} = 11.7 Hz, C16 and C20), 128.7 (d, ¹J_{PC} = 60.5 Hz, C14), 125.5 (s, C4), 108.8 (s, C7), 105.5 (s, C_{cymene}), 104.5 (s, C_{cymene}), 87.5 (s, C_{cymene}), 86.0 (s, C_{cymene}), 85.2 (s, C_{cymene}), 84.6 (s, C_{cymene}), 42.4 (d, ³J_{PC} = 14.3 Hz, C11), 31.2 (s, C_{cymene}), 24.8 (d, ¹J_{PC} = 39.0 Hz, C13), 24.4 (s, C12), 22.2 (s, 2C, C_{cymene}), 19.1 (s, C_{cymene}) ppm.

³¹P NMR (161.98 MHz, CDCl₃, 20 °C): δ 28.30 (s) ppm.

IR $\tilde{\nu}$ (cm⁻¹): 3328 (w), 3100 (w), 2970 (w), 1739 (s), 1593 (m), 1560 (s), 1525 (w), 1458 (w), 1434 (m), 1375 (m), 1351 (m), 1260 (w), 1231 (m), 1203 (m), 1104 (m), 1054 (w), 1024 (w), 990 (w), 852 (w), 792 (w), 769 (w), 732 (m), 688 (m).

5.11 Synthesis of Pyrimidine Ligands with a Paracyclophane Backbone

5.11.1 (*E*)-3-(Dimethylamino)-1-(1-hydroxy[2.2]paracyclophane)prop-2-en-1-one (20)



1.00 g (3.80 mmol) of 5-acetyl-4-hydroxy[2.2]paracyclophane (AHPC) and 13.0 mL (97.0 mmol) of DMF-DMA were mixed and refluxed at 110 °C for 24 hours under nitrogen atmosphere. After evaporating the solvent, the residue was washed three times with 20 ml hexane and three times with 20 ml diethyl ether.

Yield: 1.20 g (3.73 mmol, 99%, yellow solid).

Elemental Analysis: C₂₁H₂₃NO₂ (321.42 g/mol).

Calculated : C: 78.47% H: 7.21% N: 4.36%

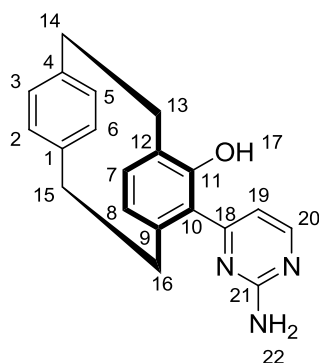
Found : C: 78.29% H: 7.17% N: 4.25%

¹H NMR (400.1 MHz, DMSO-*d*₆, 20 °C): δ 13.48 (s, 1H, H₂₁), 7.80 (d, ³J_{HH} = 12.2 Hz, 1H, H₁₉), 6.86 (dd, ³J_{HH} = 7.7 Hz and ⁴J_{HH} = 1.8 Hz, 1H, H_{pc}), 6.61 (dd, ³J_{HH} = 7.8 Hz and ⁴J_{HH} = 1.7 Hz, 1H, H_{pc}), 6.45-6.40 (m, 2H, H_{pc}), 6.29 (dd, ³J_{HH} = 7.7 Hz and ⁴J_{HH} = 1.8 Hz, 1H, H_{pc}), 6.24 (d, ³J_{HH} = 7.6 Hz, 1H, H₇), 5.34 (d, ³J_{HH} = 12.2 Hz, 1H, H₁₈), 3.76-3.70 (m, 1H, H_{pc}), 3.22-3.16 (m, 4H, H_{pc} and H_{20a}), 3.03-2.92 (m, 3H, H_{pc}), 2.90-2.83 (m, 4H, H_{pc}, H_{20b}), 2.72-2.65 (m, 1H, H_{pc}), 2.49-2.44 (m, 1H, H_{pc}) ppm.

¹³C NMR (100.6 MHz, DMSO-*d*₆, 20 °C): δ 190.5 (s, C₁₇), 160.2 (s, C₁₁), 154.3 (s, C₁₉), 140.6 (s, C_{pc}), 139.1 (s, C_{pc}), 138.0 (s, C_{pc}), 136.9 (s, C_{pc}), 132.7 (s, C_{pc}), 131.9 (s, C_{pc}), 130.8 (s, C_{pc}), 127.1 (s, C_{pc}), 126.2 (s, C_{pc}), 123.7 (s, C_{pc}), 96.0 (s, C₁₈), 44.8 (s, C_{20a}), 37.3 (s, C_{20b}), 36.6 (s, C_{pc}), 34.6 (s, C_{pc}), 33.4 (s, C_{pc}), 29.5 (s, C_{pc}) ppm.

IR $\tilde{\nu}$ (cm⁻¹): 2942 (w), 2852 (w), 2798 (w), 1740 (w), 1624 (s), 1568 (m), 1540 (s), 1491 (w), 1451 (w), 1436 (w), 1423 (m), 1401 (s), 1359 (m), 1330 (m), 1270 (s), 1231 (s), 1157 (w), 1084 (s), 1019 (m), 976 (m), 956 (w), 938 (m), 871 (m), 856 (m), 803 (m), 795 (s), 757 (m), 735 (w), 716 (m), 692 (w), 657 (m).

5.11.2 1-Hydroxy-2-(2-aminopyrimidin-4-yl)[2.2]paracyclophane (21)



140 mg (6.20 mmol) of sodium were dissolved in a solution of 570 mg (4.70 mmol) of guanidine nitrate in 20 mL of dry EtOH under nitrogen atmosphere. After refluxing for about 30 minutes, 1.00 g (3.10 mmol) of (*E*)-3-(dimethylamino)-1-(1-hydroxy[2.2]paracyclophane)prop-2-en-1-one (**20**) were added and the mixture was refluxed for 24 hours. The solvent was evaporated and the residue was dissolved in CH₂Cl₂. The organic phase was washed three times with water and dried over Na₂SO₄. The solvent was removed under reduced pressure.

Yield: 650 mg (2.10 mmol, 66 %, yellow solid).

Elemental Analysis: C₂₀H₁₉N₃O (317.38 g/mol).

Calculated : C: 75.69% H: 6.03% N: 13.24%

Found : C: 74.05% H: 6.21% N: 12.77%

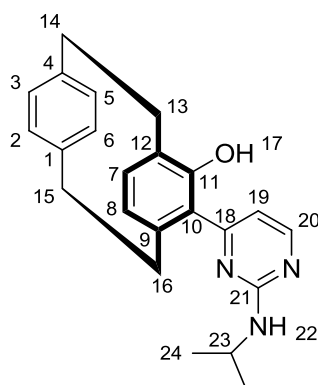
¹H NMR (400.1 MHz, DMSO-*d*₆, 20 °C): δ 13.34 (s, 1H, H17), 8.28 (d, ³*J*_{HH} = 5.3 Hz, 1H, H20), 7.12 (s, 2H, H22), 7.01 (dd, ³*J*_{HH} = 7.7 Hz and ⁴*J*_{HH} = 1.8 Hz, 1H, H_{pc}), 6.71 (d,

$^3J_{\text{HH}} = 5.3$ Hz, 1H, H₁₉), 6.61 (dd, $^3J_{\text{HH}} = 7.8$ Hz and $^4J_{\text{HH}} = 1.8$ Hz, 1H, H_{pc}), 6.48 (dd, $^3J_{\text{HH}} = 7.8$ Hz and $^4J_{\text{HH}} = 1.7$ Hz, 1H, H_{pc}), 6.45 (d, $^3J_{\text{HH}} = 7.6$ Hz, 1H, H_{pc}), 6.32 (d, $^3J_{\text{HH}} = 7.6$ Hz, 1H, H_{pc}), 6.22 (dd, $^3J_{\text{HH}} = 7.7$ Hz and $^4J_{\text{HH}} = 1.8$ Hz, 1H, H_{pc}), 3.66-3.59 (m, 1H, H_{pc}), 3.41-3.35 (m, 1H, H_{pc}), 3.29-3.22 (m, 1H, H_{pc}), 3.07-2.99 (m, 2H, H_{pc}), 2.93-2.84 (m, 2H, H_{pc}), 2.57-2.52 (m, 1H, H_{pc}) ppm.

^{13}C NMR (100.6 MHz, DMSO-*d*₆, 20 °C): δ 164.2 (s, C₁₈), 161.5 (s, C₂₁), 159.1 (s, C₂₀), 158.1 (s, C₁₁), 140.2 (s, C_{pc}), 139.2 (s, C_{pc}), 138.0 (s, C_{pc}), 136.4 (s, C_{pc}), 132.7 (s, C_{pc}), 132.1 (s, C_{pc}), 130.2 (s, C_{pc}), 127.8 (s, C_{pc}), 127.3 (s, C_{pc}), 127.1 (s, C_{pc}), 120.2 (s, C_{pc}), 110.2 (s, C₁₉) ppm.

IR $\tilde{\nu}$ (cm⁻¹): 3437 (m), 3290 (w), 3150 (w), 2931 (w), 1631 (s), 1565 (s), 1551 (s), 1498 (m), 1467 (s), 1451 (s), 1433 (w), 1406 (s), 1363 (w), 1337 (m), 1286 (m), 1263 (w), 1218 (s), 1144 (w), 1096 (w), 1016 (m), 984 (w), 927 (w), 896 (w), 878 (w), 829 (m), 816 (m), 796 (m), 747 (w), 717 (w), 688 (m).

5.11.3 1-Hydroxy-2-(2-(isopropylamino)pyrimidin-4-yl)[2.2]paracyclophane (22a)



1.50 g (65.3 mmol) of sodium were dissolved in a solution of 7.50 g (25.0 mmol) of 1-isopropylguanidine sulfate in 50 ml of dry EtOH under nitrogen atmosphere. After refluxing for about 30 minutes, 1.00 g (3.10 mmol) of (*E*)-3-(dimethylamino)-1-(1-hydroxy[2.2]paracyclophane)prop-2-en-1-one (**20**) were added and the mixture was refluxed for 24 hours. The solvent was evaporated and the residue was dissolved in CH₂Cl₂. The organic phase was washed three times with water and dried over Na₂SO₄. The solvent was removed under reduced pressure.

Yield: 590 g (1.65 mmol, 55 %, yellow solid).

Elemental Analysis: C₂₃H₂₅N₃O (359.46 g/mol) + 0.2H₂O.

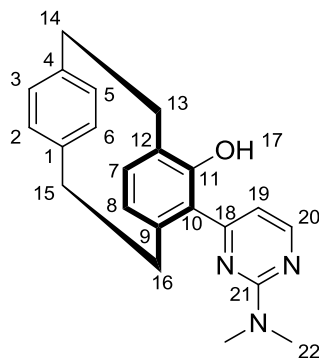
Calculated : C: 76.09% H: 7.05% N: 11.57%

Found : C: 75.98% H: 6.85% N: 11.63%

¹H NMR (400.1 MHz, DMSO-*d*₆, 20 °C): δ 13.23 (s, 1H, H17), 8.32 (d, ³J_{HH} = 5.2 Hz, 1H, H20), 7.61 (s, 1H, H22), 6.98 (d, ³J_{HH} = 5.2 Hz, 1H, H19), 6.61 (dd, ³J_{HH} = 7.8 Hz and ⁴J_{HH} = 1.7 Hz, 1H, H_{pc}), 6.50-6.44 (m, 2H, H_{pc}), 6.33 (d, ³J_{HH} = 7.6 Hz, 1H, H7), 6.23 (d, ³J_{HH} = 7.6 Hz, 1H, H8), 4.04 (br. s, 1H, H23), 3.66-3.56 (m, 1H, H_{pc}), 3.26 (ddd, ²J_{HH} = 12.5 Hz, ³J_{HH} = 9.2 Hz and ³J_{HH} = 3.2 Hz, 1H, H_{pc}), 3.08-2.96 (m, 2H, H_{pc}), 2.93-2.84 (m, 2H, H_{pc}), 2.57-2.52 (m, 2H, H_{pc}), 1.27 (d, ³J_{HH} = 6.5 Hz, 6H, H24) ppm.

¹³C NMR (100.6 MHz, DMSO-*d*₆, 20 °C): δ 164.0 (s, C18), 159.6 (s, C21), 158.7 (s, C11), 157.9 (s, C18), 140.2 (s, C_{pc}), 139.2 (s, C_{pc}), 138.0 (s, C_{pc}), 136.4 (s, C_{pc}), 132.7 (s, C_{pc}), 132.1 (s, C_{pc}), 130.1 (s, C_{pc}), 127.7 (s, C_{pc}), 127.2 (s, C_{pc}), 127.1 (s, C_{pc}), 120.4 (s, C_{pc}), 110.0 (s, C19), 42.4 (s, C23), 35.3 (s, C_{pc}), 34.3 (s, C_{pc}), 33.4 (s, C_{pc}), 30.0 (s, C_{pc}), 22.4 (s, C24a), 22.3 (s, C24b) ppm.

5.11.4 1-Hydroxy-2-(2-(dimethylamino)pyrimidin-4-yl)[2.2]paracyclophane (22b)



200 mg (8.70 mmol) of sodium were dissolved in a solution of 1.30 g (5.00 mmol) of *N,N*-dimethylguanidine sulfate in 20 ml dry EtOH under nitrogen atmosphere. Then, 300 mg (1.00 mmol) of (*E*)-3-(dimethylamino)-1-(1-hydroxy[2.2]paracyclophane)prop-2-en-1-one (**20**) were added and the mixture was refluxed for 24 hours. The solvent was evaporated and the residue was dissolved in CH₂Cl₂. The organic phase was washed three times with water and dried over Na₂SO₄. The solvent was removed under reduced pressure.

Yield: 280 mg (0.81 mmol, 87 %, yellow solid).

Elemental Analysis: C₂₂H₂₃N₃O (345.44 g/mol).

Calculated : C: 76.49% H: 6.71% N: 12.16%

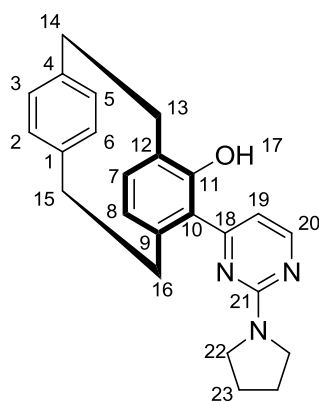
Found : C: 75.93% H: 6.69% N: 12.01%

¹H NMR (400.1 MHz, DMSO-*d*₆, 20 °C): δ 13.00 (s, 1H, H17), 8.40 (d, ³*J*_{HH} = 5.2 Hz, 1H, H20), 6.96 (dd, ³*J*_{HH} = 7.7 Hz and ⁴*J*_{HH} = 1.8 Hz, 1H, H_{pc}), 6.75 (d, ³*J*_{HH} = 5.2 Hz, 1H, H19), 6.60 (dd, ³*J*_{HH} = 7.8 Hz and ⁴*J*_{HH} = 1.8 Hz, 1H, H_{pc}), 6.48 (d, ³*J*_{HH} = 7.7 Hz, 2H, H7), 6.36 (d, ³*J*_{HH} = 7.7 Hz, 1H, H8), 6.27 (dd, ³*J*_{HH} = 7.8 Hz and ⁴*J*_{HH} = 1.8 Hz, 1H, H_{pc}), 3.64-3.58 (m, 1H, H_{pc}), 3.29-3.23 (m, 7H, H22 and H_{pc}), 3.07-2.99 (m, 2H, H_{pc}), 2.93-2.85 (m, 2H, H_{pc}), 2.57-2.53 (m, 1H, H_{pc}), 2.47-2.42 (m, 1H, H_{pc}) ppm.

¹³C NMR (100.6 MHz, DMSO-*d*₆, 20 °C): δ 164.3 (s, C18), 160.4 (s, C21), 159.3 (s, C11), 158.0 (s, C20), 140.7 (s, C_{pc}), 139.7 (s, C_{pc}), 138.4 (s, C_{pc}), 136.9 (s, C_{pc}), 133.3 (s, C_{pc}), 132.6 (s, C_{pc}), 130.5 (s, C_{pc}), 128.2 (s, C_{pc}), 127.7 (s, C_{pc}), 127.5 (s, C_{pc}), 121.0 (s, C_{pc}), 110.1 (s, C19), 37.4 (s, C22), 35.7 (s, C_{pc}), 34.6 (s, C_{pc}), 33.8 (s, C_{pc}), 30.4 (s, C_{pc}) ppm.

IR $\tilde{\nu}$ (cm⁻¹): 2923 (s), 2853 (m), 1739 (m), 1556 (s), 1530 (m), 1457 (m), 1428 (m), 1397 (m), 1377 (w), 1338 (m), 1290 (w), 1254 (w), 1217 (m), 1201 (m), 1155 (w), 1120 (w), 1097 (m), 1061 (w), 999 (m), 986 (m), 975 (m), 942 (w), 931 (m), 870 (m), 826 (m), 797 (m), 777 (w), 735 (w), 718 (m), 709 (m), 688 (m), 655 (w).

5.11.5 1-Hydroxy-2-(2-(pyrrolidin-1-yl)pyrimidin-4-yl)[2.2]paracyclophane (22c)



300 mg (12.5 mmol) of sodium were dissolved in a solution of 2.50 g (7.80 mmol) of pyrrolidine-1-carboximidamide sulfate in 25 ml dry EtOH under nitrogen atmosphere. Then, 500 mg (1.60 mmol) of (*E*)-3-(dimethylamino)-1-(1-hydroxy[2.2]paracyclophane)prop-2-en-1-one (**20**) were added and the mixture was refluxed for 24 hours. The solvent was evaporated and the residue was dissolved in CH₂Cl₂. The organic phase was washed three times with water and dried over Na₂SO₄. The solvent was removed under reduced pressure.

Yield: 276 mg (0.74 mmol, 48 %, yellow solid).

Elemental Analysis: C₂₄H₂₅N₃O (371.47 g/mol) + 0.55H₂O.

Calculated : C: 75.58% H: 6.90% N: 11.02%

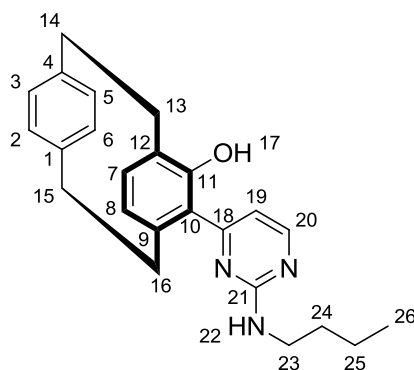
Found : C: 75.88% H: 6.65% N: 10.65%

¹H NMR (400.1 MHz, CDCl₃, 20 °C): δ 13.25 (s, 1H, H17), 8.33 (d, ³J_{HH} = 5.4 Hz, 1H, H20), 7.06 (dd, ³J_{HH} = 7.8 Hz and ⁴J_{HH} = 1.6 Hz, 1H, H_{pc}), 6.66 (d, ³J_{HH} = 5.4 Hz, 1H, H19), 6.61 (dd, ³J_{HH} = 7.8 Hz and ⁴J_{HH} = 1.6 Hz, 1H, H_{pc}), 6.50 (dd, ³J_{HH} = 7.8 Hz and ⁴J_{HH} = 1.5 Hz, 1H, H_{pc}), 6.47 (d, ³J_{HH} = 7.6 Hz, 1H, H7), 6.38-6.33 (m, 2H, H_{pc}), 3.83 (br. s, 1H, H_{pc}), 3.72-3.64 (m, 4H, H22), 3.42 (ddd, ²J_{HH} = 12.8 Hz, ³J_{HH} = 10.1 Hz and ³J_{HH} = 2.3 Hz, 1H, H_{pc}), 3.23-3.16 (m, 1H, H_{pc}), 3.09-3.03 (m, 1H, H_{pc}), 2.99-2.87 (m, 2H, H_{pc}), 2.65-2.52 (m, 2H, H_{pc}), 2.13 (br. s, 4H, H23) ppm.

^{13}C NMR (100.6 MHz, CDCl_3 , 20 °C): δ 165.7 (s, C18), 162.4 (s, C21), 158.9 (s, C11), 157.2 (s, C20), 140.7 (s, C_{pc}), 139.9 (s, C_{pc}), 138.2 (s, C_{pc}), 137.3 (s, C_{pc}), 132.9 (s, C_{pc}), 132.4 (s, C_{pc}), 130.6 (s, C_{pc}), 128.8 (s, C_{pc}), 127.6 (s, C_{pc}), 127.5 (s, C_{pc}), 120.7 (s, C_{pc}), 109.8 (s, C19), 47.1 (s, C22), 36.0 (s, C_{pc}), 35.0 (s, C_{pc}), 33.8 (s, C_{pc}), 30.4 (s, C_{pc}), 26.0 (s, C23) ppm.

IR $\tilde{\nu}$ (cm^{-1}): 2930 (w), 2856 (w), 1740 (m), 1552 (s), 1528 (s), 1478 (m), 1457 (m), 1437 (w), 1426 (w), 1335 (m), 1316 (m), 1287 (m), 1218 (m), 1154 (w), 1127 (w), 1095 (w), 1005 (m), 985 (m), 957 (w), 930 (m), 871 (w), 823 (m), 792 (m), 747 (w), 718 (m), 710 (m), 685 (m).

5.11.6 1-Hydroxy-2-(2-butylamino-1-yl)pyrimidin-4-yl)[2.2]paracyclophane (22d)



500 mg (21.0 mmol) of sodium were dissolved in a solution of 2.60 g (8.00 mmol) of 1-butylguanidine sulfate in 20 ml dry EtOH under nitrogen atmosphere. Then, 300 mg of (1.00 mmol) (*E*)-3-(dimethylamino)-1-(1-hydroxy[2.2]paracyclophane)prop-2-en-1-one (**20**) were added and the mixture was refluxed for 24 hours. The solvent was evaporated and the residue was dissolved in CH_2Cl_2 . The organic phase was washed three times with water and dried over Na_2SO_4 . After washing three times with diethyl ether, the solvent was removed under reduced pressure and the pure compound was obtained.

Yield: 180 mg (0.48 mmol, 48 %, yellow solid).

Elemental Analysis: C₂₄H₂₇N₃O (373.49 g/mol).

Calculated : C: 77.18% H: 7.29% N: 11.25%

Found : C: 75.99% H: 7.29% N: 11.51%

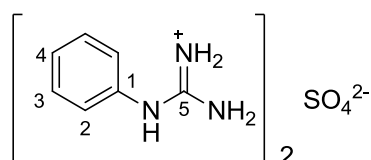
¹H NMR (400.1 MHz, CDCl₃, 20 °C): δ 12.90 (s, 1H, H17), 8.25 (d, ³J_{HH} = 4.8 Hz, 1H, H20), 7.05 (dd, ³J_{HH} = 7.8 Hz and ⁴J_{HH} = 1.5 Hz, 1H, H_{pc}), 6.69 (d, ³J_{HH} = 4.8 Hz, 1H, H19), 6.62 (dd, ³J_{HH} = 7.9 Hz and ⁴J_{HH} = 1.8 Hz, 1H, H_{pc}), 6.51 (dd, ³J_{HH} = 7.8 Hz and ⁴J_{HH} = 1.5 Hz, 1H, H_{pc}), 6.47 (d, ³J_{HH} = 7.8 Hz, 1H, H7), 6.36-6.33 (m, 2H, H_{pc}), 3.66-3.55 (m, 2H, H_{pc}), 3.53-3.40 (m, 2H, H23), 3.20 (ddd, ²J_{HH} = 12.8 Hz, ³J_{HH} = 10.1 Hz and ³J_{HH} = 5.5 Hz, 1H, H_{pc}), 3.10-3.03 (m, 1H, H_{pc}), 2.98-2.90 (m, 2H, H_{pc}), 2.67-2.52 (m, 2H, H_{pc}), 1.77-1.74 (m, 2H, H24), 1.55 (sext, ³J_{HH} = 7.4 Hz, 2H, H25), 1.03 (t, ³J_{HH} = 7.4 Hz, 3H, H26) ppm.

¹³C NMR (100.6 MHz, CDCl₃, 20 °C): δ 165.7 (s, C18), 160.1 (s, C21), 158.5 (s, C11), 157.5 (s, C20), 140.4 (s, C_{pc}), 140.2 (s, C_{pc}), 138.3 (s, C_{pc}), 137.4 (s, C7), 132.9 (s, C_{pc}), 132.5 (s, C_{pc}), 130.7 (s, C_{pc}), 128.8 (s, C_{pc}), 127.7 (s, C_{pc}), 127.5 (s, C8), 120.7 (s, C_{pc}), 111.5 (s, C19), 41.8 (s, C23), 35.9 (s, C_{pc}), 35.0 (s, C_{pc}), 34.1 (s, C_{pc}), 31.7 (s, C24), 31.1 (s, C_{pc}), 20.4 (s, C25), 14.0 (s, C26) ppm.

IR $\tilde{\nu}$ (cm⁻¹): 3271 (w), 3016 (w), 2949 (w), 2925 (m), 2870 (w), 1739 (m), 1574 (s), 1546 (s), 1465 (s), 1411 (m), 1366 (m), 1315 (w), 1286 (m), 1227 (m), 1218 (m), 1156 (m), 1120 (w), 1102 (m), 1018 (w), 997 (w), 987 (w), 978 (w), 934 (m), 895 (w), 825 (s), 792 (s), 735 (w), 711 (m), 688 (m), 657 (m).

5.12 Synthesis of Aryl Substituted Guanidinium Salts

5.12.1 1-Phenyl guanidinium Sulfate (23a)



This compound was prepared according to the literature.^[182] Freshly distilled 55.9 g (600 mmol) aniline and 27.0 g (300 mmol) 2-methyl-2-thiopseudourea-hemisulfate were heated until the solid was melted (around 3 hours). After the reaction was cooled to the room temperature, the solid residue was washed several times by ethanol.

Yield: 38.3 g (100 mmol, 35 %, colorless solid).

Elemental Analysis: C₁₄H₂₀N₆O₄S (368.41 g/mol)

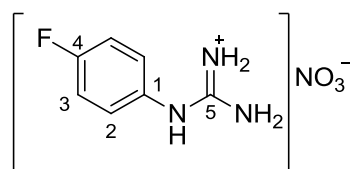
Calculated : C: 45.64% H: 5.47% N: 22.81% S: 8.70%

Found : C: 45.06% H: 5.36% N: 23.02% S: 8.66%

¹H NMR (400.1 MHz, D₂O, 20 °C): δ 7.49–7.46 (t, ³J_{HH} = 7.5 Hz, 2H, H3), 7.40–7.37 (t, 1H, H4), 7.29 (d, 2H, H2) ppm.

¹³C NMR (100.6 MHz, D₂O, 20 °C): δ 156.3 (s, C5), 134.1 (s, C1), 129.9 (s, C3), 128.0 (s, C4), 125.8 (s, C2) ppm.

5.12.2 1-(4-Fluorophenyl)guanidinium Nitrate (23b)



1.80 g (40.0 mmol) of concentrated HNO₃ was added to a solution of the 2.20 g (20.0 mmol) 4-fluoroaniline in 30 ml ethanol followed by a (30.0 mmol) 50% aqueous solution of cyanamide. The reaction mixture was heated under reflux for 16 hours and then cooled to 0 °C followed by the addition of diethyl ether. This solution was kept in the refrigerator for 12 hours at 0 °C. The resulting solid was filtered off and dried in *vacuo*.

Yield: 2.70 g (12.5 mmol, 63 %, colorless solid).

Elemental Analysis: C₇H₉FN₄O₃ (216.17 g/mol)

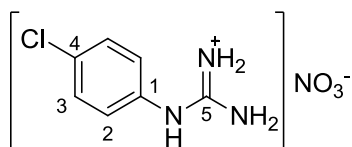
Calculated : C: 38.89% H: 4.20% N: 25.92%

Found : C: 39.04% H: 4.49% N: 26.02%

¹H NMR (400.1 MHz, D₂O, 20 °C): δ 7.35–7.29 (m, 2H, H2), 7.25–7.16 (m, 2H, H3) ppm.

¹³C NMR (100.6 MHz, D₂O, 20 °C): δ 161.8 (d, ¹J_{FC} = 245.5 Hz, C4), 156.6 (s, C5), 130.0 (s, C1), 128.5 (d, ³J_{FC} = 9.1 Hz, C2), 116.7 (d, ²J_{FC} = 23.2 Hz, C3) ppm.

5.12.3 1-(4-Chlorophenyl)guanidinium Nitrate (23c)



1.80 g (40.0 mmol) of concentrated HNO₃ was added to a solution of the 2.60 (20.0 mmol) 4-chloroaniline in 30 ml ethanol followed by a (30.0 mmol) 50% aqueous solution of cyanamide. The reaction mixture was heated under reflux for 16 hours and then cooled to 0 °C followed by the addition of diethyl ether. This solution was kept in the refrigerator for 12 hours at 0 °C. The resulting solid was filtered off and dried in *vacuo*.

Yield: 2.70 g (11.6 mmol, 58 %, colorless solid).

Elemental Analysis: C₇H₉ClN₄O₃ (232.62 g/mol)

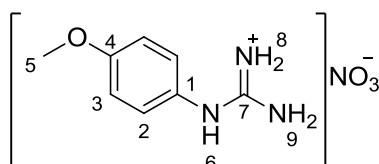
Calculated : C: 36.14% H: 3.90% N: 24.08%

Found : C: 36.05% H: 3.96% N: 24.04%

¹H NMR (400.1 MHz, D₂O, 20 °C): δ 7.48 (d, ³J_{HH} = 8.6 Hz, 2H, H3), 7.29–7.16 (m, 2H, H2) ppm.

^{13}C NMR (100.6 MHz, D_2O , 20 °C): δ 156.3 (s, C5), 133.0 (s, C1), 132.9 (s, C4), 129.9 (s, C3), 127.4 (s, C2) ppm.

5.12.4 1-(4-Methoxyphenyl)guanidinium Nitrate (23d)



1.80 g (40.0 mmol) of concentrated HNO_3 was added to a solution of the 2.50 g (20.0 mmol) *para*-anisidine in 30 ml ethanol followed by a (30.0 mmol) 50% aqueous solution of cyanamide. The reaction mixture was heated under reflux for 16 hours and then cooled to 0 °C followed by the addition of diethyl ether. This solution was kept in the refrigerator for 12 hours at 0 °C. The resulting solid was filtered off and dried in *vacuo*.

Yield: 3.80 g (16.7 mmol, 83 %, grey solid).

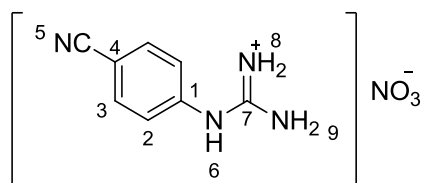
Elemental Analysis: $\text{C}_8\text{H}_{12}\text{N}_4\text{O}_4$ (228.21 g/mol)

Calculated : C: 42.11% H: 5.30% N: 24.55%

Found : C: 42.05% H: 5.31% N: 24.43%

^1H NMR (400.1 MHz, $\text{DMSO-}d_6$, 20 °C): δ 9.40 (s, 1H, H6), 7.23 (br. s, 4H, H8 and H9), 7.18 (d, $^3J_{\text{HH}} = 8.8$ Hz, 2H, H2). 7.00 (d, $^3J_{\text{HH}} = 8.8$ Hz, 2H, H3), 3.77 (s, 3H, H5) ppm.

^{13}C NMR (100.6 MHz, $\text{DMSO-}d_6$, 20 °C): δ 158.2 (s, C4), 156.3 (s, C7), 127.5 (s, C1), 127.3 (s, C2), 114.9 (s, C3), 55.4 (s, C5) ppm.

5.12.5 1-(4-Cyanophenyl)guanidinium Nitrate (23e)

1.80 g (40.0 mmol) of concentrated HNO₃ was added to a solution of the 2.40 g (20.0 mmol) 4-aminobenzonitrile in 30 ml ethanol followed by a (30.0 mmol) 50% aqueous solution of cyanamide. The reaction mixture was heated under reflux for 16 hours and then cooled to 0 °C followed by the addition of diethyl ether. This solution was kept in the refrigerator for 12 hours at 0 °C. The resulting solid was filtered off and dried in *vacuo*.

Yield: 1.40 g (6.27 mmol, 32 %, colorless solid).

Elemental Analysis: C₈H₉N₅O₃ (223.19 g/mol)

Calculated : C: 43.05% H: 4.06% N: 31.38%

Found : C: 43.07% H: 3.75% N: 30.92%

¹H NMR (400.1 MHz, DMSO-*d*₆, 20 °C): δ 10.04 (s, 1H, H6), 7.88 (d, ³J_{HH} = 8.6 Hz, 2H, H3), 7.66 (br. s, 4H, H8 and H9), 7.40 (d, ³J_{HH} = 8.6 Hz, 2H, H2) ppm.

¹³C NMR (100.6 MHz, DMSO-*d*₆, 20 °C): δ 155.3 (s, C7), 140.7 (s, C4), 133.9 (s, C3), 123.4 (s, C2), 118.6 (s, C1), 107.5 (s, C5) ppm.

6 References

- [1] E. K. van den Beuken, B. L. Feringa, *Tetrahedron* **1998**, *54*, 12985-13011.
- [2] W. W. Cleland, *Biochim. Biophys. Acta* **1963**, *67*, 188-196.
- [3] J. R. Knowles, *Annu. Rev. Biochem.* **1980**, *49*, 877-919.
- [4] H. S. Toogood, N. S. Scrutton, *Curr. Opin. Chem. Biol.* **2014**, *19*, 107-115.
- [5] C. A. Denard, H. Huang, M. J. Bartlett, L. Lu, Y. Tan, H. Zhao, J. F. Hartwig, *Angew. Chem. Int. Ed.* **2014**, *53*, 465-469; *Angew. Chem.* **2014**, *126*, 475-479.
- [6] P. A. Vigato, S. Tamburini, D. E. Fenton, *Coord. Chem. Rev.* **1990**, *106*, 25-170.
- [7] E. I. Solomon, U. M. Sundaram, T. E. Machonkin, *Chem. Rev.* **1996**, *96*, 2563-2606.
- [8] Hemocyanin. Retrieved February 1, 2015,
<http://en.wikipedia.org/wiki/Hemocyanin#mediaviewer/File:Hemocyanin2.jpg>.
- [9] Tyrosinase. Retrieved February 1, 2015,
http://en.wikipedia.org/wiki/Tyrosinase#mediaviewer/File:PPO_figure.jpeg.
- [10] R. H. Holm, P. Kennepohl, E. I. Solomon, *Chem. Rev.* **1996**, *96*, 2239-2314.
- [11] J. A. Tainer, E. D. Getzoff, J. S. Richardson, D. C. Richardson, *Nature* **1983**, *306*, 284-287.
- [12] R. Poilblanc, *Inorg. Chim. Acta* **1982**, *62*, 75-86.
- [13] R. Robson, *Inorg. Nucl. Chem. Lett.* **1970**, *6*, 125-128.
- [14] D. E. Fenton, U. Casellato, P. A. Vigato, M. Vidali, *Inorg. Chim. Acta* **1984**, *95*, 187-193.

- [15] L. K. Thompson, V. T. Chacko, J. A. Elvidge, A. B. P. Lever, R. V. Parish, *Can. J. Chem.* **1969**, *47*, 4141-4152.
- [16] R. Robson, *Aust. J. Chem.* **1970**, *23*, 2217-2224.
- [17] A. L. Gavrilova, B. Bosnich, *Chem. Rev.* **2004**, *104*, 349-384.
- [18] C. Hemmert, M. Verelst, J.-P. Tuchagues, *Chem. Commun.* **1996**, 617-618.
- [19] A. Tiripicchio, A. M. M. Lanfredi, M. Ghedini, F. Neve, *J. Chem. Soc., Chem. Commun.* **1983**, 97-98.
- [20] W. R. Tikkanen, C. Krueger, K. D. Bomben, W. L. Jolly, W. Kaska, P. C. Ford, *Inorg. Chem.* **1984**, *23*, 3633-3638.
- [21] P. Gamez, J. von Harras, O. Roubeau, W. L. Driessen, J. Reedijk, *Inorg. Chim. Acta* **2001**, *324*, 27-34.
- [22] R. Gupta, S. Mukherjee, R. Mukherjee, *J. Chem. Soc., Dalton Trans.* **1999**, 4025-4030.
- [23] L. Fanfoni, A. Meduri, E. Zangrando, S. Castillon, F. Felluga, B. Milani, *Molecules* **2011**, *16*, 1804-1824.
- [24] P. Espinet, K. Soulantica, *Coord. Chem. Rev.* **1999**, *193-195*, 499-556.
- [25] G. R. Newkome, *Chem. Rev.* **1993**, *93*, 2067-2089.
- [26] S. Maggini, *Coord. Chem. Rev.* **2009**, *253*, 1793-1832.
- [27] N. D. Jones, B. R. James, *Adv. Synth. Catal.* **2002**, *344*, 1126-1134.
- [28] R. A. Copeland, in *Enzymes: A Practical Introduction to Structure, Mechanism and Data Analysis*, Wiley-VCH, Inc, **2000**.

- [29] C. Bohr, K. Hasselbalch, A. Krogh, *Skand. Arch. Physiol.* **1904**, *16*, 402-412.
- [30] A. Whitty, *Nat. Chem. Biol.* **2008**, *4*, 435-439.
- [31] C. A. Hunter, H. L. Anderson, *Angew. Chem. Int. Ed.* **2009**, *48*, 7488-7499; *Angew. Chem.* **2009**, *121*, 7624-7636.
- [32] M. H. Pérez-Temprano, J. A. Casares, P. Espinet, *Chem.–Eur. J.* **2012**, *18*, 1864-1884.
- [33] J. Park, S. Hong, *Chem. Soc. Rev.* **2012**, *41*, 6931-6943.
- [34] H. Steinlagen, G. Helmchen, *Angew. Chem. Int. Ed.* **1996**, *35*, 2339-2342; *Angew. Chem.* **1996**, *108*, 2489-2492.
- [35] E. L. Dias, R. H. Grubbs, *Organometallics* **1998**, *17*, 2758-2767.
- [36] M. E. Broussard, B. Juma, S. G. Train, W.-J. Peng, S. A. Laneman, G. G. Stanley, *Science* **1993**, *260*, 1784-1788.
- [37] C. J. McKenzie, R. Robson, *J. Chem. Soc., Chem. Commun.* **1988**, 112-114.
- [38] M. Kitamura, S. Suga, K. Kawai, R. Noyori, *J. Am. Chem. Soc.* **1986**, *108*, 6071-6072.
- [39] J. M. Serrano-Becerra, A. F. G. Maier, S. González-Gallardo, E. Moos, C. Kaub, M. Gaffga, G. Niedner-Schatteburg, P. W. Roesky, F. Breher, J. Paradies, *Eur. J. Org. Chem.* **2014**, 4515-4522.
- [40] N. Wheatley, P. Kalck, *Chem. Rev.* **1999**, *99*, 3379-3420.
- [41] M. Shibasaki, M. Kanai, S. Matsunaga, N. Kumagai, *Acc. Chem. Res.* **2009**, *42*, 1117-1127.

- [42] T. Arai, H. Sasai, K.-i. Aoe, K. Okamura, T. Date, M. Shibasaki, *Angew. Chem. Int. Ed.* **1996**, *35*, 104-106; *Angew. Chem.* **1996**, *108*, 103-105.
- [43] H. Sasai, T. Suzuki, S. Arai, T. Arai, M. Shibasaki, *J. Am. Chem. Soc.* **1992**, *114*, 4418-4420.
- [44] H. Sasai, T. Arai, Y. Satow, K. N. Houk, M. Shibasaki, *J. Am. Chem. Soc.* **1995**, *117*, 6194-6198.
- [45] K.-i. Yamada, S. J. Harwood, H. Gröger, M. Shibasaki, *Angew. Chem. Int. Ed.* **1999**, *38*, 3504-3506; *Angew. Chem.* **1999**, *111*, 3713-3715.
- [46] R. Choukroun, D. Gervais, J. Jaud, P. Kalck, F. Senocq, *Organometallics* **1986**, *5*, 67-71.
- [47] R. Choukroun, A. Iraqi, D. Gervais, J. C. Daran, Y. Jeannin, *Organometallics* **1987**, *6*, 1197-1201.
- [48] M. A. Esteruelas, M. P. Garcia, A. M. Lopez, L. A. Oro, *Organometallics* **1991**, *10*, 127-133.
- [49] W.-Z. Lee, T.-L. Wang, H.-C. Chang, Y.-T. Chen, T.-S. Kuo, *Organometallics* **2012**, *31*, 4106-4109.
- [50] N. Tsukada, N. Ohnishi, S. Aono, F. Takahashi, *Organometallics* **2012**, *31*, 7336-7338.
- [51] M. J. Katz, K. Sakai, D. B. Leznoff, *Chem. Soc. Rev.* **2008**, *37*, 1884-1895.
- [52] M. C. Gimeno, A. Laguna, *Chem. Soc. Rev.* **2008**, *37*, 1952-1966.
- [53] M. Grzelczak, J. Perez-Juste, P. Mulvaney, L. M. Liz-Marzan, *Chem. Soc. Rev.* **2008**, *37*, 1783-1791.
- [54] H. Hakkinen, *Chem. Soc. Rev.* **2008**, *37*, 1847-1859.

- [55] A. S. K. Hashmi, M. Rudolph, *Chem. Soc. Rev.* **2008**, *37*, 1766-1775.
- [56] A. Corma, H. Garcia, *Chem. Soc. Rev.* **2008**, *37*, 2096-2126.
- [57] G. J. Hutchings, M. Brust, H. Schmidbaur, *Chem. Soc. Rev.* **2008**, *37*, 1759-1765.
- [58] M. M. Hansmann, M. Rudolph, F. Rominger, A. S. K. Hashmi, *Angew. Chem. Int. Ed.* **2013**, *52*, 2593-2598; *Angew. Chem.* **2013**, *125*, 2653-2659.
- [59] D. J. Gorin, F. D. Toste, *Nature* **2007**, *446*, 395-403.
- [60] A. S. K. Hashmi, *Angew. Chem. Int. Ed.* **2005**, *44*, 6990-6993; *Angew. Chem.* **2005**, *117*, 7150-7154.
- [61] G. Dyker, *Angew. Chem. Int. Ed.* **2000**, *39*, 4237-4239; *Angew. Chem.* **2000**, *112*, 4407-4409.
- [62] Z. Li, C. Brouwer, C. He, *Chem. Rev.* **2008**, *108*, 3239-3265.
- [63] R. A. Widenhoefer, X. Han, *Eur. J. Org. Chem.* **2006**, 4555-4563.
- [64] A. Fürstner, P. W. Davies, *Angew. Chem. Int. Ed.* **2007**, *46*, 3410-3449; *Angew. Chem.* **2007**, *119*, 3478-3519.
- [65] M. Lein, M. Rudolph, S. K. Hashmi, P. Schwerdtfeger, *Organometallics* **2010**, *29*, 2206-2210.
- [66] R. V. Parish, *Gold Bull.* **1997**, *30*, 55-62.
- [67] R. V. Parish, *Gold Bull.* **1997**, *30*, 3-12.
- [68] Y. Ito, M. Sawamura, T. Hayashi, *J. Am. Chem. Soc.* **1986**, *108*, 6405-6406.
- [69] R. G. Pearson, *Inorg. Chim. Acta* **1995**, *240*, 93-98.

- [70] M. J. McKeage, L. Maharaj, S. J. Berners-Price, *Coord. Chem. Rev.* **2002**, *232*, 127-135.
- [71] Z. Assefa, B. G. McBurnett, R. J. Staples, Fackler, P. John, *Inorg. Chem.* **1995**, *34*, 4965-4972.
- [72] E. Mizushima, K. Sato, T. Hayashi, M. Tanaka, *Angew. Chem. Int. Ed.* **2002**, *41*, 4563-4565; *Angew. Chem.* **2002**, *114*, 4745-4747.
- [73] V. W.-W. Yam, E. C.-C. Cheng, *Chem. Soc. Rev.* **2008**, *37*, 1806-1813.
- [74] H. Schmidbaur, A. Schier, *Chem. Soc. Rev.* **2012**, *41*, 370-412.
- [75] H. Schmidbaur, W. Graf, G. Müller, *Angew. Chem. Int. Ed.* **1988**, *27*, 417-419; *Angew. Chem.* **1988**, *100*, 439-441.
- [76] P. Lange, A. Schier, H. Schmidbaur, *Z. Naturforsch.* **1997**, *52*, 769-771.
- [77] C. Sarcher, S. Lebedkin, M. M. Kappes, O. Fuhr, P. W. Roesky, *J. Organomet. Chem.* **2014**, *751*, 343-350.
- [78] C. Khin, A. S. K. Hashmi, F. Rominger, *Eur. J. Inorg. Chem.* **2010**, 1063-1069.
- [79] C. Wetzel, P. C. Kunz, I. Thiel, B. Spingler, *Inorg. Chem.* **2011**, *50*, 7863-7870.
- [80] N. D. Brunet J-J, *Catalytic Hydrofunctionalization*, Wiley-VCH, **2001**.
- [81] T. E. Müller, K. C. Hultsch, M. Yus, F. Foubelo, M. Tada, *Chem. Rev.* **2008**, *108*, 3795-3892.
- [82] R. J. Puddephatt, *Comprehensive Organometallic Chemistry*, Vol. 2, Pergamon Press, Oxford, **1982**.
- [83] Y. U. Fukuda, K.; Nozaki, H., *Heterocycles* **1987**, *25*, 297.

- [84] E. Mizushima, T. Hayashi, M. Tanaka, *Org. Lett.* **2003**, *5*, 3349-3352.
- [85] Y. Luo, Z. Li, C.-J. Li, *Org. Lett.* **2005**, *7*, 2675-2678.
- [86] J. Zhang, C.-G. Yang, C. He, *J. Am. Chem. Soc.* **2006**, *128*, 1798-1799.
- [87] S. Farsadpour, L. T. Ghoochany, Y. Sun, W. R. Thiel, *Eur. J. Inorg. Chem.* **2011**, 4603-4609.
- [88] Y. Sun, A. Hienzsch, J. Grasser, E. Herdtweck, W. R. Thiel, *J. Organomet. Chem.* **2006**, *691*, 291-298.
- [89] Y. Sun, M. Ahmed, R. Jackstell, M. Beller, W. R. Thiel, *Organometallics* **2004**, *23*, 5260-5267.
- [90] J. M. Lopez-Valbuena, E. C. Escudero-Adan, J. Benet-Buchholz, Z. Freixa, P. W. N. M. van Leeuwen, *Dalton Trans.* **2010**, *39*, 8560-8574.
- [91] I. A. Guzei, K. Li, G. A. Bikzhanova, J. Darkwa, S. F. Mapolie, *Dalton Trans.* **2003**, 715-722.
- [92] M. K. Richmond, S. L. Scott, G. P. A. Yap, H. Alper, *Organometallics* **2002**, *21*, 3395-3400.
- [93] J.-C. Hierso, R. Smaliy, R. Amardeil, P. Meunier, *Chem. Soc. Rev.* **2007**, *36*, 1754-1769.
- [94] J. P. Farr, M. M. Olmstead, F. Wood, A. L. Balch, *J. Am. Chem. Soc.* **1983**, *105*, 792-798.
- [95] P. Braunstein, R. Bender, J. Kervennal, *Organometallics* **1982**, *1*, 1236-1238.
- [96] A.-K. Pleier, H. Glas, M. Grosche, P. Sirsch, W. R. Thiel, *Synthesis* **2001**, 55-62.
- [97] A. V. Kel'in, A. Maioli, *Curr. Org. Chem.* **2003**, *7*, 1855-1886.

- [98] C. Simon, T. Constantieux, J. Rodriguez, *Eur. J. Org. Chem.* **2004**, 4957-4980.
- [99] R. Levine, J. K. Sneed, *J. Am. Chem. Soc.* **1951**, 73, 5614-5616.
- [100] A. V. Kel'in, *Curr. Org. Chem.* **2003**, 7, 1691-1711.
- [101] J. L. Burdett, M. T. Rogers, *J. Am. Chem. Soc.* **1964**, 86, 2105-2109.
- [102] J. V. Greenhill, *Chem. Soc. Rev.* **1977**, 6, 277-294.
- [103] E. Bejan, H. A. Haddou, J. C. Daran, G. G. A. Balavoine, *Synthesis* **1996**, 1012-1018.
- [104] M. Sugiura, M. Kumahara, M. Nakajima, *Chem. Commun.* **2009**, 3585-3587.
- [105] Y. K. Ramtohul, A. Chartrand, *Org. Lett.* **2007**, 9, 1029-1032.
- [106] R. F. Abdulla, R. S. Brinkmeyer, *Tetrahedron* **1979**, 35, 1675-1735.
- [107] Y.-I. Lin, S. A. Lang, *J. Org. Chem.* **1980**, 45, 4857-4860.
- [108] M. Darabantu, L. Bouilly, A. Turck, N. Plé, *Tetrahedron* **2005**, 61, 2897-2905.
- [109] H. Hofmeier, U. S. Schubert, *Chem. Soc. Rev.* **2004**, 33, 373-399.
- [110] K. P. Tellmann, V. C. Gibson, A. J. P. White, D. J. Williams, *Organometallics* **2004**, 24, 280-286.
- [111] J. M. Thomas, *Angew. Chem. Int. Ed.* **1994**, 33, 913-937; *Angew. Chem.* **1994**, 106, 963-989.
- [112] W. R. Thiel, J. Eppinger, *Chem. Eur. J.* **1997**, 3, 696-705.
- [113] L. T. Ghoochany, S. Farsadpour, Y. Sun, W. R. Thiel, *Eur. J. Inorg. Chem.* **2011**, 3431-3437.

- [114] A. Alberola, C. Andrés, A. G. Ortega, R. Pedrosa, M. Vicente, *Synth. Commun.* **1987**, *17*, 1309-1314.
- [115] E. Payet, A. Auffrant, X. F. Le Goff, P. L. Floch, *J. Organomet. Chem.* **2010**, *695*, 1499-1506.
- [116] J.-F. Zhang, X. Gan, Q.-Q. Xu, J.-H. Chen, M. Yuan, W.-F. Fu, *Z. Anorg. Allg. Chem.* **2007**, *633*, 1718-1722.
- [117] D.-J. Cui, Q.-S. Li, F.-B. Xu, X.-B. Leng, Z.-Z. Zhang, *Organometallics* **2001**, *20*, 4126-4128.
- [118] Q.-S. Li, F.-B. Xu, D.-J. Cui, K. Yu, X.-S. Zeng, X.-B. Leng, H.-B. Song, Z.-Z. Zhang, *Dalton Trans.* **2003**, 1551-1557.
- [119] M. Colombo, M. Giglio, I. Peretto, *J. Heterocycl. Chem.* **2008**, *45*, 1077-1081.
- [120] Z. Abdullah, N. Tahir, M. Abas, Z. Aiyub, B. Low, *Molecules* **2004**, *9*, 520-526.
- [121] R. Ding, Y. He, X. Wang, J. Xu, Y. Chen, M. Feng, C. Qi, *Molecules* **2011**, *16*, 5665-5673.
- [122] D. Cheng, L. Croft, M. Abdi, A. Lightfoot, T. Gallagher, *Org. Lett.* **2007**, *9*, 5175-5178.
- [123] B. Stanovnik, J. Svete, *Chem. Rev.* **2004**, *104*, 2433-2480.
- [124] A. J. Cocuzza, F. W. Hobbs, C. R. Arnold, D. R. Chidester, J. A. Yarem, S. Culp, L. Fitzgerald, P. J. Gilligan, *Bioorg. Med. Chem. Lett.* **1999**, *9*, 1057-1062.
- [125] L. Fishbein, J. A. Gallaghan, *J. Am. Chem. Soc.* **1954**, *76*, 3217-3219.
- [126] P. B. Balbo, C. N. Patel, K. G. Sell, R. S. Adcock, S. Neelakantan, P. A. Crooks, M. A. Oliveira, *Biochemistry* **2003**, *42*, 15189-15196.

- [127] F. X. Tavares, J. A. Boucheron, S. H. Dickerson, R. J. Griffin, F. Preugschat, S. A. Thomson, T. Y. Wang, H.-Q. Zhou, *J. Med. Chem.* **2004**, *47*, 4716-4730.
- [128] D. Spasyuk, D. G. Gusev, *Organometallics* **2012**, *31*, 5239-5242.
- [129] R. Ahmed, A. Altieri, D. M. D'Souza, D. A. Leigh, K. M. Mullen, M. Papmeyer, A. M. Z. Slawin, J. K. Y. Wong, J. D. Woollins, *J. Am. Chem. Soc.* **2011**, *133*, 12304-12310.
- [130] S. Gu, D. Xu, W. Chen, *Dalton Trans.* **2011**, *40*, 1576-1583.
- [131] M. Melnínk, R. V. Parish, *Coord. Chem. Rev.* **1986**, *70*, 157-257.
- [132] C. Elschenbroich, A. Salzer, *Organometallics- A concise Introduction*, 2 ed., Wiley-VCH, Weinheim, **1992**.
- [133] J. B. Foley, A. E. Bruce, M. R. M. Bruce, *J. Am. Chem. Soc.* **1995**, *117*, 9596-9597.
- [134] V. Wing-Wah Yam, K. Kam-Wing Lo, *Chem. Soc. Rev.* **1999**, *28*, 323-334.
- [135] A. K. Al-Sa'Ady, C. A. McAuliffe, R. V. Parish, J. A. Sandbank, R. A. Potts, W. F. Schneider, in *Inorg. Synth.*, John Wiley & Sons, Inc., **2007**, pp. 191-194.
- [136] M. Bardaji, P. G. Jones, A. Laguna, M. D. Villacampa, N. Villaverde, *Dalton Trans.* **2003**, 4529-4536.
- [137] O. Kühn, *Phosphorous-31 NMR Spectroscopy: A concise Introduction for the Synthetic Organic and Organometallic Chemist*, Springer, **2008**.
- [138] D. Evans, J. A. Osborn, G. Wilkinson, *J. Chem. Soc. A* **1968**, 3133-3142.
- [139] D. J. C.-H. Micheal C. Simpson, *Coord. Chem. Rev.* **1996**, *155*, 163-207.
- [140] F. H. Jardine, *Polyhedron* **1982**, *1*, 569-605.

- [141] M. J. Howard, M. D. Jones, M. S. Roberts, S. A. Taylor, *Catal. Today* **1993**, *18*, 325-354.
- [142] J. M. Brown, *Angew. Chem. Int. Ed.* **1987**, *26*, 190-203; *Angew. Chem.* **1987**, *99*, 169-182.
- [143] J. A. Osborn, F. H. Jardine, J. F. Young, G. Wilkinson, *J. Chem. Soc. A* **1966**, 1711-1732.
- [144] J. M. Ernsting, S. Gaemers, C. J. Elsevier, *Magn. Reson. Chem.* **2004**, *42*, 721-736.
- [145] S. O. Grim, R. A. Ference, *Inorg. Nucl. Chem. Lett.* **1966**, *2*, 205-208.
- [146] G. M. Sammis, H. Danjo, E. N. Jacobsen, *J. Am. Chem. Soc.* **2004**, *126*, 9928-9929.
- [147] R. B. Kawthekar, W.-t. Bi, G.-J. Kim, *Appl. Organomet. Chem.* **2008**, *22*, 583-591.
- [148] A. M. Trzeciak, J. J. Ziółkowski, *Coord. Chem. Rev.* **1999**, *190–192*, 883-900.
- [149] R. B. Coapes, F. E. S. Souza, R. L. Thomas, J. J. Hall, T. B. Marder, *Chem. Commun.* **2003**, 614-615.
- [150] L. Zhang, D. Ye, Y. Zhou, G. Liu, E. Feng, H. Jiang, H. Liu, *J. Org. Chem.* **2010**, *75*, 3671-3677.
- [151] C. Sarcher, S. Farsadpour, L. Taghizadeh Ghoochany, Y. Sun, W. R. Thiel, P. W. Roesky, *Dalton Trans.* **2014**, *43*, 2397-2405.
- [152] A. S. K. Hashmi, C. Lothschütz, R. Döpp, M. Rudolph, T. D. Ramamurthi, F. Rominger, *Angew. Chem. Int. Ed.* **2009**, *48*, 8243-8246; *Angew. Chem.* **2009**, *121*, 8392-8395.

- [153] B. Panda, T. K. Sarkar, *Chem. Commun.* **2010**, 46, 3131-3133.
- [154] C. Brouwer, C. He, *Angew. Chem. Int. Ed.* **2006**, 45, 1744-1747; *Angew. Chem.* **2006**, 118, 1776-1779.
- [155] M. J. Frisch, G. W. Trucks, H. B. Schlegel, G. E. Scuseria, M. A. Robb, J. R. Cheeseman, G. Scalmani, V. Barone, B. Mennucci, G. A. Petersson, H. Nakatsuji, M. Caricato, X. Li, H. P. Hratchian, A. F. Izmaylov, J. Bloino, G. Zheng, J. L. Sonnenberg, M. Hada, M. Ehara, K. Toyota, R. Fukuda, J. Hasegawa, M. Ishida, T. Nakajima, Y. Honda, O. Kitao, H. Nakai, T. Vreven, J. A. Montgomery Jr., J. E. Peralta, F. Ogliaro, M. J. Bearpark, J. Heyd, E. N. Brothers, K. N. Kudin, V. N. Staroverov, R. Kobayashi, J. Normand, K. Raghavachari, A. P. Rendell, J. C. Burant, S. S. Iyengar, J. Tomasi, M. Cossi, N. Rega, N. J. Millam, M. Klene, J. E. Knox, J. B. Cross, V. Bakken, C. Adamo, J. Jaramillo, R. Gomperts, R. E. Stratmann, O. Yazyev, A. J. Austin, R. Cammi, C. Pomelli, J. W. Ochterski, R. L. Martin, K. Morokuma, V. G. Zakrzewski, G. A. Voth, P. Salvador, J. J. Dannenberg, S. Dapprich, A. D. Daniels, Ö. Farkas, J. B. Foresman, J. V. Ortiz, J. Cioslowski, D. J. Fox, **2009**.
- [156] P. A. Shelton, C. R. Hilliard, M. Swindling, L. McElwee-White, *ARKIVOC* **2010**, 160-166.
- [157] L. Sleno, D. A. Volmer, *J. Mass Spectrom.* **2004**, 39, 1091-1112.
- [158] M. Kawatsura, J. F. Hartwig, *J. Am. Chem. Soc.* **2000**, 122, 9546-9547.
- [159] H. Qian, X. Han, R. A. Widenhoefer, *J. Am. Chem. Soc.* **2004**, 126, 9536-9537.
- [160] Y. Oe, T. Ohta, Y. Ito, *Chem. Commun.* **2004**, 1620-1621.
- [161] B. Schlummer, J. F. Hartwig, *Org. Lett.* **2002**, 4, 1471-1474.
- [162] X. Giner, C. Nájera, *Org. Lett.* **2008**, 10, 2919-2922.
- [163] X.-Y. Liu, C.-H. Li, C.-M. Che, *Org. Lett.* **2006**, 8, 2707-2710.

- [164] H. M. Senn, P. E. Blöchl, A. Togni, *J. Am. Chem. Soc.* **2000**, *122*, 4098-4107.
- [165] G. Kovács, G. Ujaque, A. Lledós, *J. Am. Chem. Soc.* **2008**, *130*, 853-864.
- [166] P. Trillo, A. Baeza, C. Nájera, *Eur. J. Org. Chem.* **2012**, 2929-2934.
- [167] N. Mézailles, L. Ricard, F. Gagosz, *Org. Lett.* **2005**, *7*, 4133-4136.
- [168] I. Krossing, I. Raabe, *Chem. Eur. J.* **2004**, *10*, 5017-5030.
- [169] M. I. Bruce, *Angew. Chem. Int. Ed.* **1977**, *16*, 73-86; *Angew. Chem.* **1977**, *89*, 75-89.
- [170] X.-L. Hou, X.-W. Wu, L.-X. Dai, B.-X. Cao, J. Sun, *Chem. Commun.* **2000**, 1195-1196.
- [171] P. J. Pye, K. Rossen, R. A. Reamer, N. N. Tsou, R. P. Volante, P. J. Reider, *J. Am. Chem. Soc.* **1997**, *119*, 6207-6208.
- [172] M. Busch, M. Cayir, M. Nieger, W. R. Thiel, S. Bräse, *Eur. J. Org. Chem.* **2013**, 6108-6123.
- [173] L. Taghizadeh Ghoochany, Ph.D. thesis, Technische Universität Kaiserslautern **2012**.
- [174] A. D. Ryabov, *Chem. Rev.* **1990**, *90*, 403-424.
- [175] J. Dupont, C. S. Consorti, J. Spencer, *Chem. Rev.* **2005**, *105*, 2527-2572.
- [176] S. Trofimenko, *Inorg. Chem.* **1973**, *12*, 1215-1221.
- [177] M. Gómez, J. Granell, M. Martinez, *Eur. J. Inorg. Chem.* **2000**, 217-224.
- [178] G. Dyker, *Chem. Ber.* **1997**, *130*, 1567-1578.

- [179] E. Laga, A. García-Montero, F. J. Sayago, T. Soler, S. Moncho, C. Cativiela, M. Martínez, E. P. Urriolabeitia, *Chem. Eur. J.* **2013**, *19*, 17398-17412.
- [180] T. Birkle, A. Carbayo, J. V. Cuevas, G. García-Herbosa, A. Muñoz, *Eur. J. Inorg. Chem.* **2012**, 2259-2266.
- [181] C. J. Sumby, P. J. Steel, *Organometallics* **2003**, *22*, 2358-2360.
- [182] G. B. L. Smith, *J. Am. Chem. Soc.* **1929**, *51*, 476-479.
- [183] J. M. M. B. Smith, *March's Advanced Organic Chemistry*, Wiley, Newyork, **2001**.
- [184] C. Hansch, A. Leo, R. W. Taft, *Chem. Rev.* **1991**, *91*, 165-195.
- [185] K. Connors, *The Study of Reaction Rates in Solution*, VCH Verlagsgesellschaft, Weinheim, Germany, **1990**.

7 Appendix

7.1 Crystal Structure Data

7.1.1 Crystal Data and Structure Refinement for 14a.

Empirical formula	C ₂₃ H ₂₁ AuClN ₄ P	
Formula weight	616.82	
Temperature	150(2) K	
Wavelength	0.71073 Å	
Crystal system	Triclinic	
Space group	P-1	
Unit cell dimensions	$a = 10.6195(4) \text{ \AA}$ $b = 12.3785(4) \text{ \AA}$ $c = 18.7756(5) \text{ \AA}$	$\alpha = 108.768(3)^\circ$ $\beta = 103.715(3)^\circ$ $\gamma = 92.291(3)^\circ$
Volume	2252.05(13) Å ³	
Z	4	
Density (calculated)	1.819 Mg/m ³	
Absorption coefficient	6.739 mm ⁻¹	
F(000)	1192	
Crystal colour and habit	Colorless needle	
Crystal size	0.35 x 0.08 x 0.04 mm ³	
Theta range for data collection	2.72 to 32.50°.	
Index ranges	-15<=h<=15, -18<=k<=16, -28<=l<=27	
Reflections collected	29506	
Independent reflections	14731 [R(int) = 0.0294]	
Completeness to theta = 25.25°	99.8 %	
Absorption correction	Semi-empirical from equivalents	
Max. and min. transmission	1.00000 and 0.42983	
Refinement method	Full-matrix least-squares on F ²	
Data / restraints / parameters	14731 / 2 / 547	
Goodness-of-fit on F ²	1.110	
Final R indices [I>2sigma(I)]	R1 = 0.0272, wR2 = 0.0635	
R indices (all data)	R1 = 0.0364, wR2 = 0.0784	
Largest diff. peak and hole	1.741 and -2.466 e.Å ⁻³	

Definitions:

$$R_1 = \frac{\sum ||F_o| - |F_c||}{\sum |F_o|}$$

$$wR_2 = \sqrt{\frac{\sum [w(F_o^2 - F_c^2)^2]}{\sum [w(F_o^2)^2]}}$$

$$GooF = \sqrt{\frac{\sum [w(F_o^2 - F_c^2)]}{(n - p)}}$$

n = number of reflections; p = number of parameters

Notes on the refinement of 14a.

The hydrogen atoms which are bound to N4 and N8, were located in the difference Fourier synthesis, and were refined semi-freely with the help of a distance restraint, while constraining their *U*-values to 1.2 times the *U*(*eq*) values of corresponding nitrogen atoms. All the other hydrogen atoms were placed in calculated positions and refined by using a riding model.

7.1.2 Crystal Data and Structure Refinement of 15a

Empirical formula	C ₂₄ H ₂₃ AuClN ₄ P	
Formula weight	630.85	
Temperature	150(2) K	
Wavelength	1.54184 Å	
Crystal system	Triclinic	
Space group	P-1	
Unit cell dimensions	<i>a</i> = 8.7810(4) Å	<i>α</i> = 84.311(4)°.
	<i>b</i> = 9.0428(3) Å	<i>β</i> = 89.392(4)°.
	<i>c</i> = 17.2336(8) Å	<i>γ</i> = 64.721(4)°.
Volume	1230.53(9) Å ³	
Z	2	
Density (calculated)	1.703 Mg/m ³	
Absorption coefficient	12.984 mm ⁻¹	
F(000)	612	
Crystal colour and habit	Colorless needle	
Crystal size	0.40 x 0.17 x 0.12 mm ³	
Theta range for data collection	5.16 to 62.67°.	
Index ranges	-10 ≤ <i>h</i> ≤ 9, -10 ≤ <i>k</i> ≤ 7, -19 ≤ <i>l</i> ≤ 19	
Reflections collected	7658	
Independent reflections	3902 [R(int) = 0.0211]	
Completeness to theta = 62.67°	98.9 %	
Absorption correction	Semi-empirical from equivalents	
Max. and min. transmission	1.00000 and 0.33505	

Refinement method	Full-matrix least-squares on F^2
Data / restraints / parameters	3902 / 1 / 283
Goodness-of-fit on F^2	1.071
Final R indices [$I > 2\sigma(I)$]	R1 = 0.0230, wR2 = 0.0583
R indices (all data)	R1 = 0.0235, wR2 = 0.0589
Largest diff. peak and hole	0.943 and -1.324 e.Å ⁻³

Definitions:

$$R_1 = \frac{\sum ||F_o| - |F_c||}{\sum |F_o|}$$

$$wR_2 = \sqrt{\frac{\sum [w(F_o^2 - F_c^2)^2]}{\sum [w(F_o^2)^2]}}$$

$$Goof = \sqrt{\frac{\sum [w(F_o^2 - F_c^2)]}{(n - p)}}$$

n = number of reflections; p = number of parameters

Notes on the refinement of 15a.

Because of the existence of severely disordered Et₂O / CH₂Cl₂ / H₂O, SQUEEZE process integrated in PLATON was used. And the detailed information has been posted in the final CIF file. The hydrogen atom H4N which is bound to the nitrogen atom N4, was located in the difference Fourier synthesis, and was then refined semi-freely with the help of a distance restraint, while constraining its *U*-value to 1.2 times the *U*(*eq*) value of N4. All the other hydrogen atoms were placed in calculated positions and refined by using a riding model.

7.1.3 Crystal Data and Structure Refinement for 22b

Empirical formula	C ₂₂ H ₂₃ N ₃ O	
Formula weight	345.43	
Temperature	150(2) K	
Wavelength	0.71073 Å	
Crystal system	Monoclinic	
Space group	P2 ₁ /n	
Unit cell dimensions	<i>a</i> = 7.6482(2) Å	<i>α</i> = 90°.
	<i>b</i> = 20.3790(5) Å	<i>β</i> = 101.497(2)°.
	<i>c</i> = 11.3733(3) Å	<i>γ</i> = 90°.
Volume	1737.10(8) Å ³	
Z	4	
Density (calculated)	1.321 Mg/m ³	
Absorption coefficient	0.083 mm ⁻¹	
F(000)	736	
Crystal colour and habit	Yellow prism	

Crystal size	0.390 x 0.360 x 0.220 mm ³
Theta range for data collection	2.896 to 32.514°.
Index ranges	-10<=h<=11, -29<=k<=30, -17<=l<=12
Reflections collected	19562
Independent reflections	5807 [R(int) = 0.0242]
Completeness to theta = 25.242°	99.9 %
Absorption correction	Semi-empirical from equivalents
Max. and min. transmission	1.00000 and 0.88230
Refinement method	Full-matrix least-squares on F ²
Data / restraints / parameters	5807 / 1 / 240
Goodness-of-fit on F ²	1.064
Final R indices [I>2sigma(I)]	R1 = 0.0593, wR2 = 0.1431
R indices (all data)	R1 = 0.0722, wR2 = 0.1509
Extinction coefficient	n/a
Largest diff. peak and hole	0.376 and -0.249 e.Å ⁻³

Definitions:

$$R_1 = \frac{\sum ||F_o| - |F_c||}{\sum |F_o|}$$

$$wR_2 = \sqrt{\frac{\sum [w(F_o^2 - F_c^2)^2]}{\sum [w(F_o^2)^2]}}$$

$$GooF = \sqrt{\frac{\sum [w(F_o^2 - F_c^2)]}{(n - p)}}$$

n = number of reflections; p = number of parameters

Notes on the refinement of 22b.

The hydrogen atom H1O which is bound to the oxygen atom O1, was located in the difference Fourier synthesis, and was refined semi-freely with the help of a distance restraint, while constraining its *U*-value to 1.2 times the *U*(*eq*) value of O1. All the other hydrogen atoms were placed in calculated positions and refined by using a riding model.

7.2 Statutory Explanation

Hiermit bestätige ich, dass ich vorliegende Arbeit gemäß der Promotionsordnung des Fachbereich Chemie der Technischen Universität Kaiserslautern selbstständig und nur unter Verwendung der angegebenen Quellen und Hilfsmittel angefertigt habe.

Kaiserslautern, April, 2015

Merve Cayir

7.3 Acknowledgements

Firstly, I would like to thank my supervisor Prof. Dr. Werner R. Thiel for his continuous support, invaluable guidance, and understanding throughout this study. His abundant knowledge, helpful discussion and friendly encouragement helped me a lot to dissolve many problems in my research. He has been always helpful and never got tired of answering my endless questions. I am feeling very lucky to work with such a nice and friendly professor. It was a great pleasure and honor to work with him. I wish to take this opportunity to express my deepest gratitudes and regards to him.

I would like to thank Prof. Dr. Gereon Niedner Schatteburg and Dipl. Chem. Johannes Lang for ESI-MS measurements and helpful discussions. It was a very productive cooperation. I am very thankful to Prof. Dr. Franc Meyer and Adam Walli at Georg-August University Göttingen for collaborations on UV-Vis measurements. I would like to thank to Prof. Dr. Stefan Bräse and his group at Karlsruhe Institute of Technology for the synthesis of precursors of paracyclophane ligands.

I would like to thank SFB/TRR 88 3MET for financial support and giving the opportunity to do very productive collaboration.

I would like to thank Dr. Yu Sun for X-Ray crystallography measurements. Many thanks are also given to Christiana Müller for NMR Measurements.

I would like to thank Simon Walg for our scientific discussions. Whenever I was hopeless, his help, encouragement and friendship made me better. We were a great team in 3MET project. I am very grateful to Isabel Munstein. I will never forget the day which we met. Since this day, she was always with me whenever I need help about anything. I cannot express my gratitudes enough for her support and friendship. Thank you my dear friend. I would like to thank Jae-Yeon Chung for her valuable friendship. I wish we met before and we could spend more time together. I would like to give many thanks to all members of AK Thiel for great working atmosphere, help and encouragement during this study.

I would like to thank my research trainee Annelies De Cuyper for the help in the laboratory.

I would like to thank my friends Gülnar Bayramoglu Barman, Neslihan Ayazoglu and Seda Anbarli from Turkey. I felt their support and friendship always with me. I thank to my friends Nil Sahin, Nazli Yonca Aydin, Luke Harless and Ezgi Keceli from Germany. They were always cheering me up through the good and bad times.

A very special thanks goes to Murat Küçükdisli for his encouragement, support and love in overcoming all difficulties in these years. Thanks for pushing me forward and helping me whenever I need. I could not have done this without you. The last but not the least, I would like to thank my parents Bedriye and Nejdet and my sister Gizem for their patience, love and support. Despite the kilometers between us, they were always with me. Thanks a lot all of you...

7.4 Curriculum Vitae

Merve Cayir (Balikesir, Turkey)

Education

10.2010-04.2015	Technical University Kaiserslautern. PhD at Department of Chemistry.
09.2008-07.2010	Middle East Technical University, Ankara. MS at Department of Chemistry.
09.2003-06.2008	Middle East Technical University, Ankara. BS at Department of Chemistry.
09.2000-06.2003	FEKAL Anatolian High School, Balikesir.

Publications

1. C-H Activation at a Bidentate Ligand Coordinated to Palladium(II): an Electrophilic Attack Supported by an External Base, M. Cayir, L. T. Goochany, Y. Sun, A. Walli, M. Busch, S. Bräse, F. Meyer, W. R. Thiel., *Eur. J. Inorg. Chem.* **2014**, 2618-2624.
2. Roadmap towards *N*-Heterocyclic [2.2]Paracyclophanes and Their Application in Asymmetric Catalysis, M. Busch, M. Cayir, M. Nieger, W. R. Thiel, S. Bräse., *Eur. J. Org. Chem.* **2013**, 6108–6123.
3. Stereoselective synthesis of optically active dihydrofurans and dihydropyrans via a ring closing metathesis reaction, M. Cayir, S. Demirci, S. Sezer, C. Tanyeli., *Tetrahedron: Asymmetry* **2011**, 22, 1161–1168.

Poster Presentation

1. 12th Ferrocene Colloquium, Innsbruck, Austria
2. 2nd International Conference on Bimetallic Complexes, Karlsruhe, Germany.
3. 46th Jahrestreffen Deutscher Katalytiker, Weimar, Germany.
4. 1st International Conference on Bimetallic Complexes, Kaiserslautern, Germany.